THE TURBULENT BOUNDARY LAYER: EXPERIMENTAL HEAT TRANSFER WITH STRONG FAVORABLE PRESSURE GRADIENTS AND BLOWING

By

D. W. Kearney, R. J. Moffat and W. M. Kays

Report No. HMT-12

Prepared Under Grant NASA NGL-05-020-134
for
The National Aeronautics and Space Administration

Thermosciences Division
Department of Mechanical Engineering
Stanford University
Stanford, California

April 1970

THE TURBULENT BOUNDARY LAYER: EXPERIMENTAL HEAT TRANSFER WITH STRONG FAVORABLE PRESSURE GRADIENTS AND BLOWING

By

D. W. Kearney, R. J. Moffat and W. M. Kays

Report No. HMT-12

Prepared Under Grant NASA NGL-05-020-134

for

The National Aeronautics and Space Administration

Thermosciences Division
Department of Mechanical Engineering
Stanford University
Stanford, California

April 1970

ACKNOWLEDGMENTS

This research was made possible through grants from the National Science Foundation, NSF GK 2201, and the National Aeronautics and Space Administration, NGL 05-020-134. The authors wish to express appreciation for the interest of Dr. Royal E. Rostenbach of NSF, and Dr. Robert W. Graham of NASA Lewis Laboratories.

The cooperation of R. J. Loyd throughout the experimental program was a necessary factor in its success. The assistance of B. Blackwell and P. Andersen in part of the testing is appreciated. Special credit is due Miss Jan Elliott for her timely and competent handling of the publication process.

ABSTRACT

Heat transfer experiments have been carried out in air on a turbulent boundary layer subjected to a strongly accelerated free-stream flow, with and without surface transpiration. Stanton number, mean temperature and mean velocity profiles, and turbulence intensity profiles were measured along the accelerated region. The tests were conducted with favorable pressure gradients denoted by values of the acceleration parameter $K\left(= \frac{\nu}{U_\infty^2} \frac{dU_\infty}{dx} \right)$ of 2.0×10^{-6} and 2.5×10^{-6}. The blowing fraction, $F\left(= \rho_o V_o / \rho_\infty U_\infty \right)$, ranged from 0.0 to 0.004. The flow was incompressible ($U_{\infty,max} = 86$ fps) with a moderate temperature difference, 25 F, across the boundary layer.

One objective of the program was to obtain detailed heat transfer data in strong accelerations, to both increase understanding in this area and to provide a base for future prediction procedures. A second, and equally important, objective was to determine whether or not relaminarization of the boundary layer occurs at $K = 2.5 \times 10^{-6}$.

The experimental results demonstrate that the Stanton number, as a function of enthalpy thickness Reynolds number, falls increasingly below the behavior observed in unaccelerated flows as K is increased, with or without blowing. The profile traverses show that, at the end of acceleration, the boundary layer is still fully turbulent.

Further heat transfer results are presented which illustrate the effects of various conditions at the start of acceleration (notably the thicknesses of the thermal and hydrodynamic layers); step-changes in blowing within the accelerated region; and an increase in the free-stream turbulence intensity.

The experimental results reported here, as well as data taken by other experimenters at lower values of K, have

been used to calculate the distribution of turbulent Prandtl number across the boundary layer. These calculations suggest that a correlation of turbulent Prandtl number which is useful for flow over a flat plate is equally valid in accelerated flows.

Using a numerical solution of the appropriate boundary layer equations, the experimental results are predicted with reasonable accuracy, including the effects of various initial conditions and free-stream turbulence intensities.

TABLE OF CONTENTS

LIST OF FIGURES

LIST OF TABLES

NOMENCLATURE

Symbol	Description
A^+	Van Driest parameter (defined by Eqn. (2.11))
C_f	Surface shear stress coefficient ($= \tau_o/(\frac{1}{2}\rho_\infty U_\infty^2)$)
c_p	Specific heat at constant pressure
D	Dissipation term in the turbulent kinetic energy equation (defined by Eqn. (2.8))
D_v	Van Driest damping factor (defined by Eqn. (2.11))
F	Mass flux ratio ($= \rho_o V_o/\rho_\infty U_\infty$)
g_c	Gravitational constant ($= 32.17$ lbm ft/lbf sec^2)
h	height of test channel in y-direction
H	shape factor (δ_1/θ)
i	Enthalpy ($= c_p T$ for air)
i_s	Stagnation enthalpy referenced to free-stream ($= (i + U^2/2g_cJ) - (i_\infty + U_\infty^2/2g_cJ)$)
J	Dimensional constant ($= 778$ ft lbf/Btu)
K	Acceleration parameter ($= \frac{\nu}{U_\infty^2}\frac{dU_\infty}{dx}$)
ℓ_t	Length scale (defined by Eqn. (2.10))
P	Pressure
P^+	Acceleration parameter ($= -K/(C_f/2)^{3/2}$)
P_e^+	Effective P^+ (defined by Eqn. (2.15))
Pr	Prandtl number ($= \nu/\alpha$)
Pr_t	Turbulent Prandtl number ($= \epsilon_M/\epsilon_H$)

Symbol	Description
ΔP_{dyn}	Dynamic pressure ($= \rho U^2/2$)
r_c	Recovery factor
Re_H	Enthalpy thickness Reynolds number ($= \Delta_2 U_\infty/\nu$)
Re_M	Momentum thickness Reynolds number ($= \theta U_\infty/\nu$)
R_t	Turbulent Reynolds number $= \frac{y\sqrt{\tau_t/\rho}}{\nu}$
R_x	x-Reynolds number ($= \int \frac{U_\infty}{\nu} dx$)
$\dot{q}''$	Heat flux
q	Turbulent kinetic energy ($= \frac{1}{2}(\overline{u'^2} + \overline{v'^2} + \overline{w'^2})$)
Q^+	Heat flux ratio ($= \dot{q}''/(\rho_\infty U_\infty i_{s,o} St)$)
St	Stanton number ($= h/c_p \rho_\infty U_\infty$)
T	Temperature
T_T	T-state temperature in mass transfer
$\overline{T}$	Normalized temperature ($= (T-T_o)/(T_\infty-T_o)$)
T^+	Normalized temperature in inner region coordinates ($= \overline{T}U_\tau/(StU_\infty)$)
U,V	Mean velocity components in streamwise and normal directions
U^+	Normalized streamwise velocity ($= U/U_\tau$)
U_τ	Shear velocity ($= \sqrt{\tau_o/\rho}$)
U_∞	Free-stream velocity in streamwise direction
u',v',w'	Fluctuating velocity components in streamwise, normal, and transverse directions

Symbol	Description
V_o^+	Mass flux parameter $(= V_o/U_\tau)$
x	Denotes streamwise direction
y	Denotes normal direction
y^+	Inner region normal coordinate $(= y U_\tau/\nu)$
z	Denotes spanwise direction
α	Molecular thermal diffusivity $(= \frac{k}{\rho c_p})$
β	Clauser equilibrium parameter $(= \frac{\delta_1}{\tau_o} \frac{dP}{dx})$
ϵ	Eddy diffusivity
Δ_2	Enthalpy thickness $(= \int_0^\infty \frac{U}{U_\infty}(\frac{t-t_\infty}{t_w-t_\infty})\,dy)$
δ	Boundary layer thickness, 0.99 - point in U/U_∞ or $\overline{T}$
δ_1	Displacement thickness $(= \int_0^\infty (1 - \frac{\rho U}{\rho_\infty U_\infty})\,dy)$
κ	Von Karman constant (≈ 0.44)
ν	Kinematic viscosity
ρ	Density
τ	Shear stress
τ^+	Shear stress ratio $(= \tau/\tau_o)$
θ	Momentum thickness $(= \int_0^\infty \frac{\rho U}{\rho_\infty U_\infty}(1 - \frac{\rho U}{\rho_\infty U_\infty})\,dy)$
$\overline{a'^2}$, $\sqrt{\overline{a'^2}}$	Denotes mean-square and root-mean-square, respectively, of any fluctuating quantity a'

Subscripts

e	Denotes turbulence
H	Denotes energy
∞	Denotes free-stream
M	Denotes momentum
o	Denotes wall
q	Denotes turbulent kinetic energy
t	Denotes turbulence ,

CHAPTER ONE

INTRODUCTION

A. General Background

The purpose of this research has been to gain insight, through experimentation, into the heat transfer behavior of turbulent boundary layers subjected to a strongly accelerated free-stream flow. Recent studies in this area have clearly indicated that the interactions between the hydrodynamic and thermal boundary layers under these conditions are not understood to the point where adequate predictions of the heat transfer are possible [1,2][1]. It has been demonstrated by numerous experimenters that when a turbulent boundary layer is subjected to a sufficiently large negative pressure gradient (free-stream acceleration), the layer will display laminar-like characteristics, apparently experiencing a retransition from a turbulent boundary layer to a laminar one. This phenomenon is accompanied by very substantial reductions in Stanton number and, for this reason, is of considerable technical significance.

It was originally thought that the abrupt decrease in the Stanton number, when a high acceleration is applied, was evidence of the retransition to a laminar boundary layer, and the term "laminarization", coined by Launder [3], has frequently been used in connection with such decreases in Stanton number. More recently it has been demonstrated [4] that even a relatively mild acceleration can cause a reduction in Stanton number, and that the degree of reduction increases continuously with the strength of the acceleration even though the layer remains turbulent. It is thus impos-

---

[1] References will be denoted by brackets throughout this report.

sible to determine from heat transfer data alone whether laminarization is taking place. Examination of mean velocity profiles, and the success of a theoretical model of the accelerated boundary layer, is used by Kays, et al. [4], as evidence that a turbulent equilibrium boundary layer can exist even though Stanton number is decreasing virtually as it would were the boundary layer entirely laminar. It appears that acceleration causes a substantial increase in the thickness of the sublayer (an increase that ultimately will envelop the entire boundary layer at sufficiently strong accelerations), while at the same time the thermal boundary layer penetrates beyond the momentum boundary layer such that it encounters a region of very low or negligible eddy conductivity. The relative importance of these two different phenomena to the reduction in heat transfer is unknown, but it is expected that the growth of the sublayer is the dominating factor.

The ability to theoretically predict the effect of strong acceleration on the heat transfer in turbulent boundary layers, be it the result of relaminarization or a less dramatic phenomena, is a necessary prerequisite to design applications. Reasonable success in this regard has been achieved by Kays, et al. [4] for boundary layers subjected to accelerations up to a value of the acceleration parameter $K\left(= \frac{\nu}{U_\infty^2} \frac{dU_\infty}{dx} \right)$ of 1.47×10^{-6} (relaminarization is thought to commence somewhere between $K = 2.0 \times 10^{-6}$ and $K = 3.5 \times 10^{-6}$). The most important factor in any prediction method for turbulent boundary layer behavior is how one chooses to model the turbulent transport terms. In flows approaching relaminarization, particularly in heat transfer where the free-stream turbulence level has promise of being an important parameter, the simultaneous solution of the turbulent kinetic energy equation in conjunction with the momentum and energy equations shows considerable promise as a prediction method

because the turbulence is invoked explicity. In this method, the turbulent transport of heat and momentum can be related to the turbulent kinetic energy in several different ways. One technique, which has been pursued in this study, is to utilize the eddy diffusivity concept for momentum, and a turbulent Prandtl number to relate the eddy diffusivity for heat to that for momentum. In such a treatment, it is important to know the effect of external parameters, such as acceleration and transpiration, on the model for the turbulent Prandtl number.

Because a requirement for wall cooling often accompanies strong accelerations in current applications, positive transpiration, or blowing, at the wall is sometimes used to provide thermal protection at the surface. Thielbahr, et al. [6] conducted an extensive experimental investigation of the combined case of transpiration, both blowing and sucking, and moderate accelerations, up to $K = 1.45 \times 10^{-6}$. The results of that study show some interesting interactions between blowing and acceleration. To pursue that aspect of heat transfer in accelerated flows, this study has been extended to cover the combined case of strong acceleration and blowing. It is recognized that practical problems often include variable-property, high velocity flows, whereas the experimental work reported here has been taken under conditions of constant properties and incompressible flow. Experience with current prediction methods, however, has repeatedly shown that the knowledge gained from this simpler case is generally applicable to more complicated flow conditions.

B. Report Organization

The present research covers three separately definable, but interrelated, topics.

First, the essential question of the relationship of the reduction in heat transfer to the possible occurrence of relaminarization has been investigated. Detailed measurements

have been obtained of both surface heat transfer, and boundary layer profiles of mean temperature, mean velocity, and streamwise fluctuation velocity, up to a value of the acceleration parameter, K , of 2.5×10^{-6} . The experimental data also include a series of tests which examine the response of the heat transfer in the accelerated turbulent boundary layer to changes in initial conditions and to steps in boundary conditions. The results of this test series provide some insight into the importance of the laminar-like outer region, where the thermal boundary layer has grown thicker than the hydrodynamic boundary layer.

Secondly, the effect of an inlet free-stream turbulence intensity of 3.9 percent on the reduction in heat transfer, at an acceleration of $K = 2.5 \times 10^{-6}$, has been tested. The measured heat transfer provides additional information about the importance of the outer region. Because the theoretical model has been found to adequately predict these experimental results, the effect of a still higher initial free-stream turbulence intensity of 10 percent is also theoretically predicted.

The third topic treated here is an experimental evaluation of turbulent Prandtl number, for no transpiration and one case of strong blowing, over a full range of acceleration from the flat plate boundary layer ($K = 0.0$) up to $K = 2.5 \times 10^{-6}$. This information is necessary to provide a reasonable basis for the turbulent Prandtl number model used to calculate the turbulent transport of heat in the boundary layer.

This thesis has been organized into three major chapters, each treating one of the topics described above. All peripheral information, such as a description of the experimental apparatus and testing techniques, and tabulation of the experimental data, is presented in supplementary sections. While there will naturally be some overlap between the three topics, each chapter is essentially treated as a self-contained unit. In a given chapter are presented the experimental and

theoretical background pertinent to its subject, the objectives of the research, the presentation of results, and conclusions.

C. Laminarization

It was in the mid-fifties that the reduction of surface heat transfer in an accelerated turbulent boundary layer was first noted, leading Wilson [7] in 1957 to suggest that the turbulent boundary layer may revert to a laminar layer in accelerated flow. Since that time there have been numerous studies of this phenomenon, starting with detailed investigations of the hydrodynamic aspects by Launder [3] in 1964 and a basic heat transfer study by Moretti and Kays [8] in 1966.

One of the inherent difficulties in this subject arises because laminarization, the reversion of a turbulent boundary layer to a laminar boundary layer, is a vaguely defined occurrence. Like forward transition from laminar to turbulent flow, there is a range in which the boundary layer is neither laminar nor turbulent, i.e., it is "in transition". Strong accelerations usually take place over short distances, and no experimenter has been able to maintain a laminarized boundary layer. Only laminar-like characteristics, both hydrodynamic and thermal, have been observed, with no distinct line of demarcation between turbulent and laminar conditions. It stands to reason that it is quite difficult to define the onset of the reversion process.

Experimental hydrodynamic studies [9,10,11] have concentrated on both the characteristics of laminarized boundary layers, and on criteria for the onset of laminarization. Noting the accumulated knowledge from several investigations, including their own, Badri and Ramjee [11] tentatively noted three states in the decidedly gradual process[1]: (1) disappearance of the large eddy structure near the wall at a

[1] Summarized in this form by Bradshaw [12].

critical value of the acceleration parameter K, (2) a departure from the inner law velocity profile at critical values of $\frac{\nu}{U_\tau^3}\frac{dP}{dx}$, i.e. P^+, or $\frac{\nu}{U_\tau^3}\frac{\partial \tau}{\partial y}$, and (3) a decay of turbulence intensity starting at a critical value of the momentum thickness Reynolds number. In regard to item (2), it has been observed that, in strong favorable pressure gradients, apparently approaching relaminarization, the shape factor H reaches a minimum value before increasing sharply [10], and the boundary layer becomes fully, but intermittently, turbulent [13]. Additionally, it has been shown by Julien [14] that departure from the inner velocity law occurs in moderate accelerations before any laminarization effects can be expected. One of the most pertinent observations remains that of Shraub and Kline [15], who noted, in a study of the turbulent structure in the sublayer, that the frequency of turbulent bursts, associated with the production of turbulence, decreases in accelerated flows. At a value of K of about 3.5×10^{-6} bursting ceases entirely, leaving only the normal dissipation processes.

Bradshaw [12] has recently formulated a model which displays significant promise, both in its proposed explanation of the underlying physics in laminarization, and its agreement with previous observations. Bradshaw argues that turbulent flow will become directly dependent on viscosity when the shear-stress-producing and dissipating ranges of eddy-size overlap. Laminarization will occur when the region independent of viscosity has disappeared. He develops an eddy Reynolds number, $\sqrt{\tau_t/\rho}\, L/\nu$, which is a measure of the degree of overlap, where τ_t is the turbulent shear stress and L is a typical length scale of the shear-stress-producing eddies. Since the edge of the sublayer in a turbulent boundary layer is a region where viscous effects are just appreciable, the critical value of the eddy Reynolds number

can be evaluated there. Setting $L = \kappa y$, Bradshaw deduces that when $\sqrt{\tau_t/\rho}\, y/\nu$ is below 30 throughout the layer, laminarization will occur. Launder and Jones [16], by incorporating the Van Driest hypothesis into the length scale L, find a critical value of about 15. Bradshaw shows general agreement between a maximum eddy Reynolds number and such earlier criteria as a minimum momentum thickness Reynolds number (320) or a critical value of $\frac{\nu}{U_\tau^3}\frac{d\tau}{dy}$ (about -0.009 [10]).

It is very difficult to deduce the onset of relaminarization from observations of a reduction in the Stanton number, because even in moderate accelerations a reduction in Stanton number proportional to the magnitude of the acceleration is evident. The acceleration parameter, K, shows no distinctive promise as a criteria for laminarization, but it is closely related to that phenomenon and has a marked advantage in that can be externally controlled in experimentation. Particularly sharp reductions in the Stanton number are noted above values of $K = 2.0 \times 10^{-6}$.

D. Constant-K Boundary Layers

The integral momentum and energy equations can be written in the form

$$\frac{dRe_M}{dR_x} = \frac{C_f}{2} - K(1 + H)Re_M + F \qquad (1.1)$$

and

$$\frac{dRe_H}{dR_x} = St + F \qquad (1.2)$$

where

$$dR_x \equiv \frac{U_\infty dx}{\nu}$$

$$F \equiv \frac{\rho_o V_o}{\rho_\infty U_\infty}$$

For the case where F and K are maintained constant, Eqn. (1.1) shows that an asymptotic condition can be reached where the momentum thickness Reynolds number will remain constant if the shape factor H does not change. This state is, in fact, attainable and in such a boundary layer Eqn. (1.1) provides a particularly simple means to determine the wall shear stress. Equation (1.2) is applicable only to the case of constant surface temperature. It implies that, for zero or positive F, the enthalpy thickness Reynolds number will continue to increase. In view of the asymptotic nature of the momentum boundary layer, one observes that the thermal boundary layer will grow outside of the hydrodynamic boundary layer under these conditions.

The state of the hydrodynamic boundary layer for constant K is more precisely defined by consideration of the differential equations of the boundary layer. Townsend [17] has shown that a "sink" flow, which is equivalent to a constant K, leads to a similarity solution of the continuity and momentum equations. Launder and Jones [18] have recently presented a solution to the resulting ordinary differential equation by utilizing a Prandtl mixing length model for the turbulent Reynolds stress. The important point is that complete similarity can be expected for prolonged accelerations at constant K. Launder and Lockwood [19] have also demonstrated that a similarity solution for the energy equation is possible for the case where the surface temperature varies in a special way. For the case of constant surface temperature, however, the similarity solution is the trivial case, $St = 0$ and $Re_H = \infty$.

It should be noted that the asymptotic boundary layer discussed here is a particular case of the equilibrium boundary layer, which in general displays self-preserving outer-region defect-velocity profiles and is defined as a layer in which the equilibrium parameter, $\beta = -\frac{\delta 1}{\tau_w}\frac{dP}{dx}$,

remains constant. By definition, $\beta = \frac{KRe_M H}{C_f/2}$, so that β is fixed in an asymptotic constant-K layer because each variable remains separately constant. In view of all these considerations, the parameters K and F were maintained constant for all the experimental tests conducted in this study, in an attempt to control the state of the hydrodynamic behavior of the turbulent boundary layer.

CHAPTER TWO

EXPERIMENTAL SURFACE HEAT TRANSFER TO STRONGLY ACCELERATED TURBULENT BOUNDARY LAYERS

A. Previous Experimental Findings

It has been well established that the Stanton number markedly decreases in strongly accelerated flows. The experimental evidence suggests that a fundamental change in structure, perhaps relaminarization of the turbulent boundary layer, occurs under these conditions. In 1965, Moretti and Kays [8] conducted the first detailed investigation of heat transfer in the turbulent boundary layer with strong favorable pressure gradients. They showed that the reduction of Stanton number was proportional to the magnitude of the acceleration parameter, K, which varied from 0.52×10^{-6} to 3.51×10^{-6} in their tests. At the strongest acceleration, however, the drop-off in Stanton number was particularly steep in St-Re_H coordinates, suggesting that relaminarization of the boundary layer was taking place. This conclusion was substantiated by the hydrodynamic findings of Shraub and Kline [15], in which the turbulence generation near the wall was apparently completely inhibited in a boundary layer at about $K = 3.5 \times 10^{-6}$. Profile data were not obtained by Moretti and Kays in conjunction with the surface heat transfer data, and it was difficult to speculate about the underlying mechanism for the reduction in Stanton number in their experiments.

More recently, experimental studies in rocket nozzles have also been concerned with understanding the heat transfer behavior. Boldman, et al. [20] report surface heat transfer data and mean profile data for average values of K up to 30×10^{-6} in the convergent section of a conical nozzle. Using the criterion that laminarization will occur when $Re_M \leq 360$, in conjunction with the momentum integral equation for an axisymmetric geometry, they derive a critical value for

the acceleration parameter K equal to 2.88×10^{-6}. The reduction in Stanton number in the nozzle, which is below the level normally associated with turbulent flow, consistently occurs at values of K above this critical value. It should be noted that the convergent portion of the nozzle measured 4.7-inches along the axis, giving the boundary layer very little time to respond to the imposed acceleration. Short regions of acceleration, however, are to be expected with high levels of K, even in an apparatus designed solely for basic experimental studies of accelerating flows.[1]

Back, et al. [2] conducted a series of tests on a cooled, conical nozzle, also including surface heat transfer data, mean velocity profiles, and mean temperature profiles within the nozzle. Low rates of heat transfer were noted when K was above $2\text{-}3 \times 10^{-6}$, lying approximately 50 percent below turbulent correlations at the higher values of K. Average values of K in the nozzle, which measured 10 inches along the axis in the convergent portion, ranged from 1×10^{-6} to 8×10^{-6}. Both temperature and velocity profiles appeared to approach predicted laminar shapes near the wall at the highest levels of K. Theoretical predictions of the experimental results were not successful in either of the nozzle studies in cases where effects attributed to laminarization were observed.

Caldwell and Seban [1] discuss experimental and theoretical results dealing with boundary layer tests in a rectangular

---

[1] This point is seen more readily by writing the definition of K, for incompressible flow, in the form

$$K = \frac{-\nu}{U_{\infty,1} A_1} \frac{dA}{dx}$$

where 1 denotes the start of acceleration.

channel. Acceleration took place over a 5-inch section in which a blister was installed on one wall. Maximum values of K reported in the three tests ranged from 5×10^{-6} to 12×10^{-6}. Surface heat transfer data were accompanied by mean velocity profiles, mean temperature profiles, and streamwise fluctuating velocity profiles. The mean profiles showed the same trends reported by Back, et al. [2]. The profiles of $\sqrt{\overline{u'^2}}/U_\infty$ indicate a reduction in the peak through the region of acceleration in any given test. They found that the measured minimum value of the peak, i.e., near the end of acceleration, was approximately equal to 0.06 in all three tests. To predict the experimental results, Caldwell and Seban utilized a simultaneous solution of the momentum, energy, and turbulent kinetic energy equations. Their model, however, was not able to predict the measured decrease in Stanton number.

An extensive test program to study heat transfer in moderately accelerated boundary layers, over a wide range of transpiration, was reported by Thielbahr, et al. [6] in 1969. This program, conducted on the same apparatus as the present study, was carried out over a range of the acceleration parameter, K, from 0.57×10^{-6} to 1.45×10^{-6}, and a range of the transpiration parameter, F, from -0.004 (sucking) to +0.006 (blowing). In conjunction with the parallel work of Julien [14], the data included mean velocity and mean temperature profiles in addition to surface heat transfer. The acceleration was imposed over distances from 2.5 to 5 feet, allowing the boundary layers to attain near-equilibrium conditions in many of the test runs. The significant feature of the no-blown results is that, for increasing K, the reduction in Stanton number, and the shape of the profiles, displayed a gradual progression towards the behavior normally associated with laminarization of the turbulent boundary layer. For example, the profile data show a substantial increase in the thickness of the sublayer in the accelerated

region, and a growth of the thermal boundary layer outside the hydrodynamic layer. The reduction in Stanton number is attributed to these two features, with the expectation that the sublayer growth is controlling, and a theoretical model based on these observations successfully predicted the experimental results [4]. For moderate blowing, acceleration usually decreased the Stanton number, just as in the unblown case. At certain combinations of strong blowing and moderate acceleration, however, the Stanton number, at the inception of acceleration, increased over the unblown $St\text{-}Re_H$ equilibrium relation for unaccelerated flow. However, by incorporating the experimental sublayer behavior into the theoretical model, the effect of interactions between moderate accelerations and transpiration on the surface heat transfer were also predicted.

B. Objectives

The present study was designed to investigate boundary layers in strongly accelerated flows at levels of K where relaminarization effects might be expected, but low enough so that the boundary layer would be reasonably close to an equilibrium state. The objectives can be enumerated as follows:

- To obtain surface heat transfer data in conjunction with mean temperature, mean velocity, and streamwise fluctuation velocity profile data for the turbulent boundary layer in the presence of a strongly accelerated free-stream flow, with and without blowing at the wall.
- To determine whether, at a value of the acceleration parameter $K(= \nu/U_\infty^2 \frac{dU_\infty}{dx})$ of 2.5×10^{-6}, the sudden reduction in Stanton number noted in preliminary experiments is a result of relaminarization of the boundary layer.
- To measure the response of the turbulent boundary layer in strongly accelerated flows to changes in initial

conditions and boundary conditions, particularly the initial ratio of thermal to hydrodynamic boundary layer integral parameters, the free-stream turbulence intensity, and steps in blowing at the wall.

- To investigate the use of the turbulent kinetic energy equation, in conjunction with the momentum and energy equations, in the prediction of boundary layer heat transfer in accelerated flows.

C. Experimental Program

C.1 Test Apparatus (Figs. 2.1-2.2)

The boundary layer was formed on the lower surface of a rectangular channel having initial cross-section dimensions of six inches by twenty inches. The entire channel is eight feet in length. The region of acceleration, extending over a distance of 20 inches, begins 16 inches downstream of a 1/16-inch high, 1/4-inch wide flat boundary layer trip. The height of the upper wall of the duct can be varied to achieve the desired free-stream velocity; in the experiments described here a linear variation of the wall was utilized in order to achieve a constant value of the acceleration parameter K.

A schematic diagram of the experimental apparatus is shown in Fig. 2.1. To illustrate the experimental setup and the free-stream conditions for an acceleration of $K = 2.5 \times 10^{-6}$, Fig. 2.2 presents a typical setting of the upper wall, and the variations of free-stream velocity and K through the region of acceleration.

The lower wall of the eight-foot channel is comprised of 24 segments of 1/4-inch thick sintered bronze, allowing for tests with transpiration when desired. Surface temperature is measured by five thermocouples imbedded in the center six-inch span of each segment. The segments are heated by wires situated in grooves in the bottom surface, spaced close

enough together that the top surface temperature perturbation, due to wire spacing, is less than 0.04 F. The heat transfer between the surface and the boundary layer is deduced from an energy balance based on power and temperature measurements in each segment. Mean flow velocity profiles were obtained with a flattened pitot probe, while temperature profiles were measured with an iron-constantan thermocouple with the junction flattened. Turbulence profiles were taken with a 0.0002-inch constant temperature platinum hot wire and a linearized anemometer system. A detailed description of the apparatus and the data reduction method is contained in Supplement 1.

Prior to the experiments reported here, an extensive program was undertaken to qualify the test apparatus for use in strong favorable pressure gradients. The low entrance velocities made it necessary to prove the development of a uniform, two-dimensional boundary layer on the wall, and satisfactory energy balances in heat transfer. After some modification to the test rig, the uniformity of the main stream flow and spanwise variations in the boundary layer were found to be within acceptable limits. Transpiration qualification tests, with no main stream flow, were conducted in which the net energy delivered to each plate agreed within about 4 percent with the measured energy transfer to the transpired air. Surface heat transfer results for the flat plate turbulent boundary layer agree with accepted correlations within 3 percent. Energy balances between the surface heat transfer data and profile measurements were typically within 10 percent in the accelerated flows.

C.2 Test Plan

The experiments can be conceptually divided into two categories: those tests, with and without blowing, in which the entering boundary layers are as close as possible to equilibrium conditions, and a series of experiments in

which both initial conditions and boundary conditions were perturbed in order to study certain characteristics associated with accelerated flows.

In the former category, tests without transpiration were conducted at free-stream accelerations corresponding to $K = 2.0 \times 10^{-6}$ and 2.5×10^{-6}. At the stronger acceleration, two blowing runs were carried out at values of the blowing parameter, F, of 0.002 and 0.004.

Five additional test runs comprise the second category. With no blowing, and at an acceleration of $K = 2.5 \times 10^{-6}$, the state of the thermal boundary layer at the start of the accelerated region was controlled in three tests in order to study the effect of the initial condition on the surface heat transfer behavior in a strong acceleration. The controlled parameters were the thicknesses of the entering thermal and hydrodynamic boundary layers, and perhaps more important, their relative size. Two test runs were also conducted to investigate the response of the boundary layer to a stepwise change in blowing during acceleration.

D. Experimental Results

D.1 Effects of Strong Acceleration, With and Without Blowing (Figs. 2.3-2.6)

The surface heat transfer data, for nominal values of the acceleration parameter K of 2.0×10^{-6} and 2.5×10^{-6}, with no transpiration, are presented in Fig. 2.3 in terms of Stanton number and the enthalpy thickness Reynolds number. Since each plate is 4 inches wide, each Stanton number represents an average over that distance. The enthalpy thickness Reynolds number is generally calculated by integration of the energy equation. An alternative method, also presented on that figure, is to evaluate the enthalpy thickness from profile measurements. The degree of agreement between these two independent methods is a measure of the

boundary layer energy balance. While the reduction in Stanton number at $K = 2.55 \times 10^{-6}$ is quite pronounced, it appears to be consistent with a mechanism whose effect gradually increased with the strength of the acceleration. To illustrate this point, Fig. 2.4 compares results for five values of K with the unaccelerated case. No sudden change in the character of the response to acceleration is discernible in the surface heat transfer results.

Boundary layer traverses of mean temperature, mean velocity, and the streamwise fluctuating velocity are presented in Fig. 2.5. The hydrodynamic data shown there, as well as all the hydrodynamic results discussed in this report, are taken from the work of Loyd [23], who studied the fluid mechanics of strongly accelerated boundary layer flows in parallel with these heat transfer tests. A hydrodynamic similarity solution is possible for constant-K turbulent boundary layers, and the mean velocity profiles appear to approach such a similarity condition near the end of acceleration. As expected from the momentum equation, surface skin friction is nearly constant. The turbulence profiles indicate that the intensity of the turbulence near the wall and in the outer regions is decreasing through the accelerated zone. In the outer regions, the last two profiles in the accelerated zone show evidence of similarity. At the end of acceleration, the peak in the streamwise fluctuating velocity normalized by the free-stream velocity, $\sqrt{\overline{u'^2}}/U_\infty$, decreases to about 9 percent, compared to 11 percent prior to acceleration. For stronger accelerations, other experimenters have found the peak value to be reduced to 6 percent [1] and 2 percent [11]. With a constant wall temperature, a thermal equivalent of the hydrodynamic similarity solution does not exist. The continuous reduction in Stanton number through the region of acceleration is reflected in the growth of the temperature profiles in T^+-y^+ coordinates.

Bradshaw [12] has proposed that relaminarization takes place when the maximum value turbulent Reynolds number, tentatively defined as $R_t = \frac{y}{\nu}\sqrt{\tau_t/\rho}$, falls below 30. Applying an integral technique to the hydrodynamic data in Fig. 2.5, Loyd [23] has calculated the total shear stress distribution for the boundary layers in this study. Knowing τ and the local velocity gradient, the turbulent shear stress, τ_t , can be determined. Carrying out this procedure, the maximum values of R_t for the profiles shown in Fig. 2.5 are, respectively from the start of acceleration, 115, 128, 100, and 68, usually occurring at about $y^+ = 275$. The minimum R_t of 68 suggests that relaminarization is not taking place.

On the other hand, Loyd [23] notes trends in the hydrodynamic data which suggest that, at $K = 2.55 \times 10^{-6}$ and $F = 0$, the final equilibrium state would indeed be a laminar one, though there is little doubt that the boundary layer shown in Fig. 2.5 is still turbulent. In Fig. 2.4 it can be noted that the slope of the Stanton number curve shows no signs of diminishing within the accelerated region at $K = 2.55 \times 10^{-6}$, whereas at lesser accelerations such a trend is apparent. This observation may be a sign of relaminarization, or simply a result of the fact that the boundary layer has not yet attained a near-equilibrium condition at $K = 2.55 \times 10^{-6}$. Profile results demonstrate that, for $K = 1.99 \times 10^{-6}$, an equilibrium state is nearly attained in the test shown in Fig. 2.4.

Through the accelerated region, the hydrodynamic layer thickness, δ_M, decreases much more rapidly than the thermal layer thickness, δ_H , resulting in a portion of the thermal layer lying outside of the momentum boundary layer. It is of interest to note the development of both the boundary layer thicknesses and the integral parameters through the accelerated region. At the start of the acceleration, the ratio δ_H/δ_M is 1.09 while Δ_2/θ equals 1.10 . Near the end of the

acceleration, the enthalpy thickness is 2.55 times greater than the momentum thickness, and the ratio δ_H/δ_M has risen to 1.37 . Since the outer region, hereafter called the "thermal superlayer", is characterized by laminar-like heat transfer mechanisms, it might be expected to substantially reduce the heat transfer rate. Evidence from the "recovery" region seems to deny this, however. In that region, where the imposed pressure gradient is removed, the Stanton number in Fig. 2.3 reverts almost immediately to the flat plate correlation, even overshooting the expected equilibrium value, for both $K = 2.0 \times 10^{-6}$ and 2.5×10^{-6} . This rapid response to the relaxation of the pressure gradient implies that the inner layers are controlling the heat transfer rate, not the thermal superlayer.

The combined effects of blowing and a strongly accelerated free-stream flow are shown in Fig. 2.6. Blowing affects heat transfer to the surface in two ways. First, and most important, the increase in the component of velocity normal to the wall convects energy away from the surface. Secondly, the structure of the sublayer is changed. Physically the thickness of the laminar-like region near the wall increases, but on an inner region scale, y^+ , the sublayer becomes thinner. Since acceleration acts to thicken the sublayer, the ultimate size of the sublayer thickness depends on the strength of the blowing and acceleration. The local shear stress and heat flux distributions through the layers are also influenced in an opposing manner by blowing and acceleration.

The experimental results verify that the effect of acceleration is reduced with increased blowing. Additionally, the Stanton number falls away from the equilibrium correlation for the unaccelerated case when the imposed pressure gradient ceases. Interestingly, the reduction in Stanton number at high blowing is greater during the relaxation period after acceleration than it is during the acceleration itself.

Thielbahr, et al. [21] found similar behavior for accelerations up to $K = 1.45 \times 10^{-6}$. They also measured temperature profiles in the recovery region which indicated that the inner layers, at a level of K as high as 1.45×10^{-6}, immediately returned to an equilibrium state for no acceleration, even at high blowing. Assuming a rapid inner layer response, one possible explanation of the heat transfer behavior is that the outer region is quite important in the blown boundary layer, which is characterized by a thin sublayer, and the thermal superlayer becomes a substantial factor in the resistance to heat transfer. It is also true that, with blowing, the relative sizes of the thermal and hydrodynamic boundary layers will be maintained over a longer distance[2] in the recovery region.

D.2 Response to Changes in Initial Conditions (Figs. 2.7-2.8)

Figure 2.7 presents the results of four test runs, nominally at $K = 2.5 \times 10^{-6}$, which differ only in the thickness of the momentum and thermal boundary layers at the start of the accelerated region. Also shown for comparison is the similarity solution for laminar wedge flows, other than the constant-K flow, in which the thermal boundary layer has grown completely outside of the hydrodynamic layer. Run 070869 was previously presented in Fig. 2.3. In run 071569, the hydrodynamic conditions were identical, but no power was applied to the wall for the first 16-inches, retarding the growth of the thermal layer. In run 092469,

---

[2] Deduced from the integral equations,

$$\frac{d\theta}{dx} = C_f/2 + F$$

$$\frac{d\Delta_2}{dx} = St + F$$

the unaccelerated boundary layer was allowed to develop over a longer distance before the acceleration was imposed. Run 100269 corresponds in hydrodynamic development to run 092469, but again the thermal boundary layer growth was delayed.

It is apparent that the heat transfer results presented in Fig. 2.7 are quite dependent on the initial conditions. In nozzle tests, Boldman, et al. [24] reported that different inlet boundary layer thicknesses produced no appreciable variation in the peak heat transfer coefficient, which roughly corresponds here to comparing the minimum Stanton number in the runs where $\Delta_2/\theta \approx 1$. In the present series of tests, it is possible that the significant inlet condition is the ratio of the boundary layer thicknesses. At the end of the acceleration region the values of the ratio Δ_2/θ are, for example, 1.75 and 3.4, respectively, for runs 071569 and 092469. If the thermal superlayer is important, then the Stanton number in the flat plate region after the acceleration should be lower for the case where the thermal boundary layer is relatively thicker. However, there is no substantial difference in the recovery performance (not shown in Fig. 2.7) of the four runs, suggesting that it is the inner layer structure which controls the heat transfer behavior throughout the accelerated region. The trends in the reduction in heat transfer give the impression that, were the acceleration to continue indefinitely, the Stanton number would asymptotically approach a single functional relationship with the enthalpy thickness Reynolds number. Consequently, it is possible that the different behaviors merely reflect the degree to which each boundary layer is initially out of an equilibrium state associated with the imposed acceleration.

Figure 2.7 demonstrates the danger of identifying relaminarization by the heat transfer behavior, since each test was carried out at, nominally, $K = 2.5 \times 10^{-6}$. In fact, the steep slope of the Stanton number curve in run 092469 appears

very similar to the results of Caldwell obtained at a much stronger favorable pressure gradient (peak $K = 5 \times 10^{-6}$), as illustrated in Fig. 2.8 .

D.3 Response to Changes in Boundary Conditions (Figs. 2.9-2.10)

Tani [25] summarizes the results of several hydrodynamic studies which investigated the response of the turbulent boundary layer to sudden perturbations. In general, the response was nearly instantaneous near the wall, but lagged in the outer regions. For example, a sudden change in pressure gradient immediately imposes a change in $\frac{\partial U}{\partial x}$, resulting in a change in $\frac{\partial U}{\partial y}$, and, consequently, the rate of production of the turbulent energy. A readjustment of the turbulence and shear stress follows. Tani suggests that, near the wall, the scale of turbulence is small enough so that the attainment of local equilibrium is rapid. In the outer regions, however, most of the turbulent energy resides in larger scale turbulence, which is associated with longer life-times and is responsible for the slower outer region adjustment. In all the acceleration studies reported here, a near stepwise change in pressure gradient is imposed and removed, respectively, at the start and end of the accelerated region. The behavior in the beginning of the accelerated region appears to show a substantial lag in the overall response of the boundary layer, while the recovery region, at the end of acceleration, indicates a considerably faster response, at least in the unblown case.

Some interesting results were obtained by introducing a step in blowing during acceleration. In Fig. 2.9, results are shown for the case where a stepwise change in blowing from no blowing to $F = 0.004$ is introduced at an axial distance of 32 inches (see Fig. 2.2). The Stanton number immediately drops to an unusually low value, apparently due

to the convective effect of blowing and the thick sublayer resulting from acceleration. It is conjectured that the blowing then acts to thin the sublayer and the behavior is thereafter similar to the results shown in Fig. 2.6. A similar quick response to a step in blowing is seen in Fig. 2.10, where the blowing is stopped at $x = 32$ inches. With the sudden removal of substantial convection away from the wall, but the residual effect of a thin sublayer due to blowing, the Stanton number immediately rises to a high value, then decreases rapidly at a rate reminiscent of run 092469 shown in Fig. 2.7 . The recovery region shows no effects which can be attributed to the wall blowing.

E. Prediction of Selected Experimental Results (Figs. 2.11-2.14)

The turbulent transport terms were modeled with a combination of a kinetic energy model of turbulence in the outer regions, and the Van Driest mixing-length model near the wall. The calculations were performed by a numerical solution[3] of the following simultaneous set of equations:

Continuity
$$\frac{\partial U}{\partial x} + \frac{\partial V}{\partial y} = 0 \qquad (2.3)$$

Momentum
$$U\frac{\partial U}{\partial x} + V\frac{\partial U}{\partial y} = U_\infty \frac{dU_\infty}{dx} + \frac{\partial}{\partial y}\left[(\epsilon_M + \nu)\frac{\partial U}{\partial y}\right] \qquad (2.4)$$

Energy
$$U\frac{\partial T}{\partial x} + V\frac{\partial T}{\partial y} = \frac{\partial}{\partial y}\left[(\epsilon_H + \alpha)\frac{\partial T}{\partial y}\right] \qquad (2.5)$$

[3] The numerical procedure employed is a modification of the Spalding/Patankar procedure [26].

Turbulent Kinetic Energy

$$U\frac{\partial q}{\partial x} + V\frac{\partial q}{\partial x} = \epsilon_M\left(\frac{\partial U}{\partial y}\right)^2 + \frac{\partial}{\partial y}\left[(\nu + \epsilon_q)\frac{\partial q}{\partial y}\right] - D \tag{2.6}$$

To obtain closure, the following model of the turbulent structure was assumed in the outer region

$$\epsilon_M = 0.22\, \ell_t \sqrt{q} \tag{2.7}$$

$$D = 0.284\, q^{3/2}/\ell_t \tag{2.8}$$

$$\epsilon_M/\epsilon_q = 1.70 \tag{2.9}$$

$$\ell_t = \kappa\, y\, D_v \tag{2.10}$$

$$D_v = 1 - \exp(-y^+ \sqrt{\tau^+}/A^+) \tag{2.11}$$

$$\epsilon_H = \epsilon_M/Pr_t \tag{2.12}$$

$$Pr_t = Pr_t(\epsilon_M/\nu) \tag{2.13}$$

Equations (2.7) through (2.9) have been suggested by the work of Spalding [26] and Wolfshtein [52].

The relationship for the turbulent Prandtl number as a function of ϵ_M/ν is based on the work of Simpson, et al. [27]. In the correlation used here, the values for Pr_t ranged from 1/Pr at the wall to 0.86 in the outer layers (this correlation is also presented in [4]). It will be shown that the effects of acceleration on the Van Driest parameter, A^+, can be adequately modeled in accelerated flows with blowing by the function $A^+(P_e^+, V_o^+)$ shown in Fig. 2.11.

This model is based on experimental results which are fully discussed by Loyd [23].

In the computational scheme, the wall region is handled separately from the main finite-difference mesh in the outer regions, primarily to avoid the necessity of a very small mesh in the region of severe temperature and velocity gradients. The Couette flow forms[4] of Eqns. (2.3) through (2.5) are utilized in the wall region, with the additional stipulation that

$$\epsilon_M = \ell_t^2 \left|\frac{dU}{dy}\right| \quad . \tag{2.14}$$

Equations (2.10) through (2.13) complete the mathematical set. This mixing-length model of the turbulent boundary layer, with a modification in the outer region, has been successfully used by Kays, et al. [4] to predict experimental results over a wide range of transpiration and favorable pressure gradients, up to $K = 1.45 \times 10^{-6}$. Since the turbulent kinetic energy equation has been incorporated into the outer region solution in the current study, the boundary condition required at the inner edge of the finite-difference grid is obtained by solving Eqns. (2.7), (2.10), and (2.14) for q at that point, where D_v and y are known from the wall region solution.

Selected predictions of the present experimental results are presented in Figs. 2.12-2.14. With no blowing, the near-equilibrium predictions shown in Fig. 2.12 agree reasonably well with the experimental data, both in the effects of acceleration on heat transfer and in the behavior in the recovery region. Figure 2.13 illustrates one case of strong blowing and strong acceleration. The influence of pressure gradient in the theoretical model tends to reduce the pre-

[4] The streamwise derivatives $\frac{\partial U}{\partial x}$ and $\frac{\partial T}{\partial x}$ are neglected.

dicted Stanton number below the experimental data, while, in the recovery region, both prediction and experiment show a trend away from the equilibrium flat plate case. Predictions for three cases with different initial conditions at the start of acceleration, at $K = 2.5 \times 10^{-6}$ and without blowing, are presented in Fig. 2.14. The trends of the experimental data are reproduced by the prediction, particularly in respect to the rate at which Stanton number decreases in the accelerated region. The recovery behavior, not shown, is similar in all three predictions.

It is important to recognize that the model for $A^+(P_e^+ , V_o^+)$ presented in Fig. 2.11 is crucial to the success of the theoretical model. The parameter A^+ is proportional to the thickness of the sublayer, so that, for example, the increase in A^+ with increasingly higher accelerations models the observed growth of the sublayer. Since the boundary layer cannot respond instantaneously to an imposed pressure gradient, it is also necessary to include the influence of the upstream history in the boundary layer. In the predictions, shown here, a lag function

$$\frac{dP_e^+}{dx^+} = 3000\left|P^+ - P_e^+\right| \qquad (2.15)$$

has been introduced, where P^+ is the equilibrium pressure gradient parameter for the known value of acceleration and skin-friction, while P_e^+ is the calculating, or effective, value used in the model which determines A^+. The lag constant, 3000, was selected by comparing prediction to experiment for various values of lag in run 070869-1 ($F = 0.0$, $K = 2.5 \times 10^{-6}$). Currently, no lag is associated with changes in blowing, but one can argue that a lag is physically justifiable and should, in fact, be included.

F. Conclusions

To summarize the findings from the experimental study, the following conclusions are offered:

(a) For the acceleration parameter, K, as high as 2.5×10^{-6} the boundary layer displays fully turbulent characteristics, and the marked reduction in Stanton number is largely due to growth of the sublayer.

(b) For the acceleration parameter, K, through 2.5×10^{-6}, the amount of the reduction in Stanton number, at a given F, increases smoothly as the magnitude of the acceleration increases. The absence of any abrupt changes supports the contention that relaminarization, if it is even occurring, manifests itself in the growth of the sublayer.

(c) The region of the thermal boundary layer outside of the hydrodynamic boundary layer is not an important factor in the reduction of Stanton number in strongly accelerated flows without transpiration, but it may play a significant role in the blown boundary layer.

(d) The initial thermal condition of the boundary layer markedly influences the surface heat transfer characteristics during acceleration. In practical applications, the length of the acceleration region is almost never long enough to remove the effect of the upstream thermal history. The response of the strongly accelerated turbulent boundary layer to steps in blowing at the wall, on the other hand, is quite rapid, thus displaying the same characteristics as the turbulent boundary layer without acceleration.

(e) The surface heat transfer in boundary layers subjected to accelerations up to $K = 2.5 \times 10^{-6}$ can be adequately predicted by a numerical solution of the momentum, energy, and turbulent kinetic energy equations, utilizing eddy-diffusivity models for the turbulence transport terms. The turbulence model, based on empirical equilibrium relationships, accounts for the behavior of the non-equilibrium flows measured in the present study, as long as the effects of upstream history are considered.

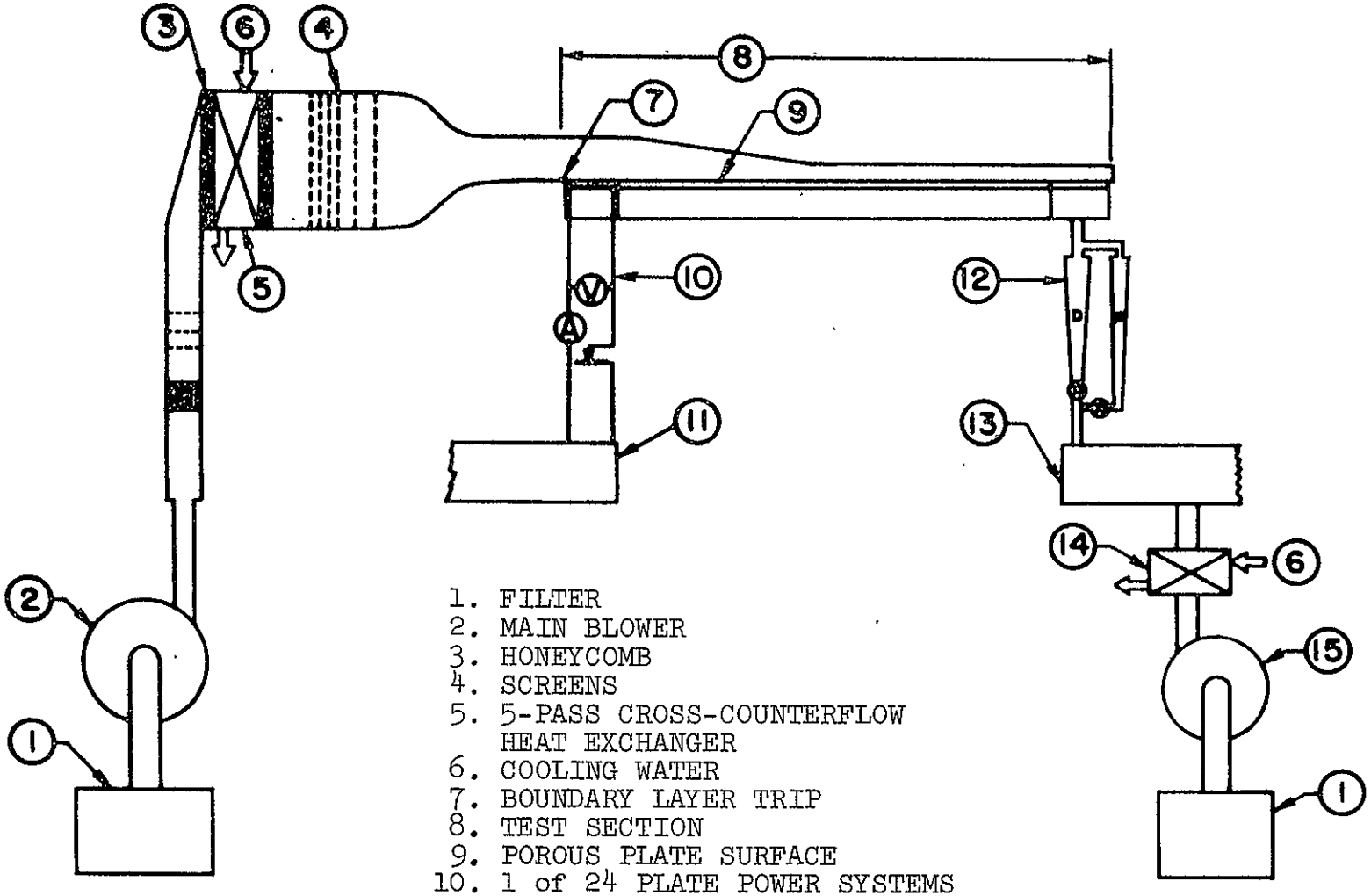

Fig. 2.1 Schematic diagram of the test apparatus

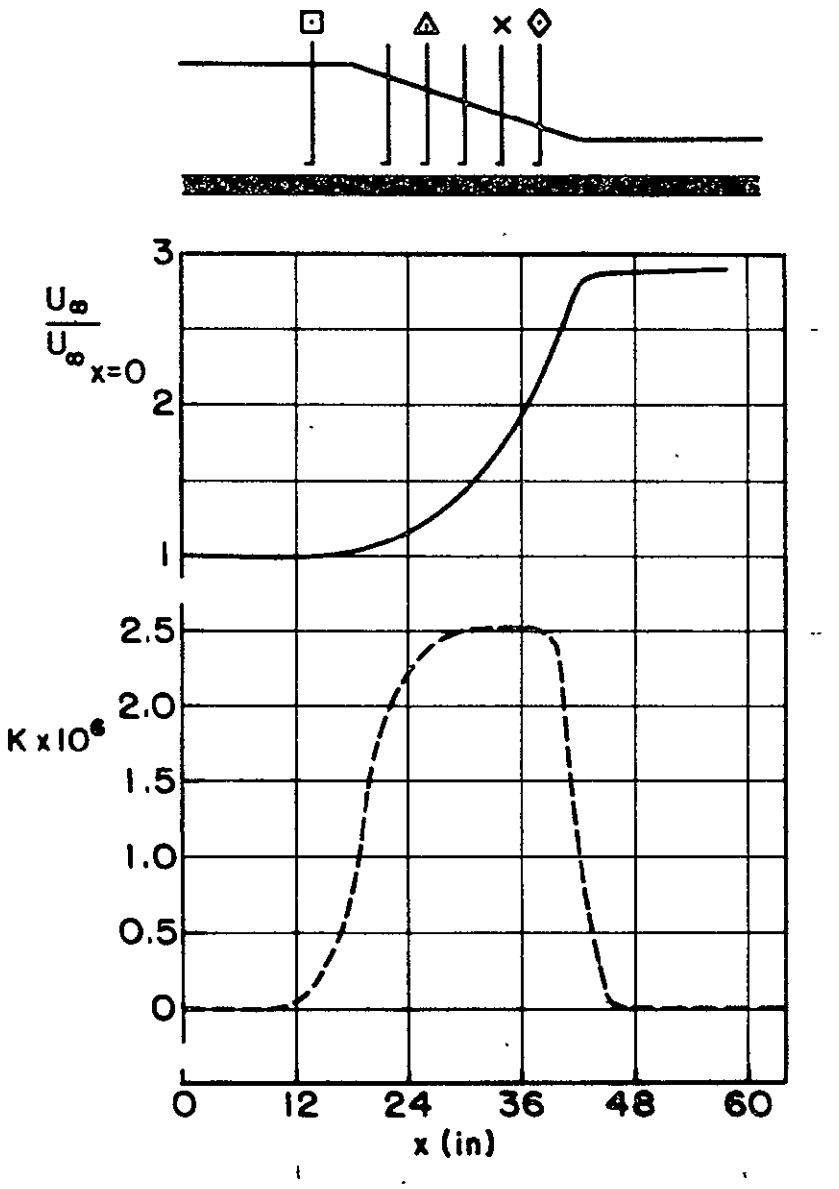

Fig. 2.2 Traverse locations and typical velocity distribution in the test apparatus for a strong acceleration

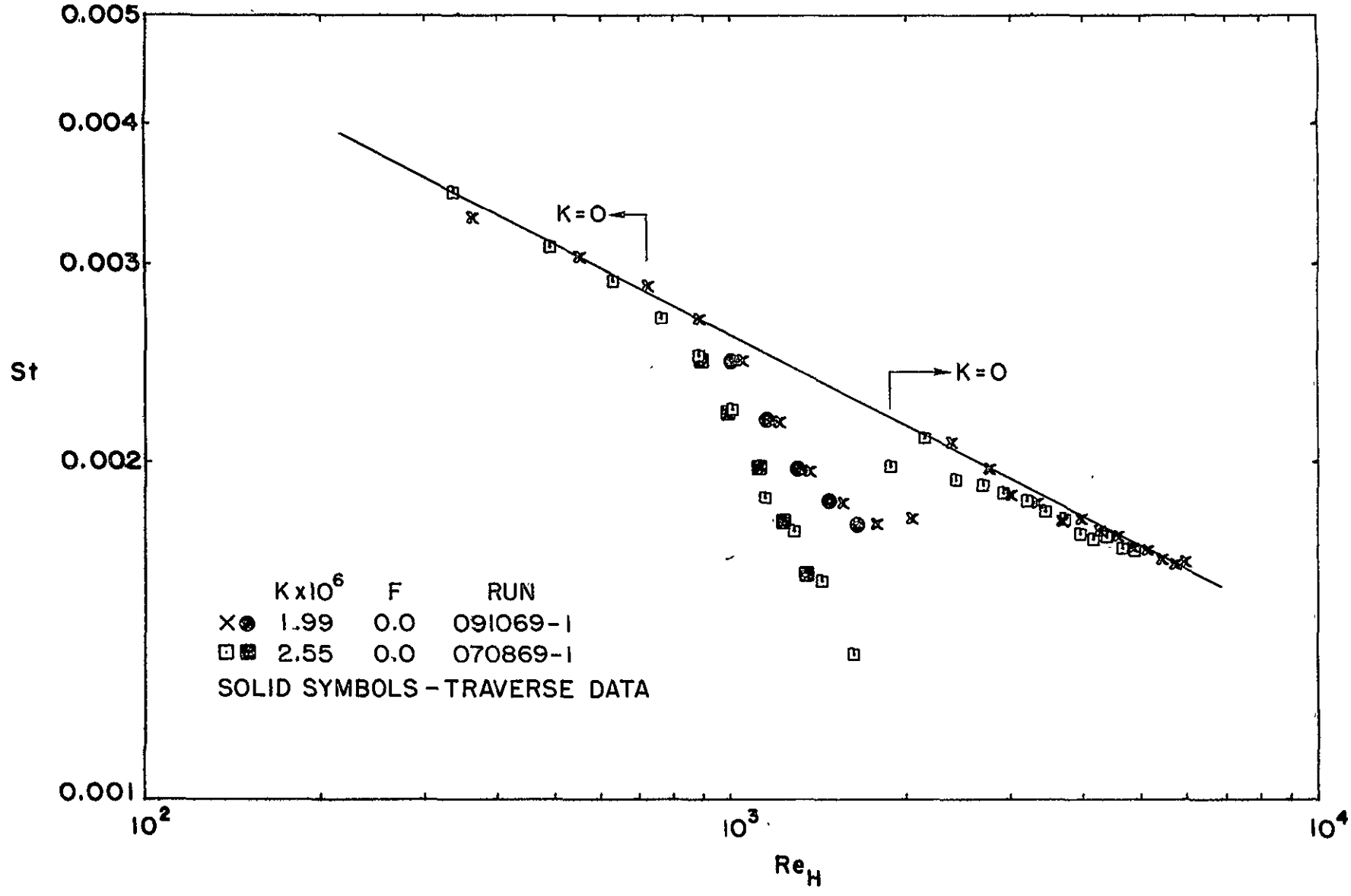

Fig. 2.3 Experimental results of surface heat transfer in a turbulent boundary layer with a strongly accelerated free-stream flow. ———, Moffat and Kays [22].

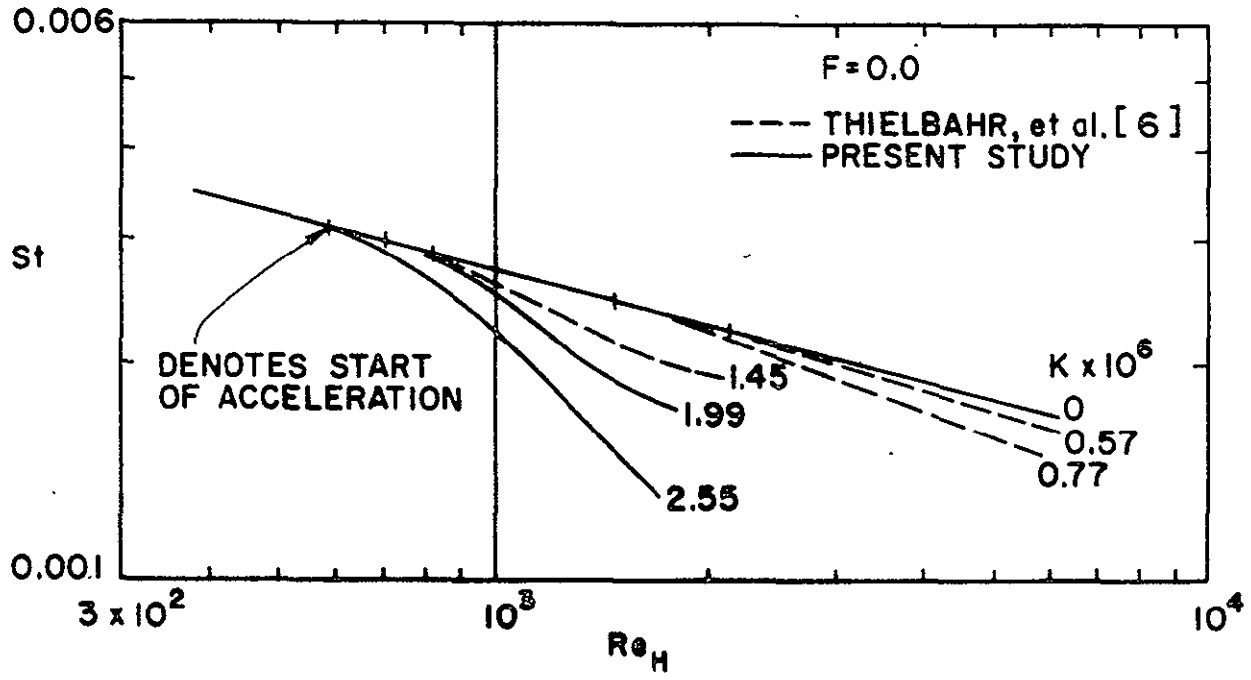

Fig. 2.4 Comparison of experimental boundary layer heat transfer in a favorable pressure gradient

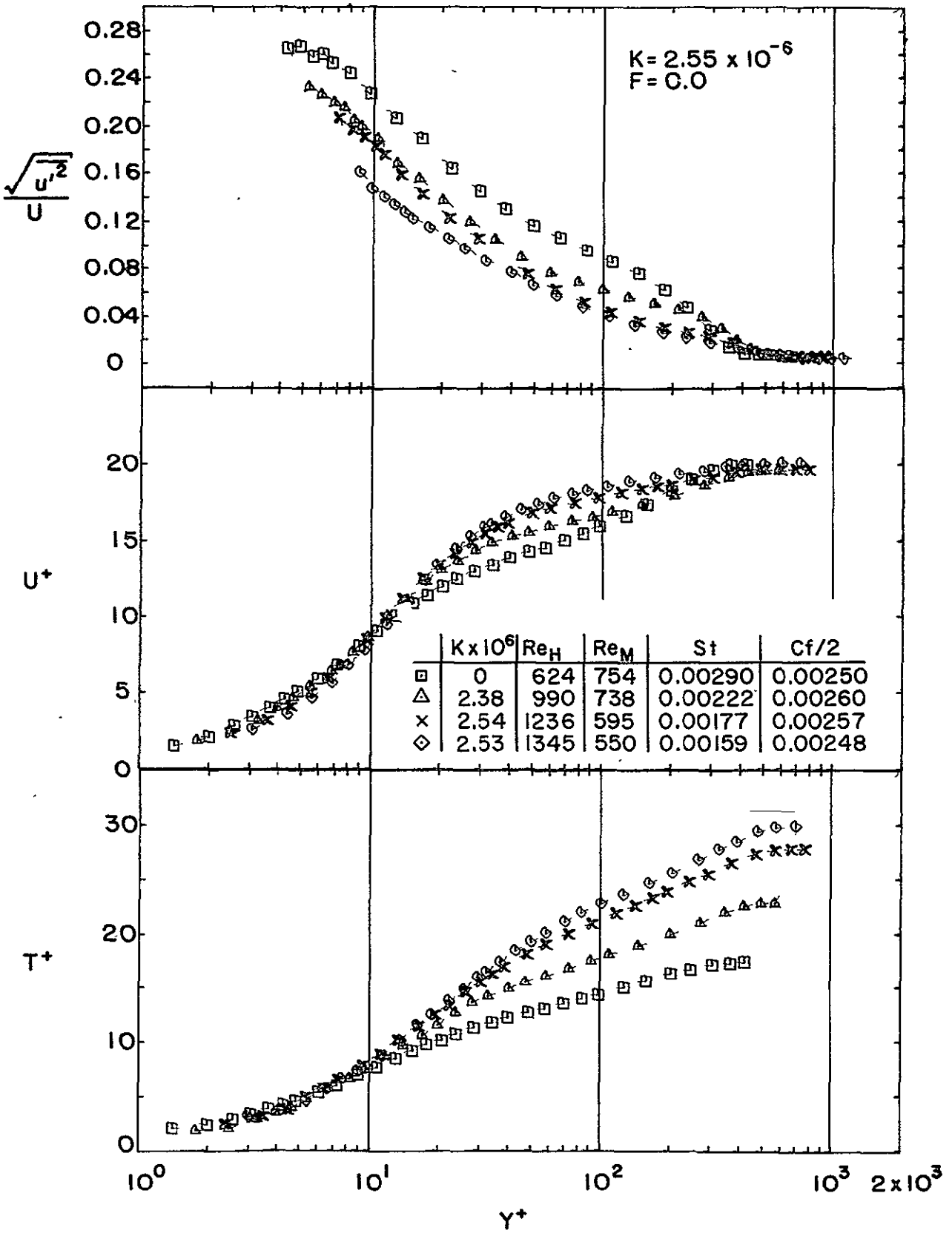

Fig. 2.5 Traverse data for the unblown turbulent boundary layer with a nominal free-stream acceleration of $K=2.5 \times 10^{-6}$. Traverse symbols correspond to Fig. 2.2.

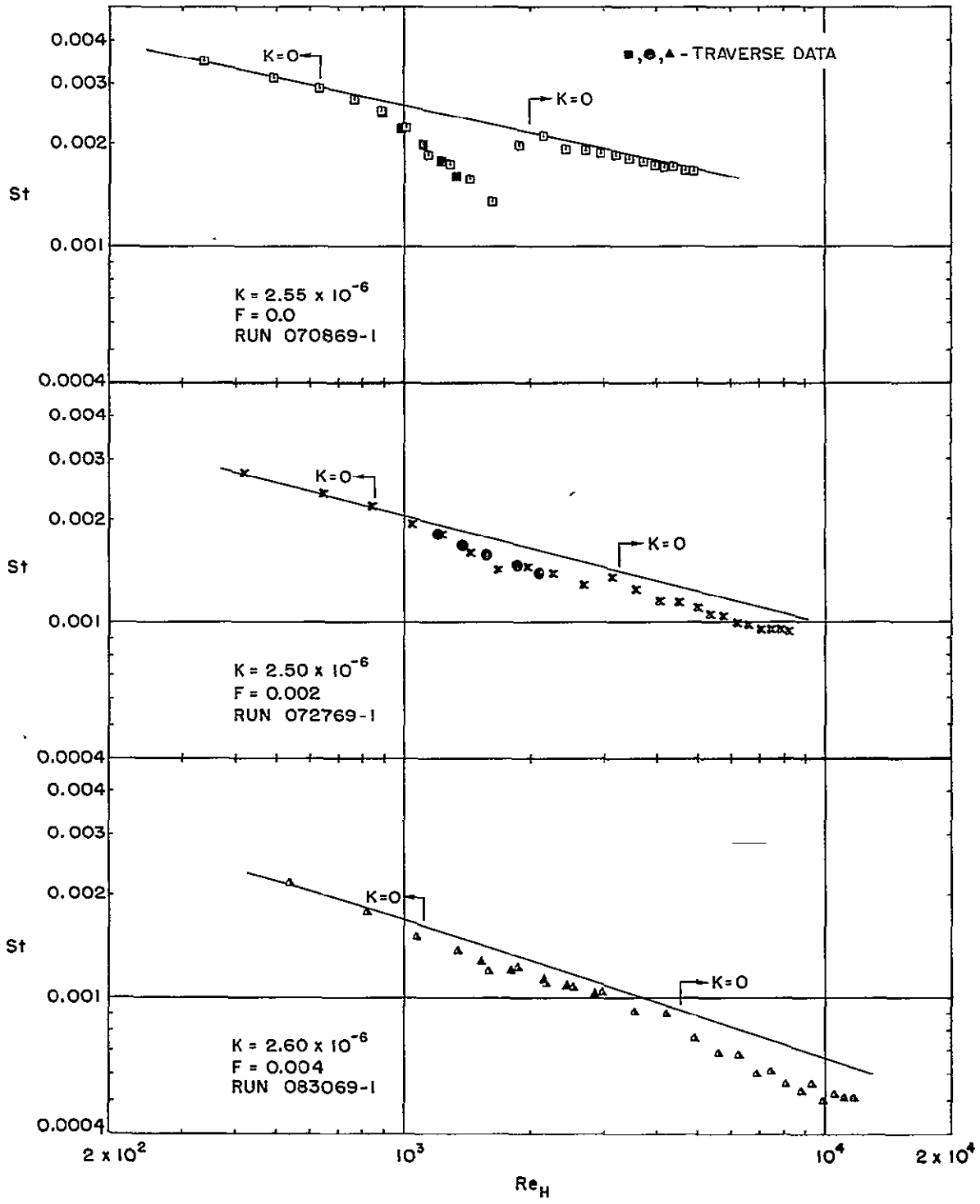

Fig. 2.6 Experimental results of surface heat transfer in a turbulent boundary layer, with and without blowing, at K≈2.55 x 10-6. ——— , Moffat and Kays [22].

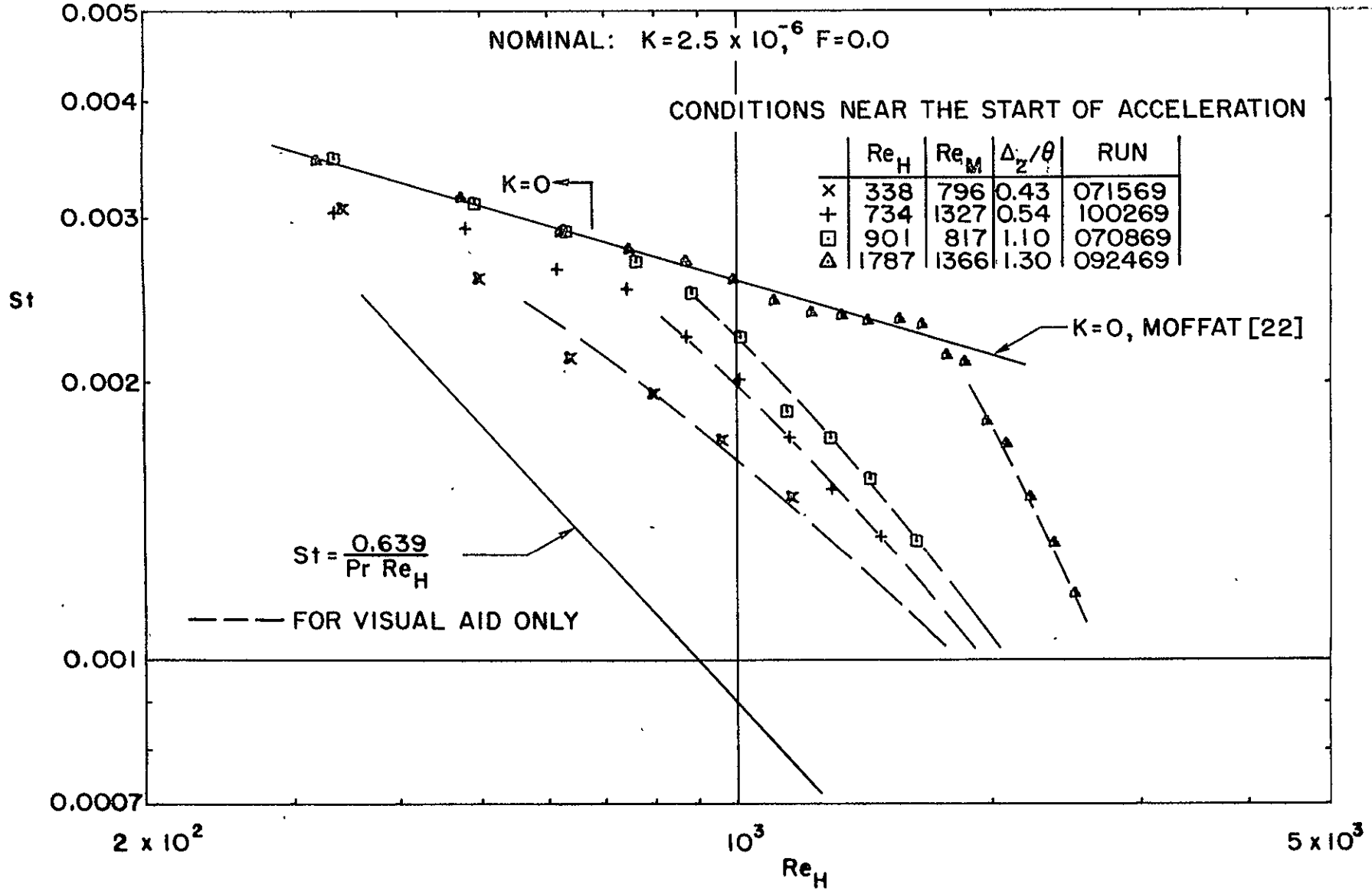

Fig. 2.7 Experimental results of surface heat transfer at $K \approx 2.55 \times 10^{-6}$ with various initial conditions at the start of acceleration. $St = 0.639/(PrRe_H)$ is the similarity solution for laminar wedge flows with a very thick thermal boundary layer

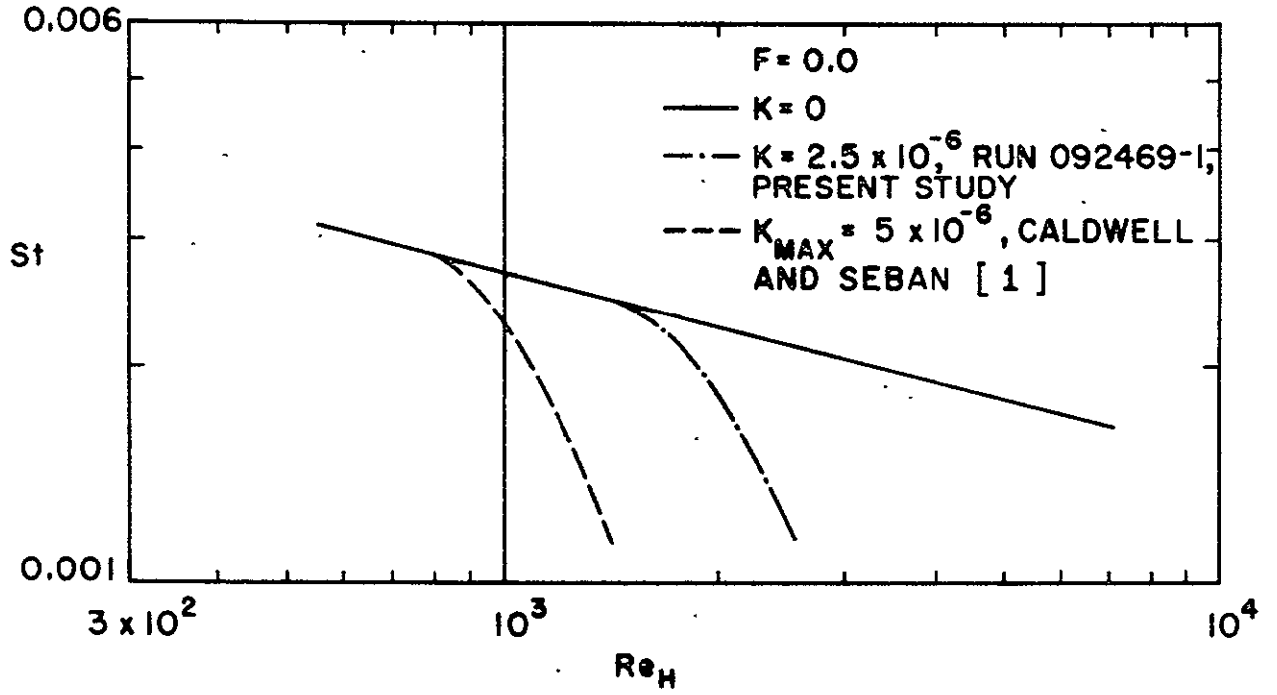

Fig. 2.8 Comparison of two runs of experimental heat transfer in a strong acceleration

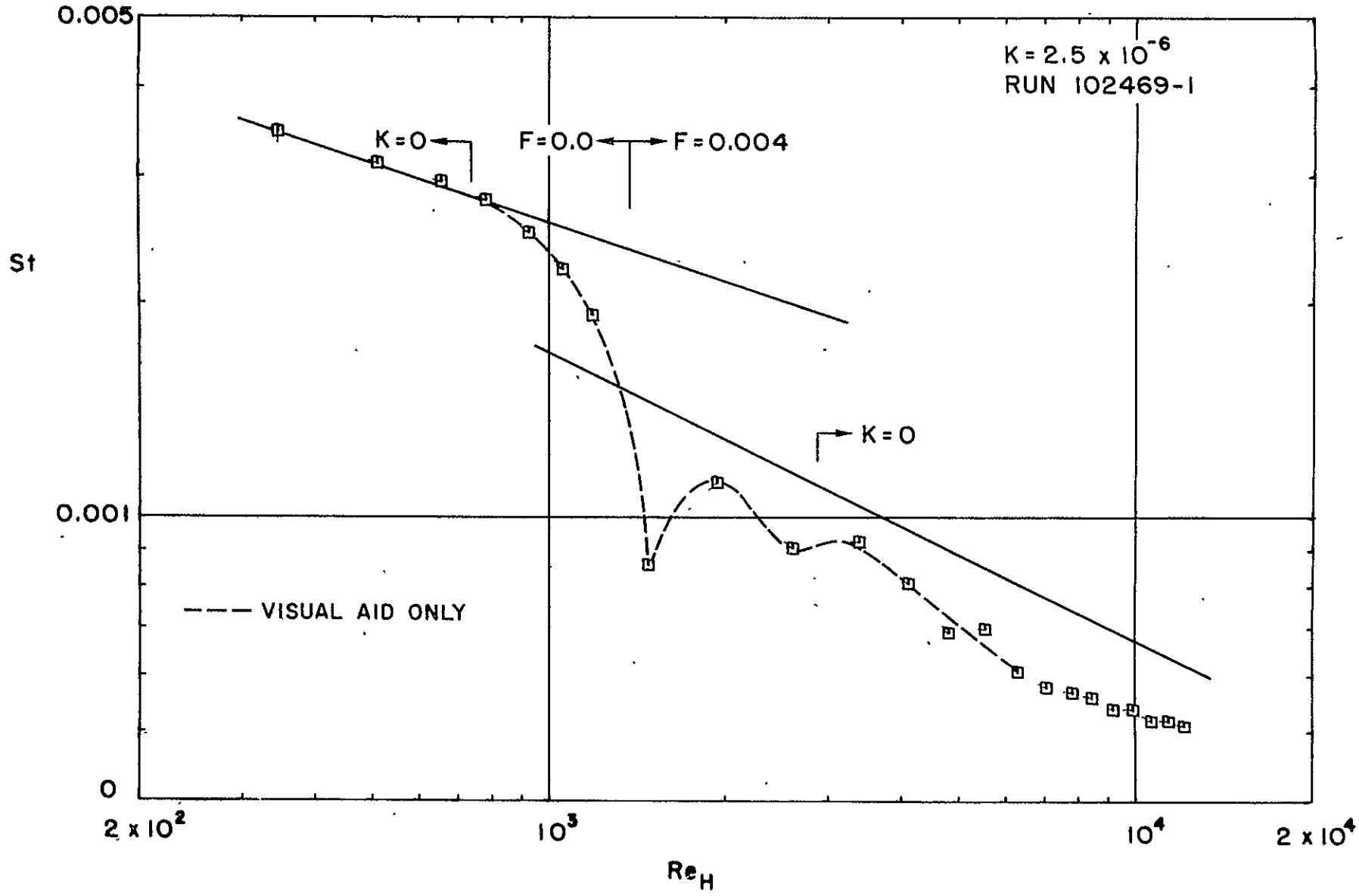

Fig. 2.9 Experimental heat transfer results in a strongly accelerated turbulent boundary layer with a step-increase in blowing

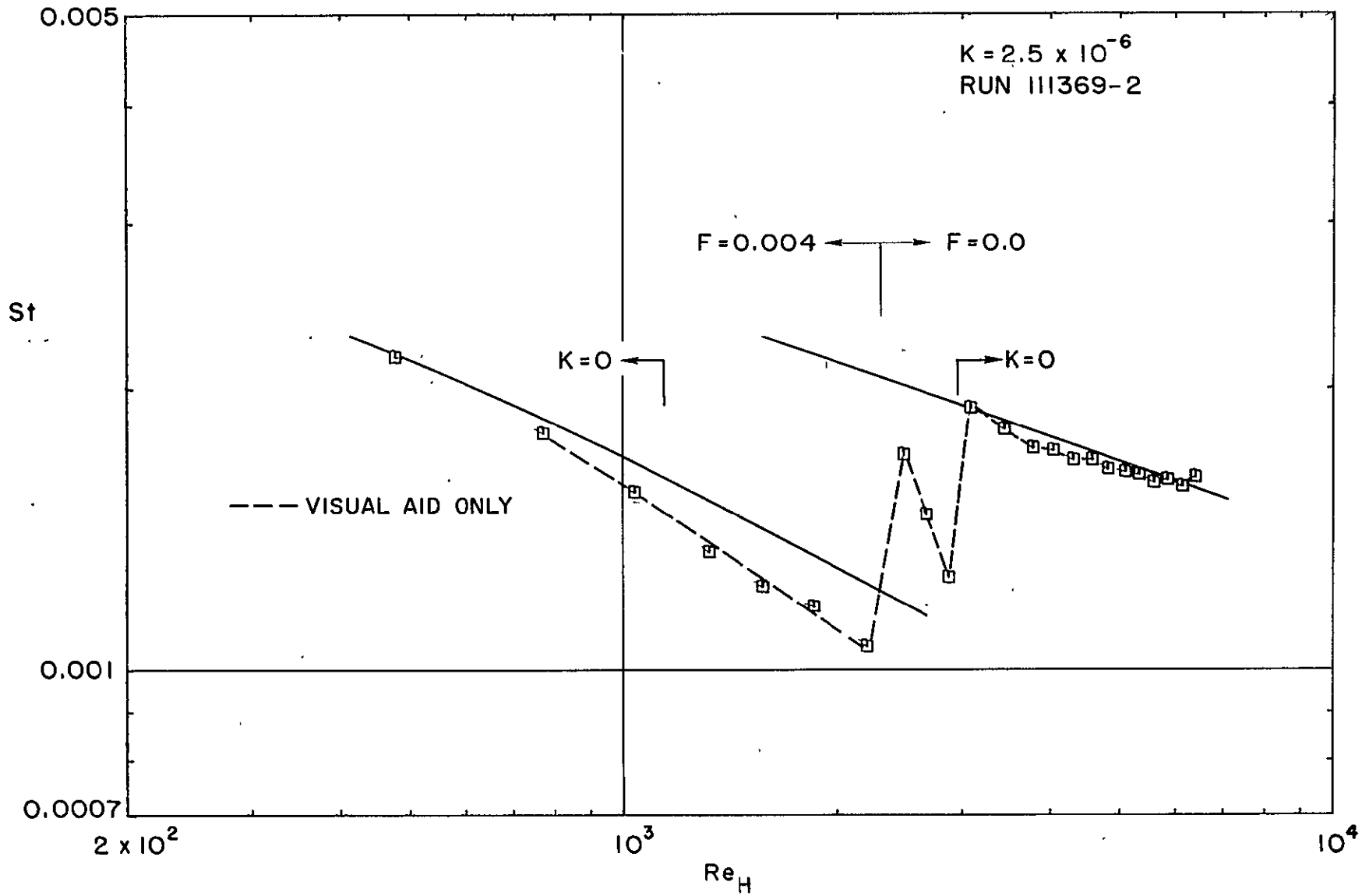

Fig. 2.10 Experimental heat transfer results in a strongly accelerated turbulent boundary layer with a step-decrease in blowing

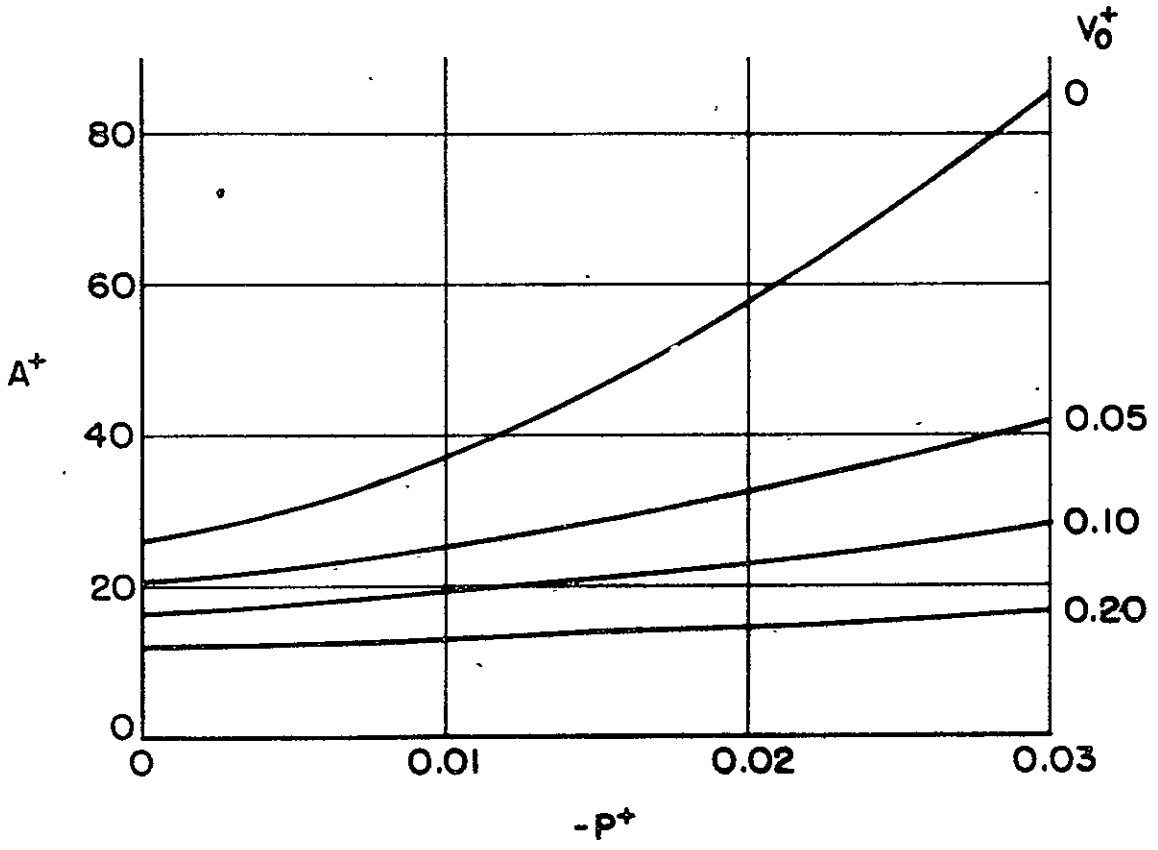

Fig. 2.11 Correlation for the Van Driest parameter in accelerating flows with blowing

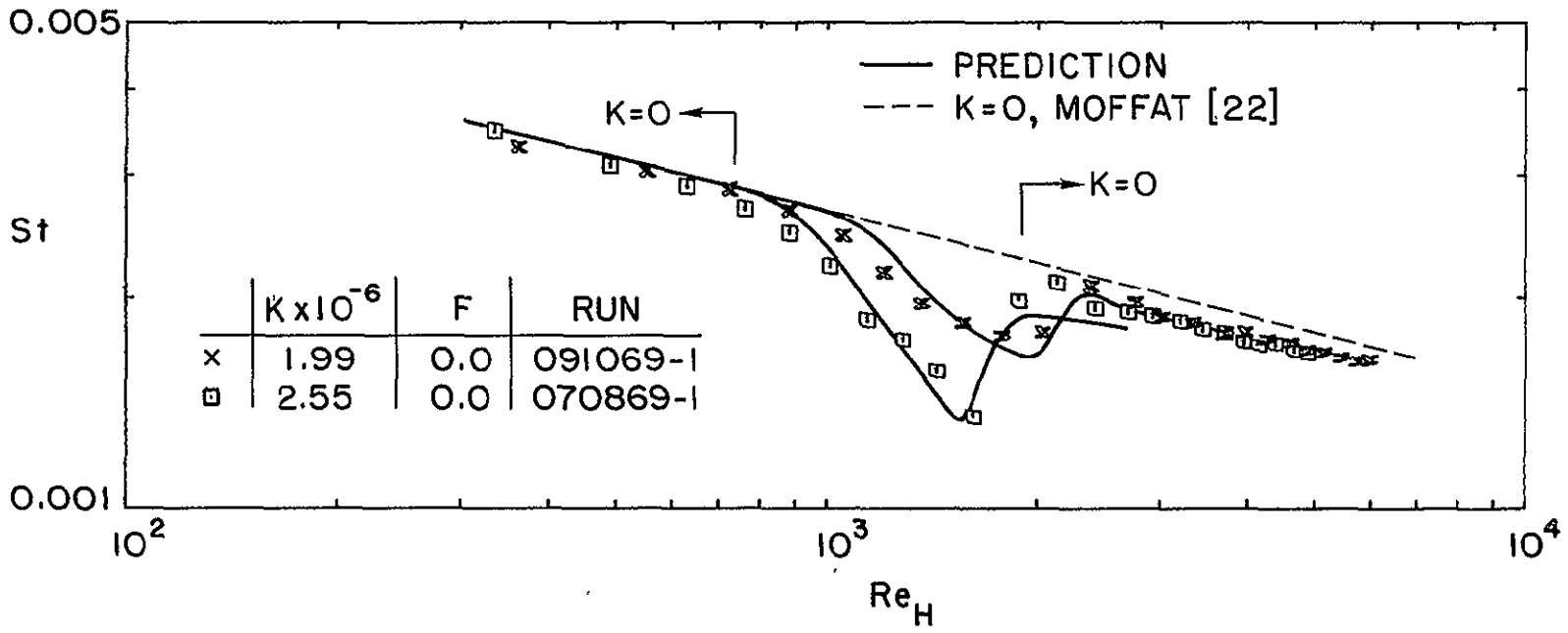

Fig. 2.12 Predictions of surface heat transfer in a turbulent boundary layer with a strongly accelerated free-stream flow.

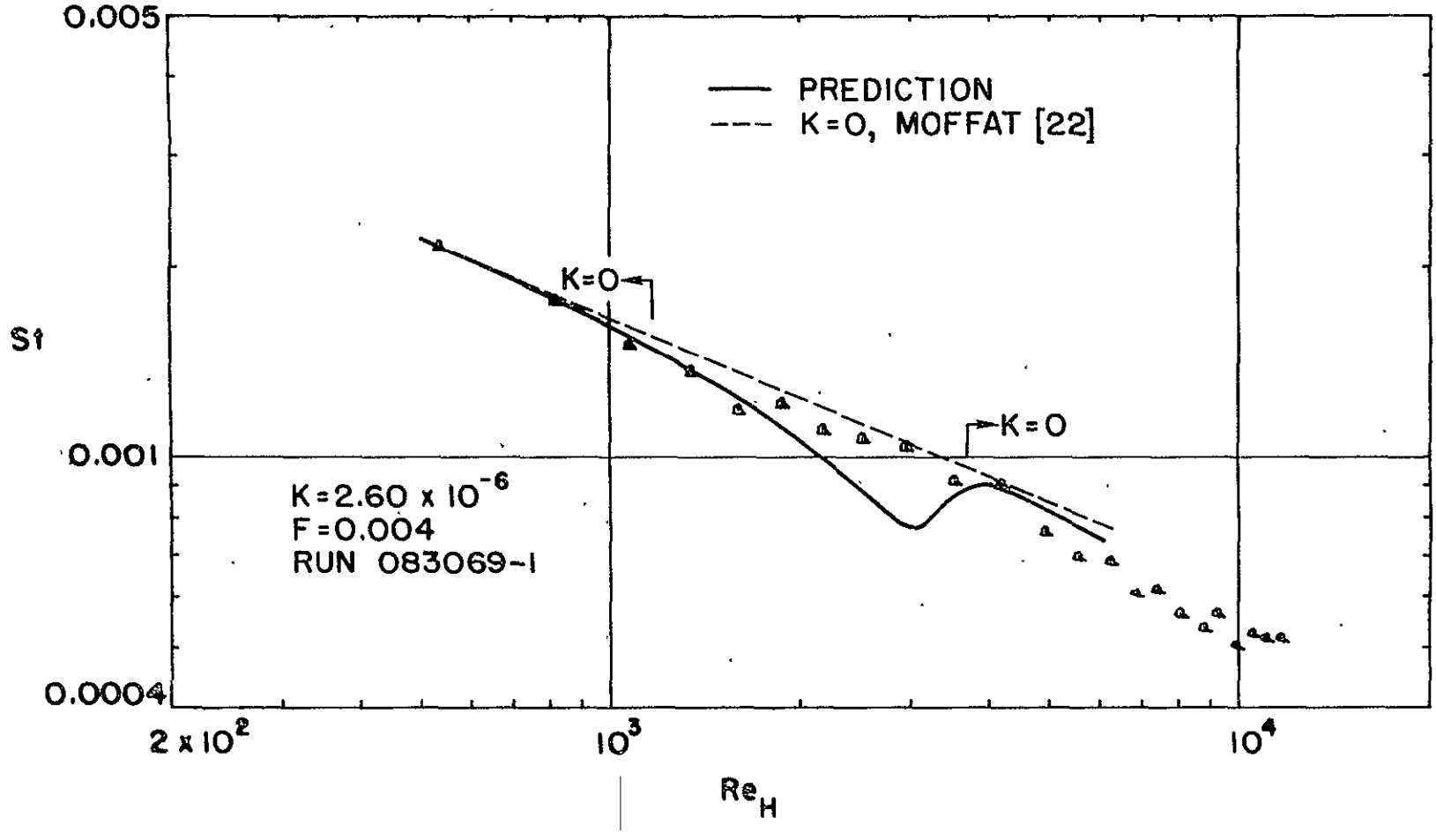

Fig. 2.13 Prediction of surface heat transfer in a turbulent boundary layer with blowing and strong acceleration

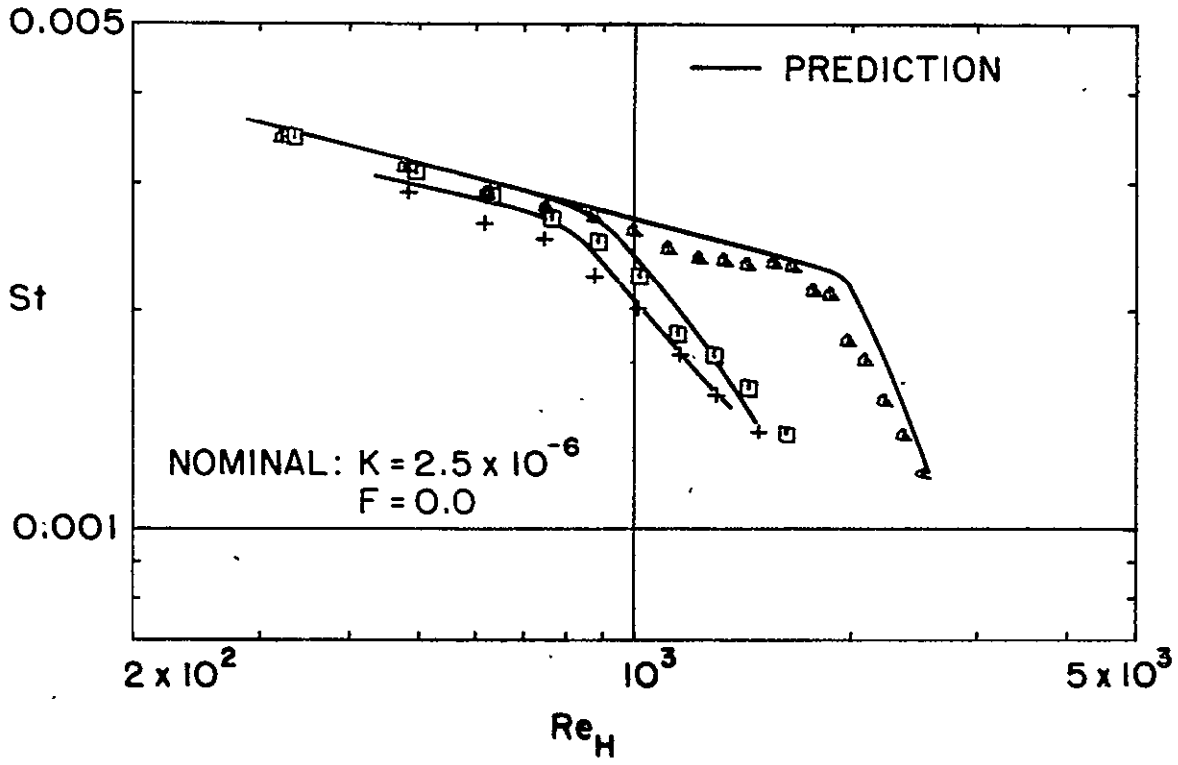

Fig. 2.14 Predictions of the effect of various initial conditions at the start of acceleration on heat transfer behavior in the turbulent boundary layer

CHAPTER THREE

THE EFFECT OF FREE-STREAM TURBULENCE ON HEAT TRANSFER TO A STRONGLY ACCELERATED TURBULENT BOUNDARY LAYER

A. Introduction

One premise put forth to explain the reduction in Stanton number in accelerated flows is that the portion of the thermal boundary layer which exists outside the hydrodynamic boundary layer, the thermal superlayer, substantially contributes to the resistance to heat transfer. An interesting question raised by this explanation is whether or not high free-stream turbulence has any substantial effect on the heat transfer performance of a strongly accelerated turbulent boundary layer. Most of the experiments have taken place in wind tunnels where turbulence level is very small, but many of the interesting technical applications (turbine blades, rocket nozzles, for example) involve highly turbulent free-stream environments. For non-accelerated boundary layers it seems that free-stream turbulence is not particularly significant [5], but this may not be the case when the outer part of the boundary layer is providing any substantial part of the overall heat transfer resistance, as it apparently does for prolonged highly accelerated flows. The answer to this question is important to the designer. For example, a rocket nozzle design, with wall cooling requirements based on the experimental data at low turbulence levels, would be inadequate if the presence of high free-stream turbulence significantly raised the heat transfer to the wall.

The experimental results in Chapter Two suggest, indirectly, that the thermal superlayer is less important than the sublayer as a cause of the reduction in Stanton number. More insight into this question can be achieved by increasing the free-stream turbulence level in the experimental apparatus. Another justification of this program derives from considering

the free-stream turbulence problem in its parametric sense: given a turbulent boundary layer in an accelerated flow field, what is the effect of free-stream turbulence on the Stanton number?

B. Previous Experimental Work

In 1966, Kestin [5] discussed in considerable detail the effect of free-stream turbulence on heat transfer in both laminar and turbulent boundary layers. He found that free-stream turbulence intensities up to 3.82 percent had no effect on local heat transfer rates in the flat plate laminar boundary layer, but intensities from 0 to 6.2 percent had increasingly noticeable effects, though modest, on the laminar boundary layer in an accelerated free-stream flow. No effect of turbulence intensities up to 4.5 percent were noted in a turbulent boundary layer in a mild favorable pressure gradient.

Two experimental investigations conducted with relatively high free-stream turbulence intensities are also of interest. Kline, et.al. [29] carried out hydrodynamic tests on a boundary layer on a flat plate with the free-stream turbulence intensity ranging from 0.5 to 20 percent. For free-stream turbulence intensities above 5 to 10 percent, they found increased boundary layer thicknesses, fuller velocity profiles, and higher values of wall shear. Boldman, et al. [51] measured heat transfer in nozzle tests and observed no change in the heat transfer coefficient when the inlet turbulence intensity was raised from 2.8 percent to 10 percent. The level of K in the nozzle was low, generally less than 1×10^{-6}. Consequently, the thermal superlayer was probably thin, so that the effect of free-stream turbulence in that region would be minimized.

C. Experimental Program

The objective of this chapter is to describe the results of some experiments at relatively high acceleration

($K = 2.5 \times 10^{-6}$) taken first under low turbulence conditions, and then with considerably higher free-stream turbulence artificially induced by a crossed-rod grid. The surface heat transfer measurements were accompanied by mean velocity and temperature traverses, but more importantly by hot-wire traverses of $\sqrt{\overline{u'^2}}$. The experimental apparatus differs from the description in Chapter Two only in that, for the high free-stream turbulence runs, a crossed-rod grid was placed 13 inches upstream of the trip. The grid consisted of 1/4-inch round wooden dowels formed into a square, interlocked mesh (i.e., all of the dowels were in the same plane) on 1-inch centers.

Two experiments were conducted with free-stream turbulence intensities, $\sqrt{\overline{u'^2}}/U_\infty$, of 0.7 percent and 3.9 percent, respectively, at the start of acceleration. The free-stream turbulence intensity decayed to 0.4 percent and 0.9 percent, respectively, in the recovery region. The level of high free-stream turbulence employed is of the same order of magnitude as used by Kestin [5] in his investigation of the effects of free-stream turbulence on a boundary layer subjected to a moderate acceleration. The free-stream energy spectra exhibited in both runs was that of normal turbulence. The grid design was based in part on the work of Uberoi and Wallis [28], in which, 29 inches downstream of a similar grid, the turbulence was found to be homogeneous with $\overline{u'^2} \approx \overline{v'^2}$. Both tests reported here were conducted with a free-stream velocity of about 23 fps.

In Fig. 3.1 is shown a plot of Stanton number versus local enthalpy thickness Reynolds number for the two cases. The differences in the data sets on Fig. 3.1 are no greater than the estimated experimental uncertainty. It appears that in the accelerated region, where the abrupt decrease in Stanton number is taking place, there is negligible difference in performance. If anything the high turbulence case yields lower St, which does not seem physically plausible. In

the recovery region, where free-stream velocity is again constant, it appears that recovery is slightly more abrupt with high free-stream turbulence, and this would be consistent with the proposed model. Thus the conclusions that one can draw are that initial free-stream turbulence levels as high as 3.9 percent have very little effect on Stanton number for strongly accelerated flows, but this fact in itself is of significance.

Figs. 3.2 and 3.3 are plots of traverses of $\sqrt{\overline{u'^2}}/U_\infty$ taken just before acceleration, and near the end of acceleration, for both the low free-stream turbulence case and the high free-stream turbulence case. Essentially they demonstrate that at this relatively high rate of acceleration the boundary layer is in fact still a turbulent one, but with a lowered turbulence intensity, especially in the wake. The results for the higher free-stream turbulence case are similar to those for low free-stream turbulence, with the differences confined primarily to the wake.

The global characteristics of the boundary layers entering the accelerated region for the two cases are quite different in nature; the test with high free-stream turbulence exhibits a very thick boundary layer with a 52 percent larger momentum thickness. It is not certain whether this effect is a direct result of the high turbulence on the growth of the layer, or whether the grid rod nearest the wall simply introduces a momentum decrement into the developing boundary layer. Nevertheless, the important point is that, in the accelerated regions, the outer layers are affected whereas the inner layers appear to display little, if any, effect of the free-stream turbulence level. In Fig. 3.4, for example, are shown the velocity profiles, in inner coordinates, at the end of the accelerated region for both cases. The profiles deviate from the accepted law of the wall for a flat plate boundary layer, as is typical of highly accelerated boundary layers, but are quite similar to each other. The temperature

profiles, also in inner coordinates, are presented in Fig. 3.5. This figure illustrates the development throughout the entire region of acceleration, for both high and low turbulence. In general, the two layers display similar thermal behavior.

D. Prediction of Experimental Results

Figure 3.6 shows the results of theoretical calculations made under the conditions of the experiments, using the prediction method described in Chapter Two. Prior to the inclusion of the turbulent kinetic energy equation, a mixing-length model of the turbulent boundary layer, with a modification in the outer region, had been successfully used to predict experimental results over a wide range of conditions including transpiration and favorable pressure gradients [4]. It was hoped that the addition of the turbulent kinetic energy model, besides providing a potential improvement in the prediction method in general, would in particular permit a prediction of the influence of free-stream turbulence.

The theoretical calculations presented in Fig. 3.6 are in reasonable agreement with the experimental findings. The deviation between the two theoretical curves is due to the fact that the boundary conditions for the variation of the free-stream velocity, i.e., the precise level and physical location of the imposed acceleration, are slightly different in the two cases. It will be shown next that, were the imposed experimental conditions identical, the theoretical model would predict nearly identical curves for the two cases.

A question naturally arises concerning the effect of still higher initial levels of free-stream turbulence under these same conditions of acceleration. To investigate the theoretical aspects of this point, three predictions were made utilizing the experimental boundary conditions and mean-flow starting profiles of the 3.9 percent case.

The results are shown in Fig. 3.7 for initial free-stream turbulence levels of 0.7 percent, 3.9 percent, and 10 percent. The curves for the lower two intensities are indistinguishable on the plot, whereas the higher turbulence level clearly decreases the effect of acceleration on Stanton number, and significantly increases Stanton number in the recovery region. Eventually, all three predictions converge on the accepted correlation for the flat-plate turbulent boundary layer.

Prior to acceleration, the free-stream turbulence for the 10 percent case is on the order of the self-generated turbulence within the boundary layer. It is not unreasonable that the heat transfer should be affected under these conditions. The study by Kline, et al. [29] substantiates the notion that a free-stream turbulence level of this magnitude has significant effects on the characteristics of the boundary layer. In the accelerated zone and thereafter, however, it is believed that the influence of the high turbulence would be manifested through a different mechanism. As the thermal layer grows outside of the momentum layer, the higher free-stream turbulence acts to increase the apparent conductivity in this laminar-like outer region, resulting in higher Stanton numbers. The modest increase in Stanton number, if it is in fact due to the effect of free-stream turbulence on the thermal superlayer, is consistent with the findings of Kestin on accelerated laminar boundary layers [5].

E. Conclusions

The following are the conclusions that may be drawn from this work:

(a) The decrease in Stanton number observed during strong acceleration is independent of initial free-stream turbulence levels up to at least 4 percent.

(b) Theoretical calculations for an initial free-stream turbulence level of 10 percent suggest that if initial free-stream turbulence is of the same order of magnitude as the self-generated turbulence within the boundary layer, an increase in Stanton number will be obtained throughout the accelerated region. In view of the experimental results of Boldman, et al. [51], however, the validity of this prediction must be viewed with caution.

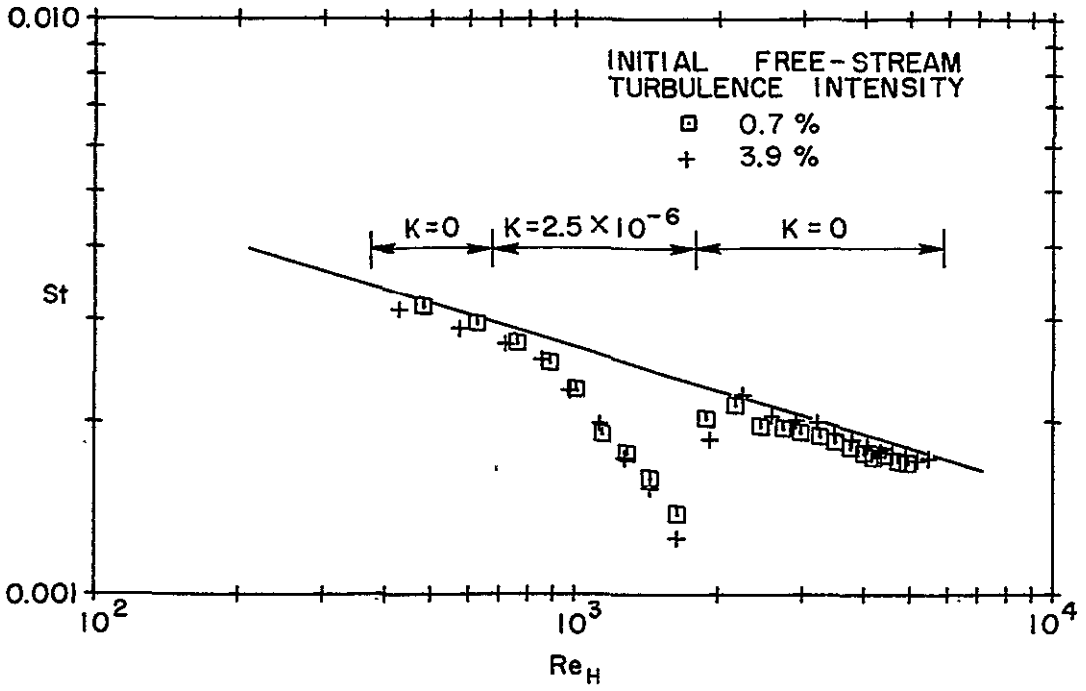

Fig. 3.1 Experimental heat transfer for low and high initial free-stream turbulence intensities in a strongly accelerated flow. ———, Moffat and Kays [22].

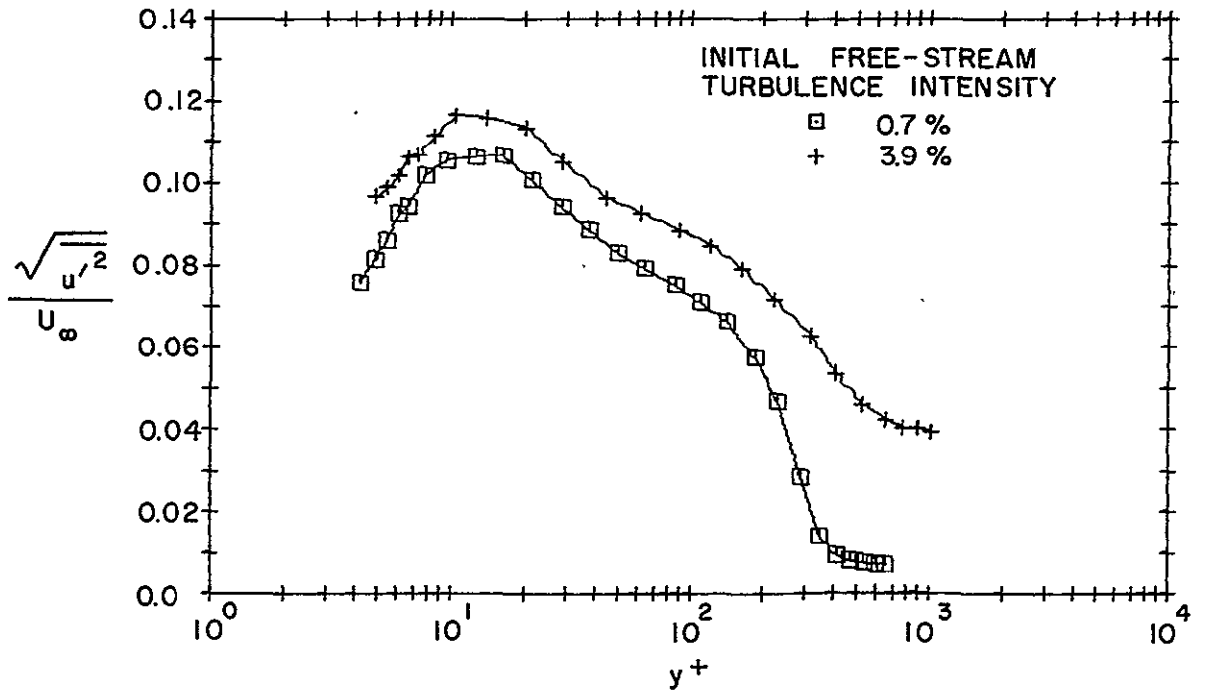

Fig. 3.2 Experimental turbulence intensity profiles in the constant U_∞ region prior to acceleration. $Re_H \approx 600$.

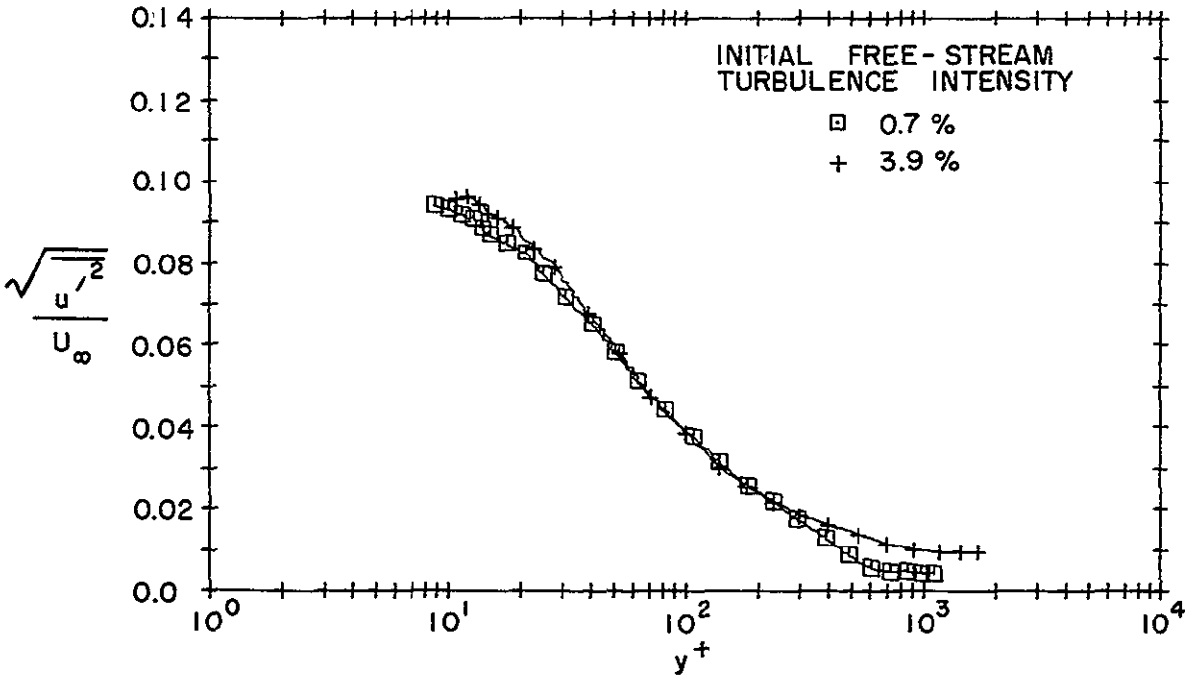

Fig. 3.3 Experimental turbulence intensity profiles near the end of the accelerated region. $Re_H \approx 1430$.

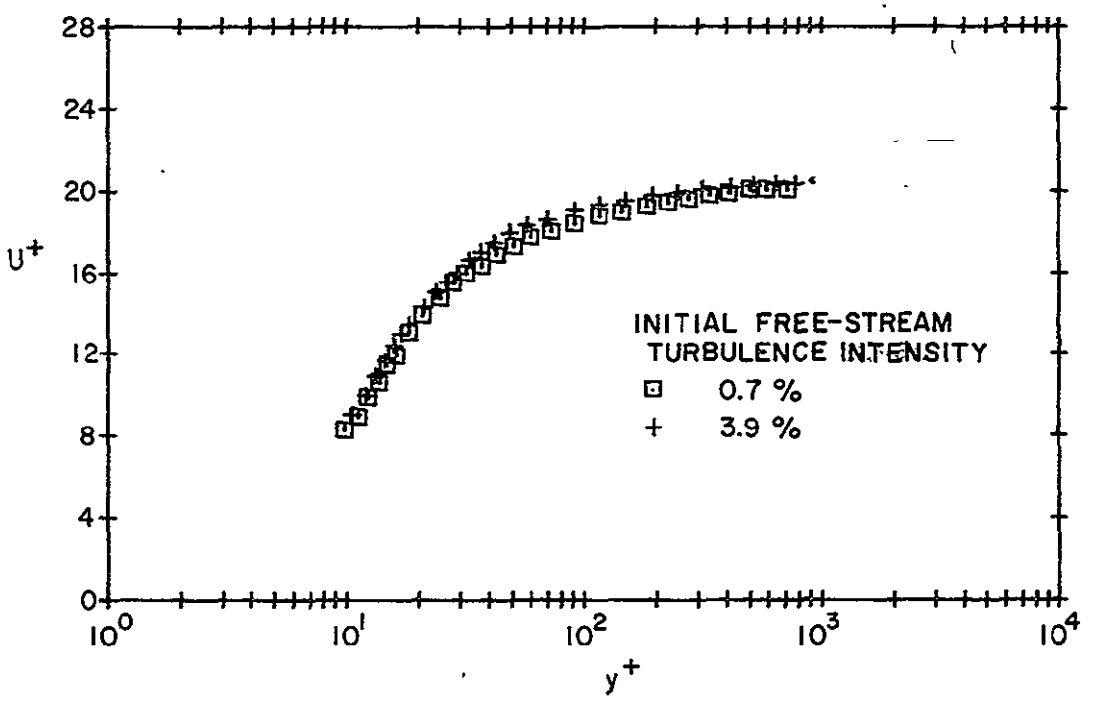

Fig. 3.4 Experimental velocity profiles near the end of the accelerated region. $Re_H \approx 1430$.

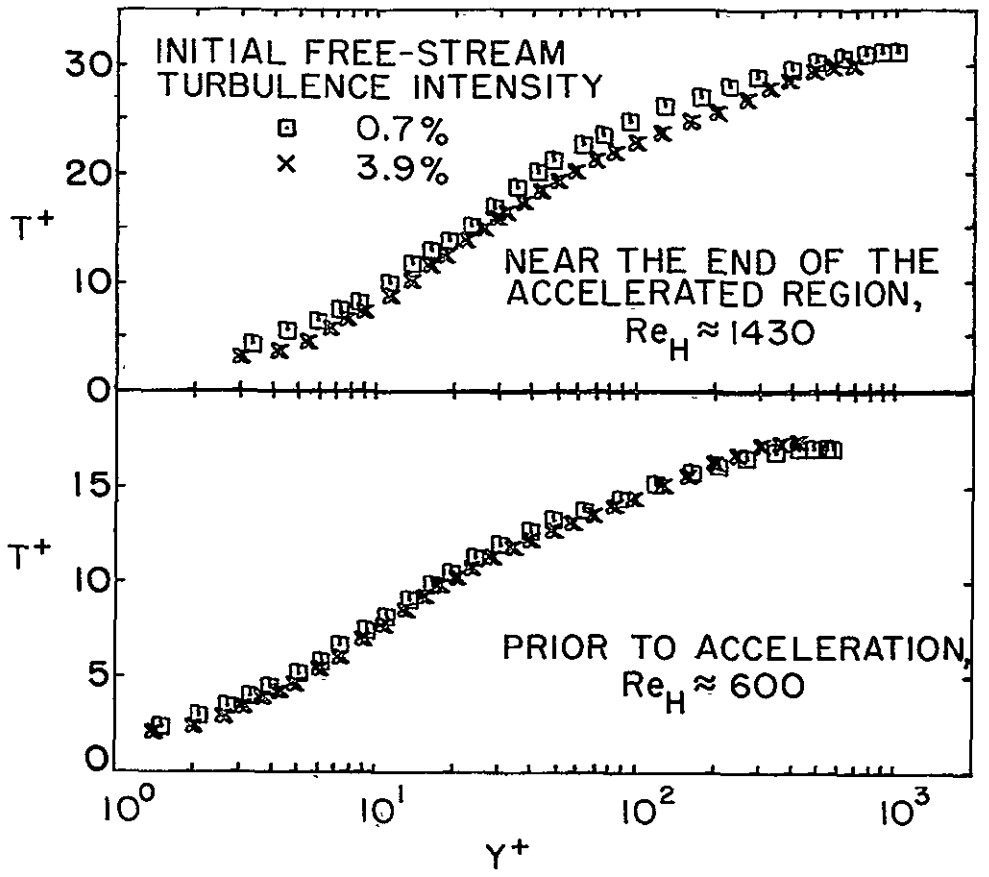

Fig. 3.5 Experimental temperature profiles for low and high initial free-stream turbulence.

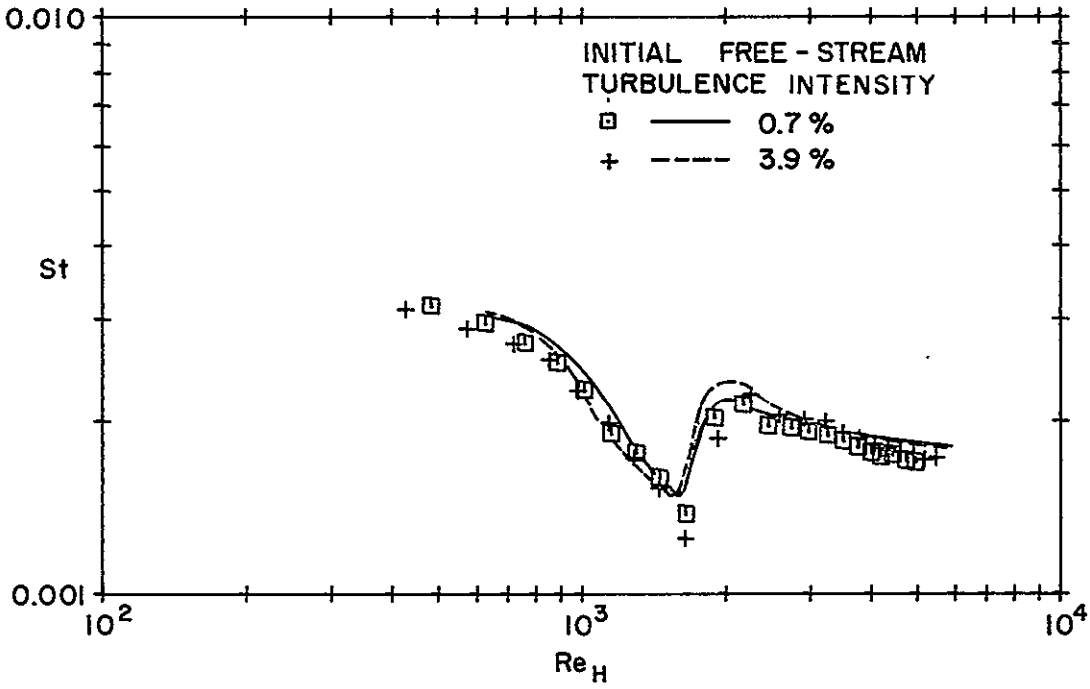

Fig. 3.6 Comparison of predicted and experimental heat transfer results.

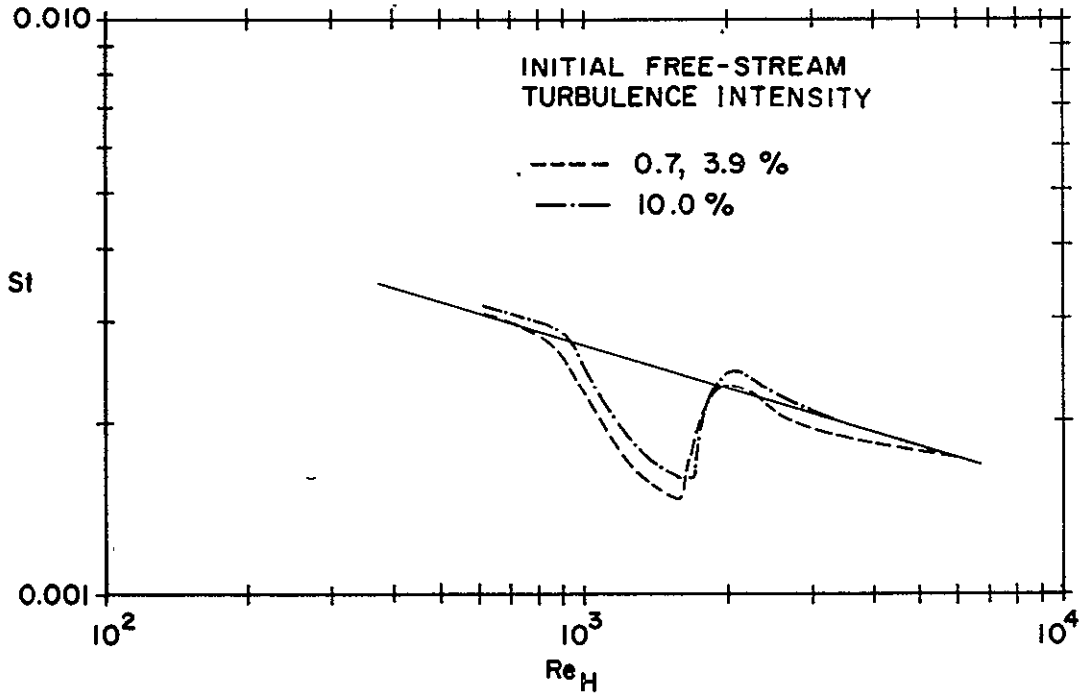

Fig. 3.7 Effect of initial free-stream turbulence level on the predicted heat transfer performance. ———, Moffat and Kays [22].

CHAPTER FOUR

AN EXPERIMENTAL STUDY OF TURBULENT PRANDTL NUMBER FOR AIR IN ACCELERATED TURBULENT BOUNDARY LAYERS

A. Introduction

Many current prediction methods for heat transfer in the turbulent boundary layer utilize the turbulent Prandtl number to relate the eddy diffusivity for heat to that for momentum. While it is generally acknowledged that the eddy diffusivity concept is not an adequate model of the physical processes occurring in the boundary layer, it is also recognized that this method, having been proven in practice, will continue to be important until significant advances in turbulent boundary layer theory are made. If the turbulent transport terms in the boundary layer equations for momentum and energy are expressed in the forms,

$$\frac{\tau_t}{\rho} = \epsilon_M \frac{\partial U}{\partial y} \tag{4.1}$$

and

$$\frac{\dot{q}''_t}{\rho c_p} = \epsilon_H \frac{\partial T}{\partial y} , \tag{4.2}$$

the eddy diffusivity for heat can be expressed as

$$\epsilon_H = \epsilon_M / Pr_t ,$$

thus defining the turbulent Prandtl number. There is no physical reason to believe, a priori, that Pr_t is not a function of the molecular Prandtl number, the position in the flow field, and hydrodynamic parameters such as the Reynolds number. Nevertheless, it has proven adequate in many calculation procedures to assume a constant value for

turbulent Prandtl number across the boundary layer, often between 0.85 and 1 [26, 30, 31]. In other cases, however, it has been necessary, in order to achieve reasonable predictions in boundary layers, to assume a variation in the turbulent Prandtl number such that it is high near the wall (on the order of 1.5 in air) and less than unity in the outer region [4,32]. Even though the solution of the heat transfer problem requires knowledge of both the eddy diffusivity for momentum and the turbulent Prandtl number, relatively few experimental studies have been directed towards the latter. Simpson, Whitten, and Moffat [27] recently reported the variations of turbulent Prandtl number in the boundary layer on a flat plate, with and without transpiration. It is the purpose of this study to extend the experimental knowledge of the turbulent Prandtl number to the case of the accelerated boundary layer, with and without blowing. The range of acceleration in this study varies from mild ($K = 0.55 \times 10^{-6}$) to that approaching relaminarization of the boundary layer ($K = 2.55 \times 10^{-6}$).

B. Theoretical Models and Previous Experimental Results

In this aspect of turbulent transport theory, it is difficult to substantiate proposed theoretical models because of the scarcity of reliable experimental results. In external boundary layers, as an example, the experimental data required to determine the local values of shear stress and heat flux are often not available. Since these quantities are more easily calculated in channel flow, most of the experimentation has been carried out in circular tubes, at both low and high molecular Prandtl numbers. In air, however, there is conflicting evidence in pipe flow on the variation of turbulent Prandtl number with distance from the wall. Kestin and Richardson [33] show the findings of several investigators in which the turbulent Prandtl number is always below unity in pipe flow, but does not consistently rise or fall

with distance from the wall. They conclude that results of Ludwieg [34] are most reliable, in which Pr_t decreases towards the center of a pipe. Azer [35], on the other hand, notes that Ludwieg's data was taken at high subsonic Mach numbers, and that the preponderance of evidence suggests that, in a pipe, Pr_t increases towards the center. There is general agreement, at least, that the turbulent Prandtl number is not constant across a tube. In the external boundary layer, Johnson [36] determined the turbulent Prandtl number from fluctuation measurements of both velocity and temperature on a flat plate downstream of a stepwise discontinuity in wall temperature, while Simpson, et al. [27] calculated Pr_t from mean profile data on a flat plate with and without transpiration. Both results are summarized in Fig. 4.1. Simpson found that the turbulent Prandtl number was greater than unity in the region close to the wall, and decreased to a value of approximately 0.7 in the outer edge of the boundary layer. No effect of transpiration, either sucking or blowing, could be detected within the uncertainty of the results.

Theoretical models for the turbulent Prandtl number have, on the whole, relied on mixing length arguments. By taking into account the molecular diffusion from or to an eddy in motion, the effect of the molecular Prandtl number on Pr_t can be modeled. Depending on the model, turbulent Prandtl number is also found to be a function of the eddy diffusivity for momentum or a hydrodynamic Reynolds number. The model of Azer and Chao [35] predicts Pr_t increasing with distance from the wall. Jenkins [37], on the other hand, predicts turbulent Prandtl numbers close to the wall greater than unity, and decreasing with distance away from the wall. A new theory has been proposed by Tyldesley and Silver [38] which considers entities of fluid in motion in a turbulent field in pipe flow. In its present state, this promising approach does not provide for the variation of the turbulent Prandtl number across the boundary layer, but it does give results

as a function of molecular Prandtl number which agree with experiment. For $Pr = 0.7$, their theory predicts $Pr_t = 1.0$. Tyldesley [39] has extended the theory to the case of free turbulent flows, not unlike the outer region of the turbulent boundary layer. In this case, a value of about 0.74 is predicted for $Pr = 0.7$, generally agreeing with earlier theories and experimental results.

C. Sources of Experimental Data

The magnitude of the accelerations utilized in this study varied from moderate to that approaching relaminarization of the turbulent boundary layer. The range of variables in the tests were,

K : 0.57×10^{-6} to 2.55×10^{-6}

U_∞ : 23.5 to 123 fps

T_∞ : 60 to 95 F

$T_o - T_\infty$: -20 to 43 F

F : 0, 0.004

The present data were obtained on the same apparatus used by Simpson, et al. [27]. The experimental data in the range, $K = 0.57 \times 10^{-6}$ to 1.45×10^{-6}, were reported by Thielbahr [6] and Julien [14]. For $K \geq 1.99 \times 10^{-6}$, the data is that of this report and the work of Loyd [23]. The performance of the test apparatus has been consistent throughout the entire series of tests. Accepted flat plate correlations for heat transfer and hydrodynamic performance are reproduced within a few percent, including skin friction, surface heat transfer, and non-dimensional mean profiles. With acceleration or transpiration, agreement with other experimenters has been adequate where comparisons are possible. The tests were all conducted at constant values of

the parameters K and F , resulting in near-equilibrium boundary layers at moderate accelerations, or with transpiration. In the accelerated flows, the velocity profile data were taken isothermally, while the temperature profiles were generally obtained at the same free-stream conditions and with a heated wall. Exploratory tests and numerical analyses established that the ratio U/U_∞ , measured in the isothermal layer, is approximately preserved in the heated layer.

Loyd [23] presents arguments to show that, in the hydrodynamic studies, the Young and Maas [40] shear correction is appropriate not only to his experimental data, but also to the data of Julien, et al. [14] and Simpson, et al. [27], which were obtained with similar total pressure probes. While some question exists concerning the justification for this correction, it has been uniformly applied to all the velocity profile data utilized in the present study of the turbulent Prandtl number. No probe corrections have been applied to the temperature data, though arguments could also be made for a displacement effect in a severe temperature gradient. In general, application of the probe correction to the velocity profile data lowers the calculated turbulent Prandtl numbers near the wall, compared to use of the uncorrected velocity data.

In the flat plate calculations of Simpson et al. [27], the experimental observation of similarity in the inner and outer regions was incorporated into the analysis of the turbulent Prandtl number. In moderate accelerations at constant K , the velocity and temperature profiles were also shown to be similar, as should be the case when the acceleration is well established. In general, similar conditions could not be achieved in accelerations above $K = 1.45 \times 10^{-6}$. For this reason, the local shear and heat flux profiles were computed by a method which makes no assumptions about the similarity of the flow or temperature fields. For comparative

purposes, the data of Simpson, et al. for K = 0, and F = 0 and 0.004, were also recalculated with the present computational method.

C.1 Local Shear Stress and Heat Flux Profiles

In the course of this study, 40 pairs of velocity and temperature profiles in the accelerated turbulent boundary layer were considered. The cases of no transpiration and moderate blowing, F = 0.004, were selected to investigate both the effect of acceleration alone, and the combined effect of blowing and acceleration, on the turbulent Prandtl number. Noting Eqns. (4.1) through (4.3), the local velocity and temperature gradients, and the local shear stress and heat flux, must be calculated from the mean profile data. The appropriate boundary layer equations

$$\frac{\partial(\rho U)}{\partial x} + \frac{\partial(\rho V)}{\partial y} = 0 \tag{4.4}$$

$$\rho U\frac{\partial U}{\partial x} + \rho V\frac{\partial U}{\partial y} + \frac{dP}{dx} - \frac{\partial \tau}{\partial y} = 0 \tag{4.5}$$

$$\rho U\frac{\partial}{\partial x}(i + \frac{U^2}{2}) + \rho V\frac{\partial}{\partial y}(i + \frac{U^2}{2}) + \frac{\partial \dot{q}''}{\partial y} - \frac{\partial}{\partial y}(\tau U) = 0 \tag{4.6}$$

are integrated with respect to y , rearranged, and non-dimensionalized, resulting in the computing forms,

$$\tau^+ = 1 + U^+V_o^+ + P^+y^+\left[1 - \frac{1}{y}\int_o^y \left(\frac{\rho U}{\rho_\infty U_\infty}\right)^2 dy\right] +$$

$$\frac{1}{U_\infty C_f/2}\frac{dU_\infty}{dx}\left[\frac{\rho U}{\rho_\infty U_\infty}\int_o^y \frac{\rho U}{\rho_\infty U_\infty}\,dy - \int_o^y \left(\frac{\rho U}{\rho_\infty U_\infty}\right)^2 dy\right] + \quad (4.7)$$

$$\frac{1}{C_f/2}\left[\frac{d}{dx}\int_o^y \left(\frac{\rho U}{\rho_\infty U_\infty}\right)^2 dy - \frac{\rho U}{\rho_\infty U_\infty}\frac{d}{dx}\int_o^y \frac{\rho U}{\rho_\infty U_\infty}\,dy\right]$$

and

$$Q^+ = 1 + \frac{1}{St}\left[F - \frac{d}{dx}\int_o^y \frac{\rho U}{\rho_\infty U_\infty}\,\frac{i_s}{i_{s,o}}\,dy -\right.$$

$$\frac{1}{\rho_\infty U_\infty i_{s,o}} \cdot \int_o^y \frac{\rho U}{\rho_\infty U_\infty}\,\frac{i_s}{i_{s,o}}\,dy \cdot \frac{d}{dx}(\rho_\infty U_\infty i_{s,o}) \quad (4.8)$$

$$\left. - \frac{i_s}{i_{s,o}}\left(F - \frac{d}{dx}\int_o^y \frac{\rho U}{\rho_\infty U_\infty}\,dy - \frac{U_\infty K}{\nu}\int_o^y \frac{\rho U}{\rho_\infty U_\infty}\,dy\right) + \frac{\tau U}{\rho_\infty U_\infty i_{s,o}}\right]$$

As $y \to \infty$, these equations assume the usual forms of the integral equations with transpiration and a pressure gradient,

$$\frac{C_f}{2} + F = \frac{d\theta}{dx} + \frac{\theta}{U_\infty}(2 + H)\frac{dU_\infty}{dx} \qquad (4.9)$$

and

$$St + F = \frac{1}{\rho_\infty U_\infty i_{s,o}} \frac{d}{dx}(\rho_\infty U_\infty i_{s,o}) \quad . \qquad (4.10)$$

The differentiations with respect to x were carried out at each data point in a given profile, using a central difference formulation and interpolated values in the adjoining profiles. As pointed out by Julien [14], in the ideal equilibrium boundary layer in a constant-K acceleration, there is no dependence on x, so that any terms containing x-derivatives were quite small in the moderate accelerations where equilibrium conditions were approached. The x-dependence was always evident in the flat plate boundary layers, and in strong accelerations where equilibrium was not attained.

Typical temperature and velocity profiles are presented in Figs. 4.2-4.5. In strong accelerations, above $K = 1.45 \times 10^{-6}$, five profiles were obtained in the accelerated region, spaced every four inches. In the moderate accelerations, three profiles were taken, spaced either 8 or 12 inches apart. At $K = 0$, three profile locations were spaced at intervals of 24 inches, presenting a formidable test of the present computational procedure. It will be shown that the results for the flat plate turbulent boundary layer, calculated in this manner, agree well with the results of Simpson, et al. [27], which relied in the same data but used an independent method of computation which does not require an explicit calculation of x-derivatives.

C.2 Selection of Experimental Data

Since the temperature or velocity gradients are zero at the outer edge of the thermal and hydrodynamic boundary layers, respectively, Eqns. (4.7) and (4.8) should calculate zero heat flux and shear stress at those locations if the experimental data, and the computation techniques, are exact. Since neither of these conditions is satisfied, due to both uncertainty in the experimental data and to computation errors (particularly where the differentiated terms are important), limits of acceptability were set on the shear stress and heat flux profiles by stipulating a maximum value of $|0.3|$ at the outer edge of the boundary layer. Of the 40 profile pairs examined, 15 were rejected on this basis. Of the 25 remaining, 16 pairs consisted of heat flux and shear stress profiles which were individually below $|0.15|$ at the outer edge. In order to smooth the experimental results, and to establish a consistent calculation procedure, the selected pairs were recalculated in a manner which forced the local shear stress and heat flux to zero at the outer boundary. To accomplish this, the coefficients,

$$\frac{1}{U_\infty \frac{C_f}{2}} \frac{dU_\infty}{dx} \qquad \text{and} \qquad \frac{d}{dx}\left(\rho_\infty U_\infty i_{s,o}\right) \quad ,$$

in Eqns. (4.7) and (4.8) were evaluated at $y = \infty$ from the equations themselves. In this way, the local heat flux and shear stress equations, which exactly match the known boundary condition at wall, are forced to satisfy the known boundary conditions in the free stream. Selected shear stress and heat flux profiles are shown in Figs. 4.2-4.5, along with mean temperature and velocity profile data and the calculated turbulent Prandtl numbers. These examples are representative of blown and unblown results at both moderate and strong accelerations. Also shown are sample values of the turbulent

Prandtl number which would have been computed had the outer boundary condition not been forced to zero. The only significant changes occur beyond y^+ of 200, where the uncertainty in the results is also quite high due to normal experimental uncertainty.

D. Turbulent Prandtl Number Distribution in Accelerated Flows, With and Without Blowing

The mean gradients required by Eqns. (4.1) and (4.2) were obtained by evaluating $\frac{d\overline{T}}{dy}$ and $\frac{d(U/U_\infty)}{dy}$ analytically. The determination of the temperature and velocity gradients at each point was accomplished by applying a least-squares quadratic curve fit through five data points, fitting either the normalized temperature or velocity as a function of log y, and analytically taking the derivative at the center point. This technique is thoroughly discussed by Simpson, et al. [27], and compared to results using various analytical approaches, in addition to graphical methods. It is concluded by Simpson that, for the flat plate turbulent boundary layer, the Pr_t distributions for various polynominal fits vary by no more than 2 percent, and agree within 5 percent with the Pr_t distribution obtained from graphical fits of $\frac{d\overline{T}}{dy}$ and $\frac{d(U/U_\infty)}{dy}$.

The turbulent Prandtl numbers computed from the selected profiles in accelerated turbulent boundary layers are presented in Figs. 4.6-4.8 as functions of y^+, y/δ, and ϵ_M/ν. An approximate uncertainty band, based on the method of Kline and McClintock [41] is included on two of the figures, as well as a comparison to the data of Simpson, et al. for the flat plate. The scatter of the experimental results, as one would expect, is greater than for the flat plate case. In the thinner boundary layers encountered in acceleration,

the uncertainty in the temperature and velocity gradients is proportionally higher than in the thicker flat plate layers. Additionally, the computational difficulties inherent in the evaluation of the local shear stress and heat fluxes contribute to the uncertainty. The combination of these effects is reflected in the uncertainty band. In view of these considerations, the collapse of the experimental results is encouraging in the inner regions.

In Figs. 4.6 and 4.7, it can be seen that the turbulent Prandtl number collapses on the inner region coordinate y^+ in the range $20 < y^+ < 200$, but correlates less well in the outer regions on y/δ. In the regions very close to the wall, $y^+ < 20$, and in the outer regions, $y/\delta > 0.3$, where one could reasonably expect correlation on one parameter and not the other, the uncertainty of the results precludes a comparison. The diffusivity ratio, ϵ_M/ν, is the parameter of the turbulent Prandtl number in the Jenkins model [37], and is itself well correlated by the inner coordinate y^+ in flat plate turbulent boundary layers [42]. It is shown in Fig. 4.8 that the present results do not correlate on this coordinate. The curves fold back because ϵ_M/ν rises to a maximum, and then decreases towards the edge of the boundary layer, i.e., as $y/\delta \rightarrow 1$.

In the intermediate range, the turbulent Prandtl number, in Fig. 7, is above unity near the wall, with a decreasing trend towards a value of about 0.8 at y^+ of 200. The mean value is on the order of unity throughout this range. There is some indication that Pr_t is higher in strong accelerations without blowing, but the evidence is not conclusive. In general, it can be stated that no effects of blowing or acceleration are evident within the uncertainty band. The results agree reasonably well with the data of Simpson, et al. [27] above y^+ of 30, when correlated with y^+. The results for the flat plate turbulent boundary layer correlate in the

outer region as well, whereas the present results in accelerated flow do not.

In Fig. 4.6, the trend of the turbulent Prandtl number very close to the wall, ignoring for a moment the uncertainty band, is substantially different than the results of Simpson, et al. Simpson's calculations showed a mean value of Pr_t continually rising towards the wall, whereas Fig. 4.6 indicates a mean value which drops off below y^+ of 30. The drop off in the present results is largely due to the use of the Young and Maas shear correction, which Simpson did not use. Conduction error in the temperature probe would also tend to reduce turbulent Prandtl number, but not to the extent noted here. Figure 4.9 shows the flat plate case, for $F = 0$ and $F = 0.004$, calculated with and without a probe correction applied to the data. The shift in Pr_t very near the wall is evident. The effect of the correction decreases as y^+ increases, until there is complete agreement above $y^+ = 100$. It is concluded that no trends in Pr_t below $y^+ = 30$ can be confirmed from this data or that of Simpson, et al. [27].

It is not too surprising, in view of these results and those of Simpson that the assumption of a constant turbulent Prandtl number on the order of 1.0 predicts heat transfer data reasonably well over a wide range of turbulent boundary layers. It can be stated with certainty, nevertheless, that the turbulent Prandtl number is not constant across the layer, and that the values presented here are not inconsistent with the concept of a high turbulent Prandtl number near the wall and a level approaching 0.7-0.8 in the wake. To formulate a model for the turbulent Prandtl number in a prediction method, the results suggest that, in the inner regions, a relationship in the form $Pr_t(y^+)$ is most appropriate.

E. Conclusions

In summary, the conclusions of this work can be stated

as follows:

(a) Experimental values of the turbulent Prandtl number have been computed from data covering a wide range of the acceleration parameter K, 0.55×10^{-6} to 2.55×10^{-6}, both with and without blowing at the wall. The calculation method is discussed in detail and results using this method on data for the flat plate turbulent boundary layer are compared to the results of Simpson, et al. [27].

(b) The turbulent Prandtl number for blown and unblown boundary layers, with free-stream acceleration up to $K = 2.55 \times 10^{-6}$ is on the order unity. The experimental values are slightly higher than unity in the inner regions, decreasing to below unity in the outer regions. There is some evidence that, for strong accelerations, the turbulent Prandtl number remains above unity over a greater portion of the boundary layer.

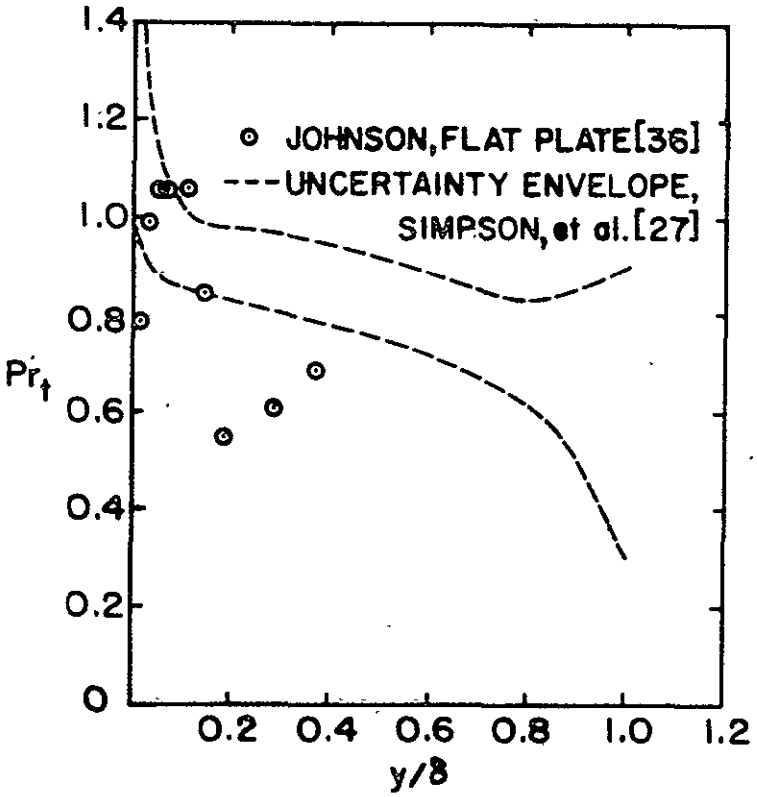

Fig. 4.1 Experimental results for turbulent Prandtl number distribution in a turbulent boundary layer on a flat plate

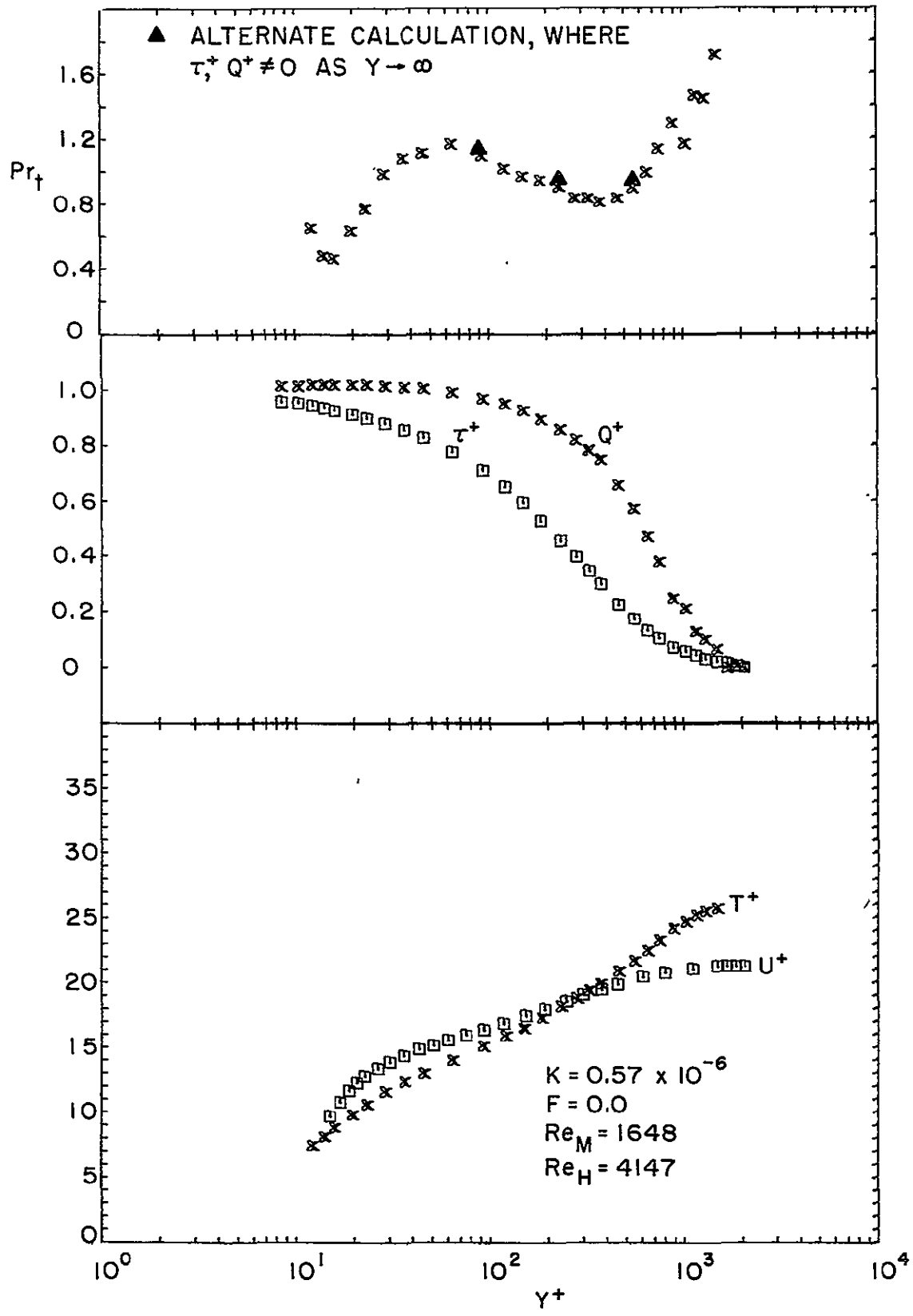

Fig. 4.2 Boundary layer profile results in a moderate acceleration with no transpiration.

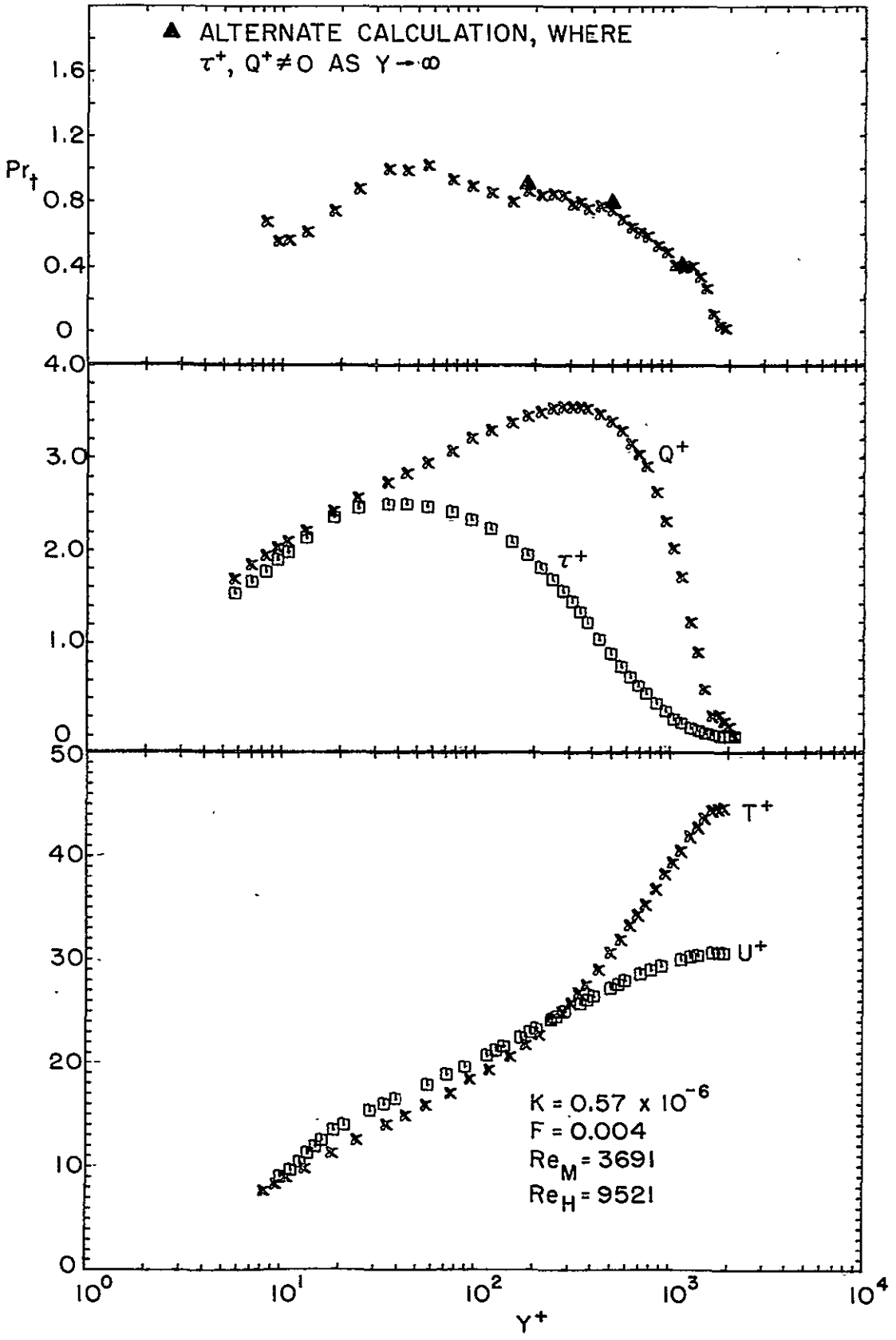

Fig. 4.3 Boundary layer profile results in a moderate acceleration with blowing.

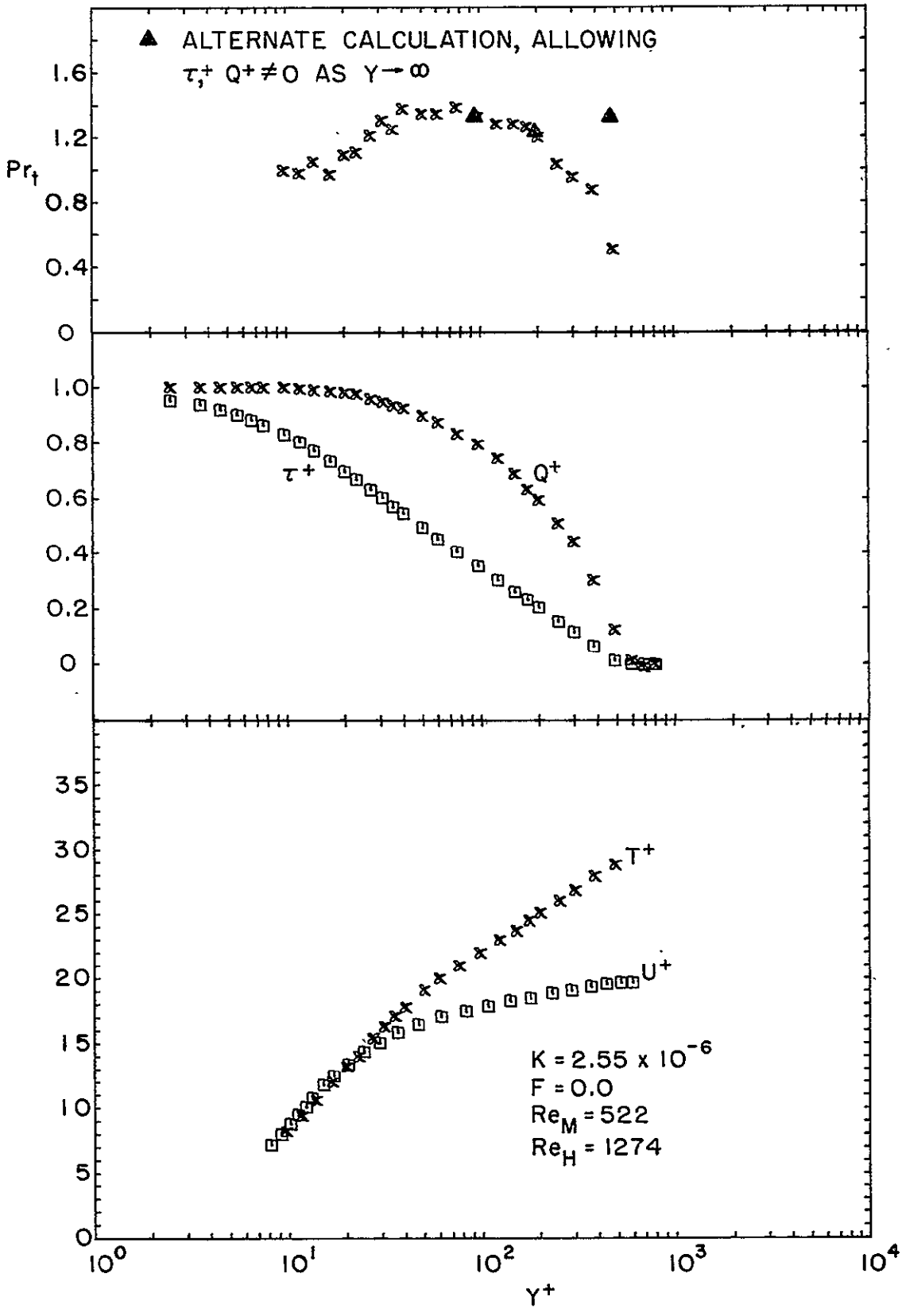

Fig. 4.4 Boundary layer profile results in a strong acceleration with no transpiration.

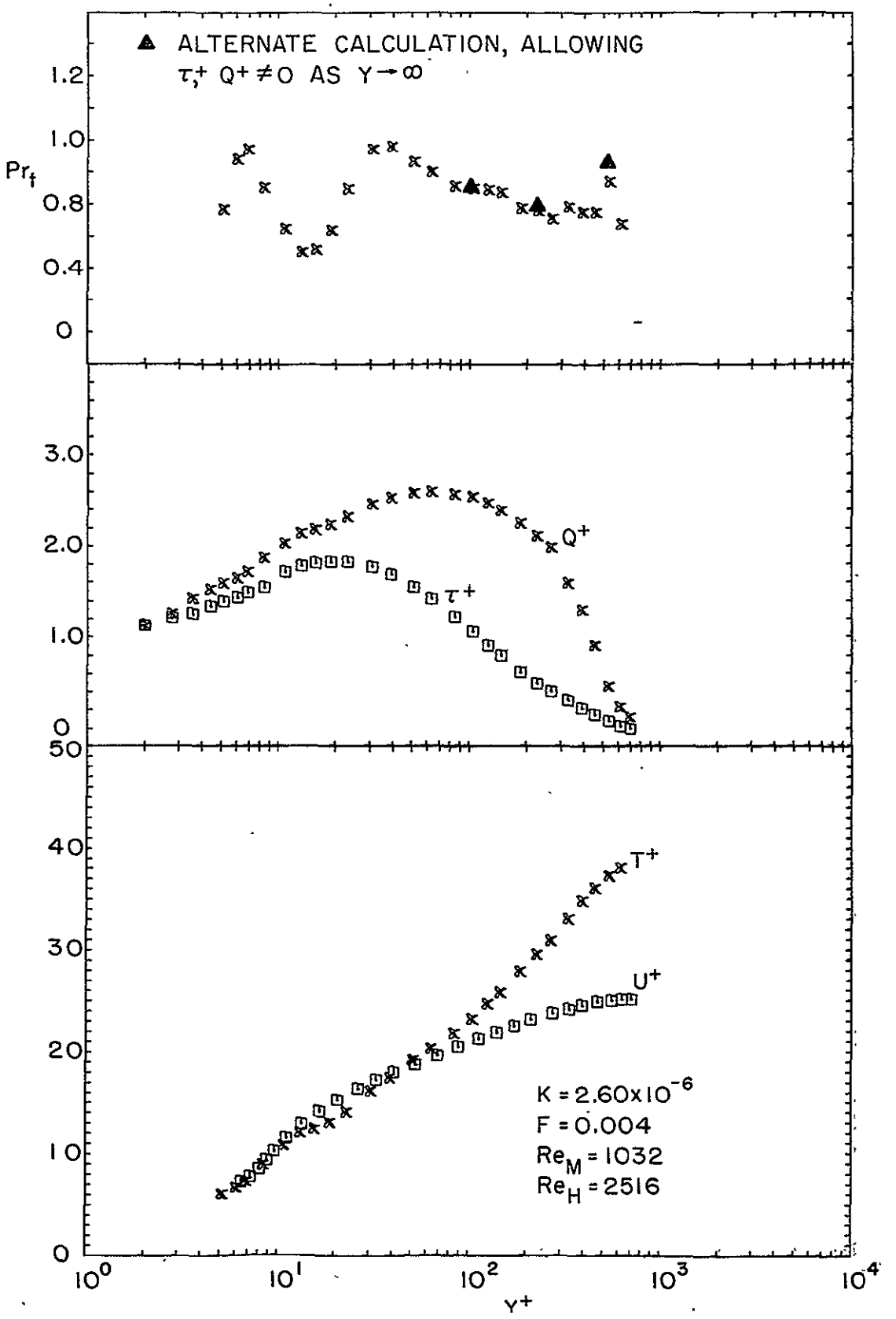

Fig. 4.5 Boundary layer profile results in a strong acceleration with blowing.

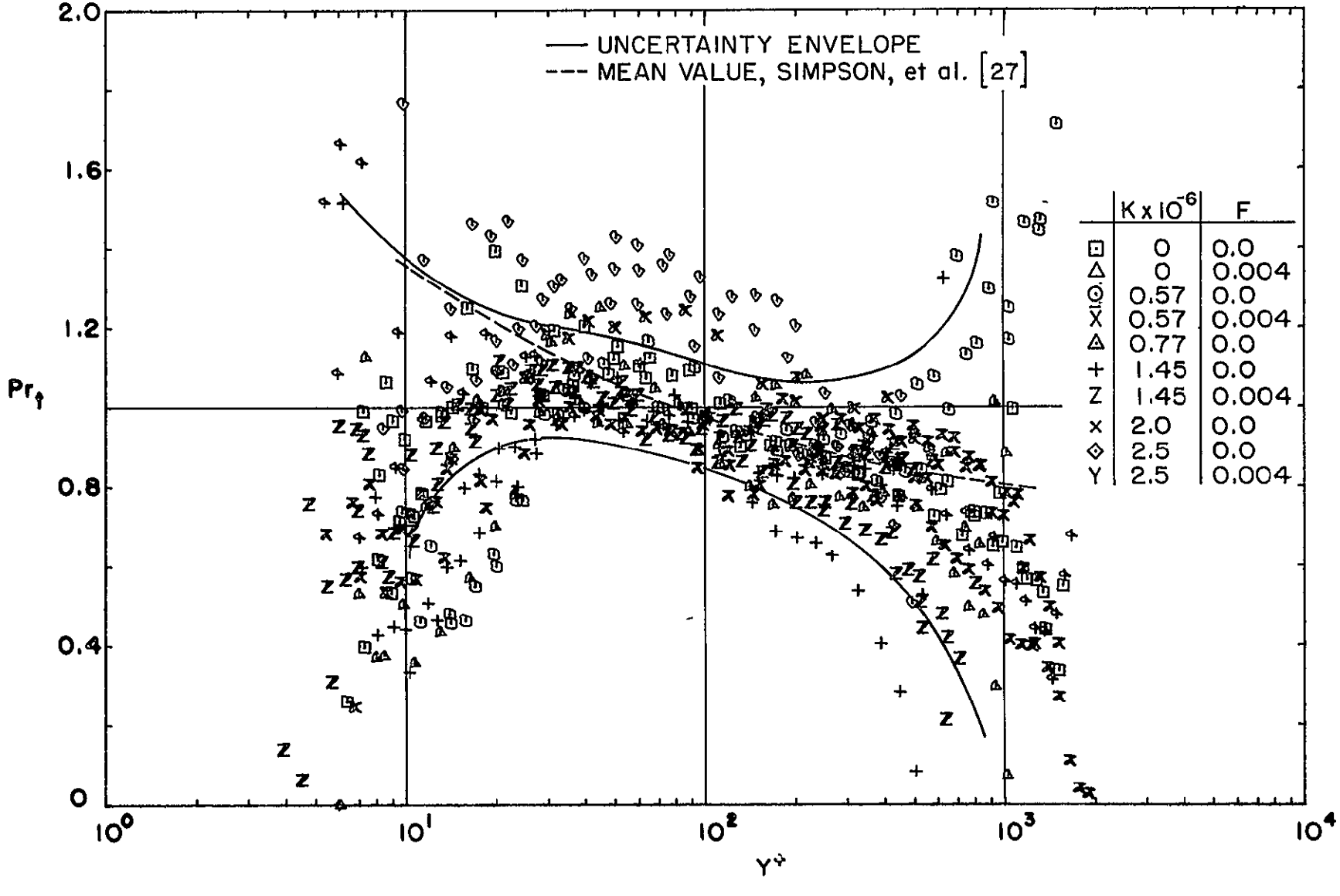

Fig. 4.6 Turbulent Prandtl number in accelerated flows-inner region plot.

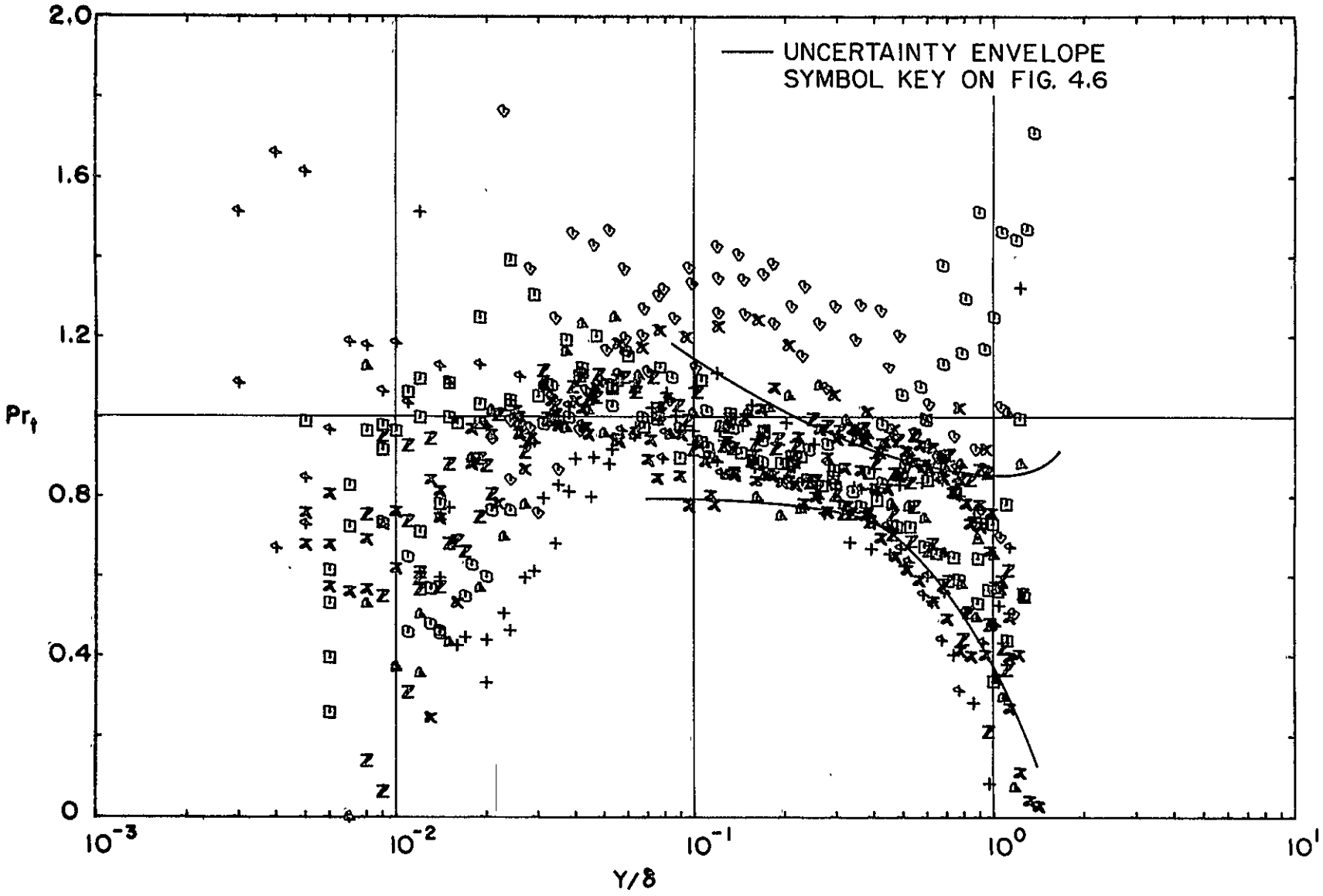

Fig. 4.7 Turbulent Prandtl number in accelerated flows-outer region plot.

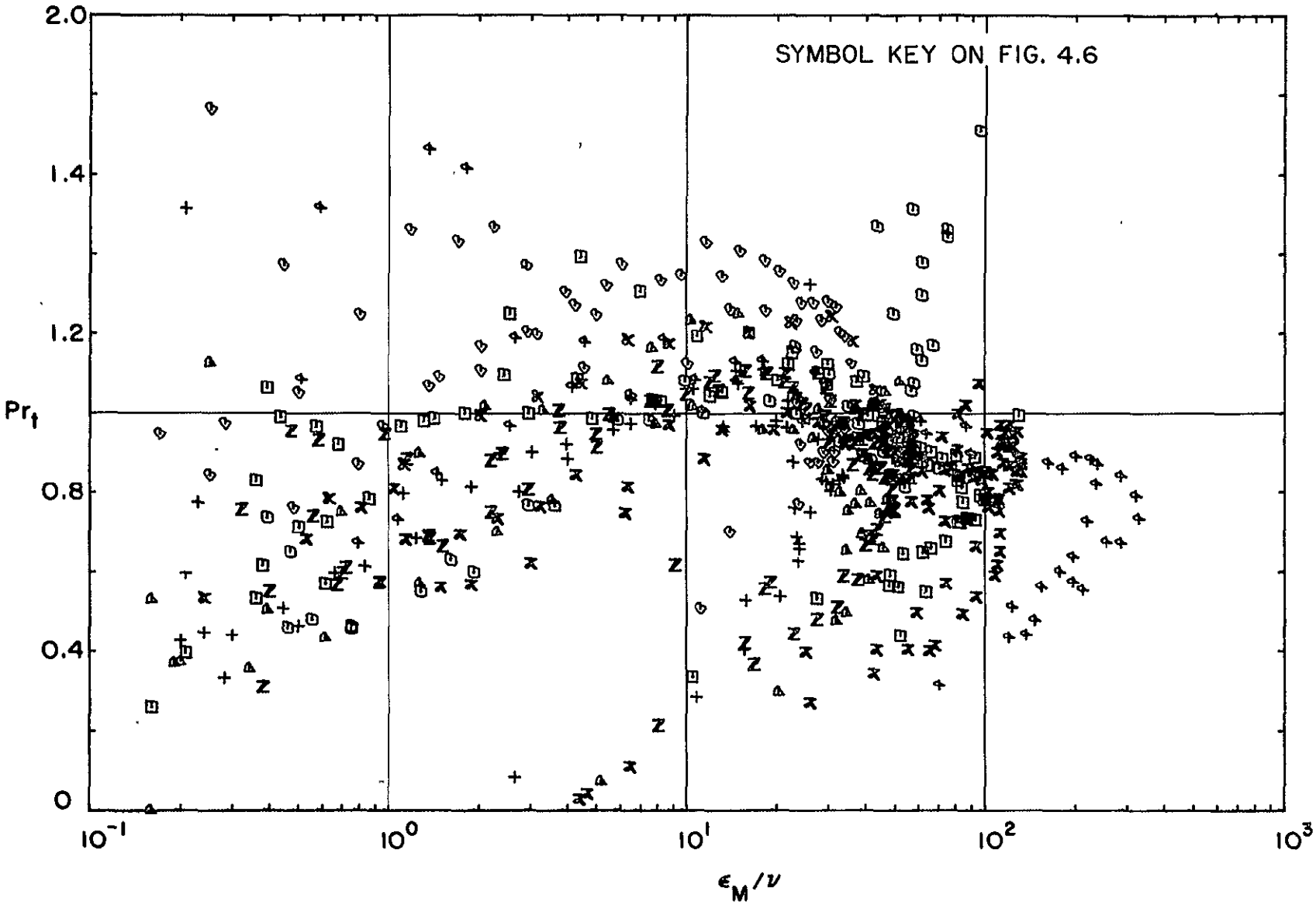

Fig. 4.8 Turbulent Prandtl number in accelerated flows as a function of ϵ_M/ν .

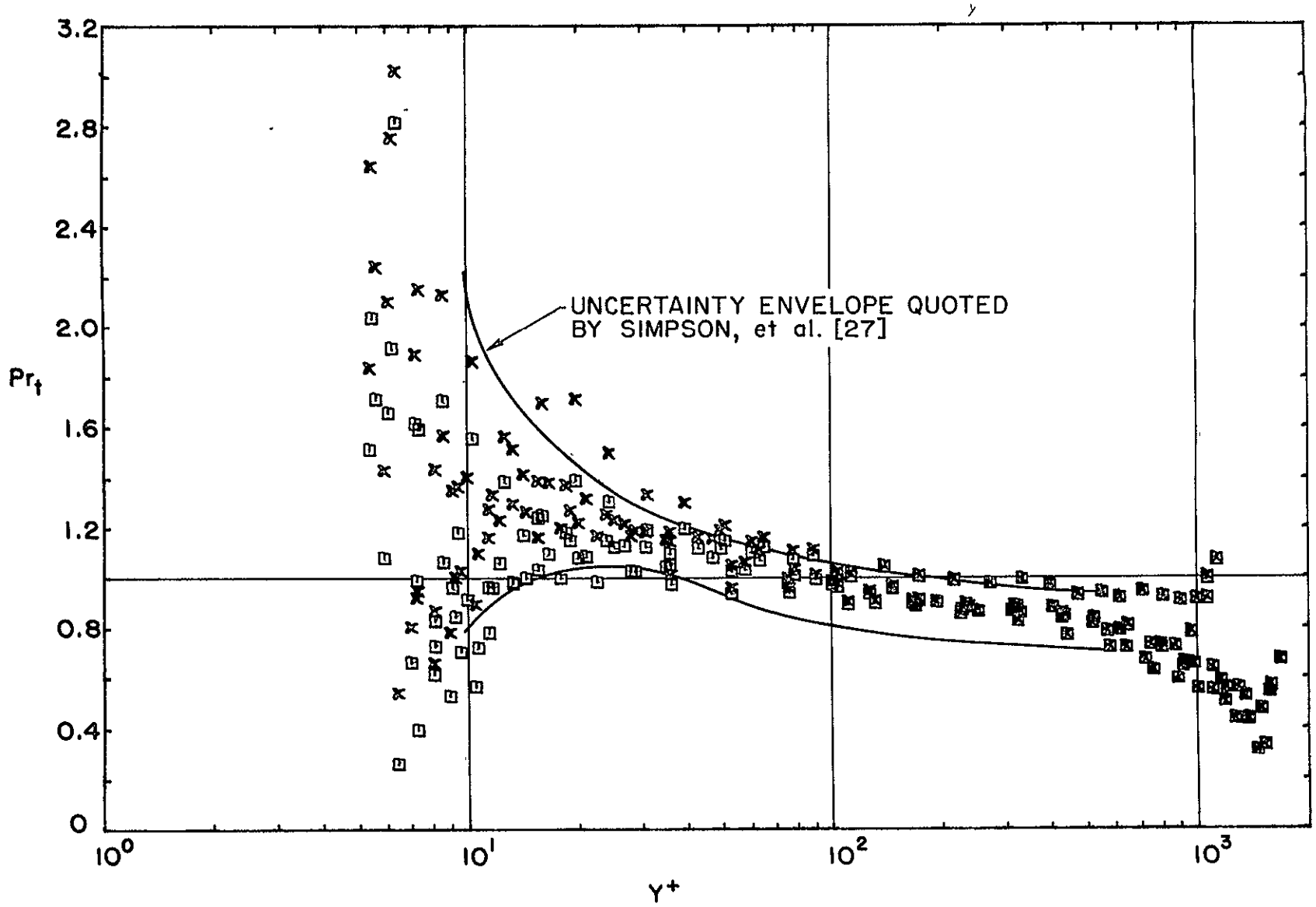

Fig. 4.9 Data of Simpson, et al. [27], for F=0 and F=0.004, recomputed with present method. ⊡ - no shear correction applied to total pressure probe data. × - shear correction applied.

REFERENCES

1. Caldwell, G. L., and R. A. Seban. "Flow and Heat Transfer in a Laminarizing Turbulent Boundary Layer," paper presented at ASME-AIChE Heat Transfer Conference, Minneapolis, Minnesota, August, 1969, ASME Paper No. 69-HT-10.

2. Back, L. H., R. F. Cuffel, and P. F. Massier. "Laminarization of a Turbulent Boundary Layer in Nozzle Flow - Boundary Layer and Heat Transfer Measurements with Wall Cooling," paper presented at ASME-AIChE Heat Transfer Conference, Minneapolis, Minnesota, August, 1969, ASME Paper No. 69-HT-56.

3. Launder, B. E. Laminarization of the Turbulent Boundary Layer in a Severe Acceleration, Journal of Applied Mechanics, 1964, 31 (4), 707-708.

4. Kays, W. M., R. J. Moffat, and W. H. Thielbahr. "Heat Transfer to the Highly Accelerated Turbulent Boundary Layer with and without Mass Addition," paper presented at ASME-AIChE Heat Transfer Conference, Minneapolis, Minnesota, August, 1969 (to be published in the Journal of Heat Transfer), ASME Paper No. 69-HT-53.

5. Kestin, J. The Effect of Free-Stream Turbulence on Heat Transfer Rates, Advances in Heat Transfer, 1966, 3, 1-32.

6. Thielbahr, W. H., W. M. Kays, and R. J. Moffat. The turbulent boundary: experimental heat transfer with blowing, suction, and favorable pressure gradient. Report HMT-5, Mechanical Engineering Department, Stanford University, Stanford, California, 1969.

7. Wilson, D. G. Equilibrium turbulent boundary layers in favorable pressure gradients. Division of Engineering and Applied Science, Harvard University, Cambridge, Mass., 1957.

8. Moretti, P. M., and W. M. Kays. Heat Transfer to a Turbulent Boundary Layer with Varying Free-Stream Velocity and Varying Surface Temperature - An Experimental Study, Int. Journal of Heat and Mass Transfer, 1966, 8 (9), 1187-1202.

9. Launder, B. E., and H. W. Stinchcombe. Non-normal similar turbulent boundary layers. Report TWF/TN/21, Mechanical Engineering Department, Imperial College of Science and Technology, London, 1967.

10. Patel, V. C., and M. R. Head. Reversion of Turbulent to Laminar Flow, J. Fl. Mech., 1968, 34 (2), 371-392.

11. Badri Narayanan, M. A., and V. Ramjee. On the Criteria for Reverse Transition in a Two-dimensional Boundary Layer Flow, J. Fl. Mech., 1969, 35 (2), 225-241.

12. Bradshaw, P. A Note on Reverse Transition, J. Fl. Mech., 1969, 35 (2), 387-390.

13. Fiedler, H., and M. R. Head. Intermittency Measurements in a Turbulent Boundary Layer, J. Fl. Mech., 1966, 25 (4), 719-735.

14. Julien, H. L., W. M. Kays, and R. J. Moffat. The turbulent boundary layer on a porous plate: experimental study of the effects of a favorable pressure gradient. Report HMT-4. Mechanical Engineering Department, Stanford University, Stanford, California, 1969.

15. Schraub, F. A., and S. J. Kline. A Study of the structure of the turbulent boundary layer with and without longitudinal pressure gradients. Report No. MD-12, Department of Mechanical Engineering, Stanford University, Stanford, California, 1965.

16. Launder, B. E., and W. P. Jones. "A Note on Bradshaw's Hypothesis for Laminarization," paper presented at ASME-AIChE Heat Transfer Conference, Minneapolis, Minnesota, August, 1969, ASME Paper No. 69-HT-12.

17. Townsend, A. A. The Structure of Turbulent Shear Flow, Cambridge University Press, 1956.

18. Launder, B. E., and W. P. Jones. Sink Flow Turbulent Boundary Layers, J. Fl. Mech., 1969, 38 (4), 817-831.

19. Launder, B. E., and F. C. Lockwood. "An Aspect of Heat Transfer in Accelerating Turbulent Boundary Layers," ASME Paper No. 68-WA/HT-13 (to be published in Journal of Heat Transfer).

20. Boldman, D. R., J. F. Schmidt, and A. K. Gallagher. Laminarization of a turbulent boundary layer as observed from heat-transfer and boundary layer measurements in conical nozzles. NASA TN D-4788. September, 1968.

21. Thielbahr, W. H., W. M. Kays, and R. J. Moffat. "The Turbulent Boundary Layer on a Porous Plate: Experimental Heat Transfer with Uniform Blowing and Suction, with Moderately Strong Acceleration," (to be submitted to the Journal of Heat Transfer).

22. Moffat, R. J., and W. M. Kays. The Turbulent Boundary Layer on a Porous Plate: Experimental Heat Transfer with Uniform Blowing and Suction, Int. J. Heat Mass Transfer, 1968, 11 (10), 1547-1566.

23. Loyd, R. J. The Turbulent boundary layer on a porous plate: an experimental study of the fluid dynamics with strong favorable pressure gradients and blowing. Ph.D. thesis. Mechanical Engineering Department, Stanford University, Stanford, California, 1970.

24. Boldman, D. R., J. F. Schmidt, and R. C. Ehlers. The Effect of Uncooled Inlet Length and Nozzle Convergence Angle on the Turbulent Boundary Layer and Heat Transfer in Conical Nozzles Operating with Air, Journal of Heat Transfer, November, 1967, 89 (4), Series C, 341-350. Also ASME Paper No. 67-HT-28.

25. Tani, I. Review of Some Experimental Results on the Response of a Turbulent Boundary Layer to Sudden Perturbations, Proceedings - Computation of Turbulent Boundary Layers - 1968, AFOSR-IFP-Stanford Conference, Vol. 1, Kline, S. J., M. Morkovin, G. Sovran, D. Cockrell, Department of Mechanical Engineering, Stanford University, Stanford, California, 483-494.

26. Spalding, D. B., and S. V. Patankar. Heat and Mass Transfer in Boundary Layers, 1967, Morgan-Grampian London.

27. Simpson, R. L., D. G. Whitten, and R. J. Moffat. An Experimental Study of the Turbulent Prandtl Number of Air with Injection and Suction (to be published in Int. J. Heat Mass Transfer).

28. Uberoi, M. S., and S. Wallis. Effect of Grid Geometry on Turbulence Decay, The Physics of Fluids, 1967, 10 (6), 1216-1224.

29. Kline, S. J., A. V. Lisin, and B. A. Waitman. Preliminary experimental investigation of effect of free-stream turbulence on turbulent boundary-layer growth. NASA TN D-368. March, 1960.

30. Bradshaw, P., and D. H. Ferriss. Calculation of boundary layer development using the turbulent energy equation, IV: heat transfer with small temperature differences. N.P.L. Aero Report 1271, A.R.C. 30 300, 1968.

31. Jones, W. P., and B. E. Launder. "On the Prediction of Laminarescent Turbulent Boundary Layers," paper presented at ASME-AIChE Heat Transfer Conference, Minneapolis, Minnesota, August, 1969, ASME Paper No. 69-HT-13.

32. Lawn, C. J. Turbulent Heat Transfer at Low Reynolds Number, Journal of Heat Transfer, ASME Transactions, 91, Series C, No. 4, November 1969, 532-536.

33. Kestin, J., and P. D. Richardson, Heat transfer across turbulent, incompressible boundary layers, Int. J. Heat Mass Transfer, 1963, 6, 147-189.

34. Ludwieg, H. Bestimung des Verhaltnisses der Austauschkoeffizienten fur Warme and Impuls bei turbulenten Grenzschichten, Z. Flugwiss, 1965, 4, 73-81.

35. Azer, N. Z., and B. T. Chao. A Mechanism of Turbulent Heat Transfer in Liquid Metals, Int. J. Heat Mass Transfer, 1960, 1, 121-138

36. Johnson, D. S. Velocity and Temperature Fluctuation Measurements in a Turbulent Boundary Layer Downstream of a Stepwise Discontinuity in Wall Temperature, Journal of Applied Mechanics, 1959, 26, 325-366.

37. Jenkins, R. Variation of the Eddy Conductivity with Prandtl Modulus and Its Use in Prediction of Turbulent Heat Transfer Coefficients, Proceedings of Heat Transfer and Fluid Mechanics Inst., 1951, 147-158.

38. Tyldesley, J. R., and R. S. Silver. The Prediction of the Transport Properties of a Turbulent Fluid, Int. J. Heat Mass Transfer, 1968, 11, 1325-1340.

39. Tyldesley, J. R. Transport Phenomena in Free Turbulent Flows, Int. J. Heat Mass Transfer, 1969, 12, 489-496.

40. Young, A. D., and J. N. Maas. The behavior of a pitot tube in a transverse total-pressure gradient. A.R.C. Report and Memoranda No. 1770. September, 1936.

41. Kline, S. J., and F. A. McClintock. "Describing Uncertainties in Single Sample Experiments," Mechanical Engineering, 1953.

42. Simpson, R. L. Characteristics of Turbulent Boundary Layers at Low Reynolds Numbers with and without Transpiration (submitted to J. Fl. Mech.).

43. London, A. L. Oblique flow headers for heat exchangers - the ideal geometries and the evaluation of losses, Mechanical Engineering Department, Tech. Rept. 63, Stanford University, Stanford, California, August, 1966.

44. Whitten, D. G. The turbulent boundary layer on a porous plate: experimental heat transfer with variable suction, blowing and surface temperature. Ph.D. thesis. Mechanical Engineering Department, Stanford University, Stanford, California, 1967.

45. Moffat, R. J. "Gas Temperature Measurement". in Temperature - Its Measurement and Control in Science and Industry, 3 (2), 553-571.

46. Bradshaw, P. The Effect of Wind-Tunnel Screens on Nominally Two-dimensional Boundary Layers, J. Fl. Mech., 1965, 22 (4), 679-687.

47. Baines, W. D., and E. G. Peterson. An Investigation of Flow Through Screens, Transactions of the ASME, July, 1951, 467-480.

48. de Bray, R. G. Some investigations into the spanwise non-uniformity of nominally two-dimensional incompressible boundary layers downstream of gauze screens. A.R.C. Report No. 29-271, July, 1967.

49. Reynolds, W. C., W. M. Kays, and S. J. Kline. Heat transfer in the turbulent incompressible boundary layer: I -Constant wall temperature. NASA MEMO 12-1-58W, 1958.

50. Kays, W. M. Convective Heat and Mass Transfer, McGraw-Hill Book Co., 1966.

51. Boldman, D. R., J. F. Schmidt, and A. Fortini. Turbulence heat-transfer, and boundary layer measurements in a conical nozzle with a controlled inlet velocity profile. NASA TND-3221. March, 1966.

52. Wolfshtein, M. The Velocity and Temperature Distribution in One-dimensional Flow with Turbulence Augmentation and Pressure Gradient, Int. J. Heat Mass Transfer, 1969, 12, 301-318.

SUPPLEMENT 1

EXPERIMENTAL APPARATUS AND TECHNIQUES

A. General Description

The test apparatus was designed for boundary layer experiments including transpiration, variable free-stream velocity, and variable surface temperature. The boundary layer is formed on the lower surface of a rectangular channel having cross-section dimensions of 6 inches high by 20 inches wide. The test channel is eight feet long, and the lower wall is made of 24 segments, or plates, each 4 inches long in the flow direction. The surface temperature and transpiration flow are each controlled individually in each plate, allowing a small-step approximation to a continuous wall boundary condition. The upper wall of the channel is adjusted to achieve the desired variation in free-stream velocity. Mean temperature, mean velocity, and streamwise fluctuation velocity profiles within the boundary layer on the lower surface are taken through access holes in the top wall. Substantial care has been taken to assure thermal and hydrodynamic uniformity in the free-stream flow throughout the channel. Heat transfer from the surface to the boundary layer, characterized by the Stanton number, is obtained from an energy balance on each plate.

A maximum free-stream velocity of about 40 fps at the inlet of the channel is available with the present installation. Plate temperature can be varied between ambient and approximately 140 F, while free-stream temperature ranges from about 70 F, if cooled, to 95 F uncooled. Energy balances on each plate which were conducted with transpiration only, i.e., no free-stream flow, close within about 4 percent over a wide range of blowing and sucking. Results of qualification tests of the uniform free-stream velocity case with no transpiration agree within several percent of accepted cor-

relations of Stanton number. A more quantitative treatment of these qualifications will be presented shortly.

The fabrication of the apparatus and its original qualification are described in considerable detail by Moffat and Kays [22]. The discussion in the following paragraphs will briefly describe some of the features mentioned above, and document the changes made to the test rig in the course of this investigation.

B. Wind Tunnel

The wind tunnel is an open-circuit unit constructed on two levels to accommodate, in a convenient manner, both the transpiration system and the instrumentation connected with the 24-plate test section. A schematic diagram of the wind tunnel and a photograph of the test duct are presented in Figs. 2.1 and S1.1 respectively. The main air flow enters the blower via a felt-type filter and passes through, in order, a preliminary screen pack, a turning header, a counter-crossflow water-cooled heat exchanger, a flow straightner and screen set, and finally a 4:1 contraction before entering the test section. The turning header prior to the heat exchanger was designed according to the guidelines set forth by London [43] to provide a uniform velocity at the inlet to the heat exchanger. The purpose of the heat exchanger is to maintain a temporally constant and spatially uniform free-stream temperature despite variations in ambient temperature during a test run. Before entering the series of six screens, the flow passes through an aluminum honeycomb-type straightener which is $1\frac{1}{2}$ inches thick with hexagonal cells on $\frac{3}{16}$ -inch centers. The screens are 32 x 32 mesh, 63 percent open-area ratio, with a $3\frac{5}{8}$ -inch spacing between the last three. A clear plexiglas wall is located just upstream of the first screen to permit easy inspection of its condition and to guard against fouling by dirt.

The 4:1 contraction extends over 26 inches, blending into an entrance section which joins the test channel. The boundary layer is tripped by a $\frac{1}{16}$ -inch high, $\frac{1}{4}$ -inch wide smooth phenolic strip located $\frac{1}{2}$ -inch before the first test plate, and 36 inches downstream of the last screen.

The major modification to the test apparatus made during the period of this investigation was a redesign of the straightening-screen set, located prior to the contraction. The primary reason for this modification was to improve the two-dimensionality of the flow through the test channel; the resulting improvement will be described in a following section. One measure of the effectiveness of the entrance arrangement is the uniformity of the free-stream flow at the entrance to the tunnel. At a free-stream velocity of about 23 fps, used for the majority of the experiments described here, the velocity is uniform to within 0.05 fps and the free-stream temperature to within 0.2 F.

C. Test Plates

The 24 test plates are mounted on thermal isolators in an aluminum frame. They are separated from each other by a 0.025 -inch strip of balsa wood and plastic putty. The pertinent physical characteristics of the plates are:

Material - sintered porous bronze
Dimensions - 18.0 x 3.975 x 0.25 inches
Particles - spherical: maximum diameter 0.0070 inches
minimum diameter 0.0023 inches
Porosity - Approximately 40%. Uniform within $\pm$6% in the center six-inch span
Roughness - Maximum of 200 microinches (RMS) measured with a stylus of radius 0.0005 inches
Thermal conductivity - 6.5 Btu/hr-ft-F, minimum
Surface emissivity - 0.37 average

Surface temperatures are measured by five iron-constantan thermocouples located in the center six-inch span. The surface thermocouples are epoxied into holes drilled from the bottom of the segment to within 0.040 inches of the surface. The plate is heated by nichrome wires located in groves in the lower surface, spaced such that the surface temperature variation, due to wire spacing, will be within 0.04 F under all conditions of surface heat transfer and transpiration. Separate power supplies, both stabilized, are available for plates 1-12 and 13-24. Additionally, power to each plate is individually controlled by a rheostat. To illustrate the nature of the plate surface, a close-up photograph is presented in Fig. S1.2.

D. Transpiration System

The transpiration system is shown in Fig. 2.1. The components of the circuit are, in order, the air filter, blower, heat exchanger, header, flow control valves, flowmeters, plate underbody, and the plate itself.

The heat exchanger is used to cool the transpiration flow to near ambient temperature, minimizing the heat transfer in the lines leading to the flowmeters so that a single measurement in the distribution header will suffice to describe the temperature at every flowmeter. Parallel circuits of ball-type flow control valves and variable-area flowmeters provide two ranges of control and measurement. To assure accurate flow measurement, the system is periodically checked for leakage. The flowmeters were individually calibrated with an ASME standard orifice in preparation for the present study. Each plate underbody has been developed to 1) provide thermally and hydrodynamically uniform flow to the underside of the entire plate and 2) allow measurement of a single temperature in the transpiration fluid just beneath the plate to provide the information necessary for energy balances. Figure S1.3 shows a view in cross-section of a typical plate.

The developments leading to this design are fully discussed by Moffat and Kays [22]. The plates are arranged in sets of six into heavy aluminum castings, which are heated (or cooled, if desired) by an auxiliary water system to reduce thermal conduction between the plates and their supports during testing. Note in Fig. S1.3 that the conduction path for heat losses to the plate support is largely limited to thin phenolic webs.

E. Instrumentation

Table I contains a listing of the instrumentation used in the experiments, plus the source of the calibration and the estimated accuracy, where appropriate.

The instrumentation which is used in the measurement of surface heat transfer is unchanged from previous investigations on the apparatus [22,44,6]. Profile measurement techniques, however, have been modified in several respects. A new temperature probe was fabricated of 0.004-inch iron-constantan wire, replacing the previous 0.010-inch wire, in order (1) to allow measurements close to the wall (the junction size was reduced from 0.009 inches to 0.005 inches in thickness) and (2) to reduce conduction losses from the junction. However, subsequent analysis of the probable conduction error using the approach of Moffat [45] showed that functionally, at the same ratio of the exposed thermocouple junction length to junction diameter (ℓ/d), the conduction error in cross flow is proportional to $\exp(-d^{1/3})$. Additionally, small wires are more subject to material inhomogeneities which result in measurement errors in a temperature gradient. A larger wire, on the order of 0.007 inches is recommended for future testing.

A calibration of the thermocouple probe was conducted in a constant temperature oil bath using a precision mercury thermometer as the standard. Even when the junction was

TABLE I. INSTRUMENTATION LIST

Measurand	Instrument or Sensing Device	Source of Calibration (where appropriate)	Estimated Accuracy
Temperature	Probe: 0.004-inch iron-constantan thermocouple wire with tip flattened to 0.005-inches	See text	See text
	Other: 0.010-inch iron-constantan thermocouple wire	Constant temperature oil bath at Stanford Linear Accelerator Standards Facility	0.25 F
Pressure	Probe: Total pressure probe with tip flattened to 0.0118-inch by 0.0355-inch		
	Static wall taps: 0.040-inch sharp-edged holes		
	Transducers: Statham PM-97 and PM-5 differential pressure transducers	Meriam Model 34FB2 20" Micromanometer	0.4-0.8%
Thermocouple or transducer output	Hewlett Packard DYMEC Integrating Digital Voltmeter Model 2401C Beckman Electronic Counter Model 5010R-11	Hewlett Packard Standards Laboratory	± 2μV
Flowrate	Transpiration: Fisher-Porter Rotameters; Tube Model Nos. B6-27-10/27 and B4-27-10/27. Float Model Nos. SS BSVT-64-A and SS BSVT-45-A	ASME standard orifices	± 2 percent
Electrical Power	Sensitive Research Company, Reference Standard Wattmeter Model U-21020	Stanford Linear Accelerator Standards Facility	1/4 percent
Fluctuating velocity	Probe: Platinum hot-wire 0.0002-inch diameter, 1/16-inch long		
	Thermo-Systems Constant Temperature Anemometer Model 1010 Thermo-Systems Linearizer Model 1005B Thermo-Systems RMS Voltmeter Model 1060		
	Quan-Tech Wave Analyzer Model 304		
	Hewlett-Packard MOSELEY Model 7001A x-y recorder		

barely immersed, in an attempt to establish a sharp gradient in the region of the tip, the agreement was within 0.3 F. It is possible, however, that measurements very close to the wall in a boundary layer, where the temperature gradients are steep, could be in error by several degrees. For purposes of uncertainty calculations, it is assumed that the accuracy is ± 0.4 F for the first fifteen profile points and ± 0.25 F in the outer regions. Comparison of the temperature data below a y^+ of 10 to the expected correlation in that region indicates that the temperature probe typically reads about 2.4 F low at $y^+ = 2$, decreasing to 0.7 F at $y^+ = 10$. Typically, the fifteenth point in the profile occurs at a y^+ of about 50. It will be shown that the effect of this error on integral parameters of the boundary layer is negligible.

The probe is manually positioned with a micrometer traversing mechanism, accurate to the closest 0.001-inch. The wall position of the thermocouple probe is established by electrical means.

Hydrodynamic measurements for this study are described by Loyd [23]. In essence, the innovations include the use of the pressure transducers in place of manometers, and the verification of pitot-tube mean velocity profiles with hot-wire data. In both the temperature and velocity profile measurements, the signal at each point was integrated by the digital voltmeter over a period of at least ten seconds. The recorded data then included both the integrated signal and the time interval.

Standard hot-wire techniques were utilized to obtain profiles of the streamwise fluctuation velocity, $\sqrt{\overline{u'^2}}$, as well as mean velocity. The data was obtained with a 0.0002-inch constant temperature platinum hot wire and a linearized anemometer system. The calibration of the hot-wire was checked frequently during testing, with a maximum estimated drift of about 3 percent. The mean velocity and the mean-

square of the streamwise fluctuation velocity were both recorded by the integration method noted above.

Free-stream velocity distribution was calculated with Bernoulli's equation for incompressible flow from a single total-pressure measurement at the entrance of the test section, and 47 wall static pressure measurements made 1-inch above the plate along one wall of the channel. Tests conducted previously [6] indicated that the static pressures measured by the wall taps were at a given x-position, constant throughout the boundary layer in moderate pressure gradients. Additional tests were conducted during the present study in the region of the most severe axial pressure gradient. It was found that perpendicular to the wall the static pressure was also constant throughout the thin boundary layer under these conditions, and increased with increasing y in the potential core such that the variation in velocity was less than 0.8%. This point is discussed further in section F.5. Additionally, the readings were identical on both sides of the channel.

F. Qualification of the Apparatus

The test apparatus was qualified for operation in several ways. An extensive set of experiments was conducted to examine the closure of energy balances over a wide range of transpiration. Secondly, tests were made to verify that an accepted correlation could be reproduced for a turbulent boundary layer with a constant free-stream velocity on an impermeable wall. Finally, the questions of surface roughness and three-dimensional flow conditions in the test section were considered.

F.1 Transpiration Energy Balances

With transpiration, the electrical energy supplied to the test segments can be accounted for as heat transferred to the boundary layer, to the transpired flow, and to the surroundings as "losses". In the first qualification of the

test rig by Moffat and Kays [22], a series of tests was conducted with no main-stream flow in order to establish correct models for the loss terms, and to achieve satisfactory energy balances for the simplified problem of transpiration only. Subsequently, these tests have been periodically conducted to confirm the repeatibility of the results, with continuing efforts expended on improvements in the model which purports to mathematically describe the performance of the apparatus. Building on the experience of the previous results, special care was taken in the current series of tests to examine some irregularities which have appeared to be associated with the rate of transpiration flow, particularly in the blowing mode. To appreciate the discussion of the modifications which have been made to the model, the modes and descriptions of the energy flows will briefly be outlined here.

The energy supplied to each plate, ENDEN[1], is distributed in the following manner,

$$\text{ENDEN} = \text{HTRANS} + \text{ECONV} + \text{LOSSES} \qquad \text{(S1.1)}$$

where

HTRANS - heat transferred from the surface to the boundary layer

ECONV - heat transferred within the plate to the transpiration flow

LOSSES - heat transferred to the surroundings by radiation from the top and bottom surfaces, and by conduction to the support structure.

It is important to recognize that the energy balance control volume is restricted to the center six-inches of the

[1]The terminology of the data reduction computer program STANTON (Supplement 3) will be used throughout this discussion.

plate. The upper and lower limits of the control volume in the y-direction are somewhat different for blowing and suction. The term LOSSES accounts for several heat transfer mechanisms: top radiation from the plate to the channel walls, back radiation from the plate to the pre-plate and casting, conduction from the plate to the casting through the web supports, conduction to the casting and pre-plate through the stagnant air which exists when no transpiration is present, and lateral conduction within the plate to or from the center six-inch control volume. The development of models for these terms are fully discussed in references [22,6].

During this study, adjustments based on experiments were made to the ECONV term, resulting in improved energy balances. The term is calculated from the equation

$$\text{ECONV} = \dot{m}'' c_p [T_o - T_T][1 + f(\dot{m}'', \text{KCONV})] \qquad (S1.2)$$

where KCONV accounts for slight measured differences in the mixed-mean temperature of the transpiration fluid leaving the plate, and the indicated plate temperature. The mass flux is obtained by the equation

$$\dot{m}'' = \frac{\dot{m}}{A}(\text{KFLOW} + \text{KFUDGE}) \ , \qquad (S1.3)$$

where KFLOW accounts for porosity variations in the plate and KFUDGE is an arbitrary correction term on the order of 1 percent.

KFLOW is the ratio of the actual transpired mass flow, passing through the center six-inch section of the plate, to the flow which would pass through that section of a uniform plate. Moffat determined the value for each plate from 72 local flow measurements. KFUDGE was introduced into the model because consistent energy unbalances existed on a plate-wise basis which could best be explained by an error

in $\dot{m}''$. Rather than change KFLOW, which could not be justified experimentally, or change the rotameter calibration, which appeared acceptable when checked, the additive term KFUDGE was introduced into the model.

Since these two correction factors are closely interrelated, action was taken along several paths in the current qualification tests to investigate this problem. First, all the flowmeters were individually calibrated against standard ASME sharp-edged orifices (which were themselves satisfactorily checked in water with a weigh tank measurement system). Two orifices of different sizes were used to measure the same flowmeter flow wherever possible, with good agreement in the resulting calibrations. Both large and small flowmeters were consistently high by 3-5 percent at the low end of their scales. In mid-range and at high flows, the flowmeters were either slightly high or agreed with the orifice. The calibration for each rotameter was curve-fit and entered into the data reduction program. Secondly, measurements were made of the flow passing through the left, right, and center six-inch portions of each plate. To do this, a small plexiglas plenum was designed which exactly covered the desired area, being sealed on the lower edges, and containing orifice holes in its upper surface. The measured pressure drop across the orifice holes allowed the calculation of the relative flow rate between each section, after suitable corrections were made for the effect of the measuring device on the flow being measured. From these measurements, values of KFLOW were recomputed. Generally, the new values are one to two percent higher than the previous values. Thirdly, the value of KFUDGE was set to zero for all plates.

With no main-stream flow, the term HTRANS in eqn. (S1.1) is zero, and the energy unbalance can be expressed by the equation,

$$HTFRAC = 1 - \frac{ECONV}{ENDEN-LOSSES} \qquad (S1.4)$$

Tests were conducted at three rates of both blowing and sucking over the full range available. As an example of the magnitudes involved, at full blow the transpiration flow rate is about 13 CFM per plate and the velocity of the fluid leaving the plate 0.44 fps. The energy unbalances for these experiments are presented in Fig. S1.4. The band of scatter is reduced over the previous results of Moffat [22] and Thielbahr [6], but no significant differences are noted. For each transpiration rate, the mean, standard deviation, and calculated uncertainty interval of the results for all plates are presented on the figure. In Table II, the mean and standard deviations for each plate and various combinations of transpiration rate are tabulated. In general, the standard deviations for all plates are within uncertainty ranges calculated for each transpiration rate. However, the results of several tests conducted under the same conditions were quite repeatable, indicating that the unbalance measurements might possibly be reasonable estimations of fixed errors, and that the true uncertainty bands are in reality not as wide as the uncertainty analysis predicts.

F.2 Boundary Layer Energy Balances

Each experimental run consists of y-traverse data, including hydrodynamic and temperature profiles, in addition to the surface heat transfer measurements. Using this information, the energy transferred to the boundary layer from the wall, calculated from the surface heat transfer data, can be compared to the increase in energy in the boundary layer as determined from the measured profiles. A simple energy balance on a two-dimensional boundary layer gives the equation

Plate	MEAN			STANDARD DEVIATION		
	Blowing and Sucking Modes	Blowing Modes Only	Sucking Modes Only	Blowing and Sucking Modes	Blowing Modes Only	Sucking Modes Only
1	-0.13	-3.27	3.00	3.29	0.73	1.21
2	-0.85	-2.03	0.33	2.19	2.40	1.02
3	-0.90	1.53	-3.33	2.65	0.26	1.46
4	-1.30	-0.33	-2.27	1.82	0.39	2.15
5	-0.67	-0.30	-1.03	0.66	0.67	0.41
6	0.97	0.67	1.27	0.79	1.02	0.19
7	-0.87	0.97	-2.70	1.91	0.66	0.36
8	-0.58	-0.67	-0.50	0.42	0.53	0.24
9	-2.05	-1.53	-2.57	0.76	0.69	0.39
10	-1.32	-1.03	-1.60	0.51	0.56	0.22
11	-0.97	-0.67	-1.27	0.58	0.33	0.62
12	0.67	0.17	1.17	0.79	0.62	0.61
13	1.35	0.10	2.60	1.80	1.31	1.28
14	0.10	-1.30	1.50	1.56	0.49	0.83
15	0.08	1.03	-0.87	1.63	0.65	1.76
16	1.82	2.40	1.23	0.88	0.71	0.61
17	-0.17	0.47	-0.80	1.17	0.17	1.37
18	1.93	0.83	3.03	2.59	0.95	3.18
19	-2.15	-1.07	-3.23	1.87	0.84	1.98
20	-0.42	0.77	-1.60	2.00	0.12	2.28
21	0.87	1.97	-0.23	1.33	0.45	0.95
22	-0.02	-0.10	0.07	1.23	0.99	1.43
23	-1.22	-2.03	-0.40	1.20	1.07	0.65
24	-0.98	-0.27	-1.70	1.03	0.95	0.45

TABLE II. TRANSPIRATION ENERGY BALANCE RESULTS: SUMMARY BY PLATE

$$St = \frac{1}{\rho_\infty U_\infty i_{s,o}} \frac{d}{dx} (\Delta_2 \rho_\infty U_\infty i_{s,o}) - F \ , \qquad (S1.5)$$

where the enthalpy thickness, Δ_2 , is defined as

$$\Delta_2(x) = \int_o^\infty \frac{\rho U}{\rho_\infty U_\infty} \cdot \frac{i_s}{i_{s,o}} \, dy \qquad (S1.6)$$

Operationally, Eqn. (S1.5) has been utilized in the following integral form to calculate Δ_2 at each plate,

$$\Delta_2(x) = \frac{1}{(\rho_\infty U_\infty i_{s,o})_x} (\rho_\infty U_\infty i_{s,o} \Delta_2)_{x=o} + \int_o^x \rho_\infty U_\infty i_{s,o} (St + F) dx \qquad (S1.7)$$

Comparing the enthalpy thickness calculated in this manner to the value calculated from profile measurements provides a check on the performance of the apparatus. The starting value required in Eqn. (S1.7) has been calculated in all test runs by assuming that the profile measurement at the first profile station represents the actual state of the boundary layer, thereby forcing agreement between Eqns. (S1.6) and (S1.7) at that x-position (where Eqn. (S1.6) is calculated using profile data). In all the runs with no transpiration, the enthalpy thickness calculated from profile measurements, Eqn. (S1.6), is consistently lower than the enthalpy thickness calculated from Eqn. (S1.7). The differences in the values of enthalpy thickness vary, in these runs, up to about 6 percent at the end of the accelerated region (no profile measurements were taken beyond this point). This difference represents a variation of approximately 10 percent between the heat transfer calculated from surface measurements and

that calculated from profile data. In runs with blowing and acceleration, the corresponding comparisons are 2 percent and 4 percent. In test 111669, at constant free-stream velocity and no transpiration, the energy unbalance over five feet of the test section is about 11 percent. It is important to note, in regard to these values, that the uncertainty intervals calculated for the enthalpy thicknesses were on the order of ± 3 percent and ± 6 percent, respectively, for Eqns. (S1.7) and (S1.6). On one hand, the absolute differences between the results of Eqns. (S1.7) and (S1.6) are within the calculated uncertainty bands, but, on the other hand, there is recognizable consistency in the trend of the energy unbalance with increasing x. A summary of representative energy unbalances and uncertainty calculations is presented in Table III.

Several possible explanations for a consistent energy unbalance have been considered. Three-dimensional effects, for example, would render the use of Eqn. (S1.7) invalid. In fact, the effects of acceleration on side wall boundary layers in the test channel would cause divergence of the main stream flow, inducing just the trends indicated by the differences noted above. However, the trend is unchanged for the constant free-stream velocity run, whereas growth of the side-wall boundary layers should, by this argument, induce convergence of the main stream under these conditions.

Three-dimensional effects could be caused by other phenomena, such as perturbations in the incoming flow or the vortices which exist in the corners of the rectangular channel. The redesign of the inlet screen pack was undertaken to forestall problems of the former type. The design of the screen pack was based on the wind tunnel work of Bradshaw [46] and others [47,48], and the results of this effort are evident in the uniformity of the free-stream conditions (to be discussed shortly) and the agreement of transverse profiles. Transverse measurements of both velocity and tempera-

Run No.	Plate	Energy Unbalance	$1-\frac{(\Delta_2)_{profile}}{(\Delta_2)_{integr.}}$	Uncertainty in Δ_2 (Eqn. S2-6)	Uncertainty in Δ_2 (Eqn. S2-7)
091069	4	0	0	6.5	2.7
$K=2.0\times10^{-6}$	6	-12.5	-3.8	5.2	2.3
$F=0.0$	7	-11.1	-4.4	5.2	2.1
	8	-9.7	-4.6	5.2	2.0
	10	-9.8	-5.7	5.1	1.8
070869	4	0	0	4.7	2.8
$K=2.5\times10^{-6}$	6	5.7	1.7	4.0	2.4
$F=0.0$	7	-4.6	-1.7	4.1	2.1
	8	-4.0	-1.8	3.7	1.9
	9	-5.9	-3.0	4.6	1.7
	10	-9.1	-5.1	3.9	1.6
072769	4	0.0	0	4.4	2.8
$K=2.5\times10^{-6}$	6	-5.3	-1.7	3.9	2.5
$F=0.002$	7	-7.9	-3.3	3.9	2.2
	8	-11.0	-5.4	3.7	2.0
	9	-6.8	-3.8	4.3	1.8
	10	-8.9	-5.5	3.7	1.7
083069	4	0.0	0.0	3.4	2.7
$K=2.5\times10^{-6}$	6	-9.1	-3.0	3.1	2.3
$F=0.004$	7	-6.3	-2.8	2.7	2.1
	8	0.3	0.1	2.5	1.8
	9	-1.9	-1.1	2.6	1.6
	10	-2.3	-1.5	2.3	1.5
092469	12	0	0.1	3.3	2.5
$K=2.5\times10^{-6}$	15	-16.3	-2.7	3.5	2.2
$F=0.0$	16	-6.9	-1.4	3.5	2.0
High initial	17	-14.5	-3.7	3.5	1.8
Re_M, Re_H	18	-13.2	-3.9	4.0	1.6
	19	-17.5	-5.8	4.0	1.5
101769	4	0	0.1	7.7	2.8
$K=2.5\times10^{-6}$	6	-19.2	-6.2	7.0	2.3
$F=0.0$	8	-13.8	-6.7	6.6	1.9
High Free-Stream Turbulence	10	-14.7	-8.7	6.9	1.7

All results are given in (%).

TABLE III. SUMMARY OF REPRESENTATIVE BOUNDARY LAYER ENERGY BALANCES

ture taken in the region just prior to acceleration and near the end of the acceleration region, with no transpiration, are quite symmetric. Figure S1.5 shows both sets of profiles, and Table IV lists the integral parameters associated with these profiles. The transverse variations in momentum and enthalpy thickness correspond, approximately, to maximum variations from the mean of 2 percent and 4.5 percent, respectively, in the skin-friction coefficient and Stanton number at plate 12. In conclusion, no obvious causes have been detected which would account for the energy unbalance trends noted in the experiments.

F.3 Flat Plate Turbulent Boundary Layer

A basic prerequisite to obtaining heat transfer data in a strong pressure gradient is a demonstration that the test rig can adequately reproduce accepted correlations for

TABLE IV

TRANSVERSE MOMENTUM THICKNESS AND ENTHALPY THICKNESS MEASUREMENTS

Quantity (in.)	x (in.)	$Kx10^6$	z = +3 in.	Center-line	z = -3 in.
θ	13.81	0	0.0690	0.0636	0.0674
Δ_2	13.81	0	0.0535	0.0534	0.0535
θ	33.59	2.5	0.0257	0.0229	0.0234
Δ_2	33.59	2.5	0.0636	0.0600	0.0605

the turbulent boundary layer with no transpiration and a constant free-stream velocity. Such a test was conducted with a free-stream velocity of 23 fps; the experimental results are presented in Fig. S1.6a and compared to the correlation obtained by Moffat and Kays [22] on the same apparatus in 1966 with a free-stream velocity of 43 fps. In Fig. S1.6b two temperature profiles from this test run are compared to another experiment. It can be seen that changes in the inlet section and the mathematical data reduction model have had a negligible effect on rig performance for this type of test run. When corrected for variable property effects by the ratio $(T_o/T_\infty)^{0.4}$, the data is adequately fitted by the expression,

$$St = 0.0128\ R_H^{-.25}\ Pr^{-.5}\ , \qquad (S1.8)$$

obtained earlier by Moffat, and within 2 percent of accepted correlations [49,50].

Temperature and velocity profiles were also obtained at three positions along the test section (14.8, 46.8, and 78.8 inches). As noted in section F.2 the measured plate heat transfer to the boundary layer was 10-11 percent higher than the increase in energy calculated from profiles.

Since other experimenters have substantiated the Stanton number correlations expected under these conditions, this test run presented an opportunity to compare actual results to expected results in an attempt to explain the small differences noted. However, careful scrutiny of both the surface heat transfer data and the profile data was again inconclusive. First, examination of the Stanton number results showed that they are not consistently high compared to the expected correlation. Next, several possible errors in the profile data, and its reduction to enthalpy thickness, were numerically investigated. A low temperature reading tends to lower the measured enthalpy thickness. To consider the magnitude of

effects due to thermocouple conduction error, the laminar Couette flow equation for no transpiration and zero pressure gradient,

$$t^+ = Pr\, y^+ \quad , \qquad (S1.9)$$

was used to predict the temperature for $y^+ \leq 10$. The computed temperatures in the sublayer ranged from 2.4 F higher than the measured temperatures near the wall to 0.7 F higher at $y^+ = 10$. The calculated enthalpy thickness at $x = 78.8$ inches, using these new values, only changed from 0.1905-inch to 0.1907-inch, whereas the enthalpy thickness computed by integration of the energy equation is 0.2079-inch. Assuming a conduction error extending into the turbulent core, where the contribution to the enthalpy thickness is greater, results in a new profile value on the order of 0.1970. Another possibility is that an error exists in the y-position in either temperature or velocity profiles, particularly due to failure to locate the wall accurately. The uncertainty analysis discussed in the previous section assumes a 0.0015 inch uncertainty in this measurement. If the y-position for all temperature profile points is arbitrarily shifted 0.0025 inches away from the wall in the case of the profile at $x = 78.8$ inches, the calculated enthalpy thickness becomes 0.1917 inches. Obviously the integral parameters of the boundary layer are not overly sensitive to any of the possible errors mentioned here, which is an indication of both their usefulness and insensitivity in experiments. The integral parameters are more sensitive to errors in the free-stream and plate temperatures, but both those measurements are much more certain than the probe temperature in a steep temperature gradient. The uncertainty analysis gives, at $x = 78.8$ inches, an uncertainty of ± 0.006 for the profile measurement of enthalpy thickness and ± 0.003 for the value obtained by integrating the energy equation. For convenience, the effects of the errors just discussed are tabulated in Table V.

TABLE V

EFFECT OF EXPERIMENTAL ERRORS ON THE CALCULATED ENTHALPY THICKNESS AT x = 78.8 INCHES IN RUN 111669 (K = 0.0, F = 0.0)

Case	Enthalpy Thickness, Δ_2
Experimental result (Eqn. S2-6)	0.1905 ± 0.006
Integration of energy equation (Eqn. S2-7)	0.2079 ± 0.003
Effect of assumed errors (evaluated by Eqn. S2-6)	
1) Couette flow valid for $y^+ < 10$	0.1907
2) Conduction error: Range 1. Linear from 2.5 F at $y^+ = 0$ to 1.0 F at $y^+ = 10$. Range 2. Linear from 1.0 F at $y^+ = 10$ to 0 F at $y^+ = 500$.	0.1970
3) y-shift of +0.0025-inch	0.1917

Within the uncertainty bands, the measurements of Stanton number and local enthalpy thickness indicate that a small percentage of the energy transferred from the wall is not accounted for by boundary layer profile measurements.

F.4 Free-stream Conditions

Uniformity of the free-stream flow was measured in both the streamwise and cross-sectional directions. All the experiments in the study were conducted with an inlet free-stream velocity of 23 fps. At this velocity, the uniformity of the free-stream velocity in the inlet plane was found to be within 0.05 fps, while the free-stream temperature in the same plane was constant within 0.2 F. The free-stream total pressure showed a maximum streamwise variation of ±0.001

inch H_2O throughout the accelerated region under the condition of strongest acceleration, $K = 2.5 \times 10^{-6}$. The free-stream stagnation enthalpy was not measured under these conditions, but the indicated thermocouple temperature was uniform in the axial direction within ± 0.2 F at a constant free-stream velocity.

The free-stream turbulence level was nominally 0.7 percent. One test series was conducted with a free-stream turbulence intensity of 3.9 percent at the start of acceleration in order to examine the effect of free-stream turbulence on heat transfer performance in strongly accelerated boundary layers. The free-stream turbulence intensity decayed to 0.4 percent and 0.9 percent, respectively, in the recovery region. In the high free-stream turbulence runs, a crossed-rod grid was placed 13 inches upstream of the trip. The grid consisted of 1/4-inch round wooden dowels formed into a square, interlocked mesh (i.e., all of the dowels were in the same plane) on 1-inch centers. The grid design was based in part on the work of Uberoi and Wallis [28], in which, 29-inches downstream of a similar grid, the turbulence was found to be homogeneous with $\overline{u'^2} \approx \overline{v'^2}$. The free-stream energy spectra exhibited in both runs was that of normal turbulence. The spectra were taken in the region just prior to acceleration and are presented in Fig. S1.7.

F.5 Effect of Pressure Gradient

Strong pressure gradients can effect the experimental velocity traverses in several ways. Streamline curvature can (1) cause a probe error due to the angle of the flow to the probe, and (2) result in a significant static pressure gradient normal to the flow streamlines, so that wall measurements of static pressure at a fixed y-position are not sufficient descriptors of the static pressure at the probe. With porous plates, there exists the additional problem in a favorable pressure gradient of a "natural" transpiration

into the upstream side of the plate (sucking) and out the downstream side (blowing), caused by the axial pressure gradient in the free-stream flow. The reversal of transpiration in a given plate occurs when forced transpiration is not present; with forced transpiration, the effect of the pressure gradient is to induce non-uniformity within the plate.

Streamline curvature effects were examined by testing the magnitude of the static pressure gradient normal to the wall. Five wall static taps (0.032 inch diameter sharp-edged holes), were drilled at distances from the wall of 0.75, 1.0, 1.5, 2.0, and 2.5 inches, at two stations in the region of the strongest pressure gradient. Static pressure readings were taken at an acceleration of $K = 2.5 \times 10^{-6}$. At the first station, where $\frac{dp}{dx} = -2.28\ (lb_f/ft^2)/ft$, the velocity varied -0.2% up to 1.5 inches and -0.7% up to 2.5 inches, both normalized by the velocity at 0.75 inches. At the second station, where $\frac{dp}{dx} = -4.45(lb_f/ft^2)/ft$ the measurements were essentially identical to those at the first station. The boundary layer thicknesses under these conditions were about 1.25 inch and 1.0 inch, respectively, at the two stations. By virtue of these results, streamline curvature effects were considered negligible within the boundary layer.

While the pressure-gradient-induced transpiration is undesirable in tests where no transpiration is desired, it is a desirable feature in the blowing tests conducted in this study. The usual objective was to achieve a boundary layer with a constant ratio of $\rho_o V_o/p_\infty U_\infty$ ($\equiv F$). Since U_∞ increases in the x-direction in the accelerated region, it is desirable if, within a given plate, the local transpiration has the same trend. A parametric study of the expected transpiration behavior at various values of K and F was conducted prior to the start of the study. The behavior of the apparatus in this regard can be modeled by assuming that a potential flow model describes the main stream flow, that

the transpiration flow is governed by laminar mechanisms in the porous plates, and that the static pressure in the cavity beneath the plate is uniform. The first two assumptions were substantiated by simple tests. At the high blowing rate, about 13 CFM, the pressure drop across a plate is approximately 12 inches of water. It was decided to limit the deviation from the desired value of the induced transpiration to $F = \pm 0.0003$, a value for which the effects of transpiration on heat transfer are known to be insignificant in constant velocity boundary layers. With this criteria in mind, a maximum limit of $K = 2.5 \times 10^{-6}$ was set for strong accelerations with no transpiration. It is possible, with blowing, to go to considerably higher values of K and still satisfy the criteria on F. The expected distribution of transpiration for the conditions of this study are presented in Fig. S1.8.

F.6 Roughness

The roughness criteria was one of the features of the porous plate taken into consideration in the initial design of the apparatus. The maximum RMS roughness, 0.0002 inch, is well within the laminar sublayer for the experiments discussed in this thesis. While the boundary layer itself becomes thinner in strong accelerations, it is also true that the relative thickness of the laminar sublayer markedly increases. Near the end of the acceleration region, at $K = 2.5 \times 10^{-6}$, with no transpiration, the sublayer thickness is about 0.008 inches. The maximum velocity in the test section was on the order of 80 fps. A study specifically directed at the effect of surface roughness in this apparatus on skin friction in a turbulent boundary layer with constant free-stream velocity is reported by Thielbahr, et al. [6]. The conclusions were that, for velocities up to 86 fps, the experimental data shows no effect of plate roughness. The conditions encountered in the present study meet this criteria.

G. Data Reduction

The method of data reduction relies on a mathematical model of the test apparatus which links the raw experimental data to appropriate representations of the results. The measurement techniques are standard, so the point of interest becomes the interpretation of the measured quantities. The purpose of this section is to clearly explain the assumptions which were made in reducing the raw data to the form of the results presented in this thesis.

G.1 Surface Heat Transfer

The surface heat flux, $\dot{q}_o''$, is presented in the form of Stanton number,

$$St = \frac{\dot{q}_o''}{\rho_\infty U_\infty i_{s,o}} \qquad (S1.10)$$

where $i_{s,o}$ is the stagnation enthalpy referenced to free-stream enthalpy. The determination of the surface heat flux has been discussed in section F.1. Equation (S1.1) is re-arranged to compute the term HTRANS, which is the heat flux, $\dot{q}_o''$. In an attempt to reduce experimental scatter in the Stanton number for the blowing runs, the transpiration energy balance results were incorporated into the computations in the following manner. A non-zero value of HTFRAC (Eqn. S1.4) in the transpiration energy balances reflects an error in one of the terms, ENDEN, ECONV, or LOSSES. Because the measurements associated with the transpiration itself are most subject to uncertainty, the error was wholly attributed, arbitrarily, to the term ECONV. The transpiration energy balance results give HTFRAC at certain values of $\dot{m}''$ over the full range of transpiration in the apparatus. Knowing $\dot{m}''$ for a given plate, and assuming a linear variation between measured energy balance points, the value of HTFRAC can be determined. HTFRAC is thus dependent both on the

plate and mass flux. Note that Eqn. (S1.4) can be written

$$\text{HTFRAC} = \text{HTRANS}/\text{ENNET}$$

where

$$\text{ENNET} = \text{ENDEN} - \text{LOSSES}$$
$$\text{HTRANS} = \text{ENNET} - \text{ECONV} .$$

In boundary layer measurements, ENNET≠ECONV, whereas in the energy balances ENNET≈ECONV. The correction to HTRANS in boundary layer measurements due to the measured energy unbalance can be expressed, approximately, by

$$\text{HTRANS}_{new} = \text{HTRANS}_{old} - (\text{HTFRAC})(\text{ECONV}) .$$

Since St∝HTRANS, the correct Stanton number is formed by writing

$$St_{new} = St_{old} \cdot \text{HTRANS}_{new}/\text{HTRANS}_{old}$$

or

$$St_{new} = St_{old} [1 - (\text{HTFRAC})(\text{ECONV})/\overline{\text{HTRANS}}_{old}]$$

The Stanton number calculations in all the blowing runs were handled in this manner. The final results show less scatter than would exist if the transpiration energy balance results were not utilized.

In the test channel, the free-stream gas temperature and total pressure are recorded 6-inches downstream of the trip, while side-wall static pressure measurements are read every 2-inches down the channel. Assuming constant free-stream total pressure, the free-stream velocity is obtained from Bernoulli's equation for incompressible flow. The free-stream stagnation enthalpy is also assumed constant throughout the channel. Both these assumptions were shown to be valid in the qualification tests. The energy equation is

integrated to obtain the enthalpy thickness at the center of each plate, assuming a starting value at the first plate. Subsequently, the enthalpy thickness at $x = 14$ inches, obtained from profile data, is used to establish the starting condition.

No adjustment to the measured plate Stanton number is applied to correct for variable property effects, since the usual correction may not be applicable to flows with blowing or strong acceleration. The surface heat transfer data is presented as a function of enthalpy thickness Reynolds number, because this dimensionless ratio has proven to be a useful and valid local descriptor of the heat transfer phenomena even with variable wall conditions (both transpiration and temperature) in a constant velocity turbulent boundary layer [44]. While this is not the case in strong acceleration, no better correlating variable has been observed.

G.2 Profile Data

Profile measurements of temperature, velocity, and streamwise velocity fluctuations were taken in the joint investigation represented by this thesis and that of Loyd [23]. A complete discussion of the hydrodynamic profile data is presented by Loyd.

The thermocouple probe measures a temperature somewhere between the static and stagnation temperatures of the flow. Since the velocities in this study are low, the magnitude of the difference between the two temperatures is, at the most, 0.5 F. It has been assumed that the thermocouple probe measures the adiabatic wall temperature; the recovery factor, an unknown function of the probe geometry and flow conditions, is taken to be given by the expression, $r_c = Pr^{1/3}$. Consequently, the static temperature is computed by the equation,

$$T = T_{probe} - r_c \, U^2/2g_c J \quad . \qquad (S1.11)$$

No other corrections were applied to the measured thermocouple readings. The effect of errors due to an incorrect interpretation of the thermocouple reading or to thermocouple position are considered in the uncertainty analysis. The enthalpy thickness at each profile station is determined by Eqn. (S1.6),

$$\Delta_2(x) = \int_0^\infty \frac{\rho U}{\rho_\infty U_\infty} \frac{i_s}{i_{s,o}} \, dy \quad .$$

All the hydrodynamic data were obtained under isothermal conditions by Loyd [23]. Since this data is required in the calculation of enthalpy and momentum thickness for the case of a heated wall, the form in which it should be combined with the temperature profile data must be considered. Thielbahr et al. [6] investigated, both experimentally and numerically by means of a computer solution of a boundary layer model, the possibility that one of the following quantities would be preserved: 1) U/U_∞ , 2) $\rho U/\rho_\infty U_\infty$, or 3) $\frac{\Delta P_{dyn}}{\Delta P_{dyn,\infty}}$. He found that, under similar free-stream conditions, the minimum error in the integral parameters calculated by mixing isothermal and non-isothermal data was achieved by assuming the preservation of U/U_∞ . The differences were less than 1 percent when $0.95 \leq T_\infty(^\circ R)/T_o(^\circ R) \leq 1.05$. The same practice has been followed in this study.

The temperature profile data are presented both in inner region coordinates, T^+ and y^+ , and outer region coordinates, $\overline{T}$ and y/δ_H .

G.3 Computer Programs

The data reduction has been accomplished entirely on an IBM 360-67 computer. The programs were written in Fortran IV. Extensive use has been made of computer plotting

routines where possible. The listings of the three basic programs used in the reduction procedure are included in Supplement 3. In brief, the programs are:

STANTON - reads raw heat transfer run data in order to compute surface heat transfer results and associated uncertainty analysis.

PROFILE - reads raw temperature profile data, and calculated velocity profile results, in order to compute temperature profile information and integral parameters, plus the associated uncertainties.

ENERGY - reads final temperature integral results, and surface heat transfer results, in order to recalculate the plate enthalpy thickness from the energy equation, and to determine the boundary layer energy balance at each profile.

G.4 Uncertainty Analysis

Errors in measured variables, such as temperature or pressure, can be accidental, fixed, or simple mistakes. The uncertainty in the measurement is related to the possible value the error might have in a given measurement. In single-sample experiments, it is not possible to make a straightforward calculation of statistical measurements of error, such as the standard deviation. Instead, the method of Kline and McClintock [29] has been utilized to determine the uncertainty in the calculated results based on estimated uncertainties in the primary measurements. The base uncertainties in the primary measurements have been chosen, following [29], to be the range within which the mean value of the measurement probably lies, given 20:1 odds. For example, by experience it is estimated that the uncertainty interval associated with the measured gas temperature is 0.25 F. This statement says that the odds are 20:1 that the true value of the gas temperature is the recorded value, within

plus or minus 0.25 F. Consequently, the uncertainty intervals which have been selected for the primary measurements are based on experience and the confidence that, at 20:1 odds, the true value lies within the stated range. The intervals used throughout this study are tabulated in Table VI.

In general the reported Stanton number is certain to at least ± 0.00010 Stanton units. The enthalpy thickness Reynolds numbers calculated from the profiles and from integration of the energy equation are, respectively, on the order of ± 6 percent and ± 3 percent uncertain. Selected samples of the uncertainty results are presented in Table VII. It should be noted that the results of the transpiration energy balances have not been incorporated into the reported uncertainties in Stanton number. To show the relation of the energy balances to the measurements, modified heat transfer results are presented, based on the convenient premise that the energy balance results associated with a given transpiration rate are completely certain and can be used to adjust the measured Stanton numbers.

H. Test Procedure

By combining the continuity equation and the definition of the acceleration parameter, K, one obtains

$$K = \frac{-\nu}{U_{\infty,1} h_1} \frac{dh}{dx} , \qquad (S1.12)$$

where the subscript, 1, denotes conditions at the start of acceleration. To achieve a constant value of K and to obtain as long an accelerated region as possible, it is apparent from Eqn. (S1.12) that the slope of the top must be constant and the inlet velocity low. Shakedown experiments determined that 23 fps was the lowest inlet velocity, $U_{\infty,1}$

TABLE VI. PRIME UNCERTAINTY INTERVALS USED (ESTIMATED AT 20:1 ODDS)

VARIABLE	VALUE ASSIGNED	VARIABLE MEANING	UNITS
SURFACE HEAT TRANSFER			
DDELP	0.0020	MANOMETER READING	IN.-H2O
DXX	0.016	STATIC TAP LOCATIONS	INCHES
DCMP	2.000	ROTOMETER READING	%
DTEMPA	0.250	GAS TEMPERATURE	DEG. F.
DTEMPP	0.150	GAS TEMPERATURE	DEG. F.
DPAMB	10.00	AMBIENT PRESSURE	LBF/FT2
DMUP	1.0	ABSOLUTE VISCOSITY	%
DP97LO	0.8000	TRANSDUCER CALIBRATION-PM97,FOR P<.05 IN.-H2O	%
DP97HI	0.4000	TRANSDUCER CALIBRATION-PM97,FOR P>.05 IN.-H2O	%
DP5LO	0.8000	TRANSDUCER CALIBRATION-PM5,FOR P<1.0 IN.-H2O	%
DP5HI	0.4000	TRANSDUCER CALIBRATION-PM5,FOR P>1.0 IN.-H2O	%
D97MIN	0.0005	MINIMUM PM97 UNCER. DUE TO ZERO SHIFT	IN.-H2O
D5MIN	0.0005	MINIMUM PM5 UNCER. DUE TO ZERO SHIFT	IN.-H2O
D97MAX	0.0030	MAXIMUM PM97 UNCER. DUE TO CALIBRATION CHECK	IN.-H2O
D5MAX	0.0030	MAXIMUM PM5 UNCER. DUE TO CALIBRATION CHECK	IN.-H2O
DQRADP	25.0	RADIATION ENERGY TRANSFER	%
DWIND	0.25	INDICATED WATTMETER READING	WATTS
DENZRP	25.0	STARTING ENTHALPY THICKNESS ESTIMATE	%
TEMPERATURE PROFILES			
DTEMPA	0.250	TEMPERATURE	DEG. F.
DPRTMP	0.400	PROBE TEMPERATURE NEAR WALL(FIRST 15 POINTS)	DEG. F.
DPAMB	10.00	AMBIENT PRESSURE	LBF/FT2
DMUP	1.0	ABSOLUTE VISCOSITY	%
DELY	0.0015	PROBE POSITION REL. TO WALL	INCHES

TABLE VII

SELECTED SAMPLES OF EXPERIMENTAL UNCERTAINTY CALCULATIONS

Run	Plate	x(in.)	$St \times 10^5$	$\Delta St \times 10^5$	Re_H	ΔRe_H
091069-1	4	14	287	7	726	21
$K = 1.99 \times 10^{-6}$	6	22	246	7	1054	26
$F = 0.0$	10	38	176	4	1781	37
	15	58	184	3	3352	63
070869-1	4	14	290	8	631	15
$K = 2.55 \times 10^{-6}$	6	22	249	7	886	18
$F = 0.0$	10	38	157	4	1433	26
	15	58	191	3	2701	45
072769-1	4	14	219	8	844	21
$K = 2.50 \times 10^{-6}$	6	22	181	8	1234	27
$F = 0.002$	10	38	139	5	2269	44
	15	58	114	5	4521	84
083069-1	4	14	151	10	1078	27
$K = 2.60 \times 10^{-6}$	6	22	119	9	1599	35
$F = 0.004$	10	38	104	7	2959	52
	15	58	68	7	6248	104
092469-1	4	14	289	8	621	16
$K = 2.50 \times 10^{-6}$	12	46	233	7	1557	30
$F = 0.0$	15	58	210	6	1866	35
	19	74	134	3	2368	43
101769-1	4	14	286	7	579	18
$K = 2.56 \times 10^{-6}$	6	22	255	7	846	21
$F = 0.0$	10	38	150	3	1411	29
	15	58	198	3	2864	51
111669-1	4	14	297	7	620	13
$K = 0.0$	10	38	236	7	1370	24
$F = 0.0$	16	62	218	6	2023	33
	22	86	210	6	2623	42

for which a turbulent boundary layer could be obtained at the start of the test section, i.e., plates 1 or 2. The inlet height of the test channel, h_1, is 6 inches. Consequently, dh/dx is uniquely determined for a selected K. At $K = 2.5 \times 10^{-6}$ about five plates, extending over 20 inches, were within the region of constant dh/dx. For most test runs, the acceleration started 18-inches from the beginning of the test channel. In tests 092469 and 100269, where a thick boundary layer was desired at the start of the accelerated region, the first bend in the top was located 53-inches from the beginning of the test channel.

In a complete test run, the experimental data consisted of surface heat transfer measurements and profile traverses with a pitot probe, hot-wire, and thermocouple probe. The configuration of the test duct and the profile locations are illustrated in Fig. S1.9. The hydrodynamic data, both pitot probe and hot-wire, was taken under nearly isothermal conditions in the test channel, usually on separate days. To obtain the surface heat transfer data and the temperature profiles, care was taken to ensure that the apparatus had been operating at a steady state condition for at least an hour prior to testing. The thermocouple probe was referenced to the free-stream temperature. If the free-stream temperature changed more than 1 F during a profile, the data was discarded. Several tests with this referencing scheme showed that, for variations up to 1 F, the calculated enthalpy thickness was virtually unchanged. Surface heat transfer runs were conducted both before and after the temperature profiles were obtained, in order to confirm the achievement of steady state conditions.

Free-stream velocity and transpiration rate measurements were taken in conjunction with both the hydrodynamic and thermal tests.

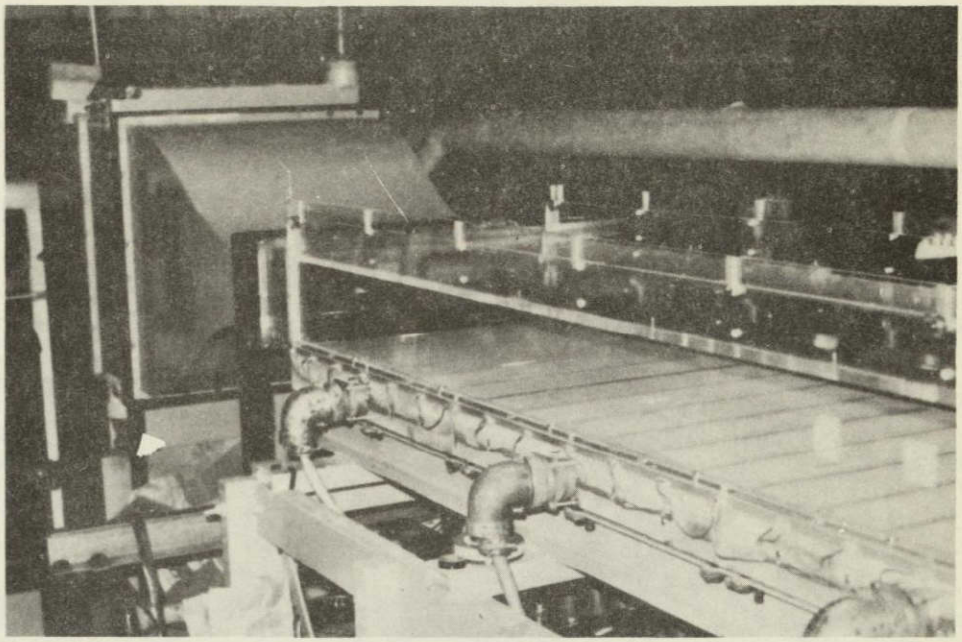

Fig. S1.1 Photograph of the test section entry region, showing the 4:1 contraction and approximately 15 of the 24 test plates.

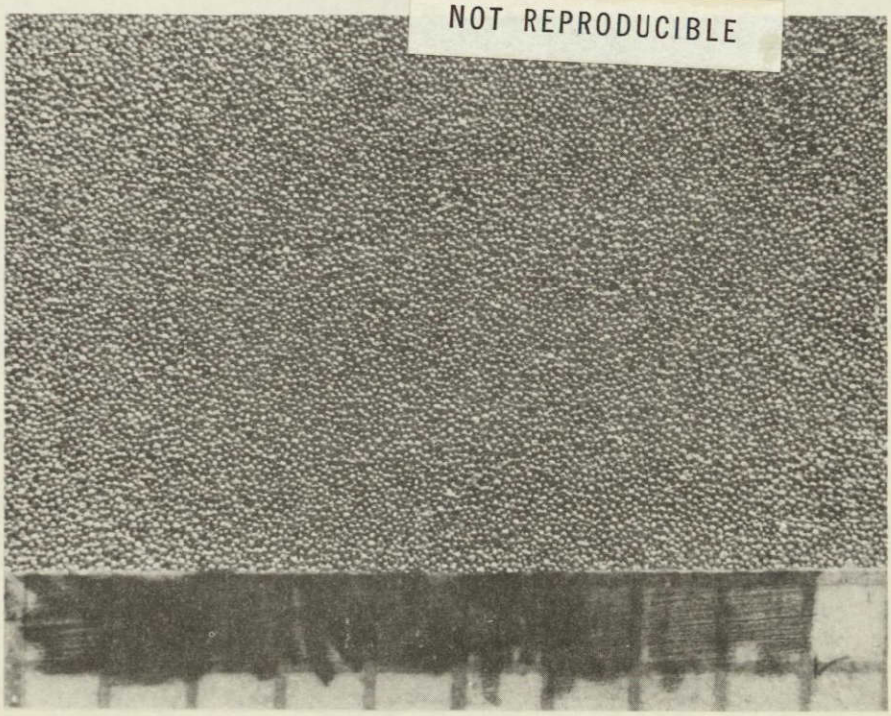

Fig. S1.2 Closeup of plate surface (1 mm squares).

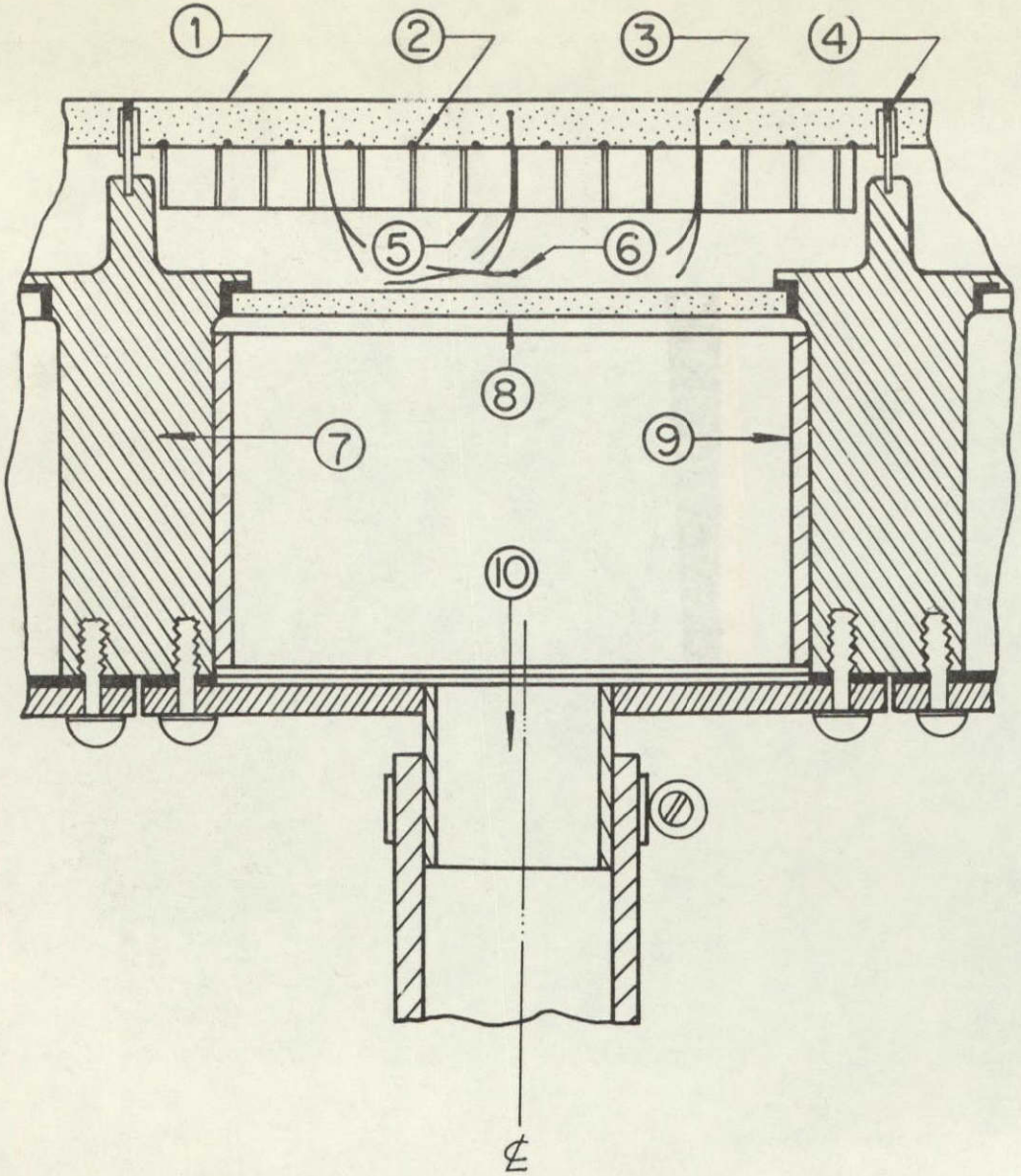

1. Porous plate
2. Heater wires
3. Thermocouples
4. Support webs
5. Honeycomb
6. Thermocouple
7. Base casting
8. Pre-plate
9. Balsa insulation
10. Delivery tube

Fig. S1.3 Cross-section view of a typical compartment.

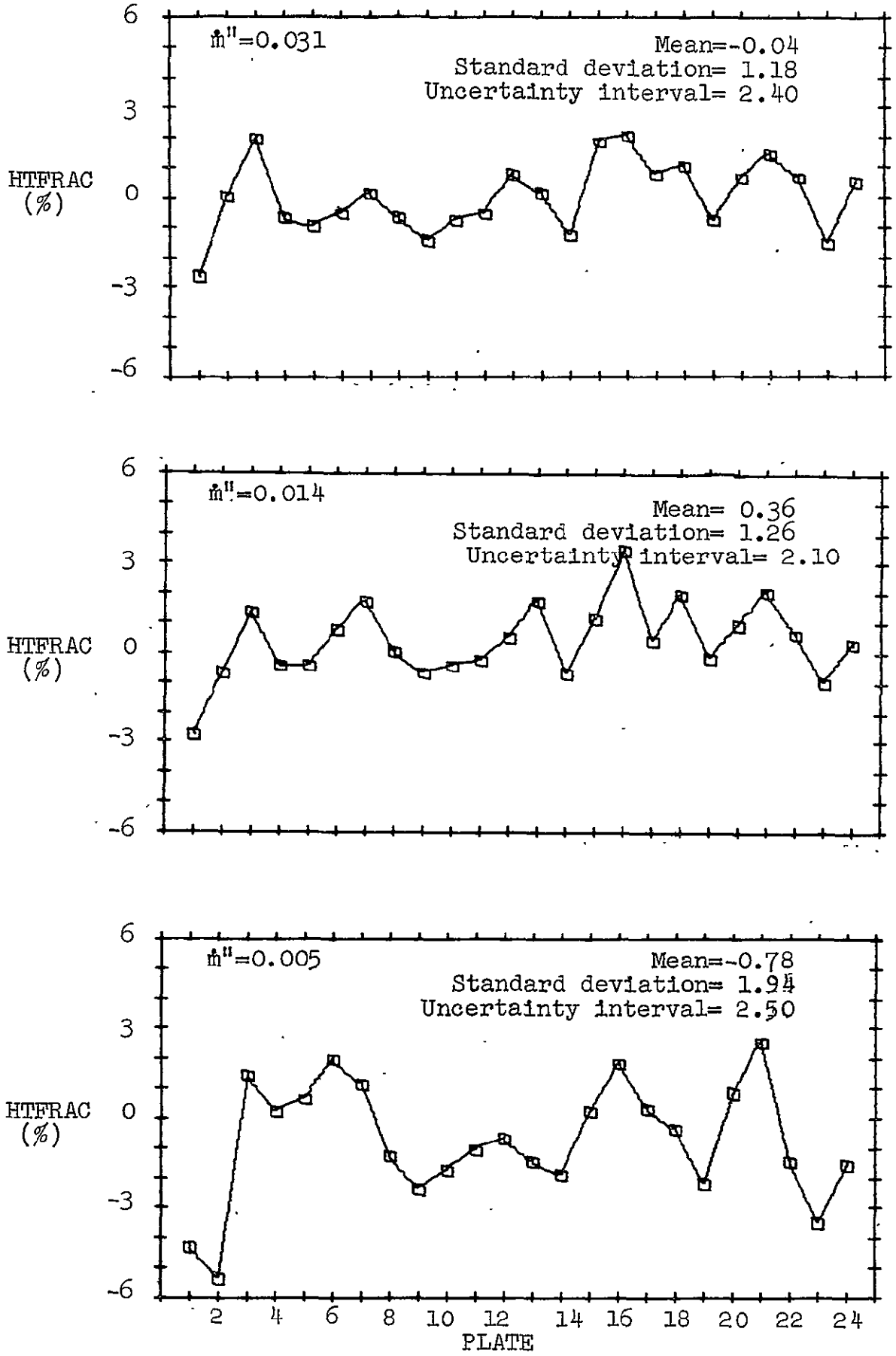

Fig. S1.4a Blowing energy balances

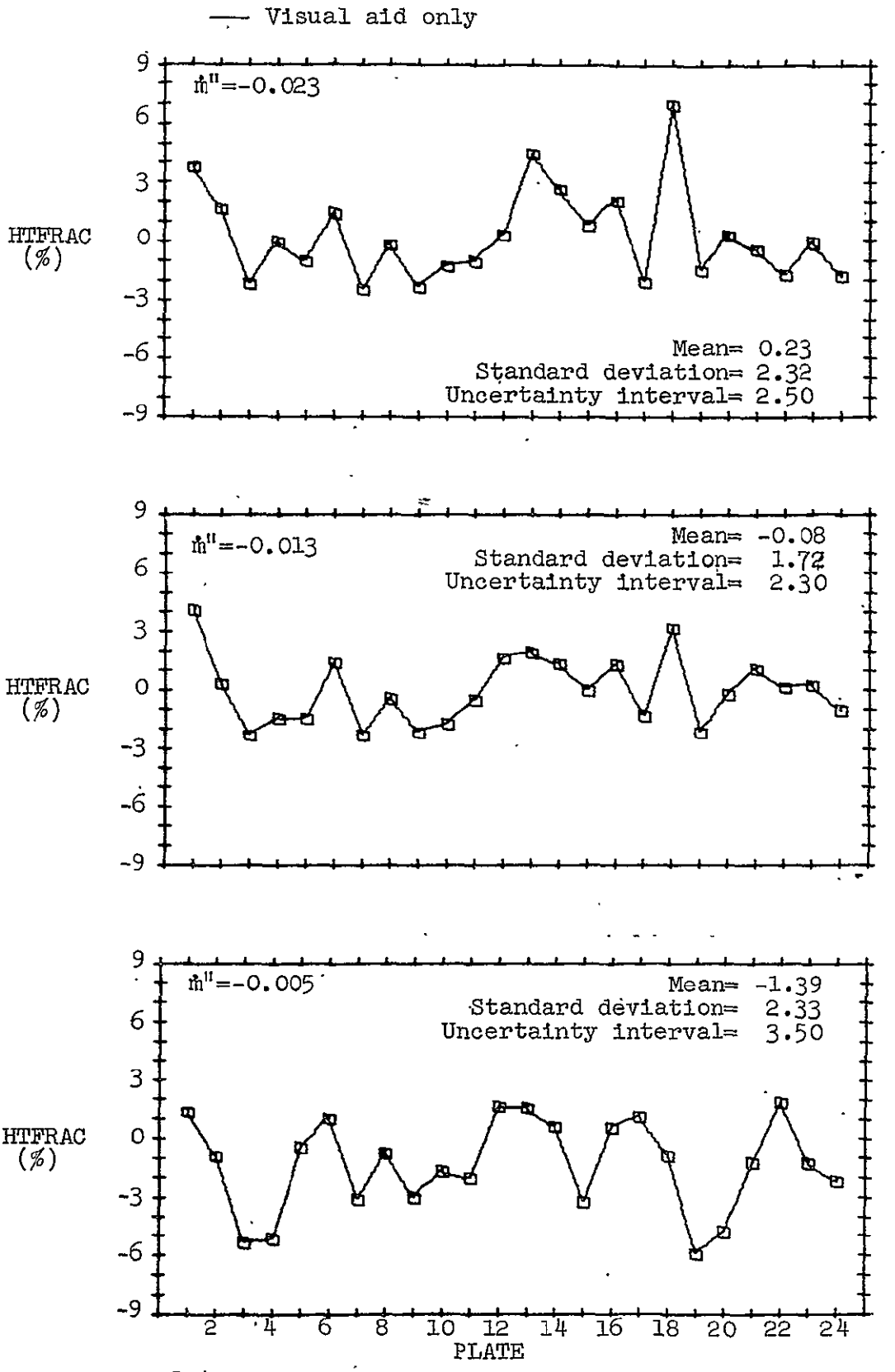

Fig. S1.4b Sucking energy balances

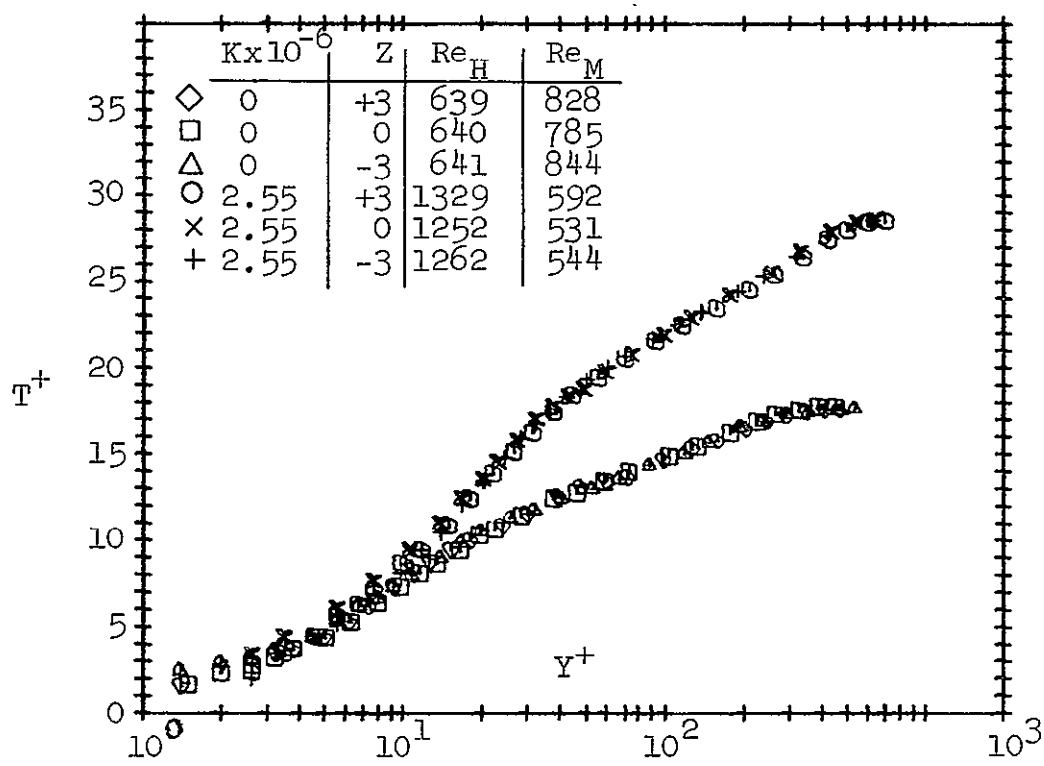

Fig. S1.5. Transverse temperature profiles in inner region coordinates.

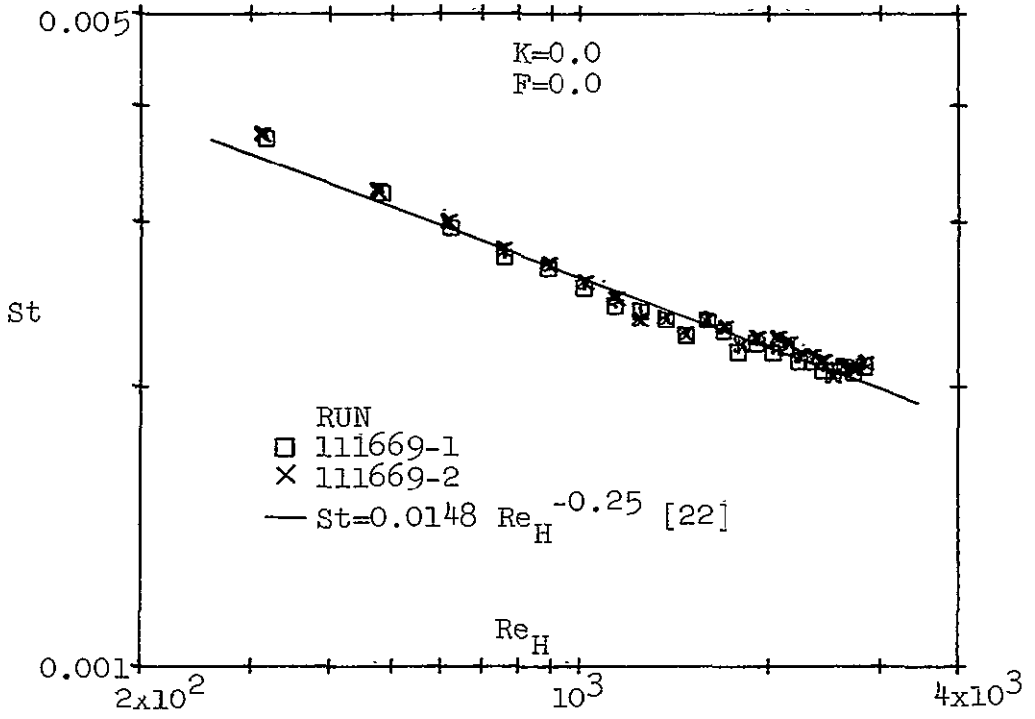

Fig. S1.6a. Surface heat transfer results for the turbulent boundary layer on a flat plate.

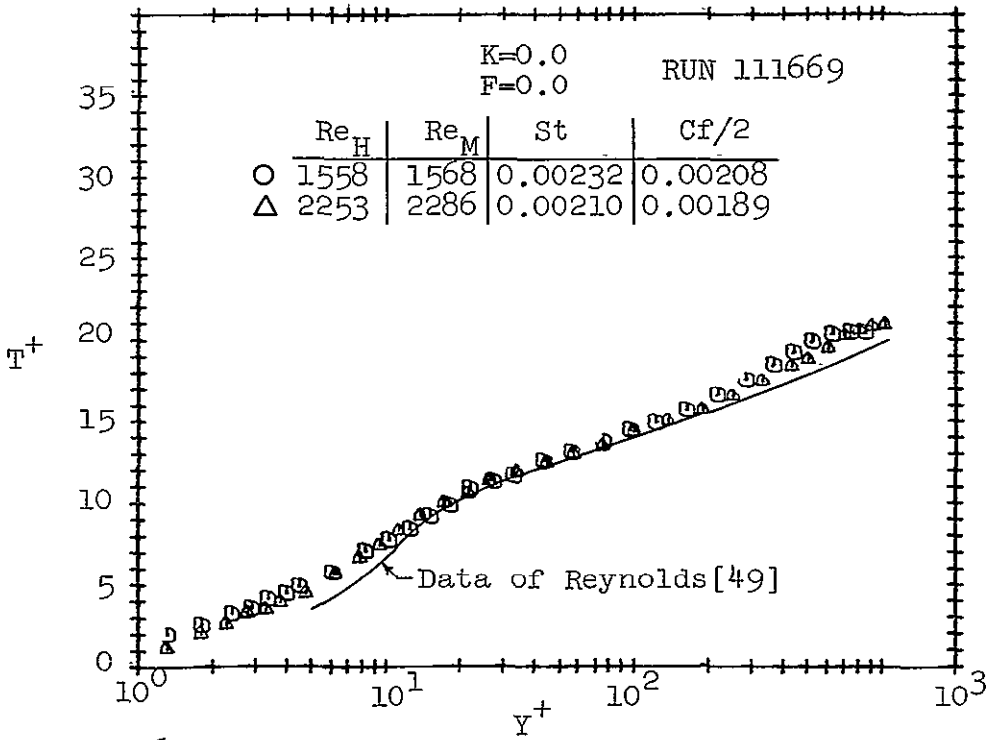

Fig. S1.6b. Temperature profile results for the turbulent boundary layer on a flat plate.

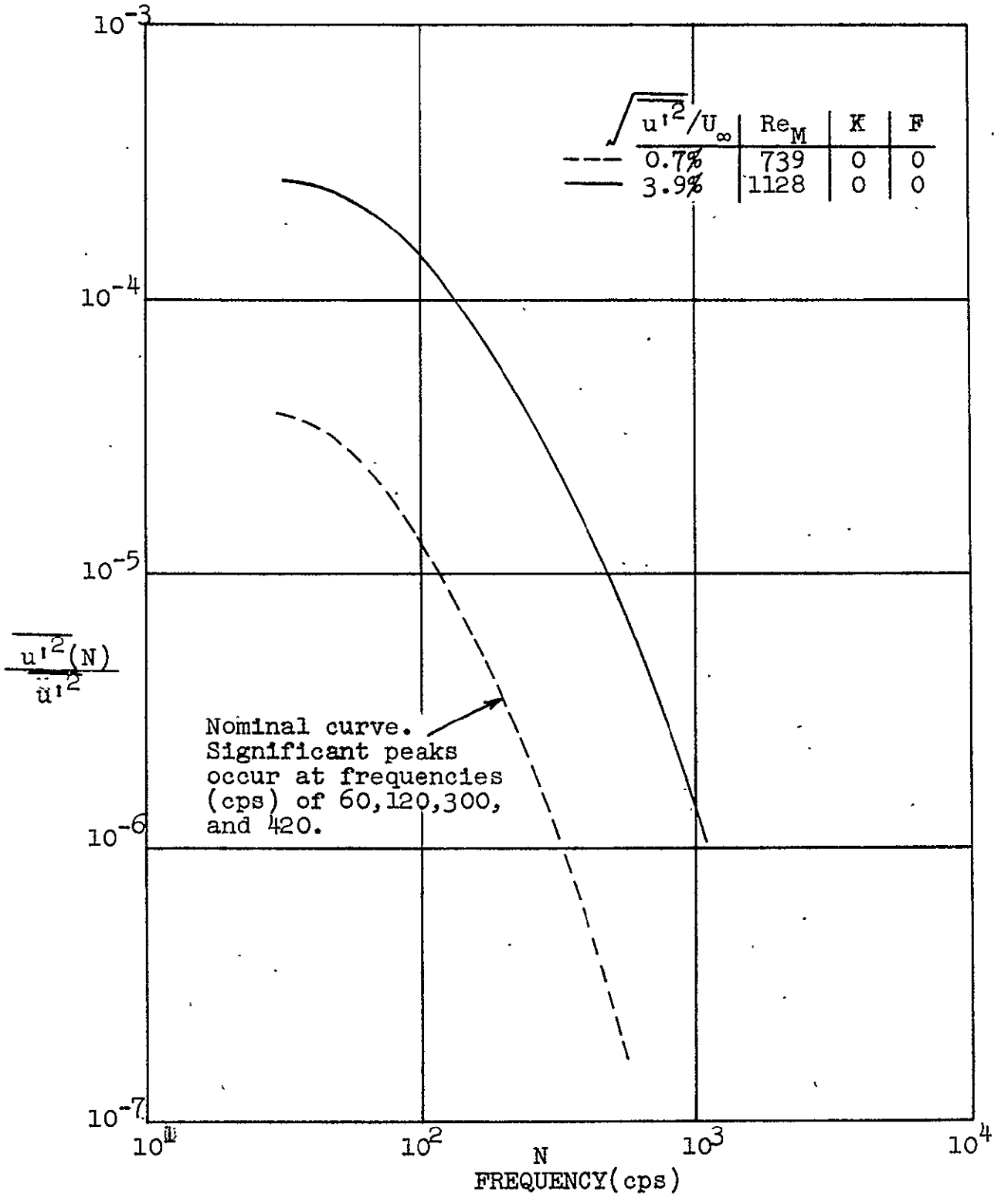

Fig. S1.7. Free-stream energy spectra for low and high turbulence. Data recorded at x=14-inches, just prior to the region of acceleration.

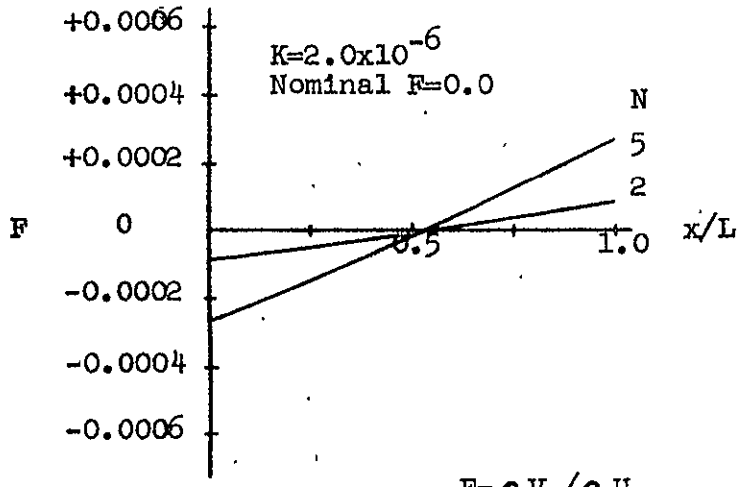

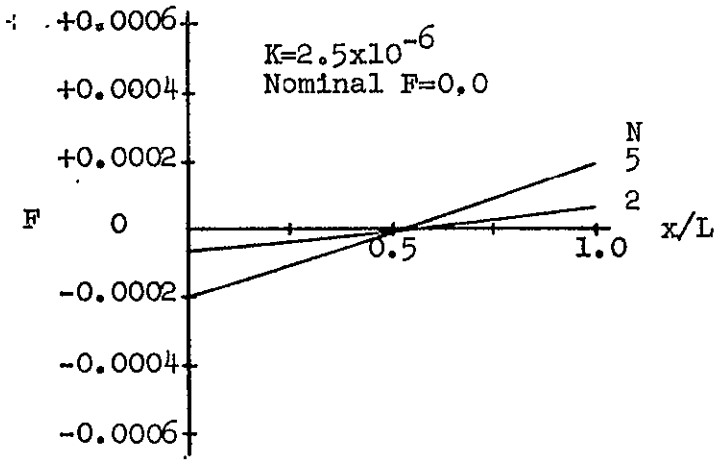

$F = \rho_o V_o / \rho_\infty U_\infty$ L=Plate width x=Streamwise coordinate(x=0 at start of each plate)

N=Order of plate in pressure gradient region

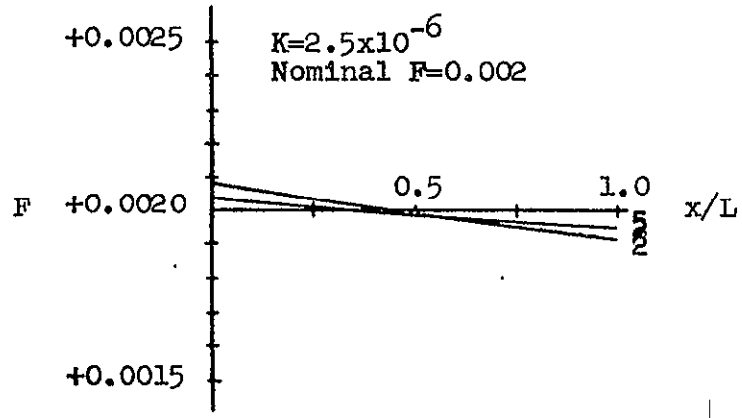

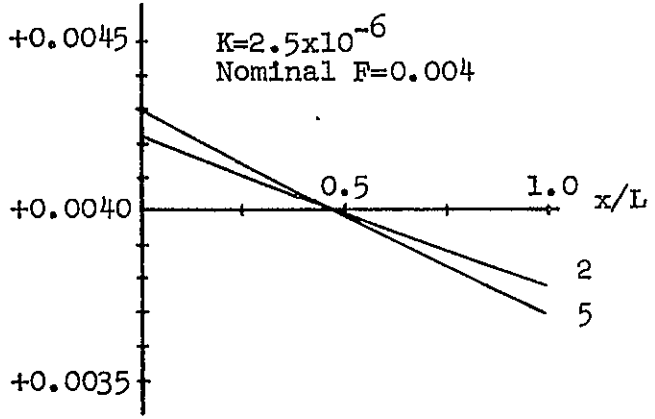

Fig. S1.8 Effect of pressure gradient on local transpiration rate in strong accelerations in present test apparatus

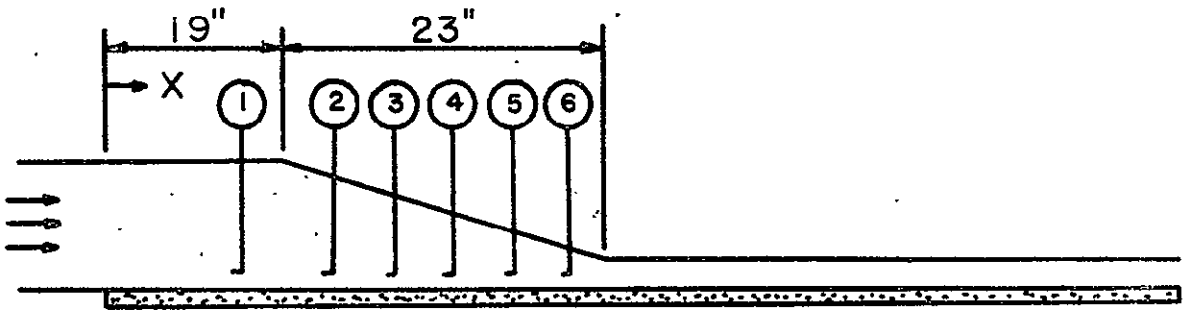

All runs except 092469 and 100269

Profile Number	Plate	x(in.)	Symbol
1	4	13.81	□
2	6	21.81	○
3	7	25.86	△
4	8	29.81	+
5	9	33.59	×
6	10	37.46	◇

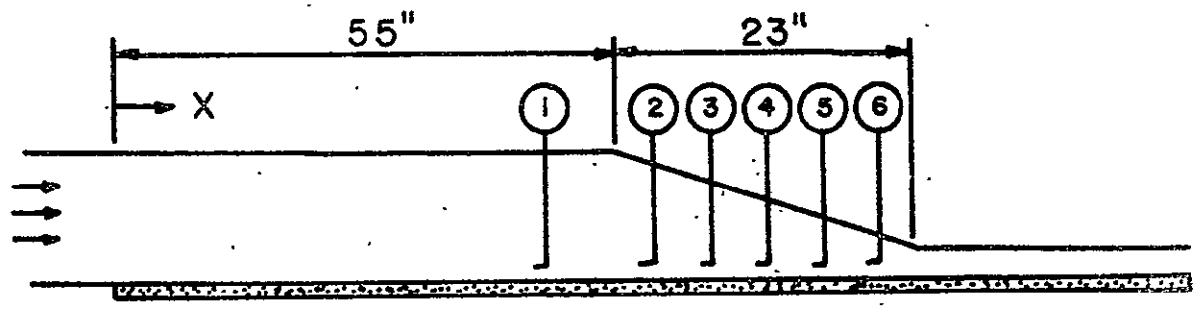

Runs 092469 and 100269

Profile Number	Plate	x(in.)	Symbol
1	12	46.76	□
2	15	58.94	○
3	16	62.86	△
4	17	66.76	+
5	18	70.69	×
6	19	74.58	◇

Fig. S1.9 Test duct configurations and profile locations

SUPPLEMENT 2

TABULATION OF EXPERIMENTAL DATA

A. Organization of Tables and Figures

General

The tabulation of experimental data consists of surface heat transfer data, temperature and velocity profiles, and plots. Each experiment, defined as a specified set of initial and boundary conditions, usually includes several surface heat transfer runs (repeated under the same conditions) and one set of profiles. The velocity profile data is taken from the work of Loyd [23]. The Stanton number quoted for each profile was obtained by interpolating from a smoothed curve of the Stanton number results. Note that selected profile information is included in the tabulation of the first surface heat transfer run. It should be noted that a constant surface temperature was maintained in all the experiments.

All of the data for a given experiment are presented together. The arrangement of the experiments is discussed below. For each experiment, the following format is used:

- Surface heat transfer data
- Summary of profile results
- Profile data
- Plots:

  $St - Re_H$

  $T^+ - y^+$

  $\overline{T} - y/\delta_H$

  $Q^+ - y/\delta_M$

The non-dimensional local heat flux, Q^+, was computed in connection with the calculation of turbulent Prandtl

number. Each plot is not presented for each experiment, though the first three are shown for all but two cases.

Careful comparison of the tabulated velocity profile data to that of Loyd [23] will reveal that the data tabulated here are interpolated from Loyd's results for the y-positions at which the temperature data was taken. The procedure followed was to assume that $U(y)/U_\infty)_{x=const}$ is similar in both the isothermal conditions of the hydrodynamic tests and the non-isothermal state in the heat transfer tests. The validity of this assumption is discussed in Supplement 1. One result of the temperature difference across the boundary layer is to slightly alter the momentum thickness Reynolds number, Re_M, compared to its isothermal value. In referring to the thesis of Loyd, a velocity run number listed here as, for example, Run 71669-1 will be listed there as Run 71669.

Nomenclature of Tables

AMB	ambient
BARO PRES	barometric pressure, in. Hg.
BASE	refers to cast substructure of test apparatus
COVER	refers to reflecting cover, facing test surface, in the rectangular channel
CF2 or CF/2	$C_f/2$
DELH or THERMAL B.L. THICKNESS	δ_H, in.
DELM or HYDRO B.L. THICKNESS	δ_M, in.
DELTA2 or ENTHALPY THICKNESS	Δ_2, in.
F	$\dot{m}''/(\rho_\infty U_\infty)$
GAS	refers to free-stream condition
K	$\frac{\nu}{U_\infty}\frac{dU_\infty}{dx}$

PL	plate number
Q^+	heat flux ratio $(= \dot{q}''/(\rho_\infty U_\infty i_{s,o} St))$
REH or ENTHALPY RE.	$Re_H = \frac{U_\infty \Delta_2}{\nu}$
REL HUM	relative humidity
REM or MOMENTUM RE.	$Re_M = \frac{U_\infty \theta}{\nu}$
ST	St
TBAR	$\overline{T} = \frac{T - T_o}{T_\infty - T_o}$
TEMP	temperature, ^oF
TGAS or TINF	T_∞, free-stream temperature, ^oF
THETA or MOMENTUM THICKNESS	θ , in.
TO	T_o , wall temperature, ^oF
TPLUS	$T^+ = \frac{\overline{T}\, U_\tau}{St\, U_\infty}$
U/UINF	U/U_∞
UPLUS	$U^+ = U/U_\tau$
VEL or UINF	U_∞ , fps
X	x-distance from start of first plate, in.
Y	y-distance normal to plate, in.
Y/DELM	y/δ_M
YPLUS	$\frac{yU_\tau}{\nu}$

Symbols and Abbreviations

Stanton runs:

Order	Symbol
-1	⊡
-2	X
-3	△

Profiles: See Fig. S1.9 for explanation. A symbol code is also shown on each plot.

Titles: The run number consists of the date and the order of the run. The acceleration parameter, K, and the blowing fraction, F, are given for each run. The letters following this information are one of four sets:

NE - near-equilibrium. The experimental conditions are such that the momentum thickness Reynolds number, Re_M, at the start of acceleration is as close as possible to the asymptotic value associated with the given K. The thermal and momentum layers are approximately of equal thickness, i.e., $\delta_H/\delta_M \approx 1$. See Chapters 1 and 2 for further details.

IC - initial condition. The initial conditions at the start of acceleration were varied, meaning either that Re_M is far away from the asymptotic value, or that $\delta_H/\delta_M \neq 1$.

BC - boundary condition. The boundary conditions were varied to examine a particular effect. The effects studies were a high free-stream turbulence level, and step-changes in blowing within the acceleration region.

FP - flat plate boundary layer

Purpose of Experiments

NE:

The near-equilibrium test series was conducted to examine the effect of acceleration, combined with blowing, on heat transfer in the turbulent boundary layer. The experiments in this series were:

Date	$K \times 10^6$	F
091069	1.99	0.0
070869	2.55	0.0
072769	2.50	0.002
083069	2.60	0.004

IC:

These tests were all conducted at nominal values of $K = 2.5 \times 10^{-6}$ and $F = 0$. For Run 071569, the first three plates in the test apparatus were unheated, with the same hydrodynamic conditions as Run 070869, so that $\delta_H/\delta_M < 1$. In Run 092469, the momentum thickness Reynolds number entering the region of acceleration is considerably higher than the asymptotic value. In Run 100269, the first ten plates were unheated, with the same hydrodynamic conditions as Run 092469, resulting in $\delta_H/\delta_M < 1$.

BC:

This test series was conducted at a nominal value of $K = 2.5 \times 10^{-6}$. The free-stream turbulence level was increased, by means of a crossed-rod grid, in Run 101769 in order to study the effect of the increased turbulence level.

In Run 102469, the blowing fraction, F, was stepped from 0 to 0.004 in the center of the acceleration region, while in Run 111369 F was stepped from 0.004 to 0 at the same location.

FP:

The flat plate turbulent boundary layer experiment was conducted in order to validate the performance of the apparatus.

B. Data

The experimental data is tabulated in the following order:

Date	$Kx10^{-6}$	F	Designation
091069	1.99	0.0	NE
070869	2.55	0.0	NE
072769	2.50	0.002	NE
083069	2.60	0.004	NE
071569	2.55	0.0	IC
092469	2.50	0.0	IC
100269	2.50	0.0	IC
101769	2.56	0.0	BC
102469	2.50	0.0	BC
111369	2.50	0.0	BC
111669	0.0	0.0	FP

Following these data, a table of some ratios formed from the boundary layer integral parameters is presented.

RUNS 091069-1
091069-2

K=1.99 x 10^{-6}

F=0.0

NE

RUN 091069-1 K=1.99X10-6 F=0.0 NE

DATE 91069 RUN NO. 1
AMB TEMP 80.30 BASE TEMP 82.06 GAS TEMP 74.37 COVER TEMP 75.38 BARO PRES 29.83 REL HUM 0.50

PL	X	VEL	K	REH	ST	REM	CF2	TO	F
2	6	29.64	0.859E-08	364.	0.00330			96.8	0.0000
3	10	29.49	-0.640E-07	553.	0.00304			96.7	0.0000
4	13.81	29.50	0.126E-06	718.	0.00284	1038.	0.00231	96.7	0.0000
5	14	29.17	0.126E-06	726.	0.00287			96.7	0.0000
6	18	29.86	0.613E-06	886.	0.00268			96.8	0.0000
6	21.81	32.20	0.168E-05	1006.	0.00246	1064.	0.00254	96.6	0.0000
6	22	31.99	0.168E-05	1054.	0.00246			96.6	0.0000
7	25.86	36.50	0.203E-05	1154.	0.00218	942.	0.00254	96.5	0.0000
7	26	36.49	0.203E-05	1213.	0.00217			96.5	0.0000
8	29.81	42.10	0.196E-05	1257.	0.00197	804.	0.00254	96.4	0.0000
8	30	42.52	0.196E-05	1263.	0.00196			96.7	0.0000
9	33.59	50.10	0.203E-05	1479.	0.00185	747.	0.00254	96.3	0.0000
9	34	51.42	0.203E-05	1501.	0.00184			96.5	0.0000
10	37.46	62.20	0.206E-05	1655.	0.00176	677.	0.00254	96.2	0.0000
10	38	64.59	0.206E-05	1701.	0.00176			96.5	0.0000
11	42	83.97	0.852E-06	2042.	0.00178			96.6	0.0000
12	46	86.40	0.846E-08	2390.	0.00200			96.5	0.0000
13	50	86.42	0.619E-08	2765.	0.00197			96.3	0.0000
14	54	86.39	-0.718E-08	3018.	0.00187			96.8	0.0000
15	58	86.32	0.361E-08	3352.	0.00184			96.7	0.0000
16	62	86.28	-0.122E-08	3690.	0.00177			96.6	0.0000
17	66	86.34	0.582E-08	3979.	0.00178			96.6	0.0000
18	70	86.49	0.321E-08	4287.	0.00174			96.6	0.0000
19	74	86.46	-0.107E-07	4601.	0.00172			96.5	0.0000
20	78	86.40	0.800E-08	4671.	0.00168			96.6	0.0000
21	82	86.53	0.449E-08	5143.	0.00167			96.7	0.0000
22	86	86.55	-0.239E-08	5436.	0.00164			96.6	0.0000
23	90	86.47	-0.974E-08	5734.	0.00162			96.6	0.0000

RUN 091069-2 K=1.99X10-6 F=0.0 NE

DATE 91069 RUN NO. 2
AMB TEMP 79.26 BASE TEMP 82.31 GAS TEMP 73.78 COVER TEMP 74.79 BARO PRES 29.83 REL HUM 0.53

PL	X	VEL	K	REH	ST	TO	F
2	6	29.70	-0.159E-06	370.	0.00327	96.4	0.0000
3	10	29.48	0.815E-07	556.	0.00302	96.2	0.0000
4	14	29.33	0.627E-07	731.	0.00283	96.2	0.0000
5	18	29.98	0.658E-06	897.	0.00267	96.2	0.0000
6	22	32.25	0.160E-05	1057.	0.00242	96.1	0.0000
7	26	36.61	0.192E-05	1218.	0.00216	96.0	0.0000
8	30	42.78	0.204E-05	1381.	0.00197	96.1	0.0000
9	34	51.60	0.200E-05	1562.	0.00183	96.1	0.0000
10	38	64.81	0.204E-05	1786.	0.00174	96.0	0.0000
11	42	84.17	0.849E-06	2058.	0.00178	96.1	0.0000
12	46	86.61	0.862E-08	2397.	0.00206	95.9	0.0000
13	50	86.66	0.648E-08	2764.	0.00196	95.6	0.0000
14	54	86.63	-0.568E-08	3033.	0.00186	96.2	0.0000
15	58	86.57	0.383E-08	3359.	0.00183	96.1	0.0000
16	62	86.55	-0.122E-08	3705.	0.00175	95.9	0.0000
17	66	86.60	0.551E-08	3991.	0.00177	96.0	0.0000
18	70	86.75	0.317E-08	4293.	0.00173	96.0	0.0000
19	74	86.71	-0.111E-07	4609.	0.00170	95.9	0.0000
20	78	86.65	0.818E-08	4882.	0.00168	96.0	0.0000
21	82	86.78	0.506E-08	5115.	0.00165	96.3	0.0000
22	86	86.81	-0.247E-08	5431.	0.00163	96.1	0.0000
23	90	86.72	-0.104E-07	5758.	0.00160	95.9	0.0000

SUMMARY OF PROFILE RESULTS

RUN C91069-1 K=1.99X10-6 F=0.0 NE

PL	X	VEL	K	F	TO	TINF	DELM	DELP
4	13.81	29.50	0.126E-06	0.0000	96.7	74.0	0.595	0.548
6	21.81	32.20	0.168E-05	0.0000	96.6	74.0	0.631	0.630
7	25.86	36.50	0.203E-05	0.0000	96.5	74.0	0.580	0.595
8	29.81	42.10	0.196E-05	0.0000	96.4	73.0	0.511	0.561
9	33.59	50.10	0.203E-05	0.0000	96.3	73.7	0.412	0.516
10	37.46	62.20	0.206E-05	0.0000	96.2	73.6	0.331	0.443

PL	X	REH	ST	REM	CF2	DELTA2	THETA
4	13.81	718.	0.00284	1038.	0.00231	0.0494	0.0714
6	21.81	1006.	0.00246	1064.	0.00254	0.0633	0.0667
7	25.86	1154.	0.00218	942.	0.00254	0.0638	0.0518
8	29.81	1297.	0.00197	804.	0.00254	0.0617	0.0379
9	33.59	1479.	0.00185	747.	0.00254	0.0588	0.0291
10	37.46	1655.	0.00176	677.	0.00254	0.0530	0.0210

RUN C91069-1 K=1.99X10-6 F=0.0 NE

TEMP. RUN 91069-1	VEL. RUN 90769-1	PLATE 4	X 13.81	ST 0.00284	CF/2 0.00231	UINF 29.5	TGAS 74.0	TO 96.7	F 0.0000
THERMAL B.L. THK. 0.548	HYDRO. B.L. THK. 0.595	ENTHALPY THK. 0.0494	MOMENTUM THK. 0.0714	ENTHALPY RE. 718.	MOMENTUM RE. 1038.	NO. DATA POINTS 28	K 0.126E-06		

YPLUS	TPLUS	UPLUS	Y	TBAR	U/UINF	Y/DELM
0.0	0.0	0.0	0.0000	0.000	0.000	0.000
1.7	2.2	1.8	0.0025	0.136	0.085	0.004
2.4	3.0	2.5	0.0035	0.176	0.119	0.006
3.1	3.8	3.2	0.0045	0.210	0.152	0.008
3.8	4.1	3.5	0.0055	0.240	0.186	0.009
5.3	5.0	5.3	0.0075	0.294	0.254	0.013
6.7	5.8	6.4	0.0095	0.345	0.307	0.016
8.1	6.6	7.5	0.0115	0.391	0.358	0.019
9.4	7.1	8.4	0.0135	0.424	0.401	0.023
11.5	8.0	9.6	0.0165	0.471	0.460	0.028
13.6	8.7	10.2	0.0195	0.511	0.497	0.033
16.5	9.3	11.1	0.0235	0.550	0.535	0.039
20.0	10.0	11.9	0.0285	0.590	0.570	0.048
23.4	10.6	12.4	0.0335	0.624	0.596	0.056
30.5	11.4	13.1	0.0435	0.664	0.631	0.073
37.6	11.8	13.6	0.0535	0.697	0.655	0.090
44.6	12.1	14.0	0.0635	0.717	0.673	0.107
55.2	12.7	14.3	0.0785	0.747	0.694	0.132
69.2	13.2	14.8	0.0985	0.776	0.716	0.165
90.5	13.8	15.3	0.1285	0.809	0.744	0.216
115.1	14.3	16.0	0.1635	0.840	0.775	0.275
150.5	14.9	16.8	0.2135	0.876	0.814	0.359
185.8	15.4	17.6	0.2635	0.905	0.848	0.443
238.8	16.0	18.4	0.3385	0.939	0.893	0.568
309.6	16.5	19.4	0.4385	0.971	0.942	0.736
380.4	16.9	20.1	0.5385	0.989	0.977	0.904
451.1	17.0	20.5	0.6385	0.998	0.994	1.072
521.7	17.0	20.6	0.7385	1.000	0.998	1.240

RUN 091069-1 K=1.99X10-6 F=0.0 NE

TEMP. RUN 91069-1	VEL. RUN 90769-1	PLATE 6	X 21.81	ST 0.00246	CF/2 0.00254	UINF 32.2	TGAS 74.0	TO 96.6	F 0.0000
THERMAL B.L. THK. 0.630	HYDRO. B.L. THK. 0.631	ENTHALPY THK. 0.0633	MOMENTUM THK. 0.0667	ENTHALPY RE. 1006.	MOMENTUM RE. 1064.	NO. DATA POINTS 28	K 0.168E-05		

YPLUS	TPLUS	UPLUS	Y	TBAR	U/UINF	Y/DELM
0.0	0.0	0.0	0.0000	0.000	0.000	0.000
2.0	2.5	1.9	0.0025	0.142	0.094	0.004
2.8	3.7	2.7	0.0035	0.182	0.131	0.006
3.6	4.5	3.4	0.0045	0.221	0.169	0.007
4.4	4.9	4.2	0.0055	0.244	0.206	0.009
5.9	5.8	5.7	0.0075	0.290	0.281	0.012
7.5	7.0	6.9	0.0095	0.344	0.344	0.015
9.2	7.6	8.1	0.0115	0.378	0.401	0.018
11.6	8.9	9.3	0.0145	0.434	0.470	0.023
14.0	9.7	10.4	0.0175	0.473	0.521	0.028
18.0	10.7	11.6	0.0225	0.524	0.583	0.036
22.6	11.6	12.4	0.0275	0.568	0.623	0.044
26.1	12.2	12.9	0.0325	0.598	0.646	0.052
30.1	12.8	13.2	0.0375	0.625	0.667	0.059
34.1	13.2	13.6	0.0425	0.644	0.684	0.067
42.2	13.9	14.1	0.0525	0.677	0.709	0.083
54.2	14.6	14.5	0.0675	0.710	0.730	0.107
66.4	15.1	14.8	0.0825	0.736	0.748	0.131
86.5	15.6	15.2	0.1075	0.762	0.773	0.170
106.7	16.2	15.7	0.1325	0.790	0.793	0.210
147.1	17.0	16.3	0.1825	0.830	0.824	0.289
187.6	17.7	16.8	0.2325	0.861	0.851	0.368
228.0	18.3	17.4	0.2825	0.889	0.877	0.448
288.7	19.0	18.0	0.3575	0.922	0.912	0.567
349.7	19.6	18.7	0.4575	0.955	0.944	0.725
450.8	20.2	19.3	0.5575	0.980	0.978	0.884
531.8	20.5	19.6	0.6575	0.994	0.993	1.042
612.8	20.6	19.7	0.7575	1.000	0.998	1.201

RUN 091069-1 K=1.94X10-6 F=0.0 NE

TEMP. RUN	VEL. RUN	PLATE	X	ST	CF/2	UINF	TGAS	TO	P
91C69-1	90769-1	7	25.86	0.00218	0.00254	36.5	74.0	96.5	0.0000

THERMAL B.L. THK.	HYDRO. B.L. THK.	ENTHALPY THK.	MOMENTUM THK.	ENTHALPY RE.	MOMENTUM RE.	NO. DATA POINTS	K
C.555	0.580	C.C636	0.0518	1154.	942.	27	0.203E-05

YPLUS	TPLUS	UPLUS	Y	TBAR	U/UINF	Y/DELM
0.0	0.0	0.0	C.0000	0.000	0.000	0.000
2.3	3.3	2.3	0.0025	0.142	0.113	0.004
3.2	4.3	3.2	0.0035	0.187	0.159	0.006
4.1	5.0	4.1	0.0045	0.221	0.204	0.008
5.0	5.7	5.0	0.0055	0.247	0.249	0.009
6.8	6.9	6.8	0.0075	0.301	0.340	0.013
8.6	8.0	8.4	C.0095	0.350	0.416	0.016
11.3	9.3	10.1	0.0125	0.405	0.502	0.022
14.1	10.4	11.4	0.0155	0.451	0.568	0.027
17.7	11.6	12.5	0.0195	0.510	0.625	0.034
21.3	12.4	13.4	C.0235	0.545	0.667	0.041
25.0	13.2	13.9	C.0275	0.578	0.693	0.047
29.6	13.9	14.4	0.0325	0.610	0.721	0.056
35.0	14.6	14.9	0.0385	0.638	0.743	0.066
40.5	15.2	15.2	C.0445	0.662	0.759	0.077
49.7	15.8	15.6	0.0545	0.650	0.779	0.094
63.4	16.5	16.0	0.0695	0.718	0.799	0.120
86.2	17.4	16.4	C.0945	0.758	0.823	0.163
109.1	18.1	16.7	0.1195	0.786	0.840	0.206
154.9	19.1	17.3	0.1695	0.828	0.867	0.292
200.7	19.8	17.7	C.2195	0.861	0.891	0.378
246.6	20.4	18.1	0.2695	0.887	0.911	0.464
315.4	21.3	18.6	0.3445	0.923	0.936	0.594
407.3	22.1	19.2	C.4445	0.958	0.966	0.766
499.2	22.7	19.6	0.5445	0.983	0.986	0.938
591.C	23.1	19.8	0.6445	0.997	0.995	1.111
682.8	23.1	19.8	C.7445	1.000	C.999	1.283

RUN 091069-1 K=1.99X10-6 F=0.0 NE

TEMP. RUN	VEL. RUN	PLATE	X	ST	CF/2	UINF	TGAS	TO	P
91C69-1	90769-1	9	33.59	0.00185	0.00254	50.1	73.7	96.3	C.0000

THERMAL B.L. THK.	HYDRO. B.L. THK.	ENTHALPY THK.	MOMENTUM THK.	ENTHALPY RE.	MOMENTUM RE.	NO. DATA POINTS	K
C.516	0.412	C.C588	0.0291	1479.	747.	30	0.203E-05

YPLUS	TPLUS	UPLUS	Y	TBAR	U/UINF	Y/DELM
0.0	0.0	0.0	C.0000	0.000	C.000	0.000
3.1	3.3	2.7	0.0025	0.145	C.130	0.006
4.3	3.9	3.8	0.0035	0.147	0.182	0.008
5.6	4.1	4.8	0.0045	0.155	0.233	0.011
6.8	4.7	5.9	0.0055	0.180	C.285	0.013
8.1	5.6	7.C	0.0065	0.214	0.337	0.016
9.3	6.7	8.C	C.0075	0.234	C.389	0.018
10.5	7.5	8.9	0.0085	0.284	0.434	0.021
13.1	8.9	10.7	C.0105	0.339	0.519	0.025
15.6	10.2	12.1	C.0125	0.389	C.585	0.030
18.C	11.1	13.0	0.0145	0.425	0.634	0.035
21.8	12.5	14.2	C.0175	0.476	C.687	0.042
25.5	13.5	14.9	0.0205	0.513	0.726	0.050
30.6	14.5	15.7	0.0245	0.551	0.763	0.059
35.6	15.4	16.1	C.0285	C.587	0.786	0.069
40.7	16.1	16.4	0.0325	0.613	C.800	0.079
46.9	16.9	16.7	C.C375	0.639	0.816	0.091
54.4	17.4	17.C	C.0435	0.658	0.831	0.105
64.4	18.1	17.4	0.0515	0.686	0.848	0.126
83.4	19.1	17.8	0.0665	0.724	0.869	0.161
108.4	20.1	18.2	C.0865	C.759	C.890	C.210
139.9	20.9	18.6	0.1115	C.792	0.909	0.270
177.6	21.8	19.C	C.1415	0.826	0.927	0.343
221.7	22.7	19.2	0.1765	0.855	0.941	0.428
284.8	23.6	19.5	0.2265	0.890	0.956	0.549
347.7	24.3	19.7	C.2765	C.918	0.967	0.671
442.4	25.2	20.0	0.3515	0.951	0.981	0.852
568.7	26.C	20.2	C.4515	0.980	0.995	1.095
694.8	26.5	20.3	0.5515	0.995	C.999	1.337
820.9	26.6	20.3	C.6515	1.000	1.000	1.580

RUN 091069-1 K=1.99X10-6 F=0.0 NE

TEMP. RUN	VEL. RUN	PLATE	X	ST	CF/2	UINF	TGAS	TO	P
91C69-1	90769-1	8	29.81	0.00197	0.00254	42.1	73.8	96.4	0.0000

THERMAL B.L. THK.	HYDRO. B.L. THK.	ENTHALPY THK.	MOMENTUM THK.	ENTHALPY RE.	MOMENTUM RE.	NO. DATA POINTS	K
C.561	0.511	0.0617	0.0379	1297.	804.	28	0.198E-05

YPLUS	TPLUS	UPLUS	Y	TBAR	U/UINF	Y/DELM
0.0	0.0	0.0	0.0000	0.000	0.000	0.000
2.6	3.9	2.5	0.0025	0.158	0.124	0.005
3.7	4.6	3.5	0.0035	0.185	C.174	0.007
4.7	5.6	4.5	0.0045	0.225	0.224	0.009
5.7	6.2	5.6	0.0055	0.249	0.273	C.011
6.7	7.0	6.6	0.0065	0.281	0.323	0.013
8.9	8.3	8.5	C.0085	0.332	0.416	0.017
11.0	9.4	9.9	0.0105	0.375	C.488	0.021
13.1	10.4	11.0	0.0125	0.416	0.543	0.024
15.2	11.1	12.C	C.0145	0.446	C.591	0.028
18.3	12.3	13.0	0.0175	0.490	0.643	0.034
21.5	13.2	13.8	0.0205	0.525	0.685	0.040
25.7	14.1	14.5	C.0245	0.563	C.719	0.048
32.0	15.1	15.3	0.0305	0.601	0.758	0.060
36.3	15.9	15.6	C.0345	0.630	0.776	0.068
46.8	16.8	16.3	C.0445	0.665	C.808	0.087
57.4	17.5	16.7	C.0545	0.697	0.826	0.107
73.2	18.3	17.1	0.0695	0.728	0.847	0.136
94.3	19.1	17.5	0.0895	0.759	0.867	0.175
126.C	20.0	17.9	0.1195	0.795	0.887	0.234
157.7	20.8	18.2	0.1495	0.824	0.902	0.293
210.6	21.7	18.6	0.1995	0.860	0.924	0.391
263.6	22.5	18.9	C.2495	0.890	0.941	0.489
343.1	23.4	19.3	C.3245	0.925	0.960	0.636
422.6	24.1	19.6	0.3995	0.954	0.977	0.782
528.7	24.8	19.8	C.4995	0.982	0.989	0.978
634.7	25.2	20.C	0.5995	0.995	0.997	1.174
740.7	25.3	20.C	0.6995	1.000	0.999	1.370

RUN 091069-1 K=1.99X10-6 F=0.0 NE

TEMP. RUN	VEL. RUN	PLATE	X	ST	CF/2	UINF	TGAS	TO	P
91C69-1	90769-1	10	37.46	0.00176	0.00254	62.4	73.6	96.2	0.0000

THERMAL B.L. THK.	HYDRO. B.L. THK.	ENTHALPY THK.	MOMENTUM THK.	ENTHALPY RE.	MOMENTUM RE.	NO. DATA POINTS	K
C.443	0.331	C.C530	0.0210	1655.	677.	26	C.206E-05

YPLUS	TPLUS	UPLUS	Y	TBAR	U/UINF	Y/DELM
0.0	0.0	C.C	C.CCCO	0.000	0.000	0.000
3.9	4.7	3.7	0.0025	0.174	0.177	0.008
5.4	5.0	5.2	0.0035	0.185	0.247	0.011
6.9	6.4	6.6	0.0045	C.234	0.318	0.014
8.5	7.6	8.1	0.0055	0.275	0.389	0.017
10.C	8.5	9.7	0.0065	0.311	0.460	0.020
11.6	9.3	11.1	C.0075	0.345	C.530	0.023
14.6	10.8	13.1	0.0095	0.398	0.626	0.029
17.7	11.8	14.1	C.0115	0.434	0.675	0.035
22.4	13.3	15.2	C.0145	0.489	0.729	0.044
27.1	14.2	15.9	0.0175	0.519	0.765	0.053
33.3	15.3	16.5	0.0215	0.560	0.794	0.065
41.0	16.4	17.0	0.0265	0.959	C.820	C.080
50.4	17.2	17.4	0.0325	0.630	0.840	0.098
66.C	18.4	18.C	0.0425	C.672	0.869	0.128
81.6	19.3	18.3	0.0525	0.702	C.883	0.159
104.5	20.2	18.7	0.0675	0.736	0.903	0.204
136.0	21.2	19.1	0.0875	0.773	0.923	0.265
175.1	22.2	19.4	0.1125	0.811	0.940	0.340
221.9	23.2	19.7	0.1425	0.844	0.955	0.431
276.6	24.1	19.9	0.1775	C.875	0.967	0.537
354.8	25.0	20.1	0.2275	0.909	0.977	0.688
433.1	25.9	20.4	C.2775	0.939	0.985	0.839
550.5	26.7	20.5	0.3525	0.969	0.992	1.066
767.0	27.3	20.6	0.4525	0.992	0.998	1.368
883.4	27.5	20.6	0.5525	1.000	C.998	1.670

RUNS 091069-1 K=1.99 x 10^{-6} F=0.0 NE
091069-2

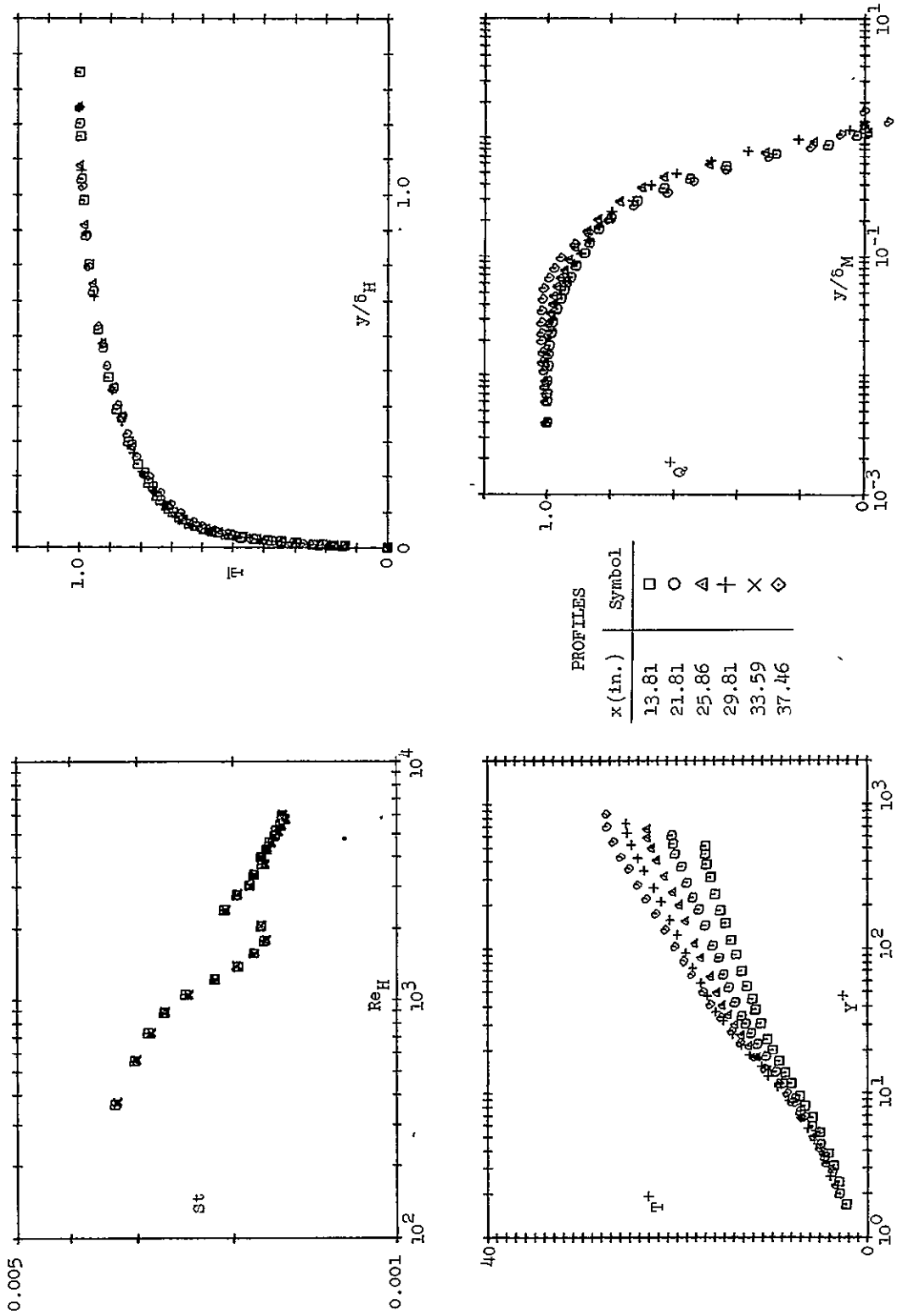

RUNS 070869-1 071669-1 K=2.55 x 10-6 F=0.0 NE
070869-2

RUN 070869-1 K=2.55X10-6 F=0.0 NE

DATE 70869 RUN NO. 1

AMB TEMP	BASE TEMP	GAS TEMP	COVER TEMP	BARO PRES	REL HUM
73.40	83.58	72.37	73.51	29.90	0.56

PL	X	VEL	K	REH	ST	REM	CF2	TC	F
2	6	23.31	0.103E-06	336.	0.00348			99.6	0.0000
3	10	23.27	-0.235E-06	492.	0.00311			99.4	0.0000
4	13.81	23.30	0.208E-06	624.	0.00290	754.	0.00250	98.7	0.0000
4	14	23.20	0.208E-06	631.	0.00290			99.5	0.0000
5	18	23.87	0.774E-06	763.	0.00269			99.5	0.0000
6	21.81	25.00	0.205E-05	895.	0.00248	817.	0.00255	98.2	0.0000
6	22	25.54	0.205E-05	886.	0.00249			99.7	0.0000
7	25.86	28.40	0.238E-05	990.	0.00222	738.	0.00260	97.0	0.0000
7	26	28.73	0.238E-05	1012.	0.00223			99.7	0.0000
8	29.81	33.00	0.252E-05	1120.	0.00198	665.	0.00260	95.2	0.0000
8	30	33.52	0.252E-05	1147.	0.00186			99.6	0.0000
9	33.59	39.00	0.254E-05	1236.	0.00177	595.	0.00257	95.3	0.0000
9	34	40.25	0.254E-05	1287.	0.00174			99.4	0.0000
10	37.46	48.30	0.253E-05	1345.	0.00159	550.	0.00248	96.0	0.0000
10	38	50.59	0.253E-05	1433.	0.00157			99.6	0.0000
11	42	65.59	0.110E-05	1627.	0.00135			99.2	0.0000
12	46	67.22	-0.312E-07	1878.	0.00198			98.9	0.0000
13	50	67.15	0.134E-07	2144.	0.00210			98.9	0.0000
14	54	67.32	0.237E-07	2425.	0.00193			98.8	0.0000
15	58	67.47	0.143E-07	2701.	0.00191			98.7	0.0000
16	62	67.56	0.882E-08	2931.	0.00188			98.9	0.0000
17	66	67.56	0.387E-08	3209.	0.00185			98.7	0.0000
18	70	67.71	0.350E-08	3449.	0.00181			98.8	0.0000
19	74	67.66	-0.173E-07	3719.	0.00178			98.6	0.0000
20	78	67.57	0.860E-08	3957.	0.00173			98.6	0.0000
21	82	67.68	0.729E-08	4164.	0.00171			98.7	0.0000
22	86	67.72	0.122E-08	4382.	0.00172			98.8	0.0000
23	90	67.68	-0.747E-08	4670.	0.00168			98.5	0.0000

RUN 070869-2 K=2.55X10-6 F=0.0 NE

DATE 70869 RUN NO. 2

AMB TEMP	BASE TEMP	GAS TEMP	COVER TEMP	BARO PRES	REL HUM
78.92	82.06	69.87	71.60	29.90	0.50

PL	X	VEL	K	REH	ST	TO	F
2	6	23.26	0.102E-06	336.	0.00342	97.4	0.0000
3	10	23.22	-0.233E-06	493.	0.00309	97.2	0.0000
4	14	23.15	0.207E-06	634.	0.00289	97.2	0.0000
5	18	23.82	0.770E-06	766.	0.00269	97.2	0.0000
6	22	25.48	0.204E-05	892.	0.00250	97.3	0.0000
7	26	28.67	0.236E-05	1019.	0.00219	97.4	0.0000
8	30	33.45	0.251E-05	1149.	0.00186	97.3	0.0000
9	34	40.21	0.252E-05	1290.	0.00173	97.2	0.0000
10	38	50.48	0.251E-05	1437.	0.00156	97.3	0.0000
11	42	65.45	0.109E-05	1629.	0.00135	97.0	0.0000
12	46	67.07	-0.310E-07	1873.	0.00196	96.7	0.0000
13	50	67.00	0.133E-07	2147.	0.00211	96.7	0.0000
14	54	67.18	0.235E-07	2429.	0.00191	96.6	0.0000
15	58	67.32	0.143E-07	2694.	0.00190	96.5	0.0000
16	62	67.41	0.877E-08	2959.	0.00189	96.5	0.0000
17	66	67.41	0.385E-08	3219.	0.00185	96.4	0.0000
18	70	67.57	0.348E-08	3456.	0.00181	96.5	0.0000
19	74	67.51	-0.172E-07	3718.	0.00178	96.4	0.0000
20	78	67.42	0.856E-08	3968.	0.00174	96.3	0.0000
21	82	67.54	0.724E-08	4180.	0.00171	96.5	0.0000
22	86	67.58	0.122E-08	4395.	0.00172	96.6	0.0000
23	90	67.54	-0.743E-08	4651.	0.00167	96.4	0.0000

RUN 071669-1 K=2.55X10-6 F=0.0 NE

DATE 71669 RUN NO. 1

AMB TEMP	BASE TEMP	GAS TEMP	COVER TEMP	BARO PRES	REL HUM
78.57	85.76	74.18	75.35	29.91	0.52

PL	X	VEL	K	REH	ST	TO	F
2	6	23.25	0.412E-07	333.	0.00350	101.7	0.0000
3	10	23.33	0.138E-06	490.	0.00313	101.6	0.0000
4	14	23.18	0.129E-06	626.	0.00293	101.8	0.0000
5	18	23.79	0.857E-06	762.	0.00273	101.7	0.0000
6	22	25.33	0.185E-05	892.	0.00252	101.6	0.0000
7	26	28.71	0.251E-05	1012.	0.00223	101.9	0.0000
8	30	33.46	0.253E-05	1146.	0.00189	101.7	0.0000
9	34	40.37	0.256E-05	1289.	0.00177	101.6	0.0000
10	38	50.57	0.254E-05	1428.	0.00156	101.8	0.0000
11	42	65.55	0.110E-05	1606.	0.00135	101.7	0.0000
12	46	67.17	0.336E-07	1824.	0.00198	101.8	0.0000
13	50	67.07	0.102E-07	2101.	0.00212	101.8	0.0000
14	54	67.22	0.220E-07	2378.	0.00194	101.7	0.0000
15	58	67.36	0.152E-07	2667.	0.00192	101.4	0.0000
16	62	67.46	0.910E-08	2940.	0.00191	101.2	0.0000
17	66	67.52	0.531E-08	3164.	0.00186	101.5	0.0000
18	70	67.59	0.000E 00	3404.	0.00181	101.6	0.0000
19	74	67.59	0.000E 00	3653.	0.00178	101.5	0.0000
20	78	67.59	0.000E 00	3904.	0.00174	101.4	0.0000
21	82	67.59	0.000E 00	4114.	0.00171	101.5	0.0000
22	86	67.59	0.000E 00	4372.	0.00172	101.4	0.0000
23	90	67.59	0.000E 00	4608.	0.00168	101.3	0.0000

SUMMARY OF PROFILE RESULTS

RUN 070869-1 K=2.55X10-6 F=0.0 NE

PL	X	VEL	K	F	TO	TINF	DELM	DELH
4	13.81	23.30	0.208E-06	0.0000	98.7	71.1	0.540	0.556
6	21.81	25.00	0.205E-05	0.0000	98.2	70.6	0.574	0.628
7	25.86	28.40	0.238E-05	0.0000	97.0	69.1	0.549	0.603
8	29.81	33.00	0.252E-05	0.0000	95.2	67.2	0.490	0.568
9	33.59	39.00	0.254E-05	0.0000	95.3	67.9	0.401	0.513
10	37.46	48.30	0.253E-05	0.0000	96.0	68.3	0.323	0.443

PL	X	REH	ST	REM	CF2	DELTA2	THETA
4	13.81	624.	0.00290	754.	0.00250	0.0536	0.0646
6	21.81	895.	0.00248	817.	0.00255	0.0700	0.0635
7	25.86	990.	0.00222	738.	0.00260	0.0689	0.0508
8	29.81	1120.	0.00198	665.	0.00260	0.0670	0.0390
9	33.59	1236.	0.00177	595.	0.00257	0.0622	0.0291
10	37.46	1345.	0.00159	550.	0.00248	0.0545	0.0214

RUNS 070869-1 071669-1 K=2.55 x 10-6 F=0.0 NE
070869-2

RUN 07C869-1 K=2.55X10-6 F=0.0 NE

TEMP. RUN	VEL. RUN	PLATE	X	ST	CF/2	UINF	TGAS	TO	F
7CE69-1	71669-1	4	13.81	0.00290	0.00250	23.3	71.1	90.7	0.0000

THERMAL B.L. THK.	HYDRO. B.L. THK.	ENTHALPY THK.	MOMENTUM THK.	ENTHALPY RE.	MOMENTUM RE.	NO. DATA POINTS	K
0.556	0.540	0.0536	0.0646	824.	754.	32	0.208E-06

YPLUS	TPLUS	UPLUS	Y	TBAR	U/UINF	Y/DELM
0.0	0.0	0.0	0.0000	0.000	0.000	0.000
1.4	2.1	1.5	0.0025	0.122	0.075	0.005
2.0	2.4	2.1	0.0035	0.143	0.105	0.006
2.6	2.9	2.8	0.0045	0.171	0.135	0.008
3.1	3.4	3.4	0.0055	0.200	0.165	0.010
3.7	3.9	4.0	0.0065	0.229	0.195	0.012
4.3	4.2	4.6	0.0075	0.247	0.225	0.014
4.9	4.6	5.1	0.0085	0.269	0.249	0.016
6.1	5.4	5.6	0.0105	0.320	0.288	0.019
7.3	6.0	6.7	0.0125	0.354	0.334	0.023
9.0	7.0	8.0	0.0155	0.410	0.397	0.029
10.8	7.7	9.0	0.0185	0.451	0.448	0.034
13.1	8.5	10.0	0.0225	0.497	0.500	0.042
15.4	9.2	10.8	0.0265	0.536	0.536	0.049
17.8	9.8	11.3	0.0305	0.564	0.565	0.056
20.7	10.2	11.9	0.0355	0.593	0.595	0.066
23.6	10.7	12.4	0.0405	0.621	0.616	0.075
26.3	11.3	12.9	0.0485	0.651	0.643	0.090
34.2	11.8	13.3	0.0585	0.681	0.667	0.108
40.0	12.2	13.8	0.0685	0.706	0.688	0.127
46.8	12.7	14.2	0.0835	0.735	0.709	0.155
57.7	13.1	14.5	0.0985	0.758	0.727	0.182
69.4	13.5	15.0	0.1185	0.781	0.749	0.219
84.1	14.0	15.4	0.1435	0.809	0.773	0.266
98.8	14.4	15.9	0.1685	0.832	0.794	0.312
120.3	15.1	16.6	0.2185	0.870	0.833	0.405
157.8	15.6	17.3	0.2685	0.900	0.868	0.497
202.0	16.3	18.1	0.3435	0.936	0.916	0.636
246.3	16.7	18.9	0.4185	0.963	0.954	0.775
305.3	17.2	19.5	0.5185	0.986	0.986	0.960
364.2	17.3	19.8	0.6185	0.996	0.998	1.145
423.2	17.4	19.8	0.7185	1.000	1.000	1.330

RUN 07C869-1 K=2.55X10-6 F=0.0 NE

TEMP. RUN	VEL. RUN	PLATE	X	ST	CF/2	UINF	TGAS	TO	F
7CE69-1	71669-1	7	25.06	0.00222	0.00260	28.4	69.1	97.0	0.0000

THERMAL B.L. THK.	HYDRO. B.L. THK.	ENTHALPY THK.	MOMENTUM THK.	ENTHALPY RE.	MOMENTUM RE.	NO. DATA POINTS	K
0.603	0.549	0.0689	0.0SCE	990.	738.	30	0.238E-05

YPLUS	TPLUS	UPLUS	Y	TBAR	U/UINF	Y/DELM
0.0	0.0	0.0	0.0000	0.000	0.000	0.000
1.8	1.9	1.8	0.0025	0.084	0.090	0.005
2.5	2.1	2.5	0.0035	0.095	0.126	0.006
3.3	2.9	3.2	0.0045	0.132	0.162	0.008
4.0	3.5	4.0	0.0055	0.156	0.197	0.010
4.7	4.0	4.7	0.0065	0.182	0.233	0.012
5.4	4.8	5.5	0.0075	0.214	0.269	0.014
6.8	5.7	6.5	0.0095	0.254	0.322	0.017
8.3	6.7	7.8	0.0115	0.300	0.384	0.021
9.7	7.5	8.8	0.0135	0.336	0.436	0.025
11.9	8.7	10.2	0.0165	0.387	0.508	0.030
14.2	9.7	11.2	0.0195	0.430	0.559	0.036
17.0	10.6	12.4	0.0235	0.475	0.620	0.043
19.9	11.6	13.2	0.0275	0.519	0.659	0.050
23.6	12.7	13.8	0.0325	0.565	0.693	0.059
28.0	14.6	14.6	0.0385	0.605	0.735	0.070
33.1	14.2	15.1	0.0455	0.629	0.753	0.083
40.4	14.9	15.6	0.0555	0.663	0.775	0.101
47.7	15.5	15.8	0.0655	0.690	0.791	0.119
58.7	16.1	16.2	0.0805	0.716	0.809	0.147
73.2	16.8	16.5	0.1005	0.744	0.826	0.183
91.6	17.6	16.8	0.1255	0.775	0.843	0.229
109.9	18.1	17.1	0.1505	0.798	0.858	0.274
146.6	18.9	17.6	0.2005	0.836	0.883	0.365
201.6	19.9	18.2	0.2755	0.880	0.915	0.502
275.1	21.0	18.5	0.3755	0.927	0.932	0.684
348.7	21.9	19.4	0.4755	0.963	0.978	0.867
422.3	22.5	19.7	0.5755	0.987	0.994	1.049
495.9	22.7	19.8	0.6755	0.999	0.999	1.231
569.3	22.7	19.8	0.7755	1.000	1.000	1.414

RUN 07C869-1 K=2.55X10-6 F=0.0 NE

TEMP. RUN	VEL. RUN	PLATE	X	ST	CF/2	UINF	TGAS	TO	F
7CE69-1	71669-1	6	21.81	0.00248	0.00255	25.0	70.6	96.2	0.0000

THERMAL B.L. THK.	HYDRO. B.L. THK.	ENTHALPY THK.	MOMENTUM THK.	ENTHALPY RE.	MOMENTUM RE.	NO. DATA POINTS	K
0.628	0.574	0.0700	0.0635	895.	817.	31	0.205E-05

YPLUS	TPLUS	UPLUS	Y	TBAR	U/UINF	Y/DELM
0.0	0.0	0.0	0.0000	0.000	0.000	0.000
1.6	2.0	1.6	0.0025	0.101	0.081	0.004
2.2	2.4	2.3	0.0035	0.124	0.113	0.006
2.8	2.9	3.1	0.0046	0.145	0.148	0.008
3.4	3.3	3.7	0.0055	0.169	0.177	0.010
4.0	3.8	4.3	0.0065	0.195	0.210	0.011
4.7	4.3	5.0	0.0075	0.222	0.242	0.013
6.0	5.1	6.0	0.0095	0.260	0.293	0.017
7.2	5.9	7.1	0.0115	0.306	0.346	0.020
9.1	6.9	8.7	0.0145	0.353	0.422	0.025
11.0	8.0	9.7	0.0175	0.408	0.471	0.030
12.8	8.7	10.7	0.0205	0.444	0.520	0.036
15.4	9.6	11.6	0.0245	0.488	0.568	0.043
17.9	10.3	12.2	0.0285	0.523	0.601	0.050
21.1	10.9	13.0	0.0335	0.553	0.634	0.058
24.9	11.8	13.6	0.0395	0.594	0.663	0.069
28.0	12.2	13.9	0.0445	0.613	0.680	0.077
34.4	12.8	14.4	0.0545	0.650	0.707	0.095
40.8	13.3	14.8	0.0645	0.672	0.728	0.114
50.3	13.9	15.2	0.0795	0.703	0.749	0.138
62.9	14.4	15.6	0.0995	0.726	0.767	0.173
82.0	15.1	16.1	0.1295	0.763	0.795	0.226
104.3	15.8	16.6	0.1645	0.797	0.819	0.286
136.0	16.6	17.2	0.2145	0.833	0.848	0.374
167.8	17.2	17.8	0.2645	0.865	0.876	0.461
215.7	18.0	18.5	0.3395	0.903	0.912	0.591
263.6	18.6	19.1	0.4145	0.934	0.944	0.722
327.5	19.3	19.7	0.5145	0.968	0.976	0.896
391.2	19.8	20.1	0.6145	0.989	0.994	1.070
455.0	20.0	20.2	0.7145	0.998	0.999	1.244
518.7	20.0	20.2	0.8145	1.000	1.000	1.418

RUN 07C869-1 K=2.55X10-6 F=0.0 NE

TEMP. RUN	VEL. RUN	PLATE	X	ST	CF/2	UINF	TGAS	TO	F
7CE69-1	71669-1	8	29.81	0.00158	0.00260	33.0	67.2	95.2	0.0000

THERMAL B.L. THK.	HYDRO. B.L. THK.	ENTHALPY THK.	MOMENTUM THK.	ENTHALPY RE.	MOMENTUM RE.	NO. DATA POINTS	K
0.56E	0.490	0.067C	0.039C	1120.	665.	32	0.252E-05

YPLUS	TPLUS	UPLUS	Y	TBAR	U/UINF	Y/DELM
0.0	0.0	0.0	0.0000	0.000	0.000	0.000
2.1	2.5	2.1	0.0025	0.101	0.106	0.005
3.0	3.0	3.0	0.0035	0.120	0.148	0.007
3.8	3.2	3.8	0.0045	0.129	0.190	0.009
4.7	4.0	4.8	0.0056	0.140	0.237	0.011
5.4	4.7	5.6	0.0065	0.188	0.275	0.013
6.3	5.3	6.4	0.0075	0.211	0.317	0.015
8.0	6.4	7.9	0.0095	0.257	0.392	0.019
9.7	7.7	9.2	0.0115	0.307	0.452	0.023
11.4	8.5	10.2	0.0135	0.341	0.507	0.028
13.9	9.7	11.6	0.0165	0.390	0.577	0.034
16.5	10.9	12.5	0.0195	0.433	0.623	0.040
19.1	11.9	13.4	0.0225	0.473	0.663	0.046
21.6	12.8	14.0	0.0255	0.510	0.696	0.052
24.2	13.5	14.6	0.0285	0.535	0.720	0.058
28.5	14.5	15.1	0.0335	0.575	0.749	0.068
32.7	15.0	15.5	0.0385	0.598	0.773	0.078
41.3	16.2	16.2	0.0485	0.645	0.820	0.099
49.8	17.3	16.6	0.0585	0.683	0.824	0.119
58.4	17.8	16.9	0.0685	0.704	0.843	0.140
71.3	18.5	17.1	0.0835	0.732	0.855	0.170
88.4	19.3	17.5	0.1035	0.762	0.875	0.211
109.8	20.0	17.8	0.1285	0.789	0.890	0.262
144.1	20.8	18.1	0.1685	0.821	0.909	0.344
187.0	21.8	18.4	0.2185	0.860	0.927	0.445
230.0	22.6	18.7	0.2685	0.888	0.942	0.547
273.0	23.2	19.0	0.3185	0.912	0.957	0.649
316.C	23.8	19.3	0.3685	0.935	0.971	0.751
380.6	24.5	19.5	0.4435	0.963	0.984	0.904
445.2	25.1	19.7	0.5185	0.984	0.993	1.057
531.3	25.3	19.8	0.6185	0.995	0.999	1.261
617.3	25.4	19.8	0.7185	1.000	1.000	1.465

RUNS 070869-1 071669-1 K=2.55 x 10^{-6} F=0.0 NE
070869-2

RUN 07C869-1 K=2.55X10-6 F=0.0 NE

TEMP. RUN	VEL. RUN	PLATE	X	ST	CF/2	UINF	TGAS	TO	F
70869-1	71669-1	9	33.59	0.00177	0.00257	39.0	67.9	95.3	0.0000

THERMAL B.L. THK.	HYDRO. B.L. THK.	ENTHALPY THK.	MOMENTUM THK.	ENTHALPY RE.	MOMENTUM RE.	NO. DATA POINTS	K
0.513	0.401	0.0622	0.0291	1236.	555.	32	0.254E-05

YPLUS	TPLUS	UPLUS	Y	TBAR	U/UINF	Y/DELH
0.0	0.0	0.0	0.0000	0.000	0.000	0.000
2.4	2.5	2.4	0.0025	0.091	0.113	0.006
3.5	3.2	3.3	0.0035	0.119	0.158	0.009
4.5	3.7	4.2	0.0045	0.136	0.203	0.011
5.4	4.9	5.1	0.0056	0.182	0.249	0.014
6.4	5.7	6.1	0.0065	0.208	0.294	0.016
7.4	6.5	7.0	0.0075	0.240	0.339	0.019
9.4	7.8	8.8	0.0095	0.284	0.421	0.024
11.3	8.9	10.2	0.0115	0.328	0.495	0.029
13.4	10.1	11.5	0.0135	0.369	0.557	0.034
16.4	11.4	12.9	0.0165	0.416	0.622	0.041
19.4	12.5	13.8	0.0195	0.458	0.671	0.049
22.3	13.3	14.6	0.0225	0.495	0.710	0.056
26.4	14.6	15.4	0.0265	0.533	0.748	0.066
30.4	15.5	16.0	0.0305	0.561	0.776	0.076
34.3	16.2	16.4	0.0345	0.590	0.798	0.086
38.4	16.9	16.7	0.0385	0.615	0.815	0.096
48.4	18.1	17.3	0.0485	0.659	0.845	0.121
58.4	19.0	17.7	0.0585	0.688	0.865	0.146
73.4	19.9	18.0	0.0735	0.723	0.882	0.183
93.5	20.9	18.3	0.0935	0.755	0.899	0.233
118.6	21.8	18.8	0.1185	0.786	0.916	0.296
143.8	22.5	19.0	0.1435	0.814	0.929	0.358
169.0	23.2	19.2	0.1685	0.840	0.938	0.420
194.1	23.8	19.4	0.1935	0.859	0.946	0.483
244.5	24.7	19.6	0.2435	0.890	0.961	0.608
294.9	25.4	19.8	0.2935	0.917	0.973	0.732
370.6	26.5	20.1	0.3685	0.953	0.986	0.919
471.6	27.3	20.3	0.4685	0.984	0.997	1.169
572.3	27.7	20.3	0.5685	0.997	1.000	1.418
673.0	27.6	20.3	0.6685	0.999	1.000	1.668
773.7	27.8	20.3	0.7685	1.000	1.000	1.917

RUN 07C869-1 K=2.55X10-6 F=0.0 NE

TEMP. RUN	VEL. RUN	PLATE	X	ST	CF/2	UINF	TGAS	TO	F
7CE6S-1	71669-1	10	37.46	0.00159	0.00248	48.3	68.3	96.0	0.0000

THERMAL B.L. THK.	HYDRO. B.L. THK.	ENTHALPY THK.	MOMENTUM THK.	ENTHALPY RE.	MOMENTUM RE.	NO. DATA POINTS	K
0.443	0.323	0.0545	0.0214	1345	550.	31	0.253E-05

YPLUS	TPLUS	UPLUS	Y	TBAR	U/UINF	Y/DELH
0.0	0.0	0.0	0.0000	0.000	0.000	0.000
3.0	3.1	2.7	0.0025	0.107	0.147	0.008
4.2	3.7	3.8	0.0035	0.125	0.178	0.011
5.4	4.6	4.9	0.0045	0.158	0.228	0.014
6.6	5.7	6.0	0.0055	0.195	0.279	0.017
7.7	6.6	7.1	0.0065	0.223	0.330	0.020
9.0	7.3	8.2	0.0075	0.249	0.381	0.023
11.4	8.7	9.9	0.0095	0.298	0.466	0.029
13.8	10.1	11.6	0.0115	0.343	0.545	0.036
16.3	11.5	13.0	0.0135	0.388	0.606	0.042
18.6	12.5	14.0	0.0155	0.423	0.659	0.048
22.3	13.8	15.2	0.0185	0.467	0.712	0.057
25.9	14.8	16.0	0.0215	0.502	0.751	0.067
29.5	16.0	16.6	0.0245	0.539	0.780	0.076
32.0	16.5	16.8	0.0265	0.557	0.795	0.082
36.5	17.4	17.4	0.0305	0.587	0.815	0.094
42.9	18.4	17.9	0.0355	0.620	0.843	0.110
50.2	19.3	18.2	0.0415	0.650	0.859	0.128
58.7	20.1	18.6	0.0485	0.675	0.880	0.150
71.0	21.1	18.9	0.0585	0.712	0.895	0.181
83.1	21.9	19.1	0.0685	0.736	0.907	0.212
101.4	22.7	19.5	0.0835	0.766	0.922	0.258
125.7	23.6	19.8	0.1035	0.791	0.936	0.320
162.4	24.6	20.1	0.1335	0.824	0.951	0.413
205.1	25.6	20.3	0.1685	0.859	0.963	0.522
266.2	26.8	20.5	0.2185	0.898	0.975	0.676
327.4	27.8	20.7	0.2685	0.929	0.984	0.831
388.6	28.5	20.8	0.3185	0.954	0.990	0.986
480.5	29.4	20.9	0.3935	0.980	0.997	1.216
572.3	29.8	21.0	0.4685	0.995	0.999	1.450
694.5	29.9	21.0	0.5685	1.000	1.000	1.759

RUNS 070869-1 071669-1 K=2.55 x 10^{-6} F=0.0 NE
070869-2

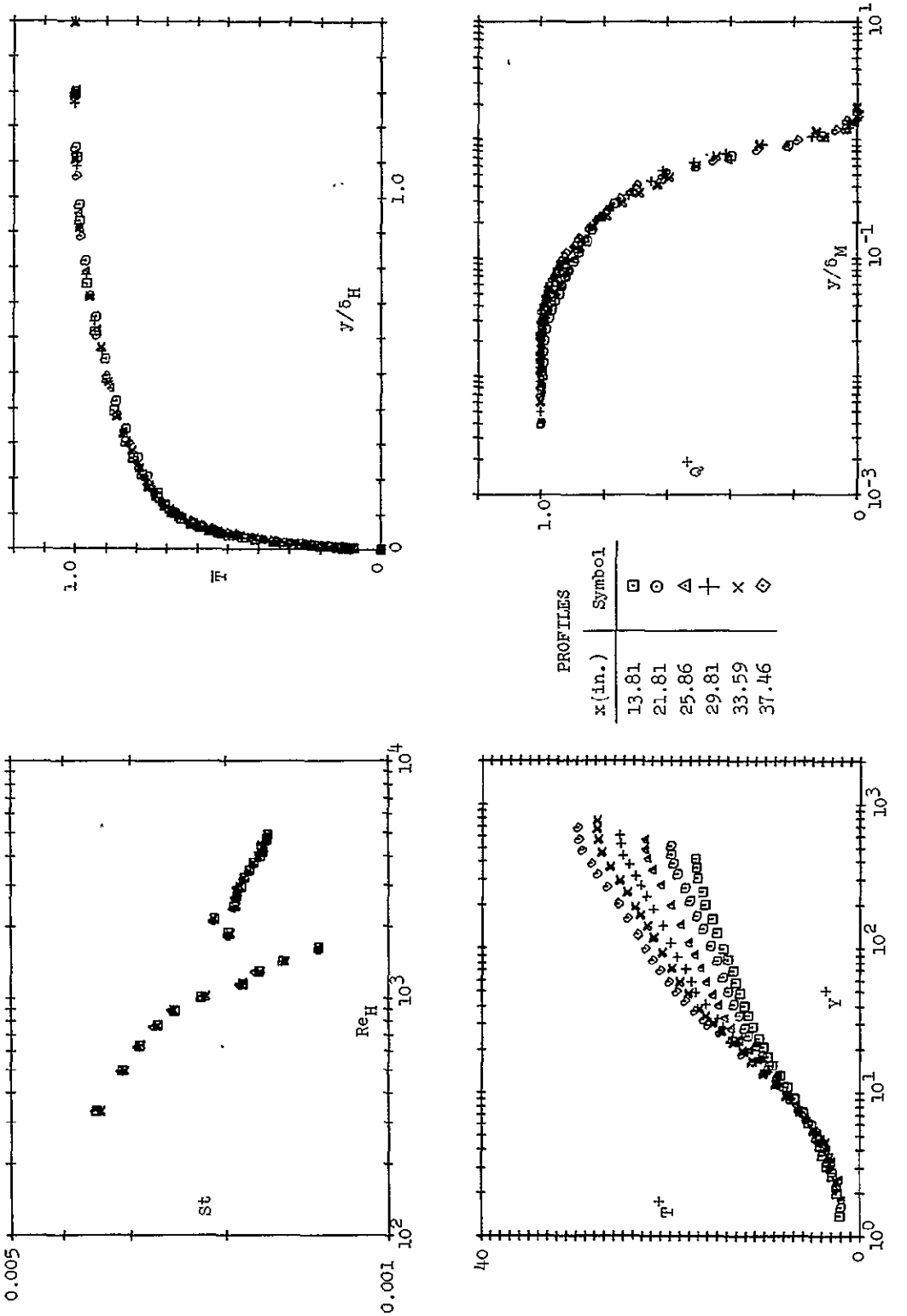

RUNS 072769-1
072769-2

K=2.55 x 10⁻⁶

F=0.002

NE

RUN 072769-1 K=2.55X10-6 F=0.002 NE

DATE 72769 RUN NO. 1

AMB TEMP	BASE TEMP	GAS TEMP	COVER TEMP	BARO PRES	REL HUM
77.39	79.89	73.17	74.24	29.95	0.53

FL	X	VEL	K	REH	ST	REH	CF2	TO	F
2	6	23.31	0.665E-07	419.	0.00273			94.7	0.0021
3	10	23.37	0.758E-07	644.	0.00237			94.5	0.0022
4	13.81	23.90	0.202E-06	835.	0.00218	966.	0.00190	94.7	0.0020
4	14	23.44	0.202E-06	844.	0.00219			94.7	0.0020
5	18	24.04	0.765E-06	1042.	0.00194			94.6	0.0020
6	21.81	26.00	0.197E-05	1204.	0.00181	1096.	0.00210	94.6	0.0021
6	22	25.65	0.197E-05	1234.	0.00181			94.6	0.0021
7	25.86	29.40	0.246E-05	1384.	0.00167	1005.	0.00210	94.6	0.0021
7	26	29.03	0.246E-05	1439.	0.00159			94.7	0.0021
8	29.81	34.20	0.247E-05	1582.	0.00156	939.	0.00210	94.5	0.0022
8	30	33.94	0.247E-05	1684.	0.00142			94.5	0.0022
9	33.59	40.70	0.258E-05	1864.	0.00146	871.	0.00210	94.1	0.0021
9	34	41.04	0.258E-05	1966.	0.00145			94.4	0.0021
10	37.46	50.40	0.255E-05	2109.	0.00138	837.	0.00210	94.4	0.0019
10	38	51.71	0.255E-05	2269.	0.00139			94.6	0.0019
11	42	67.36	0.106E-05	2678.	0.00129			94.6	0.0020
12	46	69.05	-0.146E-07	3143.	0.00135			94.6	0.0020
13	50	69.02	0.114E-07	3566.	0.00125			94.7	0.0019
14	54	69.06	-0.672E-08	4051.	0.00115			94.4	0.0020
15	58	68.93	-0.737E-08	4521.	0.00114			94.3	0.0020
16	62	68.83	-0.753E-08	4967.	0.00110			94.1	0.0020
17	66	68.79	-0.901E-05	5353.	0.00105			94.3	0.0020
18	70	68.88	0.233E-08	5151.	0.00104			94.4	0.0019
19	74	68.83	-0.114E-07	6206.	0.00059			94.2	0.0020
20	78	68.80	0.123E-07	6382.	0.00098			94.3	0.0019
21	82	68.81	0.592E-08	7031.	0.00095			94.2	0.0020
22	86	68.95	-0.349E-05	7435.	0.00056			94.2	0.0020
23	90	68.90	-0.773E-08	7854.	0.00055			94.1	0.0019

RUN G72769-2 K=2.55X10-6 F=0.002 NE

DATE 72769 RUN NO. 2

AMB TEMP	BASE TEMP	GAS TEMP	COVER TEMP	BARO PRES	REL HUM
75.66	79.85	73.31	74.20	29.95	0.51

FL	X	VEL	K	REH	ST	TO	F
2	6	23.35	0.661E-07	430.	0.00276	94.6	0.0020
3	10	23.41	0.753E-07	651.	0.00237	94.5	0.0021
4	14	23.49	0.200E-06	846.	0.00218	94.7	0.0020
5	18	24.09	0.760E-06	1050.	0.00197	94.5	0.0020
6	22	25.69	0.196E-05	1242.	0.00181	94.6	0.0021
7	26	29.07	0.245E-05	1451.	0.00157	94.6	0.0021
8	30	33.57	0.247E-05	1655.	0.00141	94.4	0.0022
9	34	41.06	0.258E-05	2003.	0.00148	94.1	0.0021
10	38	51.72	0.255E-05	2296.	0.00141	94.4	0.0019
11	42	67.37	0.106E-05	2702.	0.00127	94.4	0.0020
12	46	69.05	-0.146E-07	3172.	0.00135	94.3	0.0020
13	50	69.03	0.114E-07	3587.	0.00125	94.5	0.0019
14	54	69.07	-0.672E-08	4076.	0.00117	94.2	0.0020
15	58	68.93	-0.736E-08	4547.	0.00112	94.0	0.0020
16	62	68.83	-0.753E-08	5035.	0.00111	93.8	0.0020
17	66	68.80	-0.896E-05	5379.	0.00105	94.1	0.0020
18	70	68.89	0.232E-08	5788.	0.00102	94.1	0.0019
19	74	68.84	-0.114E-07	6217.	0.00097	94.0	0.0020
20	78	68.80	0.123E-07	6626.	0.00098	94.0	0.0019
21	82	68.92	0.581E-08	7067.	0.00094	93.9	0.0020
22	86	68.96	-0.350E-05	7466.	0.00093	93.9	0.0020
23	90	68.91	-0.772E-08	7876.	0.00093	93.9	0.0019

SUMMARY OF PROFILE RESULTS

RUN 072769-1 K=2.55X10-6 F=0.002 NE

PL	X	VEL	K	F	TO	TINF	DELM	DELH
4	13.81	23.90	0.2026-06	0.0020	94.7	72.3	0.617	0.627
6	21.81	26.00	0.197E-05	0.0021	94.4	72.3	0.694	0.736
7	25.86	29.40	0.2466-05	0.0021	94.6	72.5	0.650	0.722
8	29.81	34.20	0.247E-05	0.0022	94.5	72.6	0.586	0.665
9	33.59	40.70	0.2586-05	0.0021	94.1	72.7	0.500	0.629
10	37.46	50.40	0.255E-05	0.0019	94.4	72.8	0.465	0.542

PL	X	REH	ST	REH	CF2	DELTAZ	THETA
4	13.81	835.	0.00218	966.	0.00190	0.0710	0.0819
6	21.81	1204.	0.00181	1096.	0.00210	0.0939	0.0850
7	25.86	1384.	0.00167	1005.	0.00210	0.0955	0.0889
8	29.81	1582.	0.00156	939.	0.00210	0.0936	0.0851
9	33.59	1864.	0.00146	871.	0.00210	0.0923	0.0823
10	37.46	2109.	0.00138	837.	0.00210	0.0838	0.0823

F=0.002

NE

RUN G72769-1 K=2.55X10-6 F=0.002 NE

TEMP. RUN	VEL. RUN	PLATE	X	ST	CF/2	UINF	TGAS	TU	F
72769-1	72069-1	4	13.81	0.00218	0.00190	23.9	72.3	94.7	0.0020

THERMAL B.L. THK.	HYDRO. B.L. THK.	ENTHALPY THK.	MOMENTUM THK.	ENTHALPY RE.	MOMENTUM RE.	NO. DATA POINTS	Y
C.627	0.617	0.0710	0.0819	835.	966.	28	0.202E-06

YPLUS	TPLUS	UPLUS	Y	TBAR	U/UINF	Y/DELM
0.0	0.0	0.0	0.0000	0.000	0.000	0.000
1.3	2.8	1.5	0.0025	0.137	0.064	0.004
1.8	3.3	2.1	0.0035	0.166	C.085	0.006
2.3	3.9	2.6	0.0045	0.197	0.115	0.007
2.9	4.5	3.2	0.0055	0.224	0.140	0.009
3.4	4.9	3.8	0.0065	0.244	0.166	0.011
4.4	5.4	4.8	0.0085	0.266	0.212	0.014
5.9	6.4	6.1	0.0115	0.319	0.265	0.019
7.6	7.3	7.2	0.0145	0.364	0.317	0.024
9.1	8.1	8.3	0.0175	0.403	0.365	0.028
10.6	8.7	9.2	0.0205	0.429	0.405	0.033
12.7	9.2	10.0	0.0245	0.455	0.441	0.040
15.3	9.9	10.9	0.0295	0.488	0.480	0.048
19.0	10.8	11.7	0.0365	0.533	0.517	0.059
24.2	11.8	12.5	0.0465	0.582	0.555	0.075
29.4	12.4	13.2	0.0565	0.609	0.583	0.092
37.3	13.0	13.9	0.0715	0.640	0.615	0.116
48.1	13.3	14.5	0.0865	0.644	0.639	0.140
55.6	13.9	15.0	0.1065	0.685	0.660	0.173
68.6	14.6	15.6	0.1315	0.722	0.691	0.213
94.8	15.8	16.6	0.1815	0.776	0.736	0.294
121.1	16.4	17.5	0.2315	0.806	0.779	0.375
160.5	17.6	18.9	0.3065	0.866	0.839	0.497
199.9	18.6	20.1	0.3815	0.909	0.890	0.619
239.4	19.3	21.0	0.4565	0.944	0.935	0.740
292.1	19.9	21.9	0.5565	0.977	0.976	0.902
344.7	20.3	22.4	0.6565	0.995	0.996	1.064
397.2	20.4	22.4	0.7565	1.000	1.000	1.227

RUN G72769-1 K=2.55X10-6 F=0.002 NE

TEMP. RUN	VEL. RUN	PLATE	X	ST	CF/2	UINF	TGAS	TU	F
72769-1	72069-1	6	21.81	0.00181	0.00210	26.C	72.3	94.4	0.0021

THERMAL B.L. THK.	HYDRO. B.L. THK.	ENTHALPY THK.	MOMENTUM THK.	ENTHALPY RE.	MOMENTUM RE.	NO. DATA POINTS	K
C.736	C.654	0.0939	0.0850	1204.	1098.	30	0.1976-05

YPLUS	TPLUS	UPLUS	Y	TBAR	U/UINF	Y/DELM
C.C	0.C	0.C	C.0000	0.000	0.000	0.000
1.5	2.5	1.6	0.0025	0.098	0.070	0.004
2.0	2.9	2.2	0.0035	0.115	0.098	0.005
2.6	3.8	2.8	0.0045	0.154	0.126	0.006
3.4	4.7	3.4	0.0056	0.186	0.157	0.008
3.9	4.7	3.9	0.0065	0.189	0.182	0.009
4.5	5.3	4.6	0.0075	0.209	0.210	0.011
5.6	5.7	5.7	0.0095	0.226	0.260	0.014
7.4	7.0	7.1	0.0125	0.275	0.324	0.018
9.7	8.8	8.7	0.0165	0.347	0.397	0.024
12.2	9.7	9.8	0.0205	0.380	0.452	0.030
14.5	10.5	10.7	0.0245	0.413	0.494	0.035
17.5	11.4	11.6	0.0295	0.445	0.536	0.042
20.5	12.2	12.2	0.0345	0.480	0.562	0.050
25.9	13.5	13.C	0.0435	0.531	0.600	0.063
34.8	14.9	13.9	0.0585	0.585	0.640	0.084
43.8	15.6	14.4	0.0735	0.611	0.665	0.106
52.7	16.2	14.9	0.0885	0.636	0.687	0.127
64.7	17.0	15.4	0.1085	0.665	0.709	0.156
79.6	17.9	15.8	0.1335	0.700	0.730	0.192
94.6	18.7	16.3	0.1585	0.731	0.751	0.228
124.6	19.7	16.9	0.2085	0.770	0.785	0.300
154.5	20.4	17.6	0.2585	0.799	0.816	0.372
199.5	21.4	18.5	0.3335	0.832	0.857	0.480
244.6	22.5	19.3	0.4085	0.877	0.895	0.588
304.7	23.7	20.2	0.5085	0.925	0.938	0.733
364.9	24.8	20.6	0.6085	0.963	0.972	0.877
425.1	25.4	21.4	0.7085	0.987	0.992	1.021
485.2	25.7	21.5	0.8085	0.996	0.998	1.165
545.2	25.7	21.5	0.9085	1.000	0.999	1.309

RUNS 072769-1 072769-2 K=2.55 x 10⁻⁶ F=0.002 NE

RUN C72769-1 K=2.55X10-6 F=0.002 NE

TEMP. RUN	VEL. RUN	PLATE	X	ST	CF/2	UINF	TGAS	TO	F
72769-1	72069-1	7	25.66	0.00167	0.00210	29.4	72.5	94.6	0.0021

THERMAL B.L. THK.	HYDRO. B.L. THK.	ENTHALPY THK.	MOMENTUM THK.	ENTHALPY RE.	MOMENTUM RE.	NO. DATA POINTS	K
0.722	0.650	0.0955	0.0689	1384.	1005.	30	0.246E-05

YPLUS	TPLUS	UPLUS	Y	TBAR	U/UINF	Y/DELM
0.0	0.0	0.0	0.0000	0.000	0.000	0.000
1.6	1.7	1.7	0.0025	0.081	0.075	0.004
2.3	3.2	2.3	0.0035	0.117	0.105	0.005
3.0	4.0	3.0	0.0045	0.148	0.136	0.007
3.6	4.8	3.7	0.0055	0.174	0.166	0.008
4.4	5.2	4.2	0.0065	0.190	0.196	0.010
5.0	5.3	4.5	0.0075	0.192	0.226	0.012
6.4	6.5	6.0	0.0095	0.241	0.277	0.015
8.3	8.1	7.7	0.0125	0.296	0.351	0.019
10.3	9.3	9.3	0.0155	0.337	0.424	0.024
12.4	10.3	10.5	0.0185	0.372	0.479	0.028
15.1	11.4	11.6	0.0225	0.416	0.542	0.035
18.4	12.7	12.6	0.0275	0.463	0.581	0.042
21.8	13.6	13.4	0.0325	0.494	0.615	0.050
26.6	14.7	14.2	0.0395	0.530	0.653	0.061
30.5	15.3	14.7	0.0455	0.557	0.677	0.070
37.3	16.2	15.3	0.0555	0.588	0.705	0.085
47.4	17.1	15.9	0.0705	0.619	0.732	0.108
60.9	18.2	16.4	0.0905	0.658	0.757	0.139
74.4	19.0	16.9	0.1105	0.686	0.776	0.170
94.7	19.7	17.3	0.1405	0.715	0.798	0.216
114.9	20.5	17.7	0.1705	0.743	0.817	0.262
148.8	21.7	18.4	0.2205	0.782	0.847	0.339
199.6	22.8	19.0	0.2955	0.823	0.881	0.455
250.3	23.9	19.7	0.3705	0.864	0.912	0.570
318.3	25.4	20.4	0.4705	0.916	0.949	0.724
386.3	26.6	21.0	0.5705	0.956	0.977	0.878
454.2	27.4	21.4	0.6705	0.983	0.993	1.032
522.1	27.8	21.5	0.7705	0.997	0.999	1.186
589.9	27.9	21.5	0.8705	1.000	1.000	1.339

RUN C72769-1 K=2.55X10-6 F=0.002 NE

TEMP. RUN	VEL. RUN	PLATE	X	ST	CF/2	UINF	TGAS	TO	F
72769-1	72069-1	8	29.81	0.00156	0.00210	34.2	72.8	94.5	0.0022

THERMAL B.L. THK.	HYDRO. B.L. THK.	ENTHALPY THK.	MOMENTUM THK.	ENTHALPY RE.	MOMENTUM RE.	NO. DATA POINTS	K
0.669	0.586	0.0936	0.0551	1582.	439.	29	0.247E-05

YPLUS	TPLUS	UPLUS	Y	TBAR	U/UINF	Y/DELM
0.0	0.0	0.0	0.0000	0.000	0.000	0.000
1.9	2.4	2.0	0.0025	0.082	0.090	0.004
2.8	3.9	2.9	0.0036	0.133	0.130	0.006
3.5	4.7	3.6	0.0045	0.161	0.162	0.008
4.2	5.4	4.4	0.0055	0.183	0.198	0.009
5.0	6.0	5.2	0.0065	0.206	0.234	0.011
5.9	6.6	5.9	0.0075	0.226	0.270	0.013
7.4	7.7	7.2	0.0095	0.263	0.328	0.016
9.7	9.2	9.0	0.0125	0.316	0.413	0.021
12.0	10.2	10.6	0.0155	0.350	0.464	0.026
15.1	11.5	12.2	0.0195	0.392	0.535	0.033
19.1	12.8	13.2	0.0245	0.439	0.603	0.042
23.0	14.0	14.1	0.0295	0.477	0.663	0.050
26.9	14.8	14.8	0.0345	0.505	0.676	0.059
34.7	16.2	15.6	0.0445	0.552	0.715	0.076
42.6	17.0	16.2	0.0545	0.578	0.742	0.093
54.3	18.1	16.8	0.0695	0.616	0.773	0.119
66.1	19.0	17.2	0.0845	0.645	0.793	0.144
85.7	20.0	17.8	0.1095	0.678	0.821	0.187
105.3	21.0	18.2	0.1345	0.712	0.840	0.229
144.7	22.3	18.9	0.1845	0.756	0.873	0.315
183.9	23.4	19.5	0.2345	0.792	0.897	0.400
223.4	24.5	19.8	0.2845	0.830	0.914	0.485
282.5	25.9	20.3	0.3595	0.876	0.939	0.613
341.8	27.2	20.8	0.4345	0.919	0.960	0.741
401.0	28.1	21.1	0.5095	0.949	0.977	0.869
480.0	29.0	21.4	0.6095	0.980	0.992	1.039
559.0	29.6	21.6	0.7095	0.997	0.998	1.210
637.8	29.6	21.6	0.8095	1.000	1.000	1.380

RUN C72769-1 K=2.55X10-6 F=0.002 NE

TEMP. RUN	VEL. RUN	PLATE	X	ST	CF/2	UINF	TGAS	TO	F
72769-1	72069-1	9	33.56	0.00146	0.00210	40.7	72.7	94.1	0.0021

THERMAL B.L. THK.	HYDRO. B.L. THK.	ENTHALPY THK.	MOMENTUM THK.	ENTHALPY RE.	MOMENTUM RE.	NO. DATA POINTS	K
0.629	0.500	0.0923	0.0423	1864.	671.	31	0.258E-05

YPLUS	TPLUS	LPLUS	Y	TBAR	U/UINF	Y/DELM
0.0	0.0	0.0	0.0000	0.000	0.000	0.000
2.3	2.3	2.4	0.0025	0.077	0.109	0.005
3.2	3.1	3.4	0.0035	0.100	0.153	0.007
4.3	3.9	4.5	0.0046	0.128	0.201	0.009
5.1	4.4	5.3	0.0055	0.144	0.240	0.011
6.0	4.2	6.3	0.0065	0.138	0.283	0.013
6.9	5.8	7.4	0.0075	0.191	0.327	0.015
7.9	7.2	8.3	0.0086	0.233	0.369	0.017
9.7	8.5	9.6	0.0105	0.278	0.431	0.021
11.5	9.5	10.9	0.0125	0.310	0.487	0.025
14.3	10.9	12.3	0.0155	0.355	0.553	0.031
18.1	12.5	13.7	0.0195	0.403	0.618	0.039
21.7	13.5	14.7	0.0235	0.431	0.662	0.047
25.5	13.8	15.3	0.0275	0.448	0.687	0.055
34.8	15.8	16.3	0.0375	0.512	0.735	0.074
44.1	17.0	17.0	0.0475	0.549	0.766	0.095
53.4	17.6	17.5	0.0575	0.571	0.788	0.115
67.4	18.8	18.0	0.0725	0.607	0.813	0.145
86.1	20.1	18.5	0.0925	0.651	0.839	0.185
104.7	21.1	19.0	0.1125	0.680	0.858	0.225
128.1	22.0	19.4	0.1375	0.709	0.880	0.275
165.6	23.4	20.0	0.1775	0.755	0.905	0.355
212.4	25.0	20.5	0.2275	0.805	0.928	0.455
259.3	26.2	20.9	0.2775	0.844	0.944	0.555
306.2	27.3	21.2	0.3275	0.879	0.958	0.655
376.6	28.6	21.5	0.4025	0.919	0.976	0.805
470.6	29.9	21.8	0.5025	0.962	0.990	1.005
564.5	30.8	22.0	0.6025	0.988	0.997	1.205
658.4	31.1	22.0	0.7025	0.997	1.000	1.405
752.1	31.1	22.0	0.8025	0.998	1.000	1.605
845.8	31.2	22.0	0.9025	1.000	1.000	1.806

RUN C72769-1 K=2.55X10-6 F=0.002 NE

TEMP. RUN	VEL. RUN	PLATE	X	ST	CF/2	UINF	TGAS	TO	F
72769-1	72069-1	10	37.46	0.00130	0.00210	50.4	72.8	94.4	0.0019

THERMAL B.L. THK.	HYDRO. B.L. THK.	ENTHALPY THK.	MOMENTUM THK.	ENTHALPY RE.	MOMENTUM RE.	NO. DATA POINTS	K
0.542	0.405	0.0838	0.0323	2189.	837.	26	0.255E-05

YPLUS	TPLUS	LPLUS	Y	TBAR	U/UINF	Y/DELM
0.0	0.0	0.0	0.0000	0.000	0.000	0.000
2.8	2.7	2.9	0.0025	0.066	0.125	0.006
4.0	4.1	4.0	0.0035	0.129	0.175	0.009
5.2	5.1	5.1	0.0045	0.162	0.225	0.011
6.2	6.2	6.3	0.0055	0.194	0.275	0.014
7.4	7.2	7.4	0.0065	0.224	0.325	0.016
8.8	8.8	9.5	0.0085	0.276	0.419	0.021
13.2	10.6	12.0	0.0115	0.333	0.530	0.028
16.6	12.0	13.6	0.0145	0.377	0.600	0.036
21.2	12.8	15.0	0.0185	0.400	0.662	0.046
28.1	14.3	16.1	0.0245	0.448	0.712	0.060
37.2	15.7	17.0	0.0325	0.489	0.754	0.080
48.8	16.9	17.7	0.0425	0.529	0.785	0.105
60.4	18.1	18.2	0.0525	0.564	0.806	0.130
77.8	19.4	18.9	0.0675	0.601	0.837	0.167
94.9	20.1	19.4	0.0825	0.627	0.858	0.204
123.7	21.6	20.0	0.1075	0.671	0.887	0.265
152.7	22.9	20.5	0.1325	0.711	0.910	0.327
181.7	24.2	20.8	0.1575	0.750	0.927	0.389
239.6	26.1	21.3	0.2075	0.811	0.949	0.512
297.6	27.7	21.6	0.2575	0.856	0.965	0.635
355.6	28.9	21.9	0.3075	0.896	0.976	0.759
442.8	30.4	22.2	0.3825	0.939	0.987	0.944
530.0	31.4	22.3	0.4575	0.970	0.995	1.129
646.1	32.1	22.4	0.5575	0.994	0.999	1.376
762.1	32.3	22.4	0.6575	1.000	1.000	1.622

RUNS 072769-1 K=2.55 x 10^{-6} F=0.002 NE
072769-2

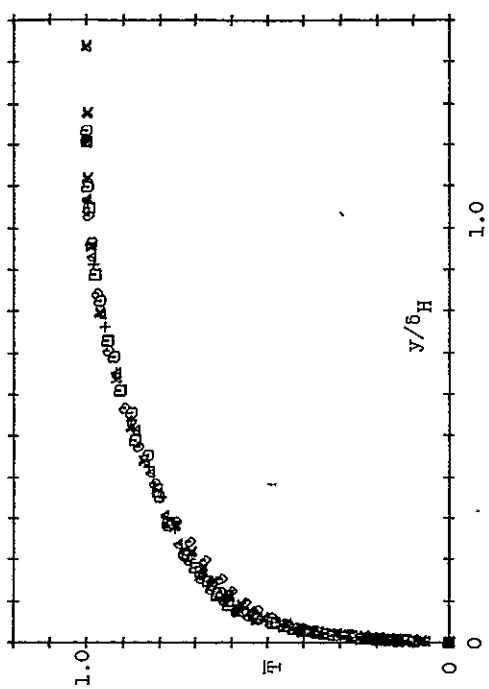

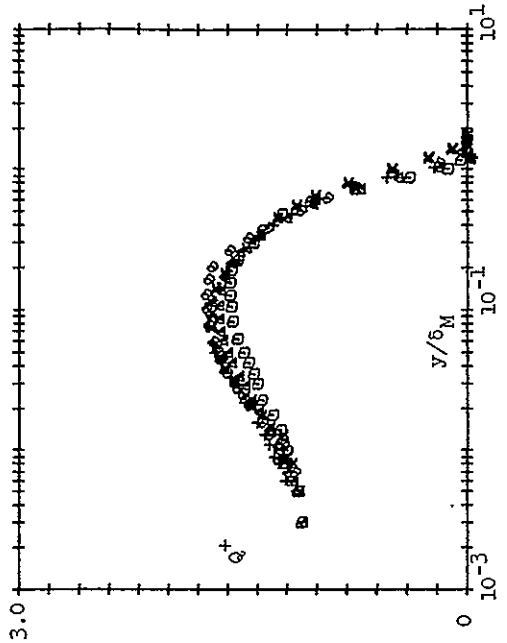

PROFILES

x(in.)	Symbol
13.81	□
21.81	○
25.86	△
29.81	+
33.59	×
37.46	◇

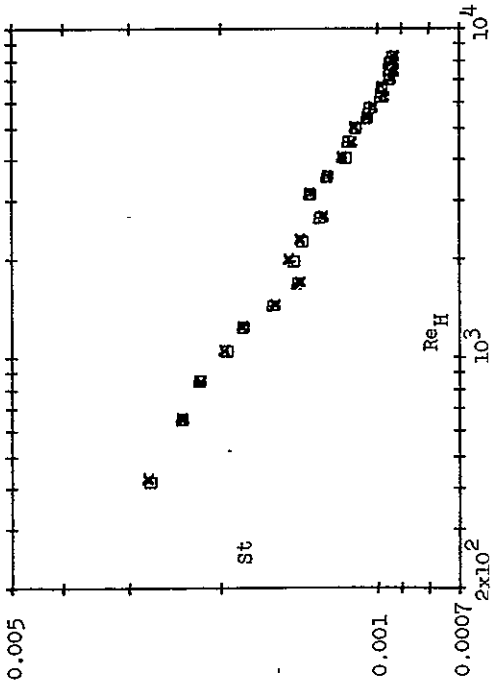

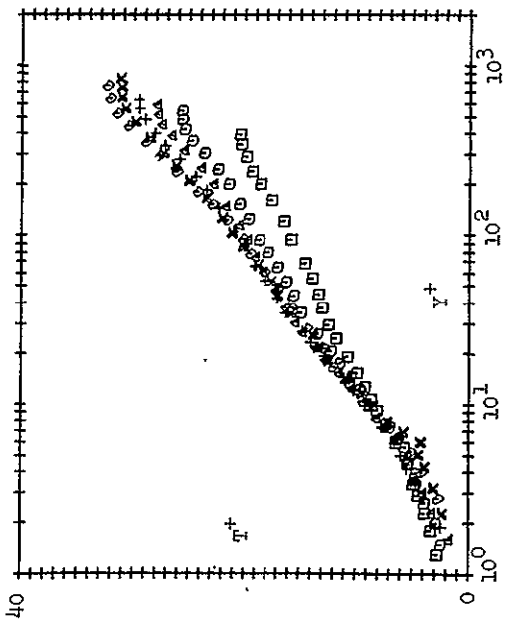

RUNS 083069-1
083069-2

K=2.60 x 10-6

F=0.004

NE

RUN 083069-1 K=2.60X10-6 F=0.004 NE

DATE 83069 RUN NO. 1
ANB TEMP 80.65 BASE TEMP 80.82 GAS TEMP 72.06 COVER TEMP 73.61 BARO PRES 29.69 REL HUM 0.48

PL	X	VEL	K	REH	ST	REH	CF2	TO	F
2	6	23.34	-C.150E-C6	538.	0.00216			98.3	0.0040
3	10	23.43	0.173E-C6	821.	0.00177			98.3	0.0041
4	13.81	23.60	0.449E-06	1066.	0.00154	1218.	0.CC13C	98.7	0.0041
4	14	23.41	C.449E-06	1C78.	0.00151			98.6	0.0041
5	18	24.14	0.706E-06	1348.	0.00137			98.4	0.0040
6	21.81	25.7C	0.192E-05	1539.	0.00127	1402.	0.00145	98.7	0.0040
6	22	26.01	0.192E-05	1556.	0.00119			98.6	0.0040
7	25.86	29.20	0.245E-05	1814.	0.CC119	1290.	0.CC15C	99.0	0.0038
7	26	29.40	0.245E-05	1876.	0.00122			98.7	0.0038
8	29.81	33.90	0.249E-05	2167.	0.00113	1185.	0.00154	98.5	0.0037
8	30	34.35	0.249E-05	2178.	0.CC110			98.9	0.CC37
9	33.59	40.40	0.254E-05	2470.	0.00108	1155.	0.00158	98.6	0.CC38
9	34	41.55	0.254E-05	2532.	0.00107			99.1	0.0038
10	37.46	50.00	0.252E-05	2862.	0.00102	1109.	0.CC159	98.7	0.0038
10	38	52.33	0.252E-05	2959.	0.00104			99.4	0.0038
11	42	68.17	0.109E-05	3541.	0.CC091			99.4	0.0038
12	46	70.25	0.125E-07	4215.	0.CC090			99.4	0.CC39
13	50	70.40	0.169E-07	4929.	0.CC076			99.0	0.0038
14	54	70.41	-0.132E-07	5590.	C.CCC65			98.9	0.0039
15	58	70.29	-0.141E-08	6240.	0.00068			98.8	0.0039
16	62	70.27	0.211E-08	6882.	0.CC060			98.8	0.0039
17	66	70.30	0.707E-09	7457.	C.00061			99.0	0.CC39
18	70	70.37	0.172E-08	8102.	0.00056			99.0	0.0038
19	74	70.33	-0.106E-07	8635.	C.CCC53			98.6	0.0039
20	78	70.29	0.776E-08	9309.	C.00056			99.0	0.0038
21	82	70.37	0.365E-08	9945.	0.00050			98.9	0.0039
22	86	70.40	0.137E-08	10542.	C.CCC52			99.0	0.0039
23	90	70.37	-0.726E-08	11110.	0.00051			99.1	0.0038

RUN 083069-2 K=2.60X10-6 F=0.004 NE

DATE 83069 RUN NO. 2
ANB TEMP 74.26 BASE TEMP 80.16 GAS TEMP 71.99 COVER TEMP 73.40 BARO PRES 29.69 REL HUM 0.49

PL	X	VEL	K	REH	ST	TO	F
2	6	23.38	-0.149E-06	537.	0.00220	97.9	0.0040
3	10	23.47	0.172E-C6	820.	0.00177	97.8	0.0041
4	14	23.52	0.446E-06	1081.	0.00155	98.1	0.0041
5	18	24.18	C.702E-06	1349.	0.00137	97.9	0.0040
6	22	26.05	0.191E-05	1607.	C.CC124	98.1	C.CC40
7	26	29.43	0.244E-05	1861.	0.00115	98.5	0.0038
8	30	34.38	0.248E-05	2219.	0.CC121	98.0	0.0037
9	34	41.57	0.253E-05	2556.	0.CC110	98.4	0.0038
10	38	52.34	0.251E-05	2572.	0.00101	98.8	0.0038
11	42	68.17	0.109E-05	3555.	C.CCC91	98.9	0.0039
12	46	70.26	0.125E-07	4235.	C.CCC89	98.8	0.0039
13	50	70.40	0.169E-07	5004.	C.00080	98.2	0.0039
14	54	70.41	-0.132E-07	5660.	C.CCCC6	98.2	0.0039
15	58	70.29	-0.141E-08	6314.	0.00068	98.1	0.0035
16	62	70.27	0.211E-08	6930.	0.00057	98.2	0.0039
17	66	70.30	C.707E-09	7532.	C.CCC55	98.3	C.CC39
18	70	70.37	0.172E-08	8218.	0.00055	98.1	0.0039
19	74	70.32	-0.106E-07	8651.	0.00052	97.8	0.0039
20	78	70.29	0.775E-08	9464.	C.CCC56	98.1	0.0038
21	82	70.37	0.364E-08	10079.	0.00051	98.1	0.0039
22	86	70.40	0.137E-08	10621.	C.CCC50	98.2	0.0039
23	90	70.37	-0.723E-08	11218.	C.CCC50	98.3	0.0039

SUMMARY OF PROFILE RESULTS

RUN 083069-1 K=2.60X10-6 F=0.004 NE

PL	X	VEL	K	F	TO	TINF	DELM	DELH
4	13.81	23.60	0.449E-06	C.CC41	98.7	72.3	0.722	0.744
6	21.81	25.7C	0.192E-05	0.0040	98.7	71.9	0.801	0.840
7	25.86	29.20	0.245E-05	C.CC38	99.C	71.9	0.753	0.840
8	29.81	33.90	0.249E-05	C.CC37	98.5	72.6	0.670	C.783
9	33.59	40.40	0.254E-05	C.0038	98.6	71.9	0.589	0.726
10	37.46	50.00	0.252E-05	C.CC38	98.7	71.9	0.470	0.639

PL	X	REH	ST	REH	CF2	DELTA2	THETA
4	13.81	1066.	0.CC154	1218.	0.CC13C	C.C910	C.1041
6	21.81	1539.	0.00127	1402.	0.00145	0.1190	0.1680
7	25.86	1814.	0.00119	1290.	0.00150	0.1242	0.0879
8	29.81	2167.	0.00113	1185.	C.00154	0.1273	C.0692
9	33.59	2470.	0.00108	1155.	0.00158	0.1213	0.0557
10	37.46	2862.	0.CC102	1109.	C.CC159	0.1139	0.0425

RUN C83069-1 K=2.60X10-6 F=0.004 NE

TEMP. PLN	VEL. RUN	PLATE	X	ST	CF/2	UINF	TGAS	TO	F
83069-1	82969-1	4	13.81	0.CC154	0.00130	23.6	72.3	98.7	0.0041

THERMAL B.L. THK.	HYDRO. B.L. THK.	ENTHALPY THK.	MOMENTUM THK.	ENTHALPY RE.	MOMENTUM RE.	NO. DATA POINTS	K
C.744	0.722	0.0910	0.1041	1066.	1218.	31	0.449E-06

YPLUS	TPLUS	UPLUS	Y	TBAR	U/UINF	Y/DELM
0.0	0.0	0.0	0.0000	0.000	0.000	0.CC0
1.0	1.6	1.4	0.0025	0.070	0.058	0.003
1.4	2.1	1.9	0.CC35	0.090	0.C87	0.CC5
1.9	2.7	2.5	0.0045	0.116	0.087	0.006
2.3	3.2	3.C	0.0055	0.136	0.106	0.008
2.7	3.6	3.6	0.0066	0.152	C.127	0.CC9
3.1	3.7	4.1	0.0075	0.162	0.144	0.010
3.9	4.2	5.C	0.0CS5	0.183	0.175	0.C13
5.2	5.2	6.2	0.0125	0.225	0.221	0.C17
6.8	6.6	7.9	0.0165	0.285	0.281	0.023
8.5	7.1	9.5	0.0205	0.305	C.335	0.028
10.2	8.0	10.4	0.0245	0.345	0.368	0.034
12.4	9.2	11.2	0.0295	0.397	0.399	0.041
14.5	9.6	11.5	C.0345	0.417	0.428	0.048
16.5	10.3	12.5	0.0395	0.447	0.448	0.055
20.7	11.4	13.5	0.C495	0.492	0.484	0.069
24.9	11.9	14.1	0.0595	0.515	0.506	0.C82
31.2	12.8	14.9	0.0745	0.551	0.536	0.103
39.7	13.8	15.8	0.0945	0.593	0.568	0.131
48.1	14.6	16.5	0.1145	0.625	0.592	0.159
58.6	15.4	17.3	0.1395	0.657	0.623	0.193
69.2	15.9	18.0	0.1645	0.682	0.647	0.228
90.3	17.1	19.2	0.2145	0.734	0.692	0.297
111.5	18.0	20.4	0.2645	0.771	0.735	0.366
143.2	19.4	22.0	0.3395	0.829	0.796	0.470
175.1	20.5	23.5	0.4145	0.874	0.850	0.574
207.0	21.4	24.5	0.4895	0.913	0.898	0.678
249.5	22.3	26.4	0.5695	0.953	C.954	0.816
292.0	23.1	27.2	0.6895	0.983	0.984	0.955
334.5	23.4	27.6	0.7895	0.996	0.997	1.093
387.5	23.5	27.6	0.9145	1.000	C.999	1.266

RUN 083069-1 K=2.60X10-6 F=0.004 NE

TEMP. RUN	VEL. RUN	PLATE	X	ST	CF/2	UINF	TGAS	TO	F
83069-1	82969-1	6	21.81	C.0C127	0.00145	25.7	71.9	98.7	0.0040

THERMAL B.L. THK.	HYDRO. B.L. THK.	ENTHALPY THK.	MOMENTUM THK.	ENTHALPY RE.	MOMENTUM RE.	NO. DATA POINTS	K
C.860	0.801	0.1190	0.1080	1539.	1402.	32	0.192E-05

YPLUS	TPLUS	UPLUS	Y	TBAR	U/UINF	Y/DELM
0.0	0.0	0.0	0.0000	0.000	0.000	0.000
1.2	1.7	1.3	0.0025	0.058	0.049	0.003
1.7	2.2	1.8	0.0035	0.075	C.068	0.004
2.2	2.8	2.3	C.0045	0.095	0.087	0.006
2.7	3.2	2.9	0.0055	0.110	C.107	0.007
3.6	4.0	3.9	0.0075	0.140	0.146	0.009
4.5	5.0	4.9	0.0095	0.171	0.180	0.012
5.5	5.7	5.9	C.0115	0.197	0.215	0.014
6.5	7.0	7.3	0.0145	0.241	0.270	0.018
8.9	8.4	9.1	C.0185	0.290	0.337	0.023
10.8	9.7	10.4	0.0225	0.332	0.384	0.028
12.8	10.4	11.3	0.0265	0.370	0.420	0.033
14.6	11.1	12.2	C.0305	0.379	0.453	0.038
17.1	12.0	13.C	0.0355	0.410	0.484	0.044
22.C	13.4	14.3	C.0455	0.457	0.529	0.057
26.8	14.3	15.C	0.0556	0.487	0.558	0.069
34.0	15.5	15.9	0.0705	0.529	0.591	0.088
41.3	16.2	16.5	0.0855	0.562	0.615	0.107
48.7	16.8	17.0	0.1005	0.590	0.634	0.125
58.3	17.9	17.6	0.1205	0.610	0.655	0.150
70.5	18.9	18.2	C.1455	0.641	0.680	0.182
82.7	19.6	18.7	0.1705	0.667	0.699	0.213
97.3	20.3	19.3	0.2005	0.689	0.721	0.250
114.3	21.1	20.C	0.2355	0.715	0.747	0.294
138.7	22.0	20.7	0.2855	0.748	0.775	0.356
175.3	23.6	21.8	C.3605	0.798	0.819	0.450
224.3	25.3	23.2	0.4605	0.856	0.870	0.575
273.3	26.6	24.4	0.5605	0.900	0.916	0.699
322.5	27.9	25.4	C.6605	0.941	0.955	0.824
396.0	29.1	26.3	C.8105	0.982	0.991	1.011
469.5	29.6	26.6	0.9605	0.999	1.000	1.196
518.5	29.7	26.6	1.0605	1.000	1.000	1.323

F=0.004

NE

RUNS 083069-1 083069-2 K=2.60 x 10⁻⁶ F=0.004 NE

RUN C83069-1 K=2.60X10-6 F=0.004 NE

TEMP. RUN	VEL. RUN	PLATE	X	ST	CF/2	UINF	TGAS	TU	F
E3069-1	82969-1	7	25.80	0.00119	0.00150	29.2	71.9	99.0	0.0038

THERMAL B.L. THK.	HYDRO. B.L. THK.	ENTHALPY THK.	MOMENTUM THK.	ENTHALPY RE.	MOMENTUM RE.	NO. DATA POINTS	K
C.640	0.753	0.1242	0.0879	1814.	1290.	31	0.2456-05

YPLUS	TPLUS	LPLUS	Y	TBAR	U/UINF	Y/DELH
0.0	0.0	0.0	C.0000	0.000	0.000	0.000
1.4	2.4	1.7	0.0025	0.076	0.066	0.003
1.9	2.6	2.4	C.0035	0.081	0.093	0.005
2.5	3.0	3.1	0.0045	0.095	0.119	0.006
3.1	3.9	3.8	C.0055	0.124	0.145	0.007
3.6	4.4	4.5	0.0065	0.138	0.172	0.009
4.7	5.5	5.8	0.0085	0.174	0.215	0.011
6.4	7.0	7.4	0.0115	0.220	0.279	0.015
8.6	8.8	9.7	0.0155	0.277	0.365	0.021
10.8	9.8	11.5	0.0195	0.310	0.434	0.026
13.0	11.1	12.8	C.0235	0.349	0.484	0.031
15.9	12.2	14.0	C.0285	0.385	0.530	0.038
19.8	13.8	15.2	0.0355	0.432	0.575	0.047
23.6	14.8	16.0	C.0425	0.464	0.606	0.056
28.1	15.6	16.7	0.0505	0.489	0.634	0.067
33.8	16.5	17.3	0.0605	0.515	0.659	0.080
42.1	17.6	18.0	C.0755	0.552	0.687	0.100
53.3	18.6	18.7	C.0955	0.580	0.712	0.127
70.2	20.0	19.3	C.1255	0.624	0.738	0.167
87.0	20.9	19.9	0.1555	0.650	0.760	0.207
115.1	22.3	20.7	0.2055	0.697	0.793	0.273
143.2	23.4	21.5	C.2555	0.727	0.821	0.339
171.5	24.7	22.2	C.3055	0.771	0.847	0.406
213.6	26.4	23.0	0.3805	0.819	0.880	0.505
256.2	27.6	23.6	0.4555	0.856	0.909	0.605
312.8	29.3	24.7	0.5555	0.905	0.946	0.738
369.5	30.7	25.3	0.6555	0.944	0.972	0.871
440.4	31.8	25.9	C.7805	0.983	0.994	1.037
511.1	32.2	26.0	0.9055	0.997	1.000	1.203
596.3	32.2	26.0	C.9555	0.999	1.000	1.269
595.8	32.3	26.0	1.0555	1.000	1.000	1.402

RUN C83069-1 K=2.60X10-6 F=0.004 NE

TEMP. RUN	VEL. RUN	PLATE	X	ST	CF/2	UINF	TGAS	TU	F
83069-1	82969-1	9	32.59	C.CC1C8	0.00158	40.4	71.9	98.0	0.0038

THERMAL B.L. THK.	HYDRO. B.L. THK.	ENTHALPY THK.	MOMENTUM THK.	ENTHALPY RE.	MOMENTUM RE.	NO. DATA POINTS	K
C.726	0.589	0.1213	0.0557	2470.	1155.	32	C.2541-05

YPLUS	TPLUS	LPLUS	Y	TBAR	U/UINF	Y/DELH
0.0	0.0	0.0	C.0000	0.000	0.000	0.000
1.9	1.1	2.4	C.0025	C.031	0.089	0.004
2.7	2.5	3.3	C.0035	0.072	0.125	0.006
3.5	4.0	4.2	0.0045	0.110	0.161	0.008
4.3	5.1	5.2	C.0055	0.144	C.197	0.009
5.1	5.6	6.2	0.0065	0.161	C.232	0.011
5.9	6.2	7.1	C.0075	0.177	C.268	0.013
6.7	6.6	7.8	0.0085	0.190	C.297	0.014
8.3	8.3	9.3	0.0105	0.235	0.354	C.018
10.6	10.0	11.6	C.0135	C.286	0.441	0.023
13.0	11.2	13.2	0.0165	0.320	C.506	C.028
15.4	11.6	14.2	C.0195	0.331	0.541	0.033
18.6	12.2	15.3	0.0235	0.347	C.583	0.040
22.5	13.1	16.3	0.0285	0.371	C.622	C.048
30.5	15.1	17.7	0.0385	0.426	0.674	C.065
38.3	16.2	18.6	0.0485	0.461	0.708	0.082
50.3	17.9	19.4	0.0635	0.505	0.742	0.108
62.3	19.0	20.1	C.0785	0.537	0.769	0.133
82.1	20.4	21.0	0.1035	0.576	0.804	0.176
102.1	21.7	21.7	0.1285	0.611	C.831	0.218
122.1	22.1	22.3	C.1535	0.648	0.864	0.260
142.1	24.2	22.7	0.1785	0.668	0.893	0.303
182.1	26.2	23.4	C.2285	0.734	0.901	C.388
222.2	27.7	23.9	C.2785	0.775	0.922	0.472
262.3	29.0	24.3	0.3285	0.812	0.939	0.557
322.7	30.9	24.9	0.4035	0.866	0.957	0.685
383.0	32.5	25.2	C.4785	0.904	C.974	C.812
443.5	33.7	25.5	0.5535	0.944	0.985	0.939
524.0	35.0	25.7	C.6535	0.978	0.994	1.109
604.4	35.6	25.8	0.7535	0.995	0.999	1.278
684.7	35.8	25.9	C.8535	0.999	1.000	1.446
765.0	35.8	25.9	C.9535	1.000	1.000	1.618

RUN C83069-1 K=2.60X10-6 F=0.004 NE

TEMP. RUN	VEL. RUN	PLATE	X	ST	CF/2	UINF	TGAS	TU	F
E3069-1	82969-1	8	25.81	C.CC113	0.00156	33.9	72.6	98.9	0.0037

THERMAL B.L. THK.	HYDRO. B.L. THK.	ENTHALPY THK.	MOMENTUM THK.	ENTHALPY RE.	MOMENTUM RE.	NO. DATA POINTS	K
C.783	0.670	0.1273	0.0692	2167.	1165.	31	0.2496-05

YPLUS	TPLUS	LPLUS	Y	TBAR	U/UINF	Y/DELH
0.0	0.0	0.0	0.0000	0.000	0.000	0.000
1.6	1.8	2.1	C.0025	0.052	0.081	0.004
2.3	2.7	3.0	C.0035	C.082	C.114	C.005
3.0	3.6	3.8	0.0045	0.106	0.146	0.007
3.6	4.5	4.6	0.0055	0.134	0.179	0.008
4.2	5.2	5.6	0.0065	0.155	0.211	0.010
5.5	6.4	7.2	0.0085	0.190	0.273	0.013
6.8	7.4	8.5	0.0105	0.210	0.322	0.016
9.5	8.3	10.9	0.0145	0.247	0.415	0.022
12.1	9.7	12.7	C.0185	0.269	0.482	0.028
15.3	11.4	14.2	0.0235	0.338	0.541	0.035
18.7	12.7	15.3	0.0285	0.375	0.582	0.043
22.5	13.5	16.2	C.0345	0.399	0.619	0.051
26.5	14.4	16.9	C.0405	0.424	C.647	0.060
33.1	15.6	17.7	0.0505	0.460	C.679	0.075
39.6	16.5	18.4	C.0605	0.486	C.704	0.090
52.8	18.0	19.2	0.0805	0.532	C.739	0.120
65.3	19.5	20.1	0.1055	0.577	0.772	0.157
85.8	21.0	20.7	C.1305	0.615	C.798	0.195
102.3	21.7	21.3	0.1555	0.634	C.819	C.232
136.3	23.4	22.1	C.2055	0.688	0.849	0.307
168.5	25.2	22.7	C.2555	C.740	0.874	0.381
201.6	26.6	23.3	0.3055	0.781	0.898	0.456
234.8	27.9	23.7	C.3555	0.815	0.915	0.530
268.0	28.9	24.1	C.4055	0.845	0.931	0.605
317.9	30.3	24.6	0.4805	0.886	0.951	C.717
367.9	31.6	25.0	0.5555	0.923	C.969	0.829
434.5	33.0	25.5	0.6555	0.963	0.988	0.978
501.1	33.6	25.7	0.7555	0.987	0.998	1.127
567.6	34.3	25.8	C.8555	0.995	1.000	1.276
633.9	34.3	25.8	C.9555	1.000	1.000	1.425

RUN C83069-1 K=2.60X10-6 F=0.004 NE

TEMP. RUN	VEL. RUN	PLATE	X	ST	CF/2	UINF	TGAS	TU	F
83069-1	82969-1	10	31.46	0.CC1C2	0.00159	50.0	71.9	98.7	0.0038

THERMAL B.L. THK.	HYDRO. B.L. THK.	ENTHALPY THK.	MOMENTUM THK.	ENTHALPY RE.	MOMENTUM RE.	NO. DATA POINTS	K
C.639	C.470	0.1129	0.0425	2862.	1145.	29	0.252L-05

YPLUS	TPLUS	LPLUS	Y	TBAR	U/UINF	Y/DELH
0.0	0.0	0.0	0.0000	0.000	0.000	0.000
2.4	3.1	3.0	C.0025	0.045	C.115	0.005
3.4	4.0	4.3	C.0035	0.109	C.161	0.007
4.4	4.7	5.5	0.0045	0.130	C.207	0.010
5.4	5.5	6.6	C.0055	0.150	0.253	0.012
6.3	6.2	7.9	0.0065	0.168	C.294	0.014
8.3	7.3	10.2	0.0085	0.199	0.361	C.018
11.2	9.1	12.4	0.0115	0.247	0.446	0.024
14.2	10.9	14.2	0.0145	0.287	0.502	0.031
18.1	12.1	15.8	0.0185	0.330	0.552	0.039
23.0	13.4	17.0	0.0235	0.366	0.638	0.050
29.0	14.8	18.0	0.0295	0.401	0.674	0.063
35.9	15.8	18.7	0.0365	0.424	0.702	0.078
43.7	16.3	19.3	C.0445	0.443	0.729	C.095
53.6	17.1	20.1	0.0545	0.464	0.756	0.116
68.4	18.6	20.5	0.0695	0.505	0.786	0.148
88.1	20.3	21.1	C.0895	0.549	0.819	0.190
112.8	22.1	22.6	0.1145	0.599	0.853	0.243
137.6	23.7	23.3	0.1395	0.641	0.880	0.297
167.4	25.2	23.8	0.1695	0.675	C.904	C.360
202.2	26.8	24.5	0.2045	0.725	0.925	C.436
251.9	28.9	25.0	C.2545	0.778	C.946	0.541
301.8	30.8	25.3	0.3045	0.828	0.961	0.647
351.7	32.1	25.6	C.3545	0.864	0.972	0.754
401.7	33.0	25.7	C.4045	0.899	0.980	0.860
476.6	35.1	26.0	0.4795	0.942	0.991	1.019
551.5	36.3	26.1	C.5545	0.971	0.998	1.179
651.4	37.2	26.2	0.6545	0.994	1.000	1.391
751.0	37.4	26.2	0.7545	1.000	1.000	1.604

RUNS 083069-1 K=2.60 x 10^{-6} F=0.004 NE
083069-2

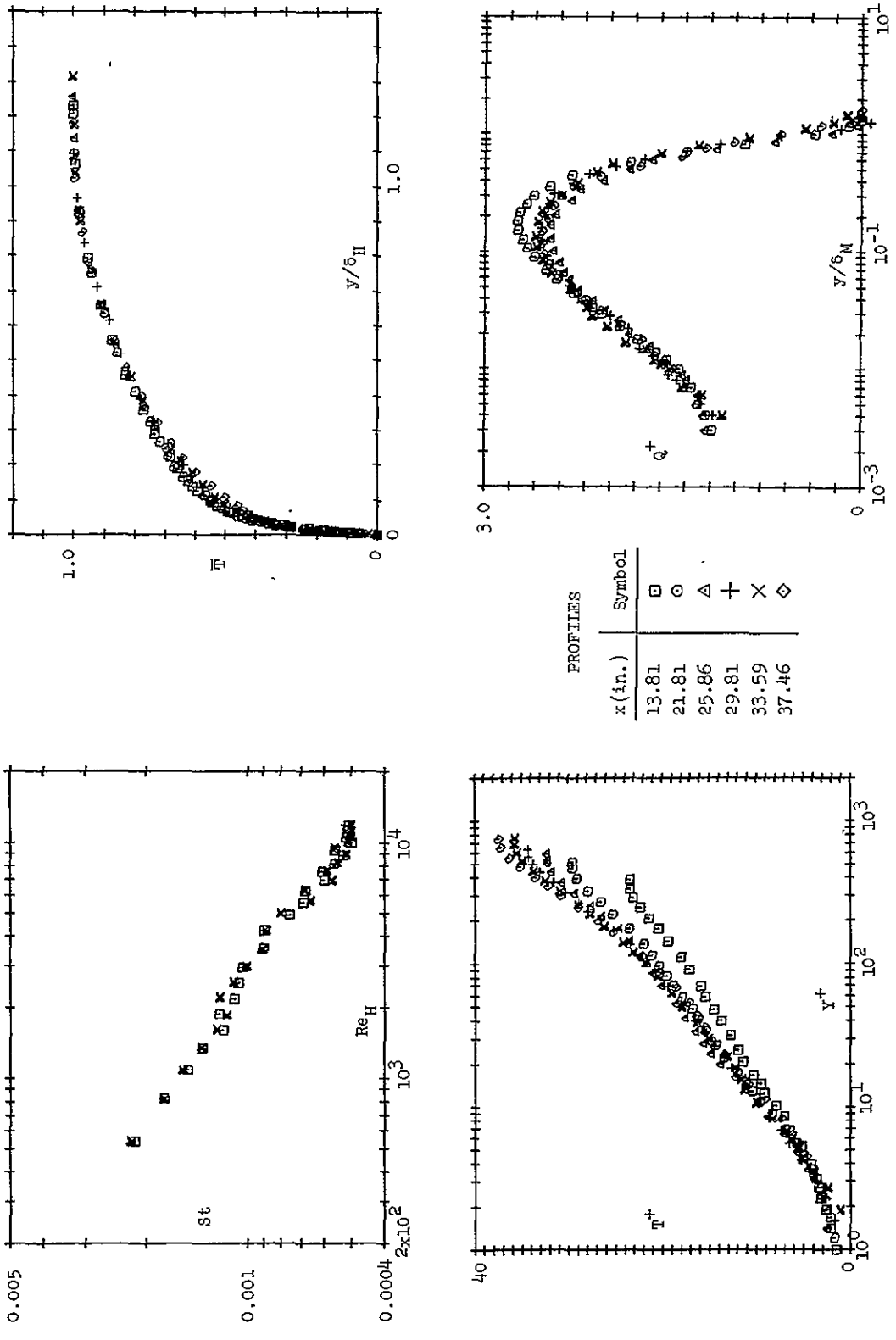

RUNS 071569-1 071569-2 K=2.55 x 10-6 F=0.0 IC

RUN 071569-1 K=2.55X1C-6 F=0.0 IC

DATE 71569 RUN NO. 1

AMB TEMP	BASE TEMP	GAS TEMP	COVER TEMP	BARO PRES	REL HUM
78.40	82.27	70.78	72.33	29.96	0.51

PL	X	VEL	K	REH	ST	REM	CF2	TO	F
2	6	23.15	-0.173E-07	502.	0.00288			72.5	0.0000
3	10	23.09	-0.635E-07	582.	0.00231			72.6	0.0000
4	14	23.15	0.914E-07	372.	0.00118			74.1	0.0000
5	18	23.52	0.826E-06	163.	0.00463			95.4	0.0000
6	21.81	25.40	0.201E-05	336.	0.00308	796.	0.00255	96.5	0.0000
6	22	25.47	0.201E-05	344.	0.00307			96.3	0.0000
7	26	28.82	0.249E-05	497.	0.00258			96.4	0.0000
8	29.81	33.40	0.245E-05	628.	0.00226	639.	0.00260	96.5	0.0000
8	30	33.58	0.245E-05	637.	0.00212			96.7	0.0000
9	34	40.40	0.253E-05	798.	0.00194			96.3	0.0000
10	37.46	49.30	0.252E-05	899.	0.00173	528.	0.00248	96.7	0.0000
10	38	50.71	0.252E-05	961.	0.00173			96.6	0.0000
11	42	65.76	0.109E-05	1164.	0.00150			96.4	0.0000
12	46	67.40	-0.318E-07	1413.	0.00216			96.3	0.0000
13	50	67.30	0.103E-07	1728.	0.00222			96.0	0.0000
14	54	67.45	0.228E-07	2017.	0.00203			96.0	0.0000
15	58	67.59	0.139E-07	2312.	0.00201			95.8	0.0000
16	62	67.68	0.876E-08	2562.	0.00198			96.0	0.0000
17	66	67.75	0.458E-08	2822.	0.00193			96.1	0.0000
18	70	67.85	0.349E-08	3065.	0.00189			96.2	0.0000
19	74	67.79	-0.184E-07	3326.	0.00184			96.2	0.0000
20	78	67.69	0.546E-08	3579.	0.00180			96.1	0.0000
21	82	67.73	-0.956E-08	3796.	0.00177			96.3	0.0000
22	86	67.95	0.380E-07	4011.	0.00176			96.5	0.0000
23	90	67.92	-0.131E-07	4305.	0.00171			96.2	0.0000

RUN 071569-2 K=2.55X1C-6 F=0.0 IC

DATE 71569 RUN NO. 2

AMB TEMP	BASE TEMP	GAS TEMP	COVER TEMP	BARO PRES	REL HUM
80.47	82.55	70.95	72.47	29.96	0.39

PL	X	VEL	K	REH	ST	TO	F
2	6	23.19	-0.172E-07	571.	0.00290	72.6	0.0000
3	10	23.13	-0.631E-07	661.	0.00239	72.7	0.0000
4	14	23.18	0.908E-07	412.	0.00121	74.3	0.0000
5	18	23.56	0.821E-06	167.	0.00457	95.6	0.0000
6	22	25.51	0.200E-05	344.	0.00302	96.6	0.0000
7	26	28.85	0.248E-05	496.	0.00256	96.6	0.0000
8	30	33.60	0.244E-05	655.	0.00218	96.2	0.0000
9	34	40.41	0.253E-05	810.	0.00197	96.2	0.0000
10	38	50.71	0.251E-05	965.	0.00173	96.7	0.0000
11	42	65.75	0.109E-05	1158.	0.00149	96.7	0.0000
12	46	67.39	-0.317E-07	1408.	0.00214	96.6	0.0000
13	50	67.29	0.102E-07	1707.	0.00222	96.6	0.0000
14	54	67.44	0.228E-07	1996.	0.00204	96.6	0.0000
15	58	67.58	0.138E-07	2287.	0.00200	96.4	0.0000
16	62	67.66	0.875E-08	2513.	0.00195	96.8	0.0000
17	66	67.74	0.457E-08	2792.	0.00192	96.7	0.0000
18	70	67.84	0.349E-08	3044.	0.00188	96.8	0.0000
19	74	67.78	-0.184E-07	3299.	0.00183	96.8	0.0000
20	78	67.68	0.546E-08	3560.	0.00180	96.7	0.0000
21	82	67.72	-0.956E-08	3778.	0.00176	96.9	0.0000
22	86	67.94	0.380E-07	3986.	0.00176	97.1	0.0000
23	90	67.90	-0.131E-07	4282.	0.00170	96.7	0.0000

SUMMARY OF PROFILE RESULTS

RUN 071569-1 K=2.55X1C-6 F=0.0 IC

PL	X	VEL	K	F	TO	TINF	DELN	DELH
6	21.81	25.40	0.201E-05	0.0000	96.5	70.8	0.574	0.383
8	29.81	33.40	0.245E-05	0.0000	96.5	71.4	0.490	0.424
10	37.46	49.30	0.252E-05	0.0000	96.7	70.4	0.323	0.363

PL	X	REH	ST	REM	CF2	DELTA2	THETA
6	21.81	336.	0.00308	796.	0.00255	0.0262	0.0616
8	29.81	628.	0.00226	639.	0.00260	0.0373	0.0376
10	37.46	899.	0.00173	528.	0.00248	0.0361	0.0206

RUNS 071569-1 K=2.55 x 10**6 F=0.0 IC
071569-2

RUN 071569-1 K=2.55X10-6 F=0.0 IC

TEMP. RUN	VEL. RUN	PLATE	X	ST	CF/2	UINF	TGAS	TO	F
71569-2	71669-1	6	21.81	0.00308	0.00255	25.4	70.8	96.5	0.0000

THERMAL B.L. THK.	HYDRO. B.L. THK.	ENTHALPY THK.	MOMENTUM THK.	ENTHALPY RE.	MOMENTUM RE.	NO. DATA POINTS	K
0.283	0.574	0.0262	0.0616	336.	796.	29	0.201E-05

YPLUS	TPLUS	UPLUS	Y	TBAR	U/UINF	Y/DELM
0.0	0.0	0.0	0.0000	0.000	0.000	0.000
1.6	2.0	1.6	0.0025	0.127	0.081	0.004
2.2	2.6	2.3	0.0035	0.162	0.113	0.006
2.9	3.3	3.0	0.0046	0.206	0.148	0.008
3.5	3.7	3.6	0.0055	0.232	0.177	0.010
4.8	4.6	4.5	0.0075	0.285	0.242	0.013
6.1	5.5	5.9	0.0095	0.338	0.293	0.017
7.4	6.2	6.9	0.0115	0.386	0.346	0.020
9.3	7.2	8.5	0.0145	0.450	0.422	0.025
11.2	8.1	9.4	0.0175	0.502	0.471	0.030
13.1	8.9	10.4	0.0205	0.550	0.520	0.036
15.1	9.5	11.3	0.0235	0.586	0.559	0.041
17.7	10.2	12.0	0.0275	0.634	0.594	0.048
19.6	10.7	12.4	0.0305	0.661	0.616	0.053
22.9	11.4	12.9	0.0355	0.703	0.644	0.062
26.1	11.8	13.4	0.0405	0.728	0.667	0.071
32.6	12.6	14.0	0.0505	0.774	0.698	0.088
39.1	13.1	14.4	0.0605	0.806	0.720	0.105
45.6	13.5	14.7	0.0705	0.829	0.736	0.123
55.3	14.0	15.1	0.0855	0.858	0.759	0.149
68.3	14.4	15.4	0.1055	0.885	0.773	0.184
84.5	14.8	15.9	0.1305	0.910	0.796	0.227
110.5	15.2	16.4	0.1705	0.937	0.822	0.297
143.0	15.6	17.0	0.2205	0.960	0.852	0.384
191.7	16.0	17.8	0.2955	0.979	0.891	0.515
256.7	16.2	18.7	0.3955	0.992	0.937	0.689
305.4	16.2	19.2	0.4705	0.996	0.964	0.819
370.3	16.3	19.7	0.5705	0.999	0.988	0.993
435.3	16.3	19.9	0.6705	1.000	0.998	1.168

RUN 071569-1 K=2.55X10-6 F=0.0 IC

TEMP. RUN	VEL. RUN	PLATE	X	ST	CF/2	UINF	TGAS	TO	F
71569-2	71669-1	10	37.46	0.00173	0.00248	49.3	70.4	96.7	0.0000

THERMAL B.L. THK.	HYDRO. B.L. THK.	ENTHALPY THK.	MOMENTUM THK.	ENTHALPY RE.	MOMENTUM RE.	NO. DATA POINTS	K
0.363	0.323	0.0361	0.0206	898.	528.	29	0.252E-05

YPLUS	TPLUS	UPLUS	Y	TBAR	U/UINF	Y/DELM
0.0	0.0	0.0	0.0000	0.000	0.000	0.000
3.0	3.3	2.7	0.0025	0.120	0.127	0.008
4.3	3.6	3.7	0.0035	0.130	0.178	0.011
5.4	4.4	4.6	0.0045	0.160	0.228	0.014
6.7	5.3	5.5	0.0055	0.196	0.279	0.017
8.0	6.5	6.9	0.0065	0.238	0.330	0.020
9.1	7.4	8.0	0.0075	0.268	0.381	0.023
11.6	8.9	9.6	0.0095	0.324	0.463	0.029
14.1	10.5	11.4	0.0115	0.382	0.549	0.036
16.5	11.9	12.6	0.0135	0.429	0.606	0.042
19.1	12.9	13.8	0.0155	0.468	0.659	0.048
22.8	14.4	14.9	0.0185	0.521	0.712	0.057
26.5	15.5	15.6	0.0215	0.558	0.751	0.067
31.6	16.6	16.4	0.0257	0.601	0.790	0.080
37.7	18.0	17.0	0.0305	0.647	0.815	0.094
43.8	19.0	17.6	0.0355	0.683	0.843	0.110
50.0	19.7	17.8	0.0405	0.711	0.857	0.125
62.5	20.9	18.4	0.0505	0.753	0.884	0.156
74.8	21.9	18.6	0.0605	0.784	0.897	0.187
81.2	22.8	18.7	0.0655	0.815	0.903	0.203
112.1	23.4	19.2	0.0905	0.840	0.928	0.280
143.2	24.3	19.5	0.1155	0.872	0.943	0.357
186.8	25.4	19.8	0.1505	0.907	0.958	0.466
236.6	26.2	20.0	0.1905	0.935	0.968	0.590
298.9	26.8	20.2	0.2405	0.959	0.979	0.744
392.3	27.5	20.5	0.3155	0.982	0.989	0.976
485.8	27.8	20.6	0.3905	0.995	0.997	1.209
579.1	27.9	20.7	0.4655	0.999	0.999	1.441
703.4	28.0	20.7	0.5655	1.000	1.000	1.750

RUN 071569-1 K=2.55X10-6 F=0.0 IC

TEMP. RUN	VEL. RUN	PLATE	X	ST	CF/2	UINF	TGAS	TO	F
71569-2	71669-1	8	29.81	0.00226	0.00260	33.4	71.4	96.5	0.0000

THERMAL B.L. THK.	HYDRO. B.L. THK.	ENTHALPY THK.	MOMENTUM THK.	ENTHALPY RE.	MOMENTUM RE.	NO. DATA POINTS	K
0.424	0.490	0.0373	0.0376	628.	639.	28	0.245E-05

YPLUS	TPLUS	UPLUS	Y	TBAR	U/UINF	Y/DELM
0.0	0.0	0.0	0.0000	0.000	0.000	0.000
2.1	2.8	2.1	0.0025	0.128	0.106	0.005
3.0	3.6	3.0	0.0035	0.168	0.148	0.007
3.8	4.3	3.8	0.0045	0.198	0.190	0.009
4.7	5.0	4.6	0.0055	0.226	0.232	0.011
5.5	5.5	5.5	0.0065	0.250	0.275	0.013
7.1	6.6	7.2	0.0085	0.301	0.356	0.017
8.8	7.8	8.6	0.0105	0.351	0.427	0.021
10.6	8.7	9.7	0.0125	0.394	0.483	0.025
12.3	9.4	10.7	0.0145	0.424	0.533	0.030
14.9	10.5	11.9	0.0175	0.478	0.595	0.036
17.4	11.6	12.7	0.0205	0.521	0.637	0.042
20.8	12.7	13.7	0.0245	0.574	0.688	0.050
26.1	13.8	14.5	0.0305	0.620	0.727	0.060
29.4	14.7	15.0	0.0345	0.665	0.755	0.070
33.6	15.4	15.5	0.0395	0.693	0.777	0.081
42.3	16.5	16.1	0.0495	0.741	0.808	0.101
50.8	17.2	16.5	0.0595	0.772	0.831	0.121
63.7	18.0	16.8	0.0745	0.806	0.849	0.152
80.9	18.7	17.2	0.0945	0.836	0.868	0.193
102.3	19.3	17.5	0.1195	0.867	0.885	0.244
145.3	20.3	18.0	0.1695	0.909	0.910	0.346
186.3	21.1	18.3	0.2195	0.941	0.927	0.448
252.7	21.6	18.7	0.2945	0.968	0.950	0.600
317.2	22.0	19.1	0.3695	0.984	0.971	0.753
403.1	22.3	19.5	0.4695	0.995	0.988	0.957
489.1	22.4	19.7	0.5695	0.999	0.997	1.161
574.9	22.4	19.7	0.6695	1.000	1.000	1.365

F=0.0

IC

RUNS 071569-1 K=2.55 x 10^{-6} F=0.0 IC
071569-2

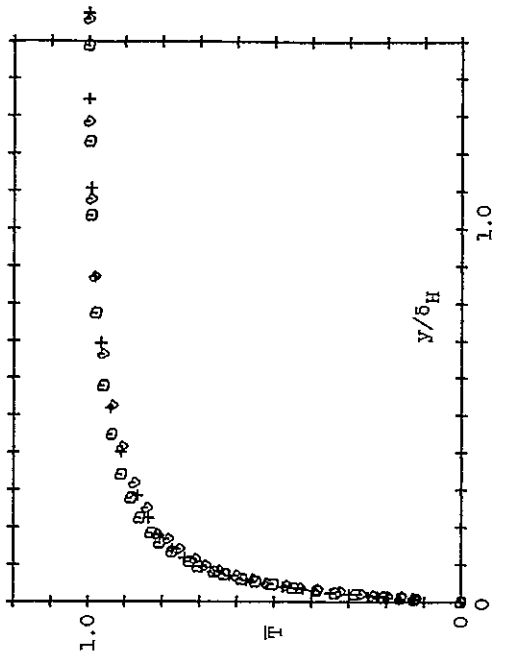

PROFILES

x(in.)	Symbol
13.81	⊡
21.81	⊙
25.86	△
29.81	+
33.59	×
37.46	◇

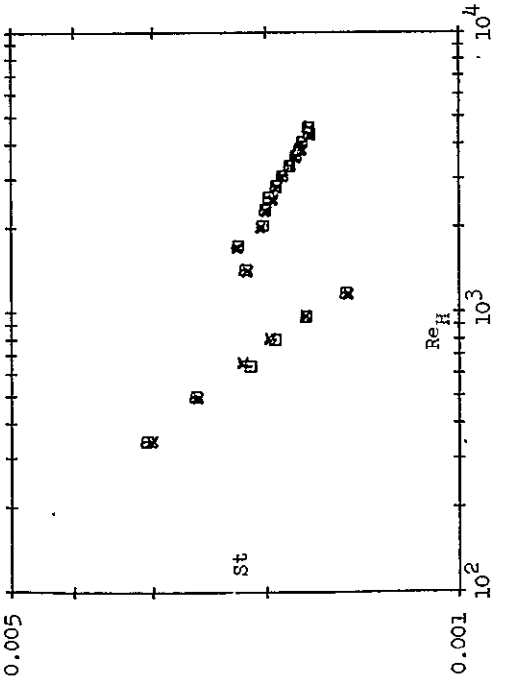

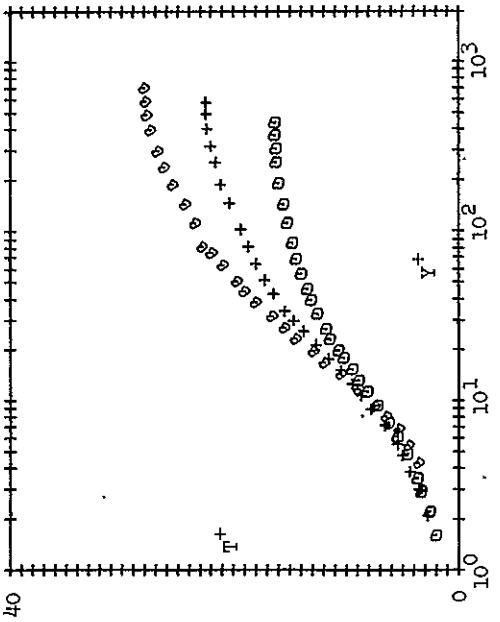

RUNS 092469-1
092469-2

K=2.50 x 10⁻⁶

F=0.0

IC

RUN 092469-1 K=2.50X10-6 F=0.0 IC

DATE 92469 RUN NO. 1
AMB TEMP 77.88 BASE TEMP 82.10 GAS TEMP 72.93 COVER TEMP 73.61 BARO PRES 29.97 REL HUM 0.55

PL	X	VEL	K	REH	ST	REH	CF2	TG	F
2	6	23.20	0.126E-06	321.	0.00345			98.9	0.0000
3	10	23.28	0.156E-C7	455.	C.CC315			98.9	0.0000
4	14	23.16	-0.217E-07	621.	0.CCC289			98.7	0.CCCC
5	18	23.14	-C.480E-C7	744.	0.00277			98.8	0.CCCC
6	22	23.10	-0.864E-C7	872.	0.00269			98.9	0.0000
7	26	23.02	0.235E-C7	992.	0.00257			98.9	0.CCCC
8	30	23.19	0.711E-07	1109.	0.00244			98.9	0.0000
9	34	23.13	0.263E-07	1225.	0.CC237			98.8	0.0000
10	38	23.29	0.647E-08	1339.	0.CC235			98.9	0.0000
11	42	23.06	-0.801E-07	1431.	0.CC232			99.1	0.0000
12	46	23.19	0.215E-06	1557.	0.CC233			98.8	0.0000
12	46.76	23.50	0.215E-06	1577.	0.00242	1529.	0.00210	99.0	0.0000
13	50	23.25	0.142E-06	1651.	C.C0230			98.9	0.0000
14	54	23.80	0.986E-06	1773.	0.00213			98.7	0.CCCC
15	58	25.52	0.178E-05	1866.	0.00210			98.9	0.CCCC
15	58.94	26.40	0.178E-C5	1843.	0.00202	1366.	0.00267	99.0	0.0000
16	62	28.96	0.244E-05	1975.	0.00181			98.9	0.CCCC
16	62.86	29.7C	0.244E-05	1976.	0.00187	1162.	0.00264	98.9	0.0000
17	66	33.57	0.248E-05	2065.	C.C0171			98.9	0.0000
17	66.76	34.60	0.248E-05	2040.	0.00170	938.	0.00257	99.0	0.0000
18	70	40.53	0.264E-C5	2212.	0.CC150			98.8	0.0000
18	70.69	42.00	0.264E-05	2165.	0.CC152	762.	0.C0243	98.7	0.0000
19	74	51.18	0.255E-05	2368.	0.00134			98.6	0.0000
19	74.58	53.20	0.255E-C5	2261.	0.00133	640.	0.00217	98.4	0.CCCC
20	78	64.04	0.728E-06	2511.	0.00118			98.7	0.CCCC
21	82	64.71	0.117E-07	2744.	C.00172			98.3	0.CCCC
22	86	64.76	0.712E-C8	2575.	0.00200			98.3	0.0000
23	90	64.73	-0.141E-07	3212.	0.00192			98.5	0.0000

RUN 092469-2 K=2.50X10-6 F=0.0 IC

DATE 92469 RUN NO. 2
AMB TEMP 76.50 BASE TEMP 82.13 GAS TEMP 72.51 COVER TEMP 74.03 BARO PRES 29.97 REL HUM 0.53

PL	X	VEL	K	REH	ST	TG	F
2	6	23.19	0.126E-06	319.	0.00345	98.4	0.0000
3	10	23.26	0.156E-C7	431.	0.CC314	98.5	0.0000
4	14	23.15	-0.217E-07	616.	0.00292	98.2	0.0000
5	18	23.13	-0.480E-07	745.	0.00279	98.4	0.0000
6	22	23.09	-0.864E-C7	865.	0.CC272	98.5	0.0000
7	26	23.01	0.235E-07	996.	0.00258	98.4	0.0000
8	30	23.18	0.711E-C7	1121.	0.CC248	98.2	0.0000
9	34	23.11	0.263E-07	1231.	0.CC240	98.3	0.0000
10	38	23.24	0.648E-08	1333.	0.CC234	98.5	0.0000
11	42	23.05	-C.800E-C7	1431.	0.CC236	98.6	0.0000
12	46	23.18	0.214E-06	1558.	0.CC232	98.4	0.0000
13	50	23.24	0.142E-06	1663.	0.CC230	98.4	0.0000
14	54	23.79	0.985E-C6	1777.	0.CC215	98.3	0.0000
15	58	25.56	0.177E-05	1872.	0.CC212	98.4	0.0000
16	62	28.95	0.243E-05	2007.	0.CC185	98.1	0.0000
17	66	33.55	0.247E-05	2102.	C.CC172	98.3	0.0000
18	70	40.52	0.264E-C5	2227.	0.CC151	98.3	0.0000
19	74	51.16	0.255E-05	2344.	0.CC135	98.3	0.0000
20	78	64.01	0.727E-06	2513.	0.CC118	98.4	0.CCCC
21	82	64.68	0.117E-07	2749.	0.00174	97.9	0.0000
22	86	64.73	0.711E-C8	2581.	0.CC200	98.0	0.0000
23	90	64.70	-0.141E-07	3221.	0.CC191	98.1	0.0000

SUMMARY OF PROFILE RESULTS

RUN 092469-1 K=2.50X10-6 F=0.0 IC

PL	X	VEL	K	F	TG	TINF	DELM	DELH
12	46.76	23.50	0.215E-06	C.CCCC	99.C	72.9	1.061	1.147
15	58.94	26.40	0.178E-05	0.0000	99.0	72.9	1.024	1.127
16	62.86	29.7C	0.244E-05	0.0000	98.9	73.0	0.983	1.029
17	66.76	34.60	0.248E-05	0.0000	99.0	72.9	0.743	0.855
18	70.69	42.0C	0.264E-05	0.0000	98.7	72.6	0.500	0.775
19	74.58	53.2C	0.255E-C5	C.CCCC	98.4	72.4	0.435	0.649

PL	X	REH	ST	REH	CF2	DELTA2	THETA
12	46.76	1577.	0.00242	1529.	0.00210	0.1354	C.1314
15	58.94	1843.	0.00202	1366.	0.00267	0.1393	0.1069
16	62.86	1976.	0.00187	1162.	0.00264	0.1314	0.0800
17	66.76	2040.	0.00170	938.	0.00257	0.1166	0.0557
18	70.69	2169.	0.00152	762.	0.00243	0.1021	0.0374
19	74.58	2261.	0.00133	640.	C.00217	0.0850	0.0249

RUN 092469-1 K=2.50X10-6 F=0.0 IC

TEMP. RUN 92469-1 | VEL. RUN 92469-1 | PLATE 12 | X 46.76 | ST 0.00242 | CF/2 0.00210 | UINF 23.5 | TGAS 72.9 | TG 99.0 | F 0.0000

THERMAL B.L. THK. 1.147 | HYDRO. B.L. THK. 1.061 | ENTHALPY THK. 0.1354 | MOMENTUM THK. 0.1314 | ENTHALPY RE. 1577. | MOMENTUM RE. 1529. | NO. DATA POINTS 29 | K 0.215E-06

YPLUS	TPLUS	UPLUS	Y	TBAR	U/UINF	Y/DELM
0.0	0.0	0.0	0.0000	0.000	0.000	0.000
1.3	1.5	1.7	0.0025	0.080	0.074	0.002
1.8	1.9	2.3	0.0035	0.097	0.104	0.003
2.4	2.3	3.0	0.0045	0.125	0.133	0.004
2.9	2.8	3.8	0.0055	0.149	0.163	0.005
3.9	3.5	4.5	0.0075	0.188	0.222	0.007
5.5	4.6	5.9	0.0105	0.243	0.289	0.010
7.7	5.7	7.5	0.0145	0.303	0.364	0.014
9.8	6.7	8.8	0.0185	0.357	0.400	0.017
11.9	7.6	9.7	0.0225	0.402	0.444	0.021
14.6	8.5	10.7	0.0275	0.450	0.486	0.026
17.7	9.0	11.4	0.0335	0.478	0.521	0.032
21.0	9.6	12.0	0.0395	0.508	0.547	0.037
26.3	10.4	12.7	0.0495	0.552	0.581	0.047
34.4	11.0	13.4	0.0645	0.584	0.610	0.061
45.1	11.7	13.5	0.0845	0.619	0.634	0.080
58.4	12.3	14.4	0.1095	0.649	0.661	0.103
85.1	13.2	15.3	0.1595	0.695	0.700	0.150
111.9	13.7	15.5	0.2095	0.722	0.729	0.197
152.2	14.4	16.8	0.2845	0.763	0.768	0.268
192.4	15.1	17.4	0.3595	0.797	0.800	0.339
246.2	15.9	18.2	0.4595	0.834	0.839	0.433
313.4	16.7	19.1	0.5845	0.874	0.681	0.551
380.8	17.4	19.6	0.7095	0.909	0.920	0.668
475.2	18.1	20.8	0.8845	0.951	0.963	0.833
515.6	18.4	21.1	0.9595	0.966	0.976	0.904
556.5	18.8	21.5	1.0395	0.987	0.994	1.045
677.4	19.1	21.6	1.2595	0.959	1.000	1.187
721.2	19.1	21.6	1.3595	1.000	1.000	1.281

RUN 092469-1 K=2.50X10-6 F=0.0 IC

TEMP. RUN 92469-1 | VEL. RUN 92469-1 | PLATE 15 | X 58.94 | ST 0.00202 | CF/2 0.00267 | UINF 26.4 | TGAS 72.9 | TU 99.0 | F 0.0000

THERMAL B.L. THK. 1.127 | HYDRO. B.L. THK. 1.024 | ENTHALPY THK. 0.1393 | MOMENTUM THK. C.1065 | ENTHALPY RE. 1843. | MOMENTUM RE. 1366. | NO. DATA POINTS 28 | K 0.178E-05

YPLUS	TPLUS	UPLUS	Y	TBAR	U/UINF	Y/DELM
0.0	0.0	0.0	0.0000	0.000	0.000	0.000
1.6	2.9	1.6	0.0025	0.114	0.083	0.002
2.4	3.8	2.2	0.0035	0.145	0.116	0.003
3.0	4.3	2.8	0.0045	0.166	C.149	0.004
3.7	4.7	3.5	0.0055	0.185	0.182	0.005
5.1	5.7	4.6	0.0075	0.219	0.248	0.007
6.4	6.6	5.7	0.0095	0.253	0.300	0.009
9.1	8.3	7.5	0.0135	0.319	0.398	0.013
11.8	9.5	8.5	0.0175	0.367	0.467	0.017
15.2	11.0	10.1	0.0225	0.424	0.532	0.022
18.6	12.0	11.1	0.0275	0.461	0.580	0.027
22.6	13.0	11.7	0.0335	0.499	0.620	0.033
26.7	14.1	12.3	0.0395	0.540	0.649	0.039
33.5	15.0	12.9	0.0495	0.573	0.679	0.048
43.7	15.9	13.5	0.0645	0.612	0.710	0.063
57.2	16.8	14.0	0.0845	0.641	0.737	0.083
77.6	17.8	14.4	0.1145	0.680	0.760	0.112
94.6	18.2	14.6	0.1395	0.695	0.775	0.136
128.7	19.1	15.0	0.1895	0.728	0.798	0.185
179.8	20.0	15.5	0.2645	0.765	0.824	0.258
230.9	20.9	16.0	0.3395	0.796	0.849	0.332
299.2	22.0	16.6	0.4395	0.835	0.878	0.429
367.7	22.8	17.1	0.5395	C.868	0.904	0.527
470.3	23.9	17.7	0.6895	0.908	0.940	0.673
573.1	24.9	18.1	0.8395	0.946	0.966	0.820
641.7	25.4	18.4	0.9395	0.965	0.981	0.918
778.8	26.2	18.7	1.1395	0.992	0.996	1.113
915.7	26.4	18.7	1.3395	1.000	0.999	1.308

F=0.0

IC

RUN 092469-1 K=2.50X10-6 F=0.0 IC

TEMP. RUN	VEL. RUN	PLATE	X	ST	CF/2	UINF	TGAS	TO	F
92469-1	92569-1	16	62.86	0.00187	0.00264	29.7	73.0	98.9	0.0000

THERMAL B.L. THK.	HYDRO. B.L. THK.	ENTHALPY THK.	MOMENTUM THK.	ENTHALPY RE.	MOMENTUM RE.	NO. DATA POINTS	K
1.029	0.883	0.1314	0.0800	1976.	1162.	32	0.244E-05

YPLUS	TPLUS	UPLUS	Y	TBAR	U/UINF	Y/DELH
0.0	0.0	0.0	0.0000	0.000	0.000	0.000
1.8	2.1	1.8	0.0025	0.077	0.092	0.003
2.7	2.5	2.5	0.0035	0.090	0.129	0.004
3.4	3.0	3.2	0.0045	0.109	0.166	0.005
4.1	3.6	3.9	0.0055	0.129	0.203	0.006
4.9	4.3	4.7	0.0065	0.155	0.240	0.007
6.3	5.3	6.0	0.0085	0.191	0.309	0.010
8.6	7.0	7.6	0.0115	0.256	0.393	0.013
10.9	8.4	9.0	0.0145	0.304	0.464	0.016
13.9	9.4	10.3	0.0185	0.359	0.536	0.021
17.0	11.1	11.4	0.0225	0.402	0.593	0.025
22.2	13.2	12.6	0.0295	0.473	0.652	0.033
27.5	14.5	13.4	0.0365	0.520	0.695	0.041
33.7	15.4	14.1	0.0445	0.553	0.730	0.050
41.3	16.6	14.5	0.0545	0.593	0.760	0.062
48.9	17.2	14.9	0.0645	0.619	0.780	0.073
60.2	17.9	15.2	0.0795	0.644	0.795	0.090
75.5	18.8	15.5	0.0995	0.673	0.810	0.113
94.5	19.5	15.8	0.1245	0.701	0.826	0.141
117.4	20.2	16.1	0.1545	0.723	0.841	0.175
155.4	21.0	16.4	0.2045	0.750	0.857	0.231
193.5	21.7	16.6	0.2545	0.775	0.871	0.288
250.7	22.7	17.0	0.3295	0.810	0.891	0.373
308.1	23.5	17.4	0.4045	0.837	0.909	0.458
384.5	24.5	17.8	0.5045	0.873	0.930	0.571
480.2	25.6	18.2	0.6295	0.911	0.954	0.713
576.0	26.6	18.6	0.7545	0.944	0.974	0.854
652.7	27.2	18.7	0.8545	0.967	0.987	0.967
729.4	27.7	18.9	0.9545	0.983	0.994	1.080
844.3	28.1	18.5	1.1045	0.997	0.999	1.250
959.0	28.1	19.0	1.2545	0.999	1.000	1.420
1035.5	28.1	19.0	1.3545	1.000	1.000	1.533

RUN 092469-1 K=2.50X10-6 F=0.0 IC

TEMP. RUN	VEL. RUN	PLATE	X	ST	CF/2	UINF	TGAS	TO	F
92469-1	92569-1	18	70.65	0.00152	0.00243	42.0	72.6	98.7	0.0000

THERMAL B.L. THK.	HYDRO. B.L. THK.	ENTHALPY THK.	MOMENTUM THK.	ENTHALPY RE.	MOMENTUM RE.	NO. DATA POINTS	K
0.735	0.580	0.1021	0.0374	2169.	762.	30	0.264E-05

YPLUS	TPLUS	UPLUS	Y	TBAR	U/UINF	Y/DELH
0.0	0.0	0.0	0.0000	0.000	0.000	0.000
2.8	3.6	2.3	0.0025	0.109	0.116	0.004
3.5	4.0	3.3	0.0035	0.121	0.163	0.006
4.6	5.3	4.1	0.0045	0.159	0.209	0.008
5.6	5.8	5.1	0.0055	0.176	0.255	0.009
6.6	6.6	6.0	0.0065	0.198	0.302	0.011
8.7	8.0	7.8	0.0085	0.242	0.391	0.015
11.7	10.0	9.0	0.0115	0.304	0.495	0.020
14.8	11.5	11.5	0.0145	0.349	0.580	0.025
19.0	13.4	13.0	0.0185	0.405	0.657	0.032
24.2	15.5	14.4	0.0235	0.464	0.725	0.041
29.2	16.8	15.2	0.0285	0.504	0.768	0.049
34.4	18.3	15.8	0.0335	0.550	0.798	0.058
39.6	19.3	16.2	0.0385	0.578	0.820	0.066
47.9	20.4	16.7	0.0465	0.611	0.846	0.080
58.3	21.6	17.1	0.0565	0.649	0.866	0.097
73.8	22.8	17.5	0.0715	0.683	0.885	0.123
94.5	23.6	17.7	0.0915	0.705	0.902	0.158
120.4	24.6	18.0	0.1165	0.735	0.915	0.201
156.7	25.4	18.2	0.1515	0.762	0.927	0.261
204.6	26.7	18.5	0.2015	0.797	0.940	0.348
260.5	27.5	18.7	0.2515	0.823	0.950	0.434
338.5	28.7	18.9	0.3265	0.857	0.962	0.563
442.6	30.1	19.1	0.4265	0.896	0.974	0.736
546.8	31.3	19.3	0.5265	0.932	0.985	0.908
677.3	32.5	19.5	0.6515	0.968	0.995	1.124
807.7	33.3	19.6	0.7765	0.990	0.998	1.339
911.8	33.6	19.5	0.8765	0.998	1.000	1.512
1015.6	33.6	19.6	0.9765	0.999	1.000	1.684
1172.0	33.6	19.6	1.1265	1.000	1.000	1.943

RUN 092469-1 K=2.50X10-6 F=0.0 IC

TEMP. RUN	VEL. RUN	PLATE	X	ST	CF/2	UINF	TGAS	TO	F
92469-1	92569-1	17	66.76	0.00170	0.00257	34.6	72.9	99.0	0.0000

THERMAL B.L. THK.	HYDRO. B.L. THK.	ENTHALPY THK.	MOMENTUM THK.	ENTHALPY RE.	MOMENTUM RE.	NO. DATA POINTS	K
0.895	0.743	0.1166	0.0557	2040.	938.	30	0.248E-05

YPLUS	TPLUS	UPLUS	Y	TBAR	U/UINF	Y/DELH
0.0	0.0	0.0	0.0000	0.000	0.000	0.000
2.2	2.9	2.1	0.0025	0.096	0.110	0.003
3.0	3.5	3.0	0.0035	0.117	0.154	0.005
3.9	4.7	3.9	0.0045	0.134	0.197	0.006
4.7	5.3	4.8	0.0055	0.176	0.241	0.007
5.6	5.8	5.5	0.0065	0.194	0.285	0.009
7.3	7.2	7.1	0.0085	0.240	0.369	0.011
10.0	8.9	8.9	0.0115	0.293	0.459	0.015
12.6	10.4	9.9	0.0145	0.346	0.507	0.020
16.1	12.2	11.7	0.0185	0.402	0.606	0.025
20.4	13.8	13.0	0.0235	0.455	0.673	0.032
24.7	15.1	13.8	0.0285	0.497	0.712	0.038
30.0	16.4	14.6	0.0345	0.539	0.753	0.046
36.2	17.6	15.1	0.0415	0.579	0.781	0.056
44.9	18.7	15.6	0.0515	0.614	0.810	0.069
53.7	19.3	16.0	0.0615	0.635	0.827	0.083
71.2	20.5	16.4	0.0815	0.675	0.849	0.110
93.0	21.4	16.7	0.1065	0.702	0.867	0.143
136.8	22.8	17.2	0.1565	0.747	0.889	0.211
180.7	23.7	17.5	0.2065	0.774	0.905	0.278
246.5	24.8	17.8	0.2815	0.812	0.924	0.379
312.4	25.8	18.0	0.3565	0.843	0.936	0.480
400.3	27.0	18.4	0.4565	0.881	0.953	0.614
488.4	28.0	18.6	0.5565	0.915	0.969	0.749
576.7	29.0	18.8	0.6565	0.943	0.981	0.883
664.8	29.7	19.0	0.7565	0.969	0.991	1.018
753.1	30.2	19.1	0.8565	0.985	0.997	1.152
841.3	30.6	19.1	0.9565	0.997	0.999	1.287
951.2	30.6	19.1	1.0815	0.999	1.000	1.455
1061.2	30.7	19.1	1.2065	1.000	1.000	1.623

RUN 092469-1 K=2.50X10-6 F=0.0 IC

TEMP. RUN	VEL. RUN	PLATE	X	ST	CF/2	UINF	TGAS	TO	F
92469-1	92569-1	19	74.58	0.00123	0.00217	53.2	72.4	98.4	0.0000

THERMAL B.L. THK.	HYDRO. B.L. THK.	ENTHALPY THK.	MOMENTUM THK.	ENTHALPY RE.	MOMENTUM RE.	NO. DATA POINTS	K
0.649	0.435	0.0850	0.0249	2261.	640.	28	0.255E-05

YPLUS	TPLUS	UPLUS	Y	TBAR	U/UINF	Y/DELH
0.0	0.0	0.0	0.0000	0.000	0.000	0.000
3.0	4.3	2.6	0.0025	0.121	0.122	0.006
4.3	5.2	3.7	0.0035	0.147	0.171	0.008
5.5	6.5	4.6	0.0045	0.182	0.220	0.010
6.8	7.2	5.7	0.0055	0.203	0.269	0.013
7.9	8.1	6.7	0.0065	0.225	0.318	0.015
9.1	8.9	7.7	0.0075	0.249	0.367	0.017
10.4	9.8	8.6	0.0085	0.276	0.409	0.020
14.0	11.6	11.2	0.0115	0.325	0.532	0.026
19.0	14.0	13.6	0.0155	0.342	0.695	0.036
23.9	16.0	15.2	0.0195	0.446	0.726	0.045
28.9	17.8	16.3	0.0235	0.495	0.779	0.054
33.9	19.2	17.0	0.0275	0.532	0.815	0.063
40.0	20.4	17.6	0.0325	0.567	0.843	0.075
48.6	21.9	18.2	0.0395	0.608	0.870	0.091
58.6	23.1	18.6	0.0475	0.642	0.892	0.109
71.0	24.4	18.9	0.0575	0.676	0.908	0.132
89.9	25.4	19.2	0.0728	0.704	0.925	0.167
120.5	26.8	19.5	0.0975	0.740	0.939	0.224
182.6	28.6	19.5	0.1475	0.788	0.957	0.339
244.6	29.6	20.0	0.1975	0.817	0.966	0.454
337.8	31.2	20.2	0.2725	0.861	0.975	0.627
462.4	33.0	20.4	0.3725	0.908	0.985	0.857
587.0	34.4	20.5	0.4725	0.948	0.993	1.087
711.7	35.6	20.6	0.5725	0.978	0.997	1.317
836.4	36.1	20.6	0.6725	0.994	0.998	1.547
960.9	36.3	20.7	0.7725	0.999	1.000	1.777
1085.3	36.4	20.7	0.8725	1.000	1.000	2.007

RUNS 092469-1 K=2.50 x 10^{-6} F=0.0 IC
092469-2

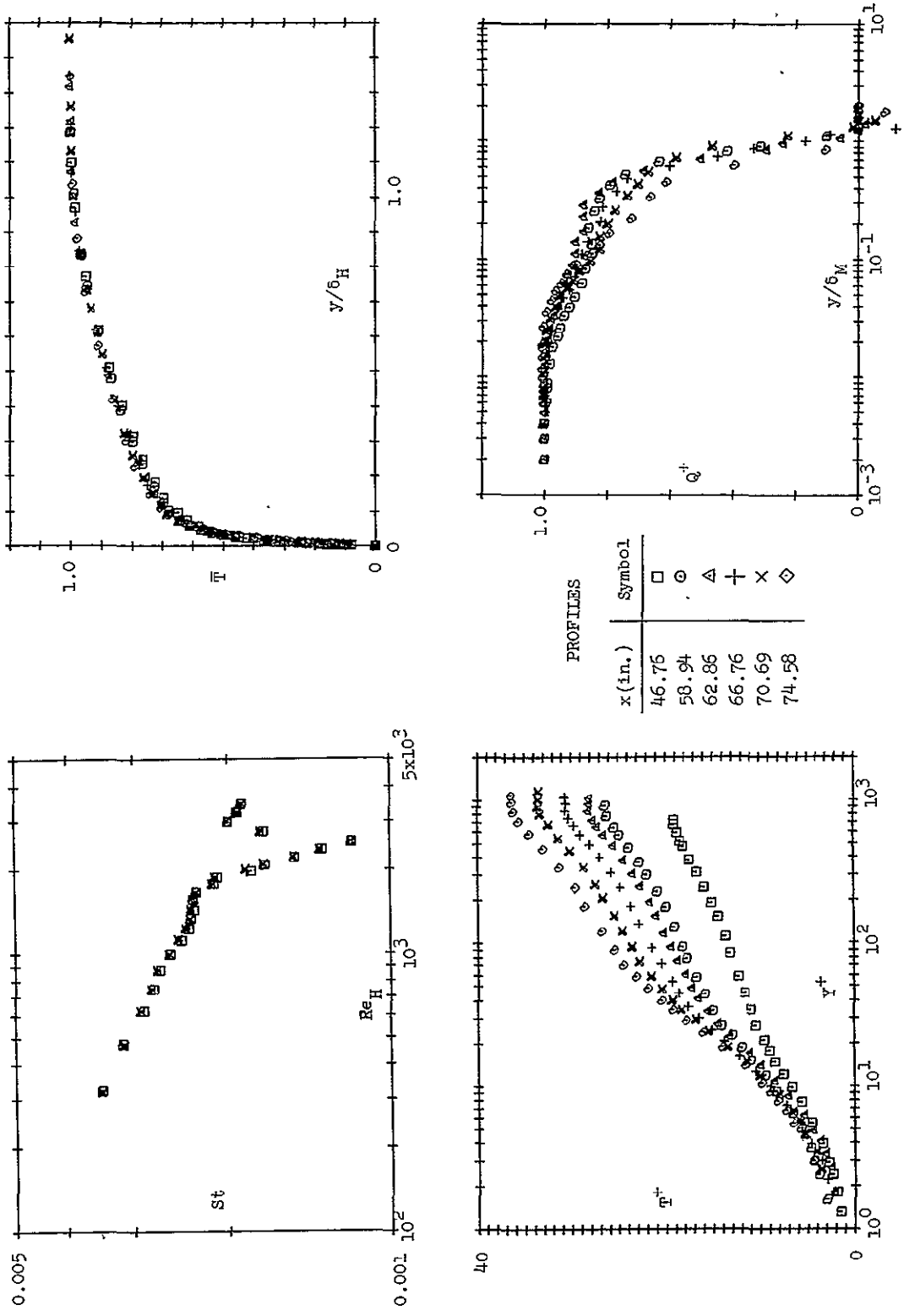

RUNS 100269-1
100269-2

K=2.50 x 10-6

F=0.0

IC

RUN 100269-1 K=2.50X10-6 F=0.0 IC

DATE 100269 RUN NO. 1

AMB TEMP	BASE TEMP	GAS TEMP	COVER TEMP	BARO PRES	REL HUM
74.97	75.59	66.32	67.88	29.80	0.46

PL	X	VEL	K	REH	ST	REM	CF2	TO	F
2	6	23.11	C.000E CC	51.	0.00166			68.4	0.0000
3	10	23.11	0.000E 00	165.	0.00146			68.4	0.0000
4	14	23.07	-0.352E-07	240.	0.00172			68.4	0.0000
5	18	23.07	C.000E 00	317.	0.00157			68.4	0.0000
6	22	23.07	C.000E 00	391.	0.00157			68.4	0.0000
7	26	23.07	C.000E 00	563.	0.00221			68.1	0.0000
8	30	23.08	-0.854E-07	678.	0.00218			68.0	0.0000
9	34	23.07	0.138E-06	727.	0.00195			68.2	0.0000
10	38	23.05	0.306E-07	457.	0.00087			69.5	0.0000
11	42	23.18	-0.146E-06	167.	0.00418			88.8	0.0000
12	46	23.16	0.200E-07	336.	0.00304			89.0	0.0000
12	46.76	23.50	C.200E-07	363.	0.00310	1456.	0.00210	89.1	0.0000
13	50	23.29	0.338E-06	480.	0.00252			88.9	0.0000
14	54	23.68	0.879E-06	615.	0.00264			88.8	0.0000
15	58	25.45	0.186E-05	744.	0.00251			88.8	0.0000
15	58.94	26.40	0.186E-05	757.	0.00243	1327.	0.00267	89.3	0.0000
16	62	28.69	0.227E-05	874.	0.00223			88.8	0.0000
17	66	33.14	0.254E-05	1007.	0.00201			88.9	0.0000
17	66.76	34.60	0.254E-05	1015.	0.00195	895.	0.00257	89.6	0.0000
18	70	40.18	0.258E-05	1153.	0.00174			88.8	0.0000
19	74	50.74	0.253E-05	1295.	0.00153			89.0	0.0000
19	74.58	53.20	0.253E-05	1372.	0.00151	595.	0.00217	87.2	0.0000
20	78	63.45	0.727E-06	1476.	0.00136			88.8	0.0000
21	82	64.17	0.176E-07	1703.	0.00202			88.8	0.0000
22	86	64.25	0.490E-08	1980.	0.00222			89.0	0.0000
23	90	64.18	-0.179E-07	2236.	0.00209			89.1	0.0000

RUN 100269-2 K=2.50X10-6 F=0.0 IC

DATE 100269 RUN NO. 2

AMB TEMP	BASE TEMP	GAS TEMP	COVER TEMP	BARO PRES	REL HUM
75.07	75.73	67.16	68.68	29.80	0.42

PL	X	VEL	K	REH	ST	TO	F
2	6	23.12	0.000E 00	116.	0.00202	68.8	0.0000
3	10	23.12	0.000E 00	205.	0.00179	68.8	0.0000
4	14	23.08	-0.352E-07	297.	0.00211	68.8	0.0000
5	18	23.08	0.000E 00	392.	0.00192	68.8	0.0000
6	22	23.08	C.000E 00	483.	0.00192	68.8	0.0000
7	26	23.08	C.000E 00	677.	C.00261	68.6	C.0000
8	30	23.09	-0.856E-07	786.	0.00246	68.6	0.0000
9	34	23.08	0.138E-06	845.	C.00222	68.7	0.0000
10	38	23.06	0.306E-07	481.	C.00089	70.1	0.0000
11	42	23.20	-0.146E-06	167.	0.00422	89.3	0.0000
12	46	23.17	C.200E-07	334.	C.00305	89.6	0.0000
13	50	23.30	0.338E-06	482.	0.00295	89.3	C.0000
14	54	23.70	0.880E-06	616.	0.00269	89.4	0.0000
15	58	25.47	0.187E-05	747.	0.00253	89.4	0.0000
16	62	28.71	0.228E-05	874.	0.00224	89.5	0.0000
17	66	33.16	0.255E-05	1009.	0.00201	89.5	0.0000
18	70	40.20	0.259E-05	1158.	0.00176	89.3	0.0000
19	74	50.76	0.253E-05	1316.	0.00156	89.3	0.0000
20	78	63.49	0.728E-06	1485.	C.00137	89.4	0.0000
21	82	64.21	0.177E-07	1707.	0.00203	89.4	0.0000
22	86	64.29	0.490E-08	1979.	0.00225	89.5	0.0000
23	90	64.22	-0.179E-07	2261.	0.00213	89.5	0.0000

SUMMARY OF PROFILE RESULTS

RUN 100269-1 K=2.50X10-6 F=0.0 IC

PL	X	VEL	K	F	TO	TINF	DELM	DELH
12	46.76	23.50	C.200E-07	0.0000	89.1	66.8	1.061	0.514
15	58.94	26.40	0.186E-05	C.0000	89.3	67.2	1.024	0.750
17	66.76	34.60	0.254E-05	0.0000	89.6	67.2	0.743	0.670
19	74.58	53.20	0.253E-05	C.0000	87.2	67.1	0.435	0.508

PL	X	REH	ST	REM	CF2	DELTA2	THETA
12	46.76	363.	0.00310	1456.	0.00210	0.0306	C.1231
15	58.94	757.	0.00243	1327.	0.00267	0.0565	0.1022
17	66.76	1015.	0.00195	895.	0.00257	0.0576	0.0530
19	74.58	1372.	0.00151	595.	0.00217	0.0511	0.0230

RUNS 100269-1 100269-2 K=2.50 x 10-6 F=0.0 IC

RUN 100269-1 K=2.50X10-6 F=0.0 IC

TEMP. RUN	VEL. RUN	PLATE	X	ST	CF/2	UINF	TGAS	TO	F
100269-2	92569-1	12	44.76	0.00310	0.00210	23.5	66.8	89.1	0.0000

THERMAL B.L. THK.	HYDRO. B.L. THK.	ENTHALPY THK.	MOMENTUM THK.	ENTHALPY RE.	MOMENTUM RE.	NO. DATA POINTS	K
0.514	1.081	0.0306	0.1231	363.	1456.	29	0.200E-07

YPLUS	TPLUS	UPLUS	Y	TBAR	U/UINF	Y/DELH
0.0	0.0	0.0	0.0000	0.000	0.000	0.000
1.3	1.9	1.6	0.0025	0.128	0.074	0.002
1.9	2.3	2.3	0.0035	0.154	0.104	0.003
2.4	2.8	3.0	0.0045	0.191	0.133	0.004
2.9	3.3	3.6	0.0055	0.223	0.163	0.005
4.1	4.0	4.8	0.0075	0.270	0.222	0.007
5.7	5.1	5.9	0.0105	0.342	0.299	0.010
7.3	6.1	7.1	0.0135	0.409	0.324	0.011
8.9	6.9	8.1	0.0165	0.465	0.371	0.016
11.1	7.8	9.2	0.0205	0.522	0.424	0.019
13.4	8.5	10.1	0.0245	0.569	0.462	0.020
15.5	9.1	10.8	0.0285	0.609	0.494	0.027
18.2	9.6	11.4	0.0335	0.643	0.521	0.032
21.6	10.2	11.8	0.0395	0.684	0.547	0.037
24.8	10.7	12.3	0.0455	0.716	0.569	0.043
30.3	11.3	12.8	0.0555	0.756	0.594	0.052
38.5	11.8	13.3	0.0705	0.798	0.617	0.066
49.5	12.4	13.8	0.0905	0.838	0.641	0.085
63.2	12.9	14.4	0.1155	0.863	0.666	0.109
77.0	13.2	14.8	0.1405	0.883	0.687	0.132
98.9	13.7	15.4	0.1805	0.916	0.713	0.170
126.4	14.1	16.0	0.2305	0.941	0.740	0.217
167.6	14.5	16.8	0.3055	0.964	0.777	0.288
208.8	14.7	17.4	0.3805	0.979	0.808	0.358
263.7	14.8	18.3	0.4805	0.988	0.847	0.453
318.6	14.9	19.0	0.5805	0.993	0.880	0.547
373.6	15.0	19.6	0.6805	0.995	0.912	0.641
428.6	15.0	20.2	0.7805	0.998	0.939	0.735
483.5	15.0	20.7	0.8805	1.000	0.962	0.830

RUN 100269-1 K=2.50X10-6 F=0.0 IC

TEMP. RUN	VEL. RUN	PLATE	X	ST	CF/2	UINF	TGAS	TO	F
100269-2	92569-1	17	66.76	0.00195	0.00257	34.6	67.2	89.6	0.0000

THERMAL B.L. THK.	HYDRO. B.L. THK.	ENTHALPY THK.	MOMENTUM THK.	ENTHALPY RE.	MOMENTUM RE.	NO. DATA POINTS	K
0.670	0.743	0.0576	0.0530	1015.	895.	30	0.254E-05

YPLUS	TPLUS	UPLUS	Y	TBAR	U/UINF	Y/DELH
0.0	0.0	0.0	0.0000	0.000	0.000	0.000
2.2	3.3	2.1	0.0025	0.125	0.110	0.003
3.0	3.9	3.0	0.0035	0.144	0.154	0.005
4.0	4.1	3.8	0.0045	0.155	0.197	0.006
4.8	5.2	4.6	0.0055	0.195	0.241	0.007
5.7	6.0	5.5	0.0065	0.225	0.285	0.009
6.6	6.4	6.3	0.0075	0.242	0.329	0.010
8.3	7.6	7.8	0.0095	0.287	0.402	0.013
10.1	8.0	8.8	0.0115	0.339	0.459	0.015
12.8	10.2	9.7	0.0145	0.385	0.507	0.020
15.4	11.0	11.2	0.0175	0.441	0.564	0.024
18.1	12.9	12.2	0.0205	0.482	0.637	0.028
21.7	14.5	13.0	0.0245	0.535	0.681	0.033
25.2	15.6	13.6	0.0285	0.579	0.712	0.038
28.8	16.3	14.1	0.0325	0.609	0.740	0.044
33.2	17.1	14.6	0.0375	0.635	0.765	0.050
37.6	17.9	15.0	0.0425	0.658	0.784	0.057
46.6	19.1	15.4	0.0525	0.712	0.812	0.071
59.9	20.4	15.9	0.0675	0.756	0.838	0.091
77.7	21.3	16.2	0.0875	0.790	0.854	0.118
104.5	22.2	16.6	0.1175	0.825	0.874	0.158
149.1	23.4	17.0	0.1675	0.866	0.893	0.225
216.0	24.5	17.4	0.2425	0.904	0.914	0.326
283.0	25.1	17.7	0.3175	0.930	0.930	0.427
372.3	25.9	17.9	0.4175	0.958	0.947	0.562
461.7	26.4	18.2	0.5175	0.974	0.963	0.696
551.0	26.7	18.5	0.6175	0.986	0.977	0.831
640.3	27.0	18.7	0.7175	0.994	0.988	0.965
729.6	27.1	18.8	0.8175	0.998	0.995	1.100
818.9	27.1	18.9	0.9175	1.000	0.998	1.234

RUN 100269-1 K=2.50X10-6 F=0.0 IC

TEMP. RUN	VEL. RUN	PLATE	X	ST	CF/2	UINF	TGAS	TO	F
100269-2	92569-1	15	58.54	0.00243	0.00267	26.4	67.2	89.3	0.0000

THERMAL B.L. THK.	HYDRO. B.L. THK.	ENTHALPY THK.	MOMENTUM THK.	ENTHALPY RE.	MOMENTUM RE.	NO. DATA POINTS	K
0.550	1.024	0.0565	0.1022	757.	1327.	31	0.185E-05

YPLUS	TPLUS	UPLUS	Y	TBAR	U/UINF	Y/DELH
0.0	0.0	0.0	0.0000	0.000	0.000	0.000
1.8	2.7	1.4	0.0025	0.116	0.083	0.002
2.6	3.5	2.0	0.0035	0.150	0.116	0.003
3.4	4.4	2.6	0.0045	0.187	0.149	0.004
4.0	5.0	3.2	0.0055	0.212	0.182	0.005
4.8	5.4	3.7	0.0065	0.229	0.215	0.006
6.3	6.2	4.8	0.0085	0.265	0.277	0.008
8.5	7.8	6.1	0.0115	0.335	0.348	0.011
10.8	9.1	7.1	0.0145	0.388	0.410	0.014
13.8	10.5	8.4	0.0185	0.446	0.481	0.018
16.7	11.9	9.3	0.0225	0.504	0.532	0.022
19.8	12.9	10.0	0.0265	0.543	0.573	0.026
23.6	13.8	10.5	0.0315	0.585	0.607	0.031
27.3	14.9	11.0	0.0365	0.628	0.634	0.036
31.8	15.6	11.5	0.0425	0.655	0.661	0.042
37.1	16.3	11.7	0.0495	0.684	0.679	0.048
44.6	17.0	12.1	0.0595	0.715	0.700	0.058
52.1	17.7	12.5	0.0695	0.743	0.717	0.068
63.4	18.4	12.7	0.0845	0.771	0.737	0.083
86.0	19.2	13.2	0.1145	0.807	0.760	0.112
116.1	20.1	13.5	0.1545	0.845	0.782	0.151
146.2	20.6	13.8	0.1945	0.866	0.800	0.190
172.6	21.2	14.0	0.2295	0.887	0.812	0.224
210.2	21.6	14.3	0.2795	0.906	0.829	0.273
266.8	22.2	14.7	0.3545	0.931	0.854	0.346
342.2	22.8	15.2	0.4545	0.956	0.882	0.444
417.7	23.2	15.7	0.5545	0.973	0.908	0.542
493.1	23.5	16.0	0.6545	0.984	0.932	0.635
606.3	23.7	16.6	0.8045	0.994	0.961	0.786
780.5	23.9	16.9	0.9255	0.998	0.980	0.908
794.8	23.9	17.1	1.0545	1.000	0.992	1.030

RUN 100269-1 K=2.50X10-6 F=0.0 IC

TEMP. RUN	VEL. RUN	PLATE	X	ST	CF/2	UINF	TGAS	TO	F
100269-2	92569-1	19	74.58	0.00151	0.00217	53.2	67.1	87.2	0.0000

THERMAL B.L. THK.	HYDRO. B.L. THK.	ENTHALPY THK.	MOMENTUM THK.	ENTHALPY RE.	MOMENTUM RE.	NO. DATA POINTS	K
0.568	0.435	0.0311	0.0230	1372.	515.	30	0.253E-05

YPLUS	TPLUS	UPLUS	Y	TBAR	U/UINF	Y/DELH
0.0	0.0	0.0	0.0000	0.000	0.000	0.000
3.1	1.5	2.6	0.0025	0.046	0.122	0.006
4.6	3.4	3.8	0.0037	0.106	0.181	0.009
5.6	3.9	4.6	0.0045	0.122	0.220	0.010
6.8	4.9	5.6	0.0055	0.152	0.269	0.012
8.1	5.7	6.6	0.0065	0.179	0.318	0.015
9.3	6.7	7.6	0.0075	0.212	0.367	0.017
11.8	8.7	9.2	0.0055	0.271	0.443	0.022
14.3	9.8	11.1	0.0115	0.310	0.532	0.026
18.1	12.2	13.1	0.0145	0.382	0.629	0.033
21.9	14.0	14.4	0.0175	0.438	0.694	0.040
25.7	15.7	15.3	0.0205	0.489	0.740	0.047
29.4	16.8	16.1	0.0235	0.523	0.779	0.054
34.5	18.4	16.8	0.0275	0.575	0.815	0.063
40.7	19.7	17.4	0.0325	0.615	0.843	0.075
53.3	21.9	18.1	0.0425	0.681	0.879	0.098
65.9	23.3	18.5	0.0525	0.725	0.900	0.121
84.7	24.6	19.0	0.0675	0.764	0.921	0.155
110.0	25.9	19.2	0.0875	0.804	0.934	0.201
141.5	26.9	19.5	0.1125	0.836	0.946	0.259
179.3	27.5	19.7	0.1425	0.867	0.956	0.328
229.8	28.9	19.8	0.1825	0.896	0.964	0.420
273.9	29.4	19.9	0.2175	0.913	0.969	0.500
337.0	30.2	20.0	0.2675	0.936	0.975	0.615
431.7	30.9	20.1	0.3425	0.960	0.982	0.788
526.5	31.6	20.2	0.4175	0.978	0.989	0.960
652.7	32.0	20.4	0.5175	0.991	0.995	1.190
778.9	32.2	20.4	0.6175	0.998	0.998	1.420
905.1	32.4	20.4	0.7175	1.000	0.999	1.650
1031.3	32.4	20.5	0.8175	1.000	1.000	1.880

RUNS 100269-1 K=2.50 x 10^{-6} F=0.0 IC
100269-2

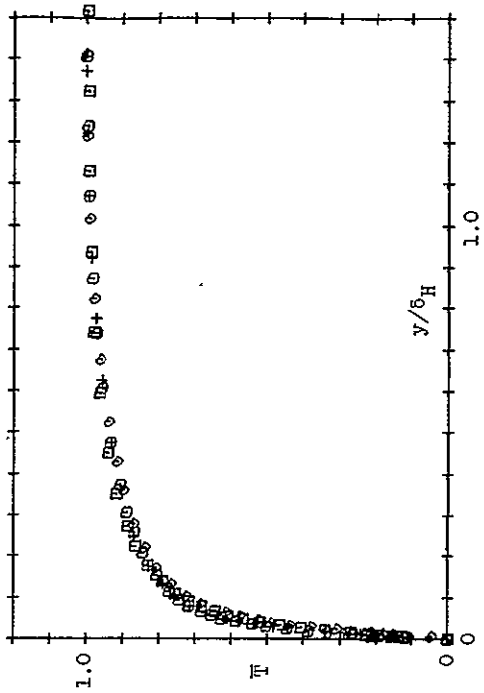

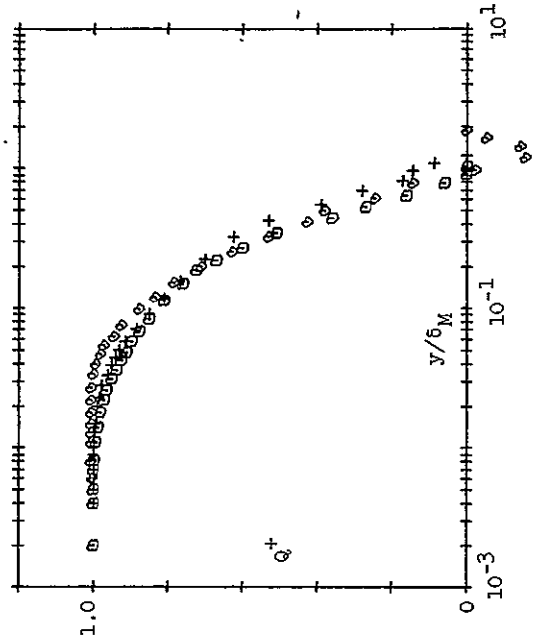

PROFILES	
x(in.)	Symbol
46.76	□
58.94	○
62.86	△
66.76	+
70.69	×
74.58	◇

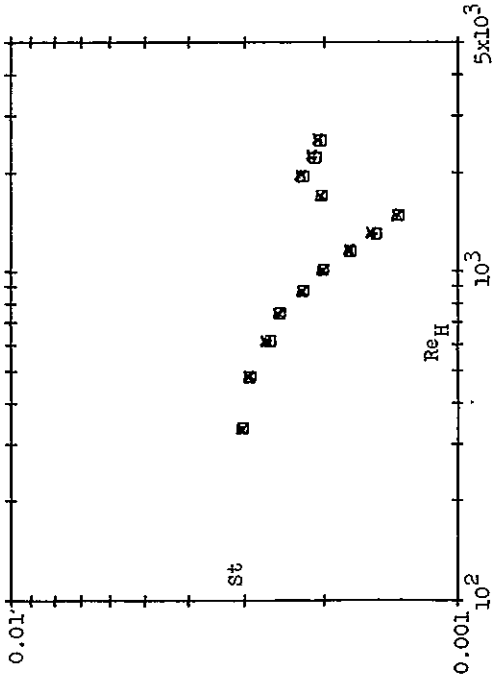

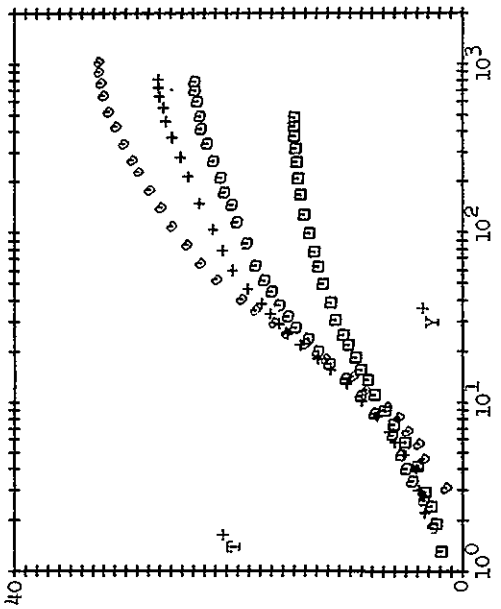

RUNS 101769-1 101769-2 K=2.56 x 10-6 F=0.0 BC

RUN 101769-1 K=2.56X10-6 F=0.0 BC

DATE 101769 RUN NO. 1

AMB TEMP	BASE TEMP	GAS TEMP	COVER TEMP	BARO PRES	REL HUM
71.49	73.47	64.75	66.03	30.04	0.51

PL	X	VEL	K	REH	ST	REM	CF2	TO	F
2	6	23.54	0.000E 00	277.	0.00324			89.4	0.0000
3	10	23.49	-0.166E-06	429.	0.00310			89.6	0.0000
4	13.81	23.20	0.208E-06	572.	0.00291	1120.	0.00253	89.4	0.0000
4	14	23.45	0.208E-06	579.	0.00286			89.4	0.0000
5	18	23.82	0.750E-06	712.	0.00275			89.5	0.0000
6	21.81	25.60	0.200E-05	788.	0.00253	1220.	0.00275	89.8	0.0000
6	22	25.62	0.200E-05	846.	0.00255			89.6	0.0000
7	26	29.29	0.253E-05	981.	0.00223			89.6	0.0000
8	29.81	34.20	0.256E-05	1038.	0.00197	825.	0.00260	89.9	0.0000
8	30	34.73	0.256E-05	1119.	0.00190			89.6	0.0000
9	34	42.44	0.258E-05	1265.	0.00170			89.6	0.0000
10	37.46	52.60	0.262E-05	1275.	0.00151	627.	0.00238	90.0	0.0000
10	38	54.74	0.262E-05	1411.	0.00150			89.9	0.0000
11	42	75.23	0.115E-05	1606.	0.00120			89.9	0.0000
12	46	77.56	0.000E 00	1870.	0.00182			89.5	0.0000
13	50	77.32	-0.198E-07	2103.	0.00215			89.5	0.0000
14	54	77.52	0.163E-07	2530.	0.00203			89.4	0.0000
15	58	77.62	0.811E-08	2864.	0.00198			89.3	0.0000
16	62	77.52	-0.807E-08	3166.	0.00193			89.4	0.0000
17	66	77.48	-0.349E-08	3457.	0.00188			89.5	0.0000
18	70	77.51	0.231E-08	3776.	0.00182			89.4	0.0000
19	74	77.45	-0.469E-08	4066.	0.00180			89.4	0.0000
20	78	77.36	-0.699E-08	4354.	0.00177			89.4	0.0000
21	82	77.51	0.115E-07	4589.	0.00174			89.6	0.0000
22	86	77.48	-0.235E-08	4853.	0.00173			89.7	0.0000
23	90	77.23	-0.198E-07	5153.	0.00176			89.6	0.0000

RUN 101769-2 K=2.56X10-6 F=0.0 BC

DATE 101769 RUN NO. 2

AMB TEMP	BASE TEMP	GAS TEMP	COVER TEMP	BARO PRES	REL HUM
72.55	73.61	64.75	66.07	30.04	0.47

PL	X	VEL	K	REH	ST	TO	F
2	6	23.44	0.000E 00	212.	0.00325	89.4	0.0000
3	10	23.40	-0.168E-06	425.	0.00313	89.6	0.0000
4	14	23.35	0.210E-06	577.	0.00289	89.2	0.0000
5	18	23.73	0.758E-06	713.	0.00278	89.3	0.0000
6	22	25.53	0.202E-05	842.	0.00257	89.5	0.0000
7	26	29.21	0.255E-05	976.	0.00221	89.6	0.0000
8	30	34.66	0.257E-05	1112.	0.00192	89.6	0.0000
9	34	42.38	0.259E-05	1254.	0.00170	89.7	0.0000
10	38	54.70	0.262E-05	1403.	0.00149	90.0	0.0000
11	42	75.19	0.116E-05	1595.	0.00120	89.9	0.0000
12	46	77.53	0.000E 00	1854.	0.00180	89.6	0.0000
13	50	77.28	-0.158E-07	2166.	0.00214	89.6	0.0000
14	54	77.49	0.163E-07	2518.	0.00201	89.5	0.0000
15	58	77.59	0.812E-08	2845.	0.00196	89.4	0.0000
16	62	77.49	-0.808E-08	3122.	0.00191	89.6	0.0000
17	66	77.44	-0.349E-08	3439.	0.00187	89.5	0.0000
18	70	77.47	0.231E-08	3741.	0.00182	89.5	0.0000
19	74	77.41	-0.470E-08	4081.	0.00181	89.2	0.0000
20	78	77.33	-0.700E-08	4313.	0.00175	89.5	0.0000
21	82	77.47	0.115E-07	4605.	0.00175	89.4	0.0000
22	86	77.44	-0.235E-08	4832.	0.00172	89.7	0.0000
23	90	77.20	-0.198E-07	5114.	0.00170	89.6	0.0000

SUMMARY OF PROFILE RESULTS

RUN 101769-1 K=2.56X10-6 F=0.0 BC

PL	X	VEL	K	F	TO	TINF	DELM	DELH
4	13.81	23.20	0.208E-06	0.0000	89.4	64.8	1.139	0.652
6	21.81	25.60	0.200E-05	0.0000	89.8	65.1	1.377	0.729
8	29.81	34.20	0.256E-05	0.0000	89.9	64.8	0.746	0.673
10	37.46	52.60	0.262E-05	0.0000	90.0	64.6	0.433	0.516

PL	X	REH	ST	REM	CF2	DELTA2	THETA
4	13.81	572.	0.00291	1120.	0.00253	0.0471	0.0922
6	21.81	788.	0.00253	1220.	0.00275	0.0595	0.0920
8	29.81	1038.	0.00197	825.	0.00260	0.0581	0.0459
10	37.46	1275.	0.00151	627.	0.00238	0.0464	0.0221

RUNS 101769-1 K=2.56 x 10-6 F=0.0 BC
101769-2

RUN 101769-1 K=2.56X10-6 F=0.0 BC

TEMP. RUN	VEL. RUN	PLATE	X	ST	CF/2	UINF	TGAS	TO	F
101769-1	101069-1	4	13.61	0.00291	0.00253	23.2	64.8	89.4	0.0000

THERMAL B.L. THK.	HYDRO. B.L. THK.	ENTHALPY THK.	MOMENTUM THK.	ENTHALPY RE.	MOMENTUM RE.	NO. DATA POINTS	K
0.652	1.139	0.0471	0.0922	572.	1120.	29	0.208E-06

YPLUS	TPLUS	UPLUS	Y	TBAR	U/UINF	Y/DELH
0.0	0.0	0.0	0.0000	0.000	0.000	0.000
1.5	2.4	1.6	0.0025	0.144	0.077	0.002
2.1	3.0	2.2	0.0035	0.162	0.108	0.003
2.7	3.5	2.8	0.0045	0.208	0.139	0.004
3.3	4.0	3.4	0.0055	0.235	0.170	0.005
3.9	4.5	4.1	0.0065	0.265	0.201	0.006
5.1	5.2	5.2	0.0085	0.305	0.260	0.007
6.2	5.8	6.2	0.0105	0.347	0.301	0.009
7.4	6.7	7.0	0.0125	0.399	0.342	0.011
9.3	7.5	8.2	0.0155	0.441	0.405	0.014
11.1	8.2	9.2	0.0185	0.481	0.451	0.016
13.5	9.1	10.2	0.0225	0.532	0.502	0.020
16.5	9.9	11.1	0.0275	0.584	0.549	0.024
19.5	10.5	11.8	0.0325	0.618	0.582	0.029
24.4	11.3	12.8	0.0405	0.666	0.631	0.036
30.4	12.0	13.1	0.0505	0.703	0.651	0.044
39.5	12.7	13.8	0.0655	0.744	0.685	0.058
48.6	13.3	14.2	0.0805	0.775	0.705	0.071
63.7	13.8	14.8	0.1055	0.811	0.735	0.093
87.8	14.4	15.5	0.1455	0.846	0.770	0.128
118.2	15.2	16.1	0.1955	0.888	0.804	0.172
163.7	15.8	16.9	0.2705	0.923	0.842	0.238
209.1	16.2	17.5	0.3455	0.944	0.875	0.303
269.8	16.6	18.2	0.4455	0.969	0.903	0.391
345.6	16.9	18.8	0.5705	0.985	0.934	0.501
421.5	17.1	19.2	0.6955	0.993	0.958	0.611
482.1	17.1	19.5	0.7955	0.997	0.969	0.699
542.7	17.1	19.6	0.8955	0.999	0.976	0.787
573.1	17.1	19.7	0.9455	1.000	0.980	0.830

RUN 101769-1 K=2.56X10-6 F=0.0 BC

TEMP. RUN	VEL. RUN	PLATE	X	ST	CF/2	UINF	TGAS	TO	F
101769-1	101069-1	8	29.81	0.00197	0.00260	34.2	64.8	89.9	0.0000

THERMAL B.L. THK.	HYDRO. B.L. THK.	ENTHALPY THK.	MOMENTUM THK.	ENTHALPY RE.	MOMENTUM RE.	NO. DATA POINTS	K
0.613	0.746	0.0581	0.0459	1038.	825.	30	0.256E-05

YPLUS	TPLUS	UPLUS	Y	TBAR	U/UINF	Y/DELH
0.0	0.0	0.0	0.0000	0.000	0.000	0.000
2.2	2.9	2.1	0.0025	0.116	0.105	0.003
3.1	4.0	3.0	0.0035	0.159	0.148	0.005
3.9	4.5	3.5	0.0045	0.180	0.190	0.006
4.9	5.3	4.7	0.0055	0.212	0.232	0.007
6.7	6.6	6.4	0.0075	0.262	0.316	0.010
9.4	8.4	8.1	0.0105	0.334	0.431	0.014
12.0	9.7	10.3	0.0135	0.386	0.515	0.018
14.7	11.1	11.7	0.0165	0.441	0.579	0.022
17.4	12.3	12.8	0.0195	0.485	0.636	0.026
20.1	13.1	13.6	0.0225	0.521	0.676	0.030
23.8	14.4	14.4	0.0265	0.573	0.717	0.036
28.2	15.3	15.1	0.0315	0.605	0.753	0.042
33.6	16.3	15.7	0.0375	0.647	0.782	0.050
39.9	17.2	16.2	0.0445	0.678	0.809	0.060
49.0	18.2	16.8	0.0545	0.718	0.831	0.073
62.5	19.1	17.1	0.0695	0.755	0.855	0.094
80.5	20.1	17.4	0.0895	0.791	0.874	0.120
103.1	20.9	17.8	0.1145	0.822	0.890	0.154
130.2	21.7	18.1	0.1445	0.851	0.904	0.194
152.8	22.1	18.2	0.1695	0.866	0.912	0.227
198.0	22.8	18.5	0.2195	0.895	0.928	0.294
265.8	23.6	18.5	0.2945	0.925	0.944	0.395
333.7	24.1	19.1	0.3695	0.947	0.955	0.496
424.2	24.7	19.3	0.4695	0.969	0.969	0.630
537.4	25.1	19.5	0.5945	0.985	0.980	0.797
650.5	25.3	19.7	0.7195	0.993	0.989	0.965
741.0	25.5	19.8	0.8195	0.997	0.993	1.099
831.5	25.5	19.8	0.9195	0.999	0.996	1.233
899.3	25.5	19.9	0.9945	1.000	0.998	1.334

RUN 101769-1 K=2.56X10-6 F=0.0 BC

TEMP. RUN	VEL. RUN	PLATE	X	ST	CF/2	UINF	TGAS	TO	F
101769-1	101069-1	6	21.81	0.00253	0.00275	25.6	65.1	89.8	0.0000

THERMAL B.L. THK.	HYDRO. B.L. THK.	ENTHALPY THK.	MOMENTUM THK.	ENTHALPY RE.	MOMENTUM RE.	NO. DATA POINTS	K
0.729	1.377	0.0595	0.0920	786.	1220.	30	0.200E-05

YPLUS	TPLUS	UPLUS	Y	TBAR	U/UINF	Y/DELH
0.0	0.0	0.0	0.0000	0.000	0.000	0.000
1.7	2.6	1.7	0.0025	0.128	0.086	0.002
2.5	3.0	2.5	0.0037	0.146	0.128	0.003
3.1	3.4	3.0	0.0045	0.167	0.156	0.003
3.8	4.0	3.7	0.0055	0.199	0.190	0.004
4.4	4.5	4.4	0.0065	0.222	0.225	0.005
5.1	5.0	5.0	0.0075	0.247	0.259	0.005
6.5	5.9	6.1	0.0095	0.293	0.317	0.007
7.9	7.0	7.1	0.0115	0.340	0.364	0.008
9.9	8.1	8.3	0.0145	0.395	0.429	0.011
12.0	9.2	9.4	0.0175	0.447	0.487	0.013
14.1	9.8	10.2	0.0205	0.480	0.529	0.015
16.9	10.9	11.0	0.0245	0.542	0.571	0.018
20.3	11.8	11.8	0.0295	0.574	0.611	0.021
24.5	12.6	12.4	0.0355	0.614	0.645	0.026
29.3	13.4	13.0	0.0425	0.651	0.674	0.031
34.9	14.1	13.3	0.0505	0.688	0.694	0.037
41.8	14.7	13.8	0.0605	0.716	0.718	0.044
52.2	15.3	14.2	0.0755	0.745	0.742	0.055
69.5	16.1	14.7	0.1005	0.780	0.769	0.073
90.4	16.9	15.1	0.1305	0.818	0.790	0.095
125.1	17.6	15.7	0.1805	0.852	0.819	0.131
177.3	18.5	16.3	0.2555	0.894	0.852	0.186
246.9	19.4	16.9	0.3555	0.933	0.886	0.258
316.5	19.8	17.4	0.4555	0.955	0.913	0.331
386.1	20.2	17.7	0.5555	0.973	0.929	0.403
490.6	20.5	18.2	0.7055	0.989	0.953	0.512
595.0	20.7	18.5	0.8555	0.995	0.968	0.621
664.6	20.7	18.6	0.9555	0.999	0.974	0.694
734.1	20.8	18.7	1.0555	1.000	0.979	0.766

RUN 101769-1 K=2.56X10-6 F=0.0 BC

TEMP. RUN	VEL. RUN	PLATE	X	ST	CF/2	UINF	TGAS	TO	F
101769-1	101069-1	10	37.46	0.00151	0.00238	52.6	64.6	90.0	0.0000

THERMAL B.L. THK.	HYDRO. B.L. THK.	ENTHALPY THK.	MOMENTUM THK.	ENTHALPY RE.	MOMENTUM RE.	NO. DATA POINTS	K
0.516	0.433	0.0464	0.0221	1275.	627.	28	0.262E-05

YPLUS	TPLUS	UPLUS	Y	TBAR	U/UINF	Y/DELH
0.0	0.0	0.0	0.0000	0.000	0.000	0.000
3.9	4.3	3.0	0.0025	0.141	0.127	0.004
4.5	5.6	4.2	0.0035	0.184	0.191	0.006
5.9	6.5	5.3	0.0045	0.214	0.246	0.010
7.2	7.5	6.6	0.0055	0.247	0.301	0.013
8.5	8.3	7.7	0.0065	0.273	0.355	0.015
11.2	9.9	10.0	0.0085	0.324	0.461	0.020
13.7	11.7	11.9	0.0105	0.379	0.549	0.024
16.3	12.9	13.3	0.0125	0.420	0.617	0.029
19.0	13.9	14.4	0.0145	0.452	0.665	0.033
23.0	15.3	15.6	0.0175	0.499	0.722	0.040
28.3	17.0	16.6	0.0215	0.553	0.773	0.050
34.9	18.8	17.6	0.0265	0.611	0.815	0.061
41.5	20.2	18.2	0.0315	0.653	0.849	0.073
48.2	21.1	18.7	0.0365	0.683	0.871	0.084
61.4	22.5	19.2	0.0465	0.730	0.895	0.107
74.7	23.5	19.6	0.0565	0.762	0.911	0.130
94.6	24.6	19.9	0.0715	0.794	0.929	0.165
127.8	26.0	20.2	0.0965	0.839	0.945	0.223
174.3	27.0	20.5	0.1315	0.872	0.959	0.304
227.5	28.0	20.7	0.1715	0.903	0.969	0.396
293.9	28.8	20.8	0.2215	0.926	0.975	0.512
393.7	29.6	20.9	0.2965	0.953	0.982	0.685
493.6	30.2	21.0	0.3715	0.973	0.987	0.858
626.6	30.7	21.1	0.4715	0.986	0.992	1.089
759.7	30.9	21.2	0.5715	0.994	0.994	1.320
892.7	31.1	21.2	0.6715	0.999	0.996	1.551
1025.6	31.1	21.2	0.7715	1.000	0.997	1.782

RUNS 101769-1 K=2.56 x 10^{-6} F=0.0 BC
101769-2

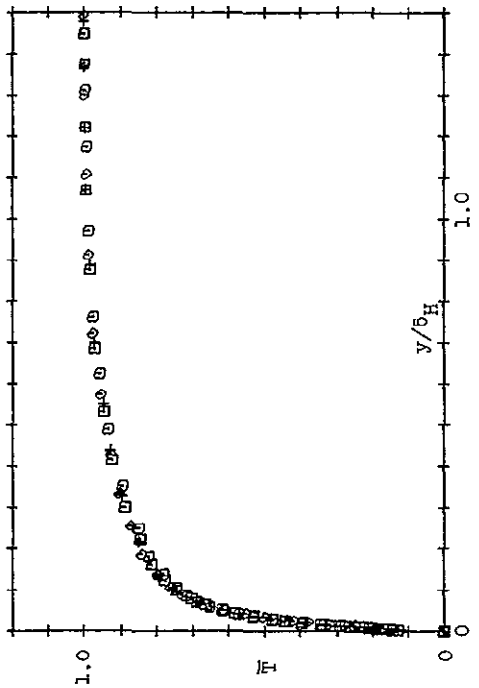

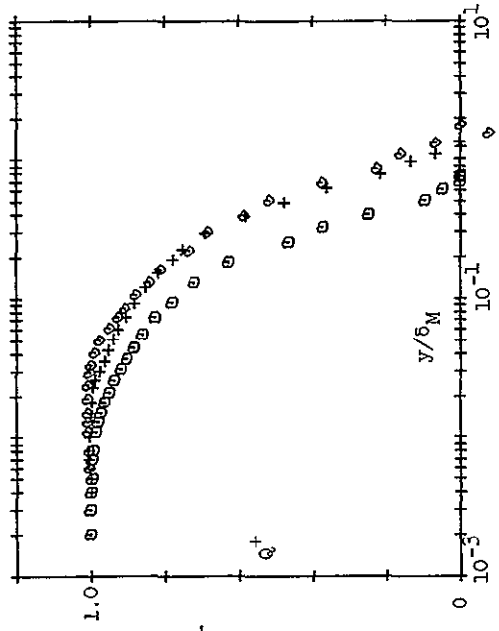

PROFILES

x(in.)	Symbol
13.81	□
21.81	○
25.86	△
29.81	+
33.59	×
37.46	◇

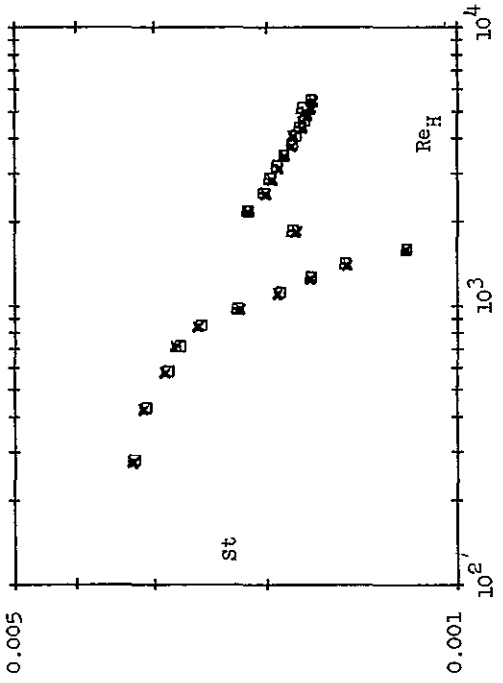

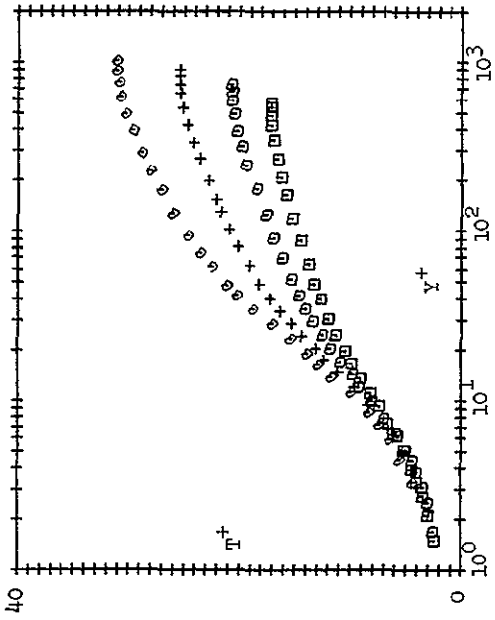

RUNS 102469-1 K=2.50 x 10^{-6} F=0.0-0.004 BC
102469-2

RUN 102469-1 K=2.50X10-6 F=0.0-0.004 BC

DATE 102469 RUN NO. 1

AMB TEMP	BASE TEMP	GAS TEMP	COVER TEMP	BARO PRES	REL HUM
72.50	74.10	65.62	66.87	29.99	0.54

PL	X	VEL	K	REH	ST	REM	CF2	TO	F
2	6	23.58	-0.298E-06	345.	C.CC347			89.5	0.0000
3	10	23.65	0.258E-06	510.	0.00313			89.3	0.0000
4	13.81	23.60	0.211E-06	656.	0.00292	796.	0.00246	89.7	0.0000
4	14	23.62	0.211E-06	656.	0.00296			89.4	0.0000
5	18	23.89	0.693E-06	779.	0.00279			90.0	0.0000
6	22	25.65	0.171E-05	922.	0.00251			89.8	0.0000
7	26	29.20	0.255E-05	1053.	0.00223			89.8	0.0000
8	30	34.34	0.255E-05	1186.	0.00192			89.9	0.0000
9	34	42.07	0.264E-05	1482.	C.CCC86			89.5	0.0039
10	38	54.32	0.269E-05	1937.	0.00112			90.1	0.0039
11	42	74.64	0.120E-05	2668.	C.00091			90.0	0.0039
12	46	77.55	-0.963E-08	3380.	C.CCC93			89.9	0.0039
13	50	77.48	0.169E-07	4122.	C.00081			90.0	0.0038
14	54	77.63	0.274E-08	4829.	C.00069			90.1	0.0039
15	58	77.54	-0.376E-08	5560.	0.00070			90.1	0.0039
16	62	77.48	0.529E-10	6318.	C.00061			90.0	0.0039
17	66	77.53	0.468E-08	7078.	0.00058			89.9	0.0039
18	70	77.65	0.165E-08	7854.	0.00057			89.6	0.0038
19	74	77.61	-0.946E-08	8465.	0.00056			89.9	0.0039
20	78	77.56	0.807E-08	9201.	C.00054			89.8	0.0038
21	82	77.68	0.545E-08	9901.	0.00054			89.8	0.0039
22	86	77.68	-0.672E-08	10635.	0.00052			89.8	0.0039
23	90	77.54	-0.112E-07	11372.	0.00052			89.7	0.0038

RUN 102469-2 K=2.50X10-6 F=0.0-0.004 BC

DATE 102469 RUN NO. 2

AMB TEMP	BASE TEMP	GAS TEMP	COVER TEMP	BARO PRES	REL HUM
72.47	74.17	65.62	66.87	29.99	0.55

PL	X	VEL	K	REH	ST	TO	F
2	6	23.59	-0.298E-06	353.	0.00348	89.4	0.0000
3	10	23.65	0.258E-06	516.	0.00312	89.3	0.0000
4	14	23.62	0.211E-06	655.	0.00292	89.6	0.0000
5	18	23.90	0.694E-06	786.	0.00279	89.9	0.0000
6	22	25.65	0.171E-05	933.	0.00252	89.6	0.0000
7	26	29.20	0.255E-05	1064.	0.CC222	89.7	0.0000
8	30	34.35	0.255E-05	1198.	0.00194	89.7	0.0000
9	34	42.07	0.264E-05	1487.	C.CCC86	89.5	0.0039
10	38	54.33	0.269E-05	1945.	0.00115	90.1	0.0039
11	42	74.64	0.120E-05	2619.	C.00095	90.0	0.0039
12	46	77.55	-0.964E-08	3397.	C.CCC94	89.9	0.0039
13	50	77.49	0.169E-07	4146.	0.00080	89.9	0.0038
14	54	77.63	0.274E-08	4850.	0.00069	90.1	0.0039
15	58	77.54	-0.376E-08	5613.	0.00071	89.9	C.CC39
16	62	77.49	0.529E-10	6351.	0.00061	89.9	0.0039
17	66	77.53	0.468E-08	7133.	0.00059	89.6	0.0039
18	70	77.65	0.165E-08	7882.	C.CCC57	89.6	0.0038
19	74	77.61	-0.947E-08	8484.	0.00055	89.8	0.0039
20	78	77.57	0.807E-08	9200.	C.00055	89.8	0.0038
21	82	77.69	0.545E-08	9962.	0.00057	89.6	0.0039
22	86	77.68	-0.672E-08	10636.	0.00052	89.7	0.0039
23	90	77.54	-0.112E-07	11404.	0.00056	89.6	0.0038

RUN 102469-1 K=2.50X10-6 F=0.0-0.004 BC

TEMP. RUN	VEL. RUN	PLATE	X	ST	CF/2	UINF	TGAS	TO	F
102469-2	102469-1	4	13.81	0.00292	0.00246	23.6	65.5	89.7	0.0000

THERMAL B.L. THK.	HYDRO. B.L. THK.	ENTHALPY THK.	MOMENTUM THK.	ENTHALPY RE.	MOMENTUM RE.	NO. DATA POINTS	K
C.559	0.553	0.0533	0.0653	650.	796.	29	0.211E-06

YPLUS	TPLUS	UPLUS	Y	TBAR	U/UINF	Y/DELH
0.0	0.0	C.C	C.0000	0.000	0.000	0.000
1.5	2.1	1.4	0.0025	0.127	C.C69	0.005
2.1	3.0	2.0	0.0035	0.180	0.097	0.006
2.7	3.2	2.6	C.0045	0.194	0.124	0.008
3.3	3.8	3.1	0.0055	0.225	0.152	0.010
4.5	4.6	4.2	0.0075	0.273	0.207	0.014
5.6	4.8	5.2	0.0095	0.284	0.254	0.017
7.4	6.2	6.5	0.0125	0.373	0.318	0.023
9.2	7.1	7.9	0.0155	0.422	0.388	0.028
11.0	8.0	9.0	0.0185	0.475	0.439	0.033
13.5	8.7	10.0	0.0225	0.517	0.492	0.041
16.5	9.4	11.C	0.0275	0.560	0.541	0.050
20.1	10.0	11.8	0.0335	0.594	0.582	0.061
25.5	10.9	12.7	0.0425	0.645	0.626	0.077
31.5	11.3	13.3	0.0525	0.673	0.654	0.095
39.3	11.9	13.8	0.0655	0.706	0.682	0.118
45.4	12.3	14.2	0.0755	0.728	0.699	0.136
60.4	12.9	14.8	0.1005	0.764	0.730	0.182
78.5	13.5	15.4	0.1305	0.799	0.760	0.236
108.7	14.2	16.3	0.1805	0.842	0.804	0.326
138.9	14.9	17.0	0.2305	0.878	0.842	0.417
169.2	15.4	17.7	0.2805	0.906	0.874	0.507
199.4	15.7	18.3	0.3305	0.929	0.906	0.597
229.7	16.1	18.8	0.3805	0.949	0.933	0.688
290.3	16.6	19.6	0.4805	0.977	0.973	0.869
350.8	16.9	20.0	C.5EC5	0.994	0.993	1.049
411.3	17.0	20.1	0.6805	0.998	0.998	1.230
471.8	17.0	20.2	C.7805	0.999	1.000	1.411
532.2	17.0	20.2	0.8805	1.000	1.000	1.592

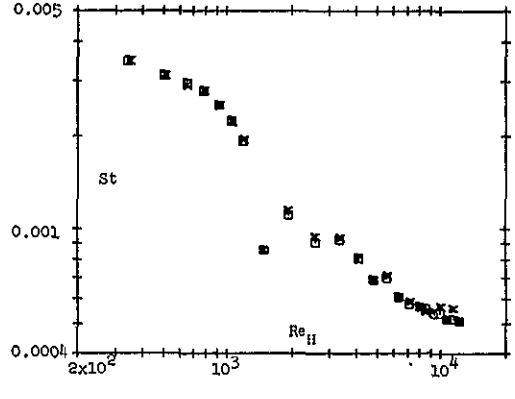

F=0.0-0.004 BC

RUNS 111369-2 111369-3 K=2.50 x 10-6 F=0.004-0.0 BC

RUN 111369-2 K=2.50X10-6 F=0.004-0.0 BC

DATE 111369 RUN NO. 2

AMB TEMP	BASE TEMP	GAS TEMP	COVER TEMP	BARO PRES	REL HUM
72.40	76.39	68.69	69.69	30.13	0.51

PL	X	VEL	K	REH	ST	REH	CF2	TO	F
2	6	23.22	-0.150E-07	478.	0.00216			94.6	0.0042
3	10	23.18	0.247E-06	766.	0.00179			94.8	0.0042
4	13.81	23.30	0.231E-06	1020.	0.00156	1210.	0.00130	95.0	0.0042
4	14	23.29	0.231E-06	1033.	0.00155			95.2	0.0042
5	18	23.82	0.879E-06	1317.	0.00134			94.9	0.0041
6	22	25.39	0.184E-05	1572.	0.00123			95.3	0.0042
7	26	28.99	0.259E-05	1848.	0.00117			95.5	0.0038
8	30	34.26	0.261E-05	2206.	0.00106			95.0	0.0038
9	34	41.98	0.262E-05	2476.	0.00170			94.7	0.0000
10	38	53.84	0.262E-05	2669.	0.00147			94.4	0.0000
11	42	72.52	0.106E-05	2869.	0.00126			94.4	0.0000
12	46	74.12	-0.146E-07	3083.	0.00191			94.6	0.0000
13	50	73.97	0.115E-07	3440.	0.00181			94.0	0.0000
14	54	74.13	0.136E-07	3778.	0.00173			93.5	0.0000
15	58	74.12	-0.649E-08	4040.	0.00172			93.5	0.0000
16	62	73.97	-0.776E-08	4304.	0.00168			93.5	0.0000
17	66	73.97	0.190E-09	4571.	0.00168			93.4	0.0000
18	70	74.13	0.000E 00	4827.	0.00164			93.4	0.0000
19	74	74.08	-0.724E-08	5099.	0.00163			93.3	0.0000
20	78	74.05	0.688E-08	5336.	0.00162			93.3	0.0000
21	82	74.21	0.141E-07	5587.	0.00159			93.3	0.0000
22	86	74.21	-0.716E-08	5839.	0.00160			93.2	0.0000
23	90	74.05	-0.141E-07	6115.	0.00157			93.1	0.0000

RUN 111369-3 K=2.50X10-6 F=0.004-0.0 BC

DATE 111369 RUN NO. 3

AMB TEMP	BASE TEMP	GAS TEMP	COVER TEMP	BARO PRES	REL HUM
72.57	76.39	69.87	70.66	30.13	0.51

PL	X	VEL	K	REH	ST	TO	F
2	6	23.24	-0.150E-07	479.	0.00220	95.1	0.0042
3	10	23.21	0.247E-06	767.	0.00185	95.3	0.0041
4	14	23.31	0.232E-06	1031.	0.00159	95.7	0.0042
5	18	23.85	0.882E-06	1314.	0.00137	95.4	0.0041
6	22	25.42	0.185E-05	1570.	0.00128	95.8	0.0042
7	26	29.03	0.260E-05	1844.	0.00119	96.0	0.0038
8	30	34.30	0.262E-05	2194.	0.00107	95.7	0.0038
9	34	42.02	0.262E-05	2470.	0.00174	95.4	0.0000
10	38	53.90	0.263E-05	2666.	0.00149	95.1	0.0000
11	42	72.60	0.106E-05	2792.	0.00125	95.7	0.0000
12	46	74.21	-0.147E-07	3084.	0.00194	95.2	0.0000
13	50	74.05	0.116E-07	3446.	0.00184	94.6	0.0000
14	54	74.21	0.136E-07	3796.	0.00174	94.1	0.0000
15	58	74.21	-0.651E-08	4042.	0.00175	94.2	0.0000
16	62	74.05	-0.778E-08	4312.	0.00171	94.2	0.0000
17	66	74.06	0.192E-09	4557.	0.00170	94.2	0.0000
18	70	74.21	0.000E 00	4831.	0.00166	94.1	0.0000
19	74	74.13	-0.726E-08	5101.	0.00166	94.1	0.0000
20	78	74.13	0.690E-08	5314.	0.00163	94.2	0.0000
21	82	74.29	0.141E-07	5617.	0.00162	94.0	0.0000
22	86	74.29	-0.718E-08	5838.	0.00163	94.1	0.0000
23	90	74.13	-0.141E-07	6104.	0.00159	94.0	0.0000

RUN 111369-2 K=2.50X10-6 F=0.004-0.0 BC

TEMP. RUN	VEL. RUN	PLATE	X	ST	CF/2	UINF	TGAS	TO	F
111369-1	111369-1	4	13.81	0.00156	0.00130	23.3	67.7	95.0	0.0042

THERMAL B.L. THK.	HYDRO. B.L. THK.	ENTHALPY THK.	MOMENTUM THK.	ENTHALPY RE.	MOMENTUM RE.	NO. DATA POINTS	K
0.725	0.706	0.0854	0.1010	1020.	1210.	30	0.231E-06

YPLUS	TPLUS	UPLUS	Y	TBAR	U/UINF	Y/DELP
0.0	0.0	0.0	0.0000	0.000	0.000	0.000
1.1	1.6	1.2	0.0025	0.072	0.043	0.004
1.5	2.3	1.7	0.0035	0.102	0.060	0.005
1.9	2.7	2.2	0.0045	0.118	0.077	0.006
2.3	3.2	2.7	0.0055	0.143	0.094	0.008
2.7	3.6	3.1	0.0065	0.160	0.111	0.009
3.2	3.9	3.6	0.0075	0.174	0.128	0.011
4.0	4.5	4.6	0.0095	0.199	0.162	0.013
4.9	5.1	5.2	0.0115	0.225	0.184	0.016
6.1	6.1	6.5	0.0145	0.268	0.229	0.021
7.9	7.6	8.1	0.0185	0.333	0.287	0.026
10.0	8.5	9.7	0.0235	0.373	0.344	0.033
12.1	9.4	10.9	0.0285	0.412	0.386	0.040
14.3	10.1	11.7	0.0335	0.443	0.416	0.047
16.4	10.3	12.4	0.0385	0.454	0.440	0.055
20.7	11.5	13.5	0.0485	0.503	0.480	0.069
27.1	12.5	14.6	0.0635	0.549	0.521	0.090
35.7	13.4	15.4	0.0835	0.586	0.551	0.118
46.4	14.4	16.5	0.1085	0.629	0.590	0.154
59.3	15.3	17.5	0.1385	0.667	0.626	0.196
70.1	16.0	18.2	0.1635	0.697	0.651	0.232
91.6	17.1	19.5	0.2135	0.744	0.700	0.302
113.2	18.1	20.7	0.2635	0.787	0.744	0.373
134.8	19.0	21.8	0.3135	0.826	0.782	0.444
157.3	20.1	23.4	0.3685	0.870	0.840	0.550
199.8	21.0	24.8	0.4635	0.910	0.892	0.656
243.2	21.9	26.3	0.5635	0.950	0.947	0.798
286.5	22.6	27.2	0.6635	0.980	0.981	0.940
329.9	23.0	27.6	0.7635	0.996	0.995	1.081
373.1	23.1	27.7	0.8635	1.000	0.999	1.223

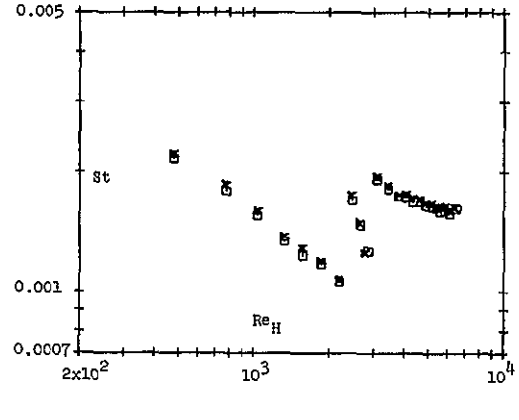

RUN 111669-1 K=0.0 X10-6 F=0.0 FP

DATE 111669 RUN NO. 1

AMB TEMP	BASE TEMP	GAS TEMP	COVER TEMP	BARO PRES	REL HUM
70.42	76.53	67.62	70.10	30.08	0.55

PL	X	VEL	K	REH	ST	REN	CF2	TO	F
2	6	23.06	-0.888E-07	516.	0.00369			97.1	0.0000
3	10	23.01	0.000E 00	480.	0.00322			97.1	0.0000
4	14	23.01	0.000E 00	620.	0.00297			97.5	0.0000
5	18	23.01	-0.451E-07	759.	0.00276			97.3	0.0000
6	22	22.96	0.000E 00	891.	0.00269			97.2	0.0000
7	26	23.01	0.447E-07	1015.	0.00256			97.1	0.0000
8	30	23.06	0.448E-07	1130.	0.00245			97.0	0.0000
9	34	23.06	0.000E 00	1246.	0.00241			97.1	0.0000
10	38	23.10	0.439E-07	1370.	0.00236			96.9	0.0000
11	42	23.10	0.444E-07	1475.	0.00227			97.0	0.0000
12	46	23.15	0.000E 00	1593.	0.00236			96.9	0.0000
12	46.76	23.10	0.000E 00	1561.	0.00232	1568.	0.00208	97.3	0.0000
13	50	23.15	0.000E 00	1656.	0.00230			97.0	0.0000
14	54	23.15	0.000E 00	1788.	0.00218			97.2	0.0000
15	58	23.15	0.000E 00	1913.	0.00223			96.9	0.0000
16	62	23.15	-0.438E-07	2023.	0.00218			96.8	0.0000
17	66	23.10	0.000E 00	2128.	0.00221			96.8	0.0000
18	70	23.10	0.000E 00	2229.	0.00213			96.8	0.0000
19	74	23.10	0.000E 00	2332.	0.00213			96.8	0.0000
20	78	23.15	0.703E-07	2424.	0.00208			96.9	0.0000
20	78.80	23.10	0.703E-07	2259.	0.00210	2286.	0.00189	97.7	0.0000
21	82	23.18	0.174E-07	2525.	0.00208			96.9	0.0000
22	86	23.25	0.440E-07	2623.	0.00210			96.9	0.0000
23	90	23.25	0.000E 00	2714.	0.00207			97.0	0.0000

RUN 111669-2 K=0.0 X10-6 F=0.0 FP

DATE 111669 RUN NO. 2

AMB TEMP	BASE TEMP	GAS TEMP	COVER TEMP	BARO PRES	REL HUM
70.17	76.87	68.86	70.66	30.08	0.48

PL	X	VEL	K	REH	ST	TO	F
2	6	23.07	-0.890E-07	513.	0.00372	97.8	0.0000
3	10	23.02	0.000E 00	476.	0.00324	97.9	0.0000
4	14	23.02	0.000E 00	618.	0.00300	98.2	0.0000
5	18	23.02	-0.452E-07	759.	0.00281	98.0	0.0000
6	22	22.97	0.000E 00	895.	0.00271	97.8	0.0000
7	26	23.02	0.448E-07	1021.	0.00259	97.8	0.0000
8	30	23.07	0.449E-07	1144.	0.00249	97.6	0.0000
9	34	23.07	0.000E 00	1249.	0.00236	97.9	0.0000
10	38	23.12	0.440E-07	1367.	0.00237	97.7	0.0000
11	42	23.12	0.445E-07	1477.	0.00228	97.7	0.0000
12	46	23.17	0.000E 00	1594.	0.00236	97.6	0.0000
13	50	23.17	0.000E 00	1704.	0.00232	97.6	0.0000
14	54	23.17	0.000E 00	1806.	0.00222	97.7	0.0000
15	58	23.17	0.000E 00	1927.	0.00226	97.4	0.0000
16	62	23.17	-0.439E-07	2067.	0.00226	97.0	0.0000
17	66	23.12	0.000E 00	2147.	0.00223	97.4	0.0000
18	70	23.12	0.000E 00	2250.	0.00216	97.4	0.0000
19	74	23.12	0.000E 00	2354.	0.00216	97.3	0.0000
20	78	23.17	0.705E-07	2443.	0.00213	97.5	0.0000
21	82	23.20	0.174E-07	2532.	0.00205	97.6	0.0000
22	86	23.26	0.440E-07	2640.	0.00210	97.5	0.0000
23	90	23.26	0.000E 00	2746.	0.00210	97.4	0.0000

SUMMARY OF PROFILE RESULTS

RUN 111669-1 K=0.0 X10-6 F=0.0 FP

PL	X	VEL	K	F	TO	TINF	DELM	DELH
12	46.76	23.10	0.000E 00	0.0000	97.3	68.7	1.073	1.150
20	78.80	23.10	0.703E-07	0.0000	97.7	68.6	1.551	1.677

PL	X	REH	ST	REN	CF2	DELTA2	THETA
12	46.76	1561.	0.00232	1568.	0.00208	0.1317	0.1326
20	78.80	2259.	0.00210	2286.	0.00189	0.1905	0.1932

RUN 111669-1 K=0.0 X10-6 F=0.0 FP

TEMP. RUN	VEL. RUN	PLATE	X	ST	CF/2	UINF	TGAS	TO	F
111669-1	111869-1	12	46.76	0.00232	0.00208	23.1	68.7	97.3	0.0000

THERMAL B.L. THK.	HYDRO. B.L. THK.	ENTHALPY THK.	MOMENTUM THK.	ENTHALPY RE.	MOMENTUM RE.	NO. DATA POINTS	K
1.150	1.073	0.1317	0.1326	1561.	1568.	31	0.000E 00

YPLUS	TPLUS	UPLUS	Y	TBAR	U/UINF	Y/DELH
0.0	0.0	0.0	0.0000	0.000	0.000	0.000
1.3	2.0	1.5	0.0025	0.101	0.067	0.002
1.8	2.6	2.1	0.0035	0.135	0.093	0.003
2.4	3.2	2.7	0.0045	0.158	0.120	0.004
2.9	3.6	3.3	0.0055	0.180	0.147	0.005
3.4	4.1	3.9	0.0065	0.205	0.173	0.006
4.0	4.4	4.5	0.0075	0.224	0.200	0.007
4.5	4.9	5.0	0.0085	0.243	0.223	0.008
6.1	5.8	6.2	0.0115	0.290	0.279	0.011
8.2	7.1	7.6	0.0155	0.352	0.353	0.014
10.3	7.8	9.2	0.0195	0.387	0.411	0.018
12.5	8.4	10.0	0.0235	0.418	0.449	0.022
15.2	9.2	10.8	0.0285	0.457	0.487	0.027
18.4	9.9	11.6	0.0345	0.493	0.523	0.032
22.1	10.9	12.3	0.0415	0.538	0.554	0.039
27.5	11.3	12.9	0.0515	0.559	0.584	0.048
32.8	11.7	13.3	0.0615	0.581	0.602	0.057
43.5	12.6	14.1	0.0815	0.620	0.636	0.076
56.9	13.1	14.6	0.1065	0.650	0.658	0.099
75.7	13.8	15.1	0.1415	0.686	0.684	0.132
97.2	14.5	15.8	0.1815	0.712	0.713	0.169
124.0	14.9	16.4	0.2315	0.735	0.741	0.216
164.4	15.7	17.2	0.3065	0.777	0.778	0.286
218.2	16.7	18.0	0.4065	0.821	0.818	0.379
285.7	17.6	19.0	0.5315	0.866	0.864	0.496
366.7	18.5	20.0	0.6815	0.906	0.911	0.635
447.9	19.2	20.9	0.8315	0.942	0.950	0.775
529.1	19.9	21.5	0.9815	0.972	0.979	0.915
637.3	20.3	21.9	1.1815	0.993	0.996	1.102
745.2	20.4	21.9	1.3815	0.999	1.000	1.288
853.1	20.4	21.9	1.5815	1.000	1.000	1.474

RUN 111669-1 K=0.0 X10-6 F=0.0 FP

TEMP. RUN	VEL. RUN	PLATE	X	ST	CF/2	UINF	TGAS	TO	F
111669-1	111869-1	20	78.80	0.00210	0.00189	23.1	68.6	97.7	0.0000

THERMAL B.L. THK.	HYDRO. B.L. THK.	ENTHALPY THK.	MOMENTUM THK.	ENTHALPY RE.	MOMENTUM RE.	NO. DATA POINTS	K
1.677	1.551	0.1905	0.1932	2259.	2286.	32	0.703E-07

YPLUS	TPLUS	UPLUS	Y	TBAR	U/UINF	Y/DELH
0.0	0.0	0.0	0.0000	0.000	0.000	0.000
1.3	1.1	1.5	0.0025	0.056	0.062	0.002
1.8	2.0	2.0	0.0035	0.100	0.086	0.002
2.3	2.6	2.6	0.0045	0.129	0.111	0.003
2.8	3.2	3.2	0.0055	0.155	0.136	0.004
3.3	3.4	3.8	0.0065	0.166	0.160	0.004
3.8	3.9	4.3	0.0075	0.193	0.185	0.005
4.8	4.5	5.2	0.0095	0.221	0.223	0.006
6.3	5.7	6.4	0.0125	0.277	0.273	0.008
7.8	6.7	7.6	0.0155	0.325	0.323	0.010
9.4	7.4	8.5	0.0185	0.362	0.363	0.012
11.4	8.3	9.6	0.0225	0.402	0.409	0.015
13.9	9.2	10.3	0.0275	0.445	0.452	0.018
17.5	10.0	11.4	0.0345	0.483	0.490	0.022
21.6	10.6	12.2	0.0425	0.516	0.523	0.027
26.7	11.3	12.9	0.0525	0.549	0.553	0.034
34.3	11.9	13.6	0.0675	0.577	0.583	0.044
44.5	12.4	14.2	0.0875	0.600	0.609	0.056
57.3	13.0	14.6	0.1125	0.628	0.629	0.073
75.1	13.5	15.2	0.1475	0.652	0.653	0.095
100.7	14.3	15.8	0.1975	0.691	0.682	0.127
139.1	15.0	16.5	0.2725	0.725	0.714	0.176
190.3	15.7	17.4	0.3725	0.759	0.753	0.240
254.4	16.6	18.3	0.4975	0.797	0.789	0.321
331.5	17.4	19.2	0.6475	0.836	0.830	0.417
434.4	18.3	20.3	0.8475	0.877	0.879	0.546
511.6	18.8	21.0	0.9975	0.902	0.912	0.643
614.8	19.5	21.5	1.1975	0.937	0.949	0.772
718.0	20.2	22.5	1.3975	0.966	0.977	0.901
821.2	20.6	22.8	1.5975	0.988	0.993	1.030
924.3	20.8	23.0	1.7975	0.996	0.998	1.159
1027.3	20.9	23.0	1.9575	1.000	1.000	1.288

RUNS 111669-1 K=0.0 F=0.0 FP

RUNS 111669-1 K=0.0 F=0.0 FP
111669-2

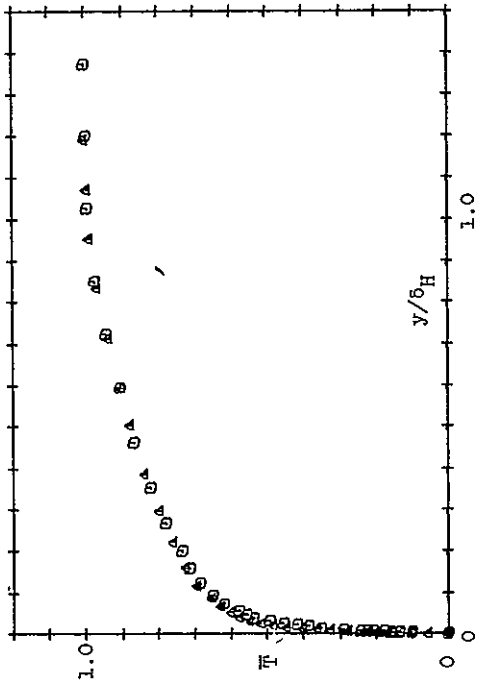

PROFILES	
x(in.)	Symbol
46.76	⊙
78.80	△

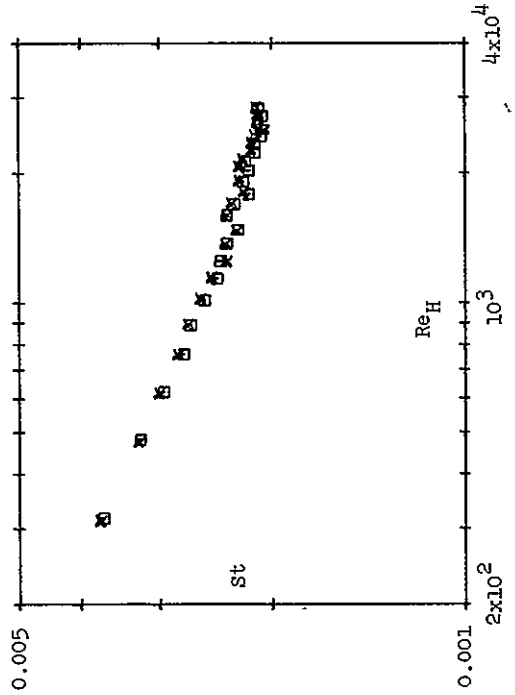

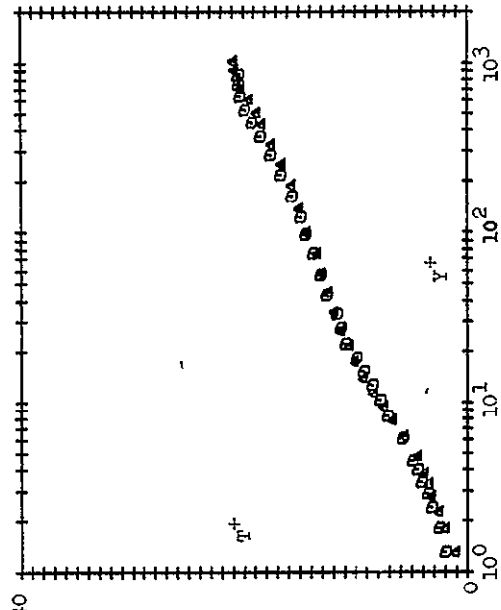

Some ratios formed from boundary layer integral parameters

Description	Plate	x[1]	Δ_2/θ	$\Delta_2/\Delta_{2,i}$	θ/θ_i	$Re_M/Re_{M,i}$	$Re_H/Re_{H,i}$
Run 070869 $\Delta_{2,i} = 0.0700$[2] $\theta_i = 0.0635$ $K=2.55\times10^{-6}$, F=0	6	21.81	1.100	1.0	1.0	1.0	1.0
	7	25.86	1.360	0.982	0.800	0.900	1.110
	8	29.81	1.720	0.958	0.613	0.814	1.265
	9	33.59	2.140	0.890	0.459	0.730	1.410
	10	37.46	2.55	0.780	0.338	0.673	1.550
Run 071569 $\Delta_{2,i} = 0.0262$ $\theta_i = 0.0616$ $K=2.55\times10^{-6}$, F=0	6	21.81	0.425	1.0	1.0	1.0	1.0
	8	29.81	0.990	1.420	0.610	0.802	1.870
	10	37.46	1.750	1.380	0.335	0.662	2.740
Run 092469 $\Delta_{2,i} = 0.1393$ $\theta_i = 0.1065$ $K=2.5\times10^{-6}$, F=0	15	58.94	1.30	1.0	1.0	1.0	1.0
	16	62.86	1.64	0.942	0.750	0.850	1.070
	17	66.76	1.46	0.838	0.522	0.685	1.100
	18	70.69	2.74	0.733	0.352	0.558	1.160
	19	74.58	3.40	0.610	0.234	0.468	2.220
Run 100269 $\Delta_{2,i} = 0.0565$ $\theta_i = 0.1022$ $K=2.5\times10^{-6}$, F=0	15	58.94	0.541	1.0	1.0	1.0	1.0
	17	66.76	1.080	1.020	0.518	0.672	1.325
	19	74.58	2.220	0.903	0.225	0.447	1.800
Run 101769 $\Delta_{2,i} = 0.0595$ $\theta_i = 0.0920$ $K=2.56\times10^{-6}$, F=0	6	21.81	0.648	1.0	1.0	1.0	1.0
	8	29.81	0.760	0.977	0.499	0.676	1.325
	10	37.46	2.100	0.780	0.240	0.512	1.670
Run 091069 $\Delta_{2,i} = 0.0633$ $\theta_i = 0.0667$ $K=1.99\times10^{-6}$, F=0	6	21.81	0.953	1.0	1.0	1.0	1.0
	7	25.86	1.230	1.007	0.777	0.884	1.155
	8	29.81	1.620	0.972	0.568	0.755	1.300
	9	33.59	2.020	0.929	0.436	0.677	1.493
	10	37.46	2.520	0.837	0.315	0.634	1.695
Run 072769 $\Delta_{2,i} = 0.0939$ $\theta_i = 0.0850$ $K=2.5\times10^{-6}$, F= 0.002	6	21.81	1.100	1.0	1.0	1.0	1.0
	7	25.86	1.380	1.018	0.810	0.917	1.150
	8	29.81	1.700	0.997	0.648	0.855	1.320
	9	33.59	2.180	0.984	0.498	0.793	1.570
	10	37.46	2.600	0.892	0.380	0.761	1.795
Run 083069 $\Delta_{2,i} = 0.1190$ $\theta_i = 0.1080$ $K=2.6\times10^{-6}$, F= 0.004	6	21.81	1.100	1.0	1.0	1.0	1.0
	7	25.86	1.410	1.045	0.813	0.918	1.180
	8	29.81	1.840	1.070	0.640	0.843	1.410
	9	33.59	2.180	1.020	0.513	0.820	1.630
	10	37.46	2.650	0.948	0.394	0.788	1.905
Run 111669 $\Delta_{2,i} = 0.0520$ $\theta_i = 0.0678$ K=0.0, F=0.0	4	13.81	0.767	1.0	1.0	1.0	1.0
	12	46.76	0.993	2.533	1.956	1.967	2.550
	20	78.80	0.986	3.663	2.850	2.868	3.687

[1] Length unit = inches

[2] Subscript "i" refers to first profile recorded in accelerated region

SUPPLEMENT 3

LISTINGS OF DATA REDUCTION PROGRAMS

STANTON PROGRAM: reads raw heat transfer data in order to compute surface heat transfer results and associated uncertainty analysis.

PROFILE PROGRAM: reads raw temperature profile data, and calculated velocity profile results, in order to compute temperature profile information and integral parameters, plus the associated uncertainties.

ENERGY PROGRAM: reads final temperature integral results, and surface heat transfer results, in order to recalculate the plate enthalpy thickness from the energy equation, and to determine the boundary layer energy balance at each profile.

STANTON PROGRAM

```
C
C
C   STANTON NUMBER AND RELATED PARAMETERS FOR PRESSURE GRADIENT RUNS ON
C   HEAT AND MASS TRANSFER RIG
C
C
C   PROGRAM REARRANGED AND UNCERTAINTY ANALYSIS ADDED BY DWKEARNEY
C   LATEST COMPILATION 120169
C
C
      REAL KCOND(24),KCONV(24),KFLOW(24),KFUDGE(24),KPROP,KS(24),
     1     KV(48),KW,MA,MDOT(24),MV,NPWR,ISO(24),TERM(25),TERMCP(25),
     2     XINT(25),XINTCP(25)
C
      INTEGER CMFLAG,DATE,ENBLFG,RUN,TITLE(18)
C
      COMMON /A/ AR,BETA,B1T1,B3T3,CMFLAG,COEF1,COEF23,CP,DATE,DEN,
     1  ENBLFG,E1,E2,EMISS,EPS,ER1,ER2,ER3,F12,F13,F22,I,INSTOT,J,KCOND,
     2    KCONV,KFLOW,KFUDGE,KPROP,KS,KV,KW,KLM,MA,MDOT,MV,NPWR,NPLATE,
     3    NSTAT,P,PBAR,PROTA, DELP ,PVAP,Q1,Q2,Q3,QHEAT,
     4    QHEATA,QHTA,QLOSS ,RA,RCF,REPS,RHOA,RHOH,RHOL,RHOV,RHOZRO,RUN,
     5    RH1,RH2,RH3,RHUM,RM,T,TAMB,TBASE,TCOV,TGAS,TROT,
     6    TROTA,T1,T2,T3,VAPH,VAPL,VEPS,WCORR,WSCALE,WSTDI,
     7  ISO,REENCP(24),ENTHCP(24),ENTHZR,
     8    AREA(24),BB(24),CFHT(24),CM(24),CONLAT(24),DELH(25),
     9    DELTAT(24),DUDX(48),DUDXS(24),ECONV(24),ED(24),ENDEN(24),
     1    ENNET(24),EO(24),ENTH(24),ET(24),EU(24),F(24),GS(24),H(24),
     2    HTFRAC(24),HTRANS(24),INSTK(48),MASSK(24),PK(48),
     A    PROT(24),PROTAB(24),PSAT(9),PSTAT(48),QCOND(24),
     3    QRAD(24),REENTH(24),REENW(25),RHOG(48),
     4    RHOSAT(9),ST(24),STCP(24),TAVG(24),TEMP(9),TIME60(48),
     5    TO(24),TOEFF(24),TD(24),TITLE,TT(24),TU(24),V(48),
     6    VISCG(48),VISCGS(24),UG(24),VZERO(24),WACT(24),WIND(24),
     7    WNET(24),WSTD(24),X(48),XS(24),XSTCP(24),XMDOT(24)
      COMMON /B/ DCMP,DDELP,DPAMB,DP5HI,DP5LO,DP97HI,DP97LO,DQRADP,
     1          DTEMPA,DTEMPP,DTBASE,DTT,DTROT,DTGAS,DWIND,DXX,F2,F3,F4,
     2            F6,F7,F8,DEL,DDUDXS(24),DISO(24),DENZRP,
     3            DB(24),DBND(24),DCM(24),DDL2(24),DDL2ND(24),DF(24),
     4            DFND(24),DHTF(24),DMDOT(24),DMDOTN(24),DPSTAT(48),
     5            DQRAD(24),DRE(24),DREND(24),DRHOG(24),DST(24),
     6            DSTND(24),DUG(24),DUGND(24),DV(48),DDUDX(48),
     7            CLR1(24),CLR2(24),CLR3(24),CLR4(24),CSR1(24),
     8            CSR2(24),CSR3(24),DVISCG(24),DEL2,DMUP,MNPLAT,
     9             D97MIN,D97MAX,D5MIN,D5MAX,PTOTAL,NPORT,MNPORT
C
C
C
C    READ AND WRITE INPUT DATA
C
C
C TRANSDUCER CALIBRATION CONSTANTS ARE READ FIRST. USED FOR K-RUN.
C
      READ(5,1353) A97,B97,C97,D97,E97,A5,B5,C5,D5,E5
 1353 FORMAT(5F10.0/5F10.0)
C
C
C UNCERTAINTY INTERVALS
C
      READ(5,1354) DCMP,DDELP,DPAMB,DP5LO,DP5HI,D5MIN,D5MAX,DP97LO,
     1             DP97HI,D97MIN,D97MAX,DQRADP,DTEMPA,DTEMPP,DWIND,
```

```
     2             DENZRP,DXX,DMUP
      DP5LO=DP5LO/100.
      DP5HI=DP5HI/100.
      DP97LO=DP97LO/100.
      DP97HI=DP97HI/100.
 1354 FORMAT( 8F10.0)
C
      PSTAT(48)=0.0
C
C    IP-PUNCH COMMAND FOR ST-REENTH DATA AND PUNCHED OUTPUT: 0 FOR NO
C     PUNCH, 1 FOR PUNCH
C    NRUNS- NUMBER OF SETS OF DATA ENTERED
C
      READ(5,36)NRUNS,IP
      DO 500 IRUN=1,NRUNS
C
C    ALL DATA READ AND PRINTED DURING THE NEXT OPERATION
C
      WRITE(6,3)
  777 FORMAT(1X,18A4,13X'THIS VERSION OF THE STANTON NUMBER DATA')
 1777 FORMAT(1X,18A4)
   36 FORMAT(I2,8X,I1)
    1 FORMAT(18A4)
    3 FORMAT(1H1)
  306 FORMAT(1H )
  308 FORMAT(1H0)
    4 FORMAT(I6,4X,I1,9X,5F10.2/6F10.0,I1)
  300 FORMAT(2X47H DATE  RUN  TAMB   TCOV   TROT   TBASE  TGAS   ,
     1 37X'REDUCTION PROGRAM WAS COMPILED 120169.')
  400 FORMAT(65H   PBAR     RHUM    E1      E2     DELP    TIME60   INST
     1   PREAD  )
  301 FORMAT(2X22H CMFLAG EN8LFG NPLATE )
  304 FORMAT(2XI6,2XI1,1X5F7.3)
  404 FORMAT(4F8.2,F8.4,4XF4.0,5XI1,4XF7.4)
    5 FORMAT(I1,9X,I1,9X,I2)
   50 FORMAT(5XI1,6XI1,6XI2)
   75 FORMAT(72H  I    EO      EU      ED      ET     WIND     CM      P
     1ROT     MASSK       )
  302 FORMAT(62H  I    EO      EU      ED      ET     WIND     CM      P
     1ROT      )
    6 FORMAT(7F10.3)
  307 FORMAT(1X,I2,4F8.3,2F8.2,F8.1)
   71 FORMAT(7F10.3,I1)
   73 FORMAT(1X,I2,7F8.3,5X,I1)
   52 FORMAT(1X,I2,4F8.3,2F8.2,F8.1,7XI1)
  303 FORMAT(55H   STATIC  PRESSURES FROM  WALL  PORTS,INCHES H2O GAGE)
  305 FORMAT(7F10.5)
  814 FORMAT(2(2X'I'5X'PO'6X'PREAD'3X'TIME60'2X'INST'10X))
  815 FORMAT (2(5X,F8.0,3X,F3.0,2X,I1,9X))
  816 FORMAT(2(1X,I2,2X,F7.4,1X,F9.3,3X,F4.0,4X,I1,12X))
C
    2 READ(5,1) TITLE
      WRITE(6,777) TITLE
      WRITE(6,300)
      READ(5,4) DATE,RUN,TAMB,TCOV,TROT,TBASE,TGAS,PBAR,RHUM,E1,
     1    E2, DELP ,TIME,INSTOT
      WRITE(6,304) DATE,RUN,TAMB,TCOV,TROT,TBASE,TGAS
C
C  CALCULATION OF  DELP
C
      PHOLD= DELP
```

```
      IF(TIME.GT.0.0)  DELP = DELP *60./TIME
      INS=INSTOT+1
      GO TO (2125,2126,2127),INS
 2126  DELP =PCAL1( DELP ,A97,B97,C97,D97,E97)
      GO TO 2125
 2127  DELP =PCAL2( DELP ,A5,B5,C5,D5,E5)
 2125 WRITE(6,400)
      WRITE(6,404) PBAR,RHUM,E1,E2, DELP ,TIME,INSTOT,PHOLD
C
C  CMFLAG:  1-SMALL ROTO   2-LARGE ROTO    3-MIXED ROTO, REQUIRES 1 OR 2
C           COL 72 OF DATA FOR EACH PLATE
C  ENBLFG:  ENTER 1 FOR ENERGY BALANCE RUN, OTHERWISE LEAVE BLANK
C  NPLATE: ENTER ONLY IF LESS THAN 24 ARE TO BE CALCULATED
C  MASSK: 1-SMALL ROTO   2-LARGE ROTO
C
      READ(5,5) CMFLAG,ENBLFG,NPLATE
      WRITE(6,301)
      WRITE(6,50) CMFLAG,ENBLFG,NPLATE
      WRITE(6,306)
      IF(CMFLAG.NE.3)GO TO 74
      WRITE(6,75)
      GO TO 76
  74  WRITE(6,302)
  76  IF(NPLATE.EQ.0) NPLATE=24
      NPORT=2*NPLATE
      MNPORT=NPORT-1
      MNPLAT=NPLATE-1
      DO 7 I=1,NPLATE
      IF(CMFLAG.NE.3)GO TO 70
      READ(5,71)EO(I),EU(I),ED(I),ET(I),WIND(I),CM(I),PROT(I),MASSK(I)
      WRITE(6,52)I,EO(I),EU(I),ED(I),ET(I),WIND(I),CM(I),PROT(I),
     1  MASSK(I)
      GO TO 7
  70  READ(5,6)EO(I),EU(I),ED(I),ET(I),WIND(I),CM(I),PROT(I)
      WRITE(6,307) I,EO(I),EU(I),ED(I),ET(I),WIND(I),CM(I),PROT(I)
    7 CONTINUE
      WRITE(6,306)
      WRITE(6,814)
      DO 817 J=1,NPORT
      IF(J.GT.24) GO TO 818
      L=J+24
      READ(5,815) PK(J),TIME60(J),INSTK(J),PK(L),TIME60(L),INSTK(L)
      DO 2215 II=J,L,24
      PHOLD=PK(II)
      IF(TIME60(II).GT.0.0) PHOLD=PHOLD*60./TIME60(II)
      INS=INSTK(II)+1
      GO TO (2202,2203,2283),INS
 2203 PSTAT(II)=PCAL1(PHOLD,A97,B97,C97,D97,E97)
      GO TO 2215
 2283 PSTAT(II)=PCAL2(PHOLD,A5,B5,C5,D5,E5)
      GO TO 2215
 2202 PSTAT(II)=PHOLD
 2215 CONTINUE
      WRITE(6,816)(II,PSTAT(II),PK(II),TIME60(II),INSTK(II),II=J,L,24)
  817 CONTINUE
  818 WRITE(6,3)
C
C
C   DATA REDUCTION BEGINS HERE
C
      DO 80 I=1,NPLATE
```

```
C
C  THE FOLLOWING BLOCK CONVERTS ANY TEMPERATURES READ IN MILLIVOLTS TO D
C
      IF(TAMB.LT.10.) TAMB=TCALIB(TAMB)
      IF(TCOV.LT.10.) TCOV=TCALIB(TCOV)
      IF(TROT.LT.10.) TROT=TCALIB(TROT)
      IF(TBASE.LT.10.) TBASE=TCALIB(TBASE)
      IF(TGAS.LT.10.) TGAS=TCALIB(TGAS)
      IF(EU(I).EQ.0.0) EU(I)=EO(I)
      IF(ED(I).EQ.0.0) ED(I)=EO(I)
      TO(I)=TCALIB(EO(I))
      TU(I)=TCALIB(EU(I))
      TD(I)=TCALIB(ED(I))
      TT(I)=TCALIB(ET(I))
   80 CONTINUE
C
C  MIXTURE COMPOSITION IS DETERMINED FROM RELATIVE HUMIDITY AND USED
C  TO GET MIXTURE GAS CONSTANT RM VIA PERFECT GAS ASSUMPTION
C
      P=PBAR*2116.0/29.96
      DO 8 N=1,9
      IF(TEMP(N).GT.TAMB) GO TO 9
    8 CONTINUE
    9 T=TEMP(N)
      EPS=T-TAMB
      VAPH=PSAT(N)
      VAPL=PSAT(N-1)
      VEPS=VAPH-VAPL
      RHOH=RHOSAT(N)
      RHOL=RHOSAT(N-1)
      REPS=RHOH-RHOL
      RHOV=RHOL+(10.0-EPS)*REPS/10.0
      RA=53.3
      PVAP=RHUM*(VAPL+(10.0-EPS)*VEPS/10.0)
      RHOA=((P-PVAP)/(RA*(TAMB+460.0))+(RHUM*RHOV))
      MV=RHUM*RHOV/RHOA
      MA=1.0-MV
      RM=1545.0*(MA/28.9+MV/18.0)
C
C  SPECIFIC HEAT IS CORRECTED FOR HUMIDITY EFFECTS IN THE FOLLOWING EQUA
C
      CP=0.240+0.205*MV
C
C TGAS IS CORRECTED TO STATIC TEMPERATURE
C
      IF(ENBLFG.EQ.1) GO TO 1104
      PTOTAL=DELP+PSTAT(3)
      DO 1103 M=1,5
      RHOG(3)=(P+5.2*PSTAT(3))/(RM*(TGAS+460.0))
      VISCG(3)=(11.0+0.0175*TGAS)/(1000000.0*RHOG(3))
      V(3)=SQRT((64.34*(PTOTAL-PSTAT(3))*(62.4/RHOG(3))/12.0))
      RCF=.7**.333
      TGAS=TGAS - RCF*V(3)*V(3)/(778.*64.34*CP)
 1103 CONTINUE
C
C  FREE STREAM DATA NOW PROCESSED
C
 1104 DO 101 J=1,NPORT
      RHOG(J)=(P+5.2*PSTAT(J))/(RM*(TGAS+460.0))
      VISCG(J)=(11.0+0.0175*TGAS)/(1000000.0*RHOG(J))
      V(J)=SQRT((64.34*(PTOTAL-PSTAT(J))*(62.4/RHOG(J))/12.0))
```

```
  101 CONTINUE
      DUDX(1)=(V(2)-V(1))/(X(2)-X(1))*12.
      KV(1)=VISCG(1)*DUDX(1)/(V(1)*V(1))
C
      DO 102 J=2,MNPORT
      DUDX(J)=12.0*(V(J+1)-V(J-1))/(X(J+1)-X(J-1))
      KV(J)=VISCG(J)*DUDX(J)/(V(J)*V(J))
  102 CONTINUE
C
C   FREE STREAM DATA FOR INDIVIDUAL PLATE IS RECORDED NOW
C
      DO 88 I=1,NPLATE
      NSTAT = 2*I - 1
      UG(I)=V(NSTAT)
      GS(I)=V(NSTAT)*RHOG(NSTAT)
      XS(I)=(2.0+(I-1)*4.0)/12.0
      KS(I)=KV(NSTAT)
      DUDXS(I)=DUDX(NSTAT)
      VISCGS(I)=VISCG(NSTAT)
   88 CONTINUE
C
C   DATA IS REDUCED FOR EACH PLATE DURING THE NEXT OPERATION
C
      DO 22 I=1,NPLATE
C
      IF(CMFLAG.NE.3) MASSK(I)=0
      NSTAT = 2*I - 1
C
C   FOLLOWING BLOCK CORRECTS INDICATED POWER FOR VOLTAGE COIL LOSS AND
C   FOR DEVIATION FROM ACTUAL PWR, PER SLAC TEST NO. 1149
C
C      WIND=0 USED AS FLAG FOR NO-POWER RUNS
C
      IF(WIND(I).LE.0.0) KW=1.0
      IF(WIND(I).LE.0.0) BETA=1.0
      IF(WIND(I).LE.0.0) GO TO 12
   10 IF(WIND(I).GE.75.0) KW=0.995
      IF(WIND(I).LT.75.0) KW=0.99
      IF(WIND(I).GE.75.0) WSCALE=150.0
      IF(WIND(I).LT.75.0) WSCALE=75.0
      NPWR=WIND(I)/WSCALE
      WCORR=NPWR*(0.0728*NPWR-0.0427*(NPWR*NPWR)-0.0292)
      WNET(I)=KW*WIND(I)+WCORR*WSCALE
      IF(I.LE.12) RC=E1/SQRT(75.0*WNET(I))
      IF(I.GT.12) RC=E2/SQRT(75.0*WNET(I))
      IF(WIND(I).LT.75.0) BETA=1.0+0.020*(1.0-1.0/RC)
      IF(WIND(I).GE.75.0) BETA=1.0+0.010*(1.0-1.0/RC)
   11 WNET(I)=BETA*WNET(I)
C
C   NEXT CALCULATES ENERGY INPUT DENSITY BTU/SECFT2 CORRECTING FOR
C   HEATER WIRE WRAPPED ACROSS ENDS, 2.3 PERCENT
C
      ENDEN(I)=WNET(I)/(1055.0*0.50*1.023)
      GO TO 13
   12 ENDEN(I)=0.0
C
C   NEXT CALCULATES HEAT LOSS BY RADIATION. SEE JULIFN 8/67 ENERGY
C   BALANCE REPORT FOR DETAILS.
C
   13 TAVG(I)=(TO(I)*3.0+TU(I)+TD(I))/5.0
      ER1=0.35
```

```
      ER2=0.20
      ER3=0.35
      F13=0.175
      AR=0.25
      KLM=1
      RH2=1.0-ER2
      RH3=1.0-ER3
      F12=1.0-F13
      F22=1.0-2.0*AR*F12
      RH1=1.0-ER1
      EMISS=0.17
      IF(PROT(I).LE.-0.1.AND.ENBLFG.EQ.1) EMISS=0.30
      T1=TAVG(I)+0.022*WIND(I)+460.0
      T3=TT(I)+460.0
      IF(PROT(I).LE.-0.1) T2=T1
      IF(PROT(I).GT.-0.1) T2=TT(I)+460.0
   14 IF(KLM.EQ.1) GO TO 15
      T1=T1+0.551*WIND(I)-0.0911*(T1-T3)
      ER1=0.90
      RH1=0.10
   15 DEN=1.0-RH2*F22-2.0*RH1*RH2*RH3*AR*F12*F12*F13-RH1*RH3*F13*F13*
     1(1.0-RH2*F22)-RH2*(RH3+RH1)*AR*F12*F12
      Q1=ER1*0.174E-08*T1*T1*T1*T1
      Q2=ER2*0.174E-08*T2*T2*T2*T2
      Q3=ER3*0.174E-08*T3*T3*T3*T3
      COEF1=1.0-RH2*F22-RH2*RH3*AR*F12*F12
      COEF23=(RH1*RH3*F12*F13+RH1*F12)*Q2+(RH1*RH2*AR*F12*F12+RH1*(1.0-
     1RH2*F22)*F13)*Q3
      B1T1=(COEF1*Q1+COEF23)/DEN
      B3T3=((RH3*(1.0+RH1*F13)*B1T1)+(RH1*Q3-RH3*Q1))/(RH1*(1.0+RH3*F13)
     1)
      IF(PROT(I).LE.-0.1) QHEATA=(ER1/RH1)*((Q1/ER1)-B1T1)
      IF(PROT(I).GT.-0.1) QHEATA=(ER3/RH3)*(B3T3-(Q3/ER3))
      IF(KLM.GE.2) GO TO 16
      KLM=2
      QHTA=QHEATA
      GO TO 14
   16 QHEAT=(0.895*QHTA+0.105*QHEATA)/3600.0
  253 QRAD(I)=0.1714*EMISS*(((TAVG(I)+460.0)/100.0)**4.0-((TCOV+460.0)/
     1100.0)**4.0)/3600.0+QHEAT
C
C  NEXT CALCULATES WEIGHT FLOW FROM ROTAMETER DATA AND GETS M''
C
      MDOT(I)=0.0
      VZERO(I) = 0.0
      RHOZRO = 0.0
      TROTA=TROT+460.0
      PROTA=PBAR+PROT(I)/25.4
      PROTAB(I)=2116.0*PROTA/29.96
      IF(CMFLAG.NE.3)GO TO 77
      IF(MASSK(I).EQ.1)GO TO 17
   77 IF(CMFLAG.EQ.1) GO TO 17
      IF(CM(I).LE.0.0) GO TO 19
C
C  NEW FIT FOR FACTORY CALIBRATION, PLUS/MINUS 0.3 PERCENT
C
      WSTDI=(0.60+0.752*CM(I)-0.50*SIN(CM(I)*3.1417/25.0))*0.075/60.0
      GO TO 18
   17 IF(CM(I).LE.0.0) GO TO 19
      WSTDI=(0.175+0.13091*CM(I)-0.067*SIN((CM(I)-2.0)*3.1417/21.0))*
     10.075/60.0
```

```
   18 WSTD(I)=WSTDI
C
C  ROTAMETER FLOW IS NEXT CORRECTED FOR DENSITY TO YIELD ACTUAL FLOW,
C  THEN CORRECTED FOR PLATE POROSITY VARIATION
C
      WACT(I)=WSTD(I)*SQRT(PROTAB(I)/(RM*TROTA*0.075))
      KFUDGE(I)=0.0
       W1=WACT(I)*1000.
      IF(CMFLAG.EQ.1) GO TO 118
      IF(CMFLAG.EQ.3.AND.MASSK(I).EQ.1) GO TO 118
C
C      CORRECTION CURVES TO FACTORY CALIBRATIONS(LARGE ROTOMETERS)
C
       IF(W1.LT.2.) W1=2.
       IF(W1.GT.15.) W1=15.
       PER=CLR1(I) + CLR2(I)*W1 + CLR3(I)*W1**2 + CLR4(I)*W1**3
      GO TO 119
  118 CONTINUE
C
C      CORRECTION CURVES TO FACTORY CALIBRATIONS(SMALL ROTOMETERS)
C
      IF(W1.LT.1.15) W1=1.15
      IF(W1.GT.4.) W1=4.0
      PER=CSR3(I)/(W1-CSR1(I))+CSR2(I)
  119  WACT(I)=WACT(I)*(1.-PER/100.)
      IF(PROT(I).LE.-0.1) MDOT(I)=WACT(I)*KFLOW(I)*2.01258
      IF(PROT(I).GT.-0.1) MDOT(I)=WACT(I)*(KFLOW(I)+KFUDGE(I))*2.01258
C
C  DENSITY OF FLOW AT PLATE SURFACE IS CALCULATED AND USED TO GET VZERO
C
      RHOZRO=(P+(    5.20    )*PSTAT(NSTAT))/(RM*(TAVG(I)+460.0))
      VZERO(I)=MDOT(I)/RHOZRO
C
C  NEXT CALCULATES HEAT LOSS BY CONDUCTION
C
  19  CONTINUE
  258 QCOND(I)=KCOND(I)*(TAVG(I)-TBASE)/30.0
      IF(MDOT(I).LE.0.0044) QCOND(I)=QCOND(I)+CONLAT(I)*((1.0-(MDOT(I)/
     10.0044)))*(TAVG(I)-TBASE)/30.0
      IF(MDOT(I).LE.0.0002) QCOND(I)=QCOND(I)+(0.015/3600.0)*12.0*
     1(TAVG(I)-TBASE)
      QLOSS=QRAD(I)+QCOND(I)
      ENNET(I)=ENDEN(I)-QLOSS
C
C  ENNET IS THE ENERGY DENSITY ON PLATE,AFTER SUBTRACTION OF HEAT LOSSES
C   FROM ENERGY DELIVERED TO THE PLATE, ENNET=Q''+ M''(IO-IT)
C
C  DISTRIBUTION OF ENERGY IS MADE NOW
C
      IF(PROT(I).GT.-0.1) GO TO 20
      MDOT(I)=0.0-MDOT(I)
      TT(I)=TAVG(I)+0.022*WIND(I)
      TOEFF(I)=TAVG(I)-0.0044*WIND(I)
      ECONV(I)=MDOT(I)*(TOEFF(I)-TT(I))*CP
      IF(ENBLFG.EQ.1)    ECONV(I)=MDOT(I)*(TGAS-TT(I))*CP
      GO TO 21
   20 ECONV(I)=MDOT(I)*(TAVG(I)-TT(I))*CP
C
C
C  EFFECTIVE SURFACE TEMPERATURE IS NOW DEFINED BASED ON MEASURED BULK
C  FLUID TEMPERATURES LEAVING THE O-STATE, THIS INCLUDES THE EFFECT ON
```

```
C  CONDUCTION ERROR, ON THE PLATE TEMPERATURE MEASUREMENT, AND ALSO THE
C  TEMPERATURE AND AREA WEIGHT FACTORS
C
      ECONV(I)=(1.0+30.0*MDOT(I)*KCONV(I))*ECONV(I)
      IF(MDOT(I).LE.0.0) TOEFF(I)=TAVG(I)
      IF(MDOT(I).GT.0.0) TOEFF(I)=TT(I)+ECONV(I)/(CP*MDOT(I))
   21 CONTINUE
C
C HTRANS- CONVECTIVE HEAT TRANSFER TO BOUNDARY LAYER
C
      HTRANS(I)=ENNET(I)-ECONV(I)
      HTFRAC(I)=HTRANS(I)/ENNET(I)*100.
      DEL=.5*1./3.
C
C  OUTPUT PARAMETERS CALCULATED NOW
C
      DELTAT(I)=TOEFF(I)-TGAS
      DELH(I) =CP*DELTAT(I)     -UG(1)*UG(I)/(64.4*778.)
      H(I)=HTRANS(I)/DELH(I)
      ST(I)=H(I)/GS(I)
      F(I)=MDOT(I)/GS(I)
      STCP(I)=ST(I)*(((TOEFF(I)+460.)/(TGAS+460.))**0.4)
C
C SEE RJM THESIS P.71 FOR EXPONENT REFERENCE
C
      BB(I)=MDOT(I)/(GS(I)*ST(I))
      DEL=1./3.
      ISO(I)=CP*(TOEFF(I)-TGAS) - UG(I)*UG(I)/(64.4*778.)
      CALL UNCERT
   22 CONTINUE
C
      IF(ENBLFG.EQ.1) GO TO 241
C
C
C  ENTHALPY THICKNESS AND ENTHALPY THICKNESS REYNOLDS NUMBER:
C THE ENERGY EQUATION IS INTEGRATED ACROSS EACH PLATED, I.E., EDGE-TO-
C EDGE.  THE VALUES AT THE CENTER ARE THEN OBTAINED BY INTERPOLATION.
C
C  THE FOLLOWING IS A CALCULATION OF INITIAL ENTHALPY THICKNESS THAT
C  EXISTS UNDER CONSTANT SURFACE TEMPERATURE AT X=0 .THE CONSTANTS WERE
C  DETERMINED EXPERIMENTALLY FROM PROFILES TAKEN 082968-1 .ENTHALPY
C  THICKNESS AT X=-3.5 EQUALS 0.039 INCHES. AT X=-3.5 THE TEMPERATURE
C  DIFFERENCE IS
C
      TRATIO= 0.47*(TGAS-TAMB +2.)/(TGAS-TOEFF(1))
      ENTHZR = 0.039*TRATIO/12.
      IF(TGAS.GT.TOEFF(1))TRATIO=0.3*(TGAS-TAMB+2.)/(TGAS-TOEFF(1)+2.5)
      IF(TGAS.GT.TOEFF(1))ENTHZR= 0.022*TRATIO/12.
C
      START=ENTHZR*UG(1)*ISO(1)
      TERM(1)=START
      XINT(1)=0.0
      NNN=NPLATE + 1
      TERMCP(1)=START
      XINTCP(1)=0.0
      DO 23 I=2,NNN
      XINT(I)=XINT(I-1) + 1./3.*(ST(I-1)*UG(I-1)*ISO(I-1) +
     1  F(I-1)*UG(I-1)*ISO(I-1))
      TERM(I)= START + XINT(I)
      ENTH(I-1)=.5*(TERM(I-1)+TERM(I))/(UG(I-1)*ISO(I-1))
      REENTH(I-1)=UG(I-1)*ENTH(I-1)/VISCGS(I-1)
```

```
C
C  INTEGRATION FOR CONSTANT PROPERTY CASE
C
      XINTCP(I)=XINTCP(I-1) + 1./3.*(STCP(I-1)*UG(I-1)*ISO(I-1) +
     1  F(I-1)*UG(I-1)*ISO(I-1))
      TERMCP(I)= START + XINTCP(I)
      ENTHCP(I-1)=.5*(TERMCP(I-1)+TERMCP(I))/(UG(I-1)*ISO(I-1))
      REENCP(I-1)=UG(I-1)*ENTHCP(I-1)/VISCGS(I-1)
   23 CONTINUE
      CALL UNCER
C
C
C  OUTPUT
C
C
  241 CONTINUE
   24 FORMAT(5H DATE,I8,5X,7HRUN NO.,I4)
   25 FORMAT(62H AMB TEMP  BASE TEMP  GAS TEMP  COVER TEMP  BARO PRES  R
     1EL HUM/1XF6.2,5XF6.2,4XF6.2,6XF6.2,6XF5.2, 6XF4.2)
   26 FORMAT(/115H UNITS:P-ROT= MM HG;  WIND= WATTS;  VEL= FT/SEC;  MDOT
     1=LB/(SEC-FT2);  HT-X, ECONV, ENNET, QCOND, QRAD= BTU/(SECFT2) )
  310 FORMAT(41H UNITS: DELTA2= IN.  ;  HTFRAC=PERCENT    )
   27 FORMAT(/5H PL  ,1X,7HTCL-AVG,5X,2HTU,6X,2HTD,7X,2HTT,5X,5HTOEFF,5X
     1,5HDEL-T,5X,2HCM,7X,4HWIND,6X,5HVEL-X/)
   63 FORMAT( /  101H PL      B         MDOT     V-ZERO       HT-X          ECO
     1NV       ENNET        QCOND        QRAD        HTFRAC /)
   28 FORMAT(I3,3XF6.2,4XF6.2,2XF6.2,3X,F6.2,3X,F6.2,3X,F6.2,2X,F6.2,4X,
     1F6.2,5X,F6.2)
   62 FORMAT(I3,3XF6.3,2XF8.4,1XF8.4,5(2XE10.3),2XF6.1)
  103 FORMAT(68H     RUN           DELP         TG        TAMB       PBAR
     1     RHUM     )
  104 FORMAT(2X,I6,1H-,I1,4X,F9.4,1X,4F10.2//)
  105 FORMAT(77H   I        X(I)     PSTAT(I)     V(I)          DUDX(I)
     1  K(I)                 ,/)
  106 FORMAT(2XI2,4X,F8.3,F10.4,2XF8.2,7XF6.2 ,5XE11.3,3XE11.3)
   30 FORMAT(/5H PL  ,1X,6HTO,EFF,4X,2HTT,7X,2HST,4X,6HREENTH,3X,
     26HDELTA2,6X'F ',6X,5HVEL-X,7X,1HK,10X5HST-CP,6X9HREENTH-CP/)
   31 FORMAT(I3,3X,F6.2,2X,F6.2,2X,F7.5,1XF6.0,4XF6.4,
     12XF8.4,3X,F6.2,2X,E10.3,5XF7.5,6XF6.0)
  131 FORMAT(I3,F6.2,F6.2,F7.5,F6.0,F6.4,
     1F8.4,F6.2,E10.3,F7.5,F6.0)
   81 FORMAT(I3,3X,F6.2,2X,F6.2,2X,F7.5,2X,F7.5,1X,
     1F6.0,2X,F8.5,2X,F5.1,2X,E10.3)
  240 FORMAT(1H1,35X,22H UNCERTAINTY INTERVALS //40X,16H ABSOLUTE VALUES
     1   /)
  225 FORMAT(3H PL,91X,6HHTFRAC)
  230 FORMAT(I3,91XF4.1)
  245 FORMAT(3H PL,22X2HST,4X15HREENTH   DELTA2,7X'F'6X'VEL-X')
  250 FORMAT(I3,I9XF7.5,2XF5.0,4XF6.4, 3X F8.4,2XF6.2)
  255 FORMAT( / 40X11HPERCENTAGES /)
  260 FORMAT(I3,21XF4.1,4XF4.1,5XF4.1, 6XF4.1,5XF4.1)
C
C
      NPRINT=1
      DO 33 J=1,NPRINT
      WRITE(6,1777) TITLE
      WRITE(6,24) DATE, RUN
      WRITE(6,26)
      WRITE(6,310)
      WRITE(6,27)
      DO 29 I=1,NPLATE
```

```
      WRITE(6,28) I, TO(I),TU(I),TD(I),TT(I),TOEFF(I),DELTAT(I),CM(I),
     1WIND(I),UG(I)
   29 CONTINUE
      WRITE (6,63)
      DO 61 I=1,NPLATE
      IF(ENBLFG.EQ.1) BB(I)=0.0
      WRITE(6,62) I,BB(I),MDOT(I),VZERO(I),HTRANS(I),ECONV(I),ENNET(I),
     1  QCOND(I),QRAD(I),HTFRAC(I)
   61 CONTINUE
      IF(ENBLFG.NE.1) GO TO 265
      WRITE(6,240)
      WRITE(6,225)
      DO 750 I=1,NPLATE
      WRITE(6,230) I,DHTF(I)
  750 CONTINUE
      GO TO 33
  265 CONTINUE
      WRITE (6,3)
      WRITE(6,103)
      WRITE(6,104) DATE,RUN, DELP ,TGAS,TAMB,PBAR,RHUM
      WRITE(6,105)
      DO 107 I=1,MNPORT
      WRITE(6,106) I,X(I),PSTAT(I),V(I),DUDX(I),KV(I)
  107 CONTINUE
      WRITE(6,3)
      WRITE(6,1777) TITLE
      IF(IP.EQ.1) WRITE(7,1777) TITLE
      WRITE(6,24) DATE,RUN
      IF(IP.EQ.1) WRITE(7,24) DATE,RUN
      WRITE(6,25) TAMB,TBASE,TGAS,TCOV,PBAR,RHUM
      IF(IP.EQ.1) WRITE(7,25) TAMB,TBASE,TGAS,TCOV,PBAR,RHUM
      WRITE(6,30)
      M=4
      DO 32 I=1,NPLATE
      ENTH(I)=ENTH(I)*12.
      WRITE(6,31) I,TOEFF(I),TT(I),ST(I),REENTH(I),
     1          ENTH(I),F(I),UG(I),KS(I),STCP(I),REENCP(I)
      IF(IP.EQ.1) WRITE(7,131) I,TOEFF(I),TT(I),ST(I),REENTH(I),
     1          ENTH(I),F(I),UG(I),KS(I),STCP(I),REENCP(I)
      IF(I.EQ.M) WRITE(6,306)
      IF(I.EQ.M) M=M+4
   32 CONTINUE
      WRITE(6,240)
      WRITE(6,245)
      DO 755 I=1,NPLATE
      WRITE(6,250) I,DST(I),DRE(I),DDL2(I),DF(I),DUG(I)
  755 CONTINUE
      WRITE(6,255)
      WRITE(6,245)
      DO 760 I=1,NPLATE
      WRITE(6,260) I,DSTND(I),DREND(I),DDL2ND(I),DFND(I),DUGND(I)
  760 CONTINUE
      WRITE(6,3)
   33 CONTINUE
C
C THE FOLLOWING SECTION PRINTS OUT INFORMATION ON THE
C UNCERTAINTY INTERVALS USED IN THE UNCERTAINTY CALCULATIONS.
C
C
C     HEADING AND EXPLANATION
      WRITE(6,900)
```

```
  900 FORMAT(//,20X,'PRIME UNCERTAINTY INTERVALS USED'
     1,3X,'(ESTIMATED AT 20:1 ODDS)'//)
      WRITE(6,901)
  901 FORMAT(2X,'VARIABLE',5X,'VALUE ASSIGNED',10X,'VARIABLE MEANING'
     1,44X,'UNITS'//)
      WRITE(6,902) DDELP
  902 FORMAT(2X'DDELP'8X,F6.4,18X,'MANOMETER READING',43X,'IN.-H2O!/)
      WRITE(6,903) DXX
  903 FORMAT(2X,'DXX',10X,F5.3,19X,'STATIC TAP LOCATIONS',40X,'INCHES'/)
      WRITE(6,905) DCMP
  905 FORMAT(2X,'DCMP ',7X,F6.3,19X,'ROTOMETER READING',43X,'%'/)
      WRITE(6,909) DTEMPA
  909 FORMAT(2X,'DTEMPA',7X,F5.3,19X,'GAS TEMPERATURE',45X,'DEG. F.'/)
      WRITE(6,1909) DTEMPP
 1909 FORMAT(2X,'DTEMPP',7X,F5.3,19X,'GAS TEMPERATURE',45X,'DEG. F.'/)
      WRITE(6,910) DPAMB
  910 FORMAT(2X,'DPAMB',8X,F5.2,19X,'AMBIENT PRESSURE',44X,'LBF/FT2'/)
      WRITE(6,911) DMUP
  911 FORMAT(2X'DMUP',7X,F5.1,21X,'ABSOLUTE VISCOSITY',42X,'%'/)
      DP97LO=DP97LO*100.
      DP97HI=DP97HI*100.
      DP5LO=DP5LO*100.
      DP5HI=DP5HI*100.
      WRITE(6,912) DP97LO
  912 FORMAT(2X,'DP97LO',7X,F6.4,18X,'TRANSDUCER CALIBRATION-PM97,',
     1'FOR P<.05 IN.-H2O',15X,'%'/)
      WRITE(6,913) DP97HI
  913 FORMAT(2X,'DP97HI',7X,F6.4,18X,'TRANSDUCER CALIBRATION-PM97,',
     1'FOR P>.05 IN.-H2O',15X,'%'/)
      WRITE(6,914) DP5LO
  914 FORMAT(2X,'DP5LO',8X,F6.4,18X,'TRANSDUCER CALIBRATION-PM5,',
     1'FOR P<1.0 IN.-H2O',16X,'%'/)
      WRITE(6,920)DP5HI
  920 FORMAT(2X,'DP5HI',8X,F6.4,18X,'TRANSDUCER CALIBRATION-PM5,',
     1'FOR P>1.0 IN.-H2O',16X,'%'/)
      DP97LO=DP97LO/100.
      DP97HI=DP97HI/100.
      DP5LO=DP5LO/100.
      DP5HI=DP5HI/100.
      WRITE(6,916) D97MIN
  916 FORMAT(2X,'D97MIN',7X,F6.4,18X,'MINIMUM PM97 UNCER. DUE TO ZERO',
     1' SHIFT',23X,'IN.-H2O'/)
      WRITE(6,917)D5MIN
  917 FORMAT(2X,'D5MIN',8X,F6.4,18X,'MINIMUM PM5 UNCER. DUE TO ZERO ',
     1' SHIFT',23X,'IN.-H2O'/)
      WRITE(6,918) D97MAX
  918 FORMAT(2X,'D97MAX',7X,F6.4,18X,'MAXIMUM PM97 UNCER.',
     1' DUE TO CALIBRATION CHECK',16X,'IN.-H2O'/)
      WRITE(6,919) D5MAX
  919 FORMAT(2X,'D5MAX',8X,F6.4,18X,'MAXIMUM PM5 UNCER.',
     1' DUE TO CALIBRATION CHECK',17X,'IN.-H2O'/)
      WRITE(6,904) DQRADP
  904 FORMAT(2X,'DQRADP',6X,F5.1,20X,'RADIATION ENERGY TRANSFER',35X,
     1  '%'/)
      WRITE(6,907) DWIND
  907 FORMAT(2X,'DWIND',8X,F4.2,20X,'INDICATED WATTMETER READING',33X,
     1  'WATTS'/)
      WRITE(6,908) DENZRP
  908 FORMAT(2X,'DENZRP',6X,F5.1,20X,'STARTING ENTHALPY THICKNESS ESTIMA
     1TE', 24X,'%'/)
      WRITE(6,925) A97,B97,C97,D97,E97,A5,B5,C5,D5,E5
```

```
  925 FORMAT(///25X'TRANSDUCER CONSTANTS'//17X'A'11X'B'11X'C'11X'D'11X,
     1'E'/3X'PM97'3X,5(2XF10.7)/3X'PM5'4X,5(2XF10.7))
      WRITE(6,3)
C
C
C
 500  CONTINUE
      STOP
      END
C
C
      FUNCTION TCALIB(TMV)
C
C THIS CONVERSION USES A CURVE FIT OF THE MV-F TABLES AND
C A CORRECTION DUE TO THE CALIBRATION BY WHITTEN. SEE FILES.
C
           TMVV=-2220.703 + 781.25*SQRT(7.950782+0.256*TMV)
           TCALIB=TMVV + 49.97 - 12.6E-04*TMVV - 32.0E-06*TMVV*TMVV
      RETURN
      END
C
C
C
C
      FUNCTION PCAL1(PMV,A97,B97,C97,D97,E97)
C     CALIBRATION FOR PM-94
      IF(PMV.LE.4.64) PCAL1=A97*PMV
      IF(PMV.GT.4.64.AND.PMV.LE.14.28) PCAL1=B97 + C97*PMV
      IF(PMV.GT.14.28) PCAL1=D97 + E97*PMV
      RETURN
      END
C
C
C
C
      FUNCTION PCAL2(PMV,A5,B5,C5,D5,E5)
C     CALIBRATION FOR PM-5
      IF(PMV.LT.1.211) PCAL2=A5*PMV
      IF(PMV.GT.1.211.AND.PMV.LE.7.626) PCAL2= B5 + C5*PMV
      IF(PMV.GT.7.626) PCAL2= D5 + E5*PMV
      RETURN
      END
C
C
C
C
      BLOCK DATA
C
      REAL KCOND(24),KCONV(24),KFLOW(24),KFUDGE(24),KPROP,KS(24),
     1     KV(48),KW,MA,MDOT(24),MV,NPWR,ISO(24)
C
      INTEGER CMFLAG,DATE,ENBLFG,RUN,TITLE(18)
C
      COMMON /A/ AR,BETA,B1T1,B3T3,CMFLAG,COEF1,COEF23,CP,DATE,DEN,
     1  ENBLFG,E1,E2,EMISS,EPS,ER1,ER2,ER3,F12,F13,F22,I,INSTOT,J,KCOND,
     2    KCONV,KFLOW,KFUDGE,KPROP,KS,KV,KW,KLM,MA,MDOT,MV,NPWR,NPLATE,
     3    NSTAT,P,PBAR,PROTA, DELP ,PVAP,Q1,Q2,Q3,QHEAT,
     4    QHEATA,QHTA,QLOSS,RA,RCF,REPS,RHOA,RHOH,RHOL,RHOV,RHOZRO,RUN,
     5    RH1,RH2,RH3,RHUM,RM,T,TAMB,TBASE,TCOV,TGAS,TROT,
     6    TROTA,T1,T2,T3,VAPH,VAPL,VEPS,WCORR,WSCALE,WSTDI,
     7  ISO,REENCP(24),ENTHCP(24),ENTHZR,
```

```
     8    AREA(24),BB(24),CFHT(24),CM(24),CONLAT(24),DELH(25),
     9    DELTAT(24),DUDX(48),DUDXS(24),ECONV(24),ED(24),ENDEN(24),
     1    ENNET(24),EO(24),ENTH(24),ET(24),EU(24),F(24),GS(24),H(24),
     2    HTFRAC(24),HTRANS(24),INSTK(48),MASSK(24),PK(48),
     A    PROT(24),PROTAB(24),PSAT(9),PSTAT(48),QCOND(24),
     3    QRAD(24),REENTH(24),REENW(25),RHOG(48),
     4    RHOSAT(9),ST(24),STCP(24),TAVG(24),TEMP(9),TIME60(48),
     5    TO(24),TOEFF(24),TD(24),TITLE,TT(24),TU(24),V(48),
     6    VISCG(48),VISCGS(24),UG(24),VZERO(24),WACT(24),WIND(24),
     7    WNET(24),WSTD(24),X(48),XS(24),XSTCP(24),XMDOT(24)
      COMMON /B/ DCMP,DDELP,DPAMB,DP5HI,DP5LO,DP97HI,DP97LO,DQRADP,
     1          DTEMPA,DTEMPP,DTBASE,DTT,DTROT,DTGAS,DWIND,DXX,F2,F3,F4,
     2            F6,F7,F8,DEL,DDUDXS(24),DISO(24),DENZRP,
     3            DB(24),D8ND(24),DCM(24),DDL2(24),DDL2ND(24),DF(24),
     4            DFND(24),DHTF(24),DMDOT(24),DMDOTN(24),DPSTAT(48),
     5            DQRAD(24),DRE(24),DREND(24),DRHOG(24),DST(24),
     6            DSTND(24),DUG(24),DUGND(24),DV(48),DDUDX(48),
     7            CLR1(24),CLR2(24),CLR3(24),CLR4(24),CSR1(24),
     8            CSR2(24),CSR3(24),DVISCG(24),DEL2,DMUP,MNPLAT,
     9             D97MIN,D97MAX,D5MIN,D5MAX,PTOTAL,NPORT,MNPORT
C
C  THE FOLLOWING ARE FIXED DATA FILLS:
C
      DATA CONLAT/
     40.0007,0.0003,0.0,0.001,0.0018,0.0018,0.0004,0.0021,0.0015,0.0014,
     50.0016,0.0006,0.0006,0.0016,0.001,0.0008,0.001,0.001,0.0,0.0007,
     60.0011,0.0010,0.0,0.0/
      DATA KCONV/
     30.020,0.020,
     40.025,0.020,0.018,0.035,0.040,0.026,0.024,0.035,0.032,0.039,0.032,
     50.024,0.016,0.014,0.018,0.020,0.019,0.015,0.017,0.013,0.030,0.015/
      DATA KCOND/
     30.00688,0.00375,
     40.00337,0.00328,0.00194,0.00194,0.00386,0.00202,0.00235,0.00264,
     50.00267,0.00243,0.00298,0.00233,0.00206,0.00231,0.00168,0.00282,
     60.00405,0.00298,0.00265,0.00168,0.00309,0.00338/
      DATA KFUDGE/
     4-0.010,0.024,0.0,-0.0025,0.0080,0.004,0.004,-0.008,0.008,0.0,0.008
     5,0.008,0.0,0.012,0.006,0.016,0.010,0.016,0.016,0.005,0.016,0.010,
     60.010,0.008/
      DATA KFLOW/
C     31.0204,1.0101,
C     41.0309,1.0417,1.0309,1.0309,1.0183,1.0493,1.0225,1.0449,1.0331,
C     51.0428,1.0504,1.0373,1.0526,1.0152,1.0341,1.0331,1.0081,1.0471,
C     61.0363,1.0428,1.0018,1.0331/
     31.033,1.045,1.026,1.041,1.047,1.032,1.03,1.062,1.06,1.062,
     41.05,1.058,1.059,1.07,1.062,1.035,1.057,1.052,1.04,1.061,
     5 1.051,1.05,1.04,1.043/
      DATA X/
     41.969,3.953,5.953,7.961,9.969,11.953,13.937,
     515.945,17.953,19.922,21.938,23.954,25.962,27.962,29.978,31.939,
     633.955,35.955,37.971,39.987,41.963,43.963,45.963,47.979,49.979,
     751.979,53.995,55.971,57.971,59.955,61.979,63.971,65.979,67.963,
     869.971,71.979,73.963,75.939,77.947,79.939,81.931,83.962,85.931,
     987.915,89.939,91.931,93.947,96.0/
      DATA TEMP/
     140.0,50.0,60.0,70.0,80.0,90.0,100.0,110.0,120.0/
      DATA PSAT/
     117.53,25.65,36.90,52.20,73.00,100.40,136.50,183.60
     2,243.70/
      DATA RHOSAT/
```

```
     10.000409,0.000587,0.000830,0.001153,
     20.001580,0.002139,0.002853,0.003770,0.004920/
      DATA F2,F3,F4,F6,F7,F8/0.752,-0.5,0.12567,0.13091,-0.067,0.14960/
      DATA CLR1/
     13.8823,4.3784,4.9672,5.3868,6.0977,7.2071,6.7488,1.224E01,4.9783,
     26.4093,2.1603,2.6746,3.5441,4.6305,4.5954,5.4947,4.1666,6.2882,
     32.6813,5.3851,2.391,1.0441,1.4687,3.3328/
      DATA CLR2/
     1-7.4872E-01,-4.5701E-01,-8.613E-01,-1.6336,-1.6978,-1.9426,-1.4491
     2,-2.4532,-6.7284E-01,-1.2452,-1.9676E-01,-4.5878E-01,-8.924E-01,
     3-1.44,-9.2705E-01,-9.9417E-01,-6.3879E-01,-1.5029,-3.6441E-01,
     4-8.4925E-01,-1.7758E-01,-1.3509E-01,-1.4061E-02,-8.1687E-01/
      DATA CLR3/
     15.6479E-02,7.3789E-03,3.7527E-02,1.5384E-01,1.5879E-01,1.8029E-01
     2,1.1898E-01,2.0284E-01,2.9397E-02,1.0067E-01,-6.4155E-03,3.7478E-0
     32,9.0667E-02,1.4625E-01,6.6932E-02,6.2717E-02,2.7366E-02,1.3727E-
     401,1.1157E-02,4.1191E-02,-1.1368E-02,-7.5722E-03,-1.1172E-02,
     57.9734E-02/
      DATA CLR4/
     1-1.3375E-03,7.5566E-04,6.5083E-04,-4.3438E-03,-4.6469E-03,-5.3748E
     2-03,-3.3093E-03,-5.5582E-03,-2.5595E-05,-2.7E-03,1.1122E-03,-8.737
     35E-04,-2.741E-03,-4.4226E-03,-1.1244E-03,-8.9969E-04,1.8686E-04,
     4-3.9184E-03,3.5851E-04,-1.7090E-04,1.1929E-03,7.9497E-04,5.1672E-0
     54,-2.2502E-03/
      DATA CSR1/
     11.0849,.8777,1.0304,.9367,.7106,.9667,.9716,.9882,.8258,1.0704,
     21.0269,1.0342,.9988,1.1026,1.1040,1.0583,.9891,1.0849,1.1065,
     31.1186,1.0742,1.0511,1.0978,1.1414/
      DATA CSR2/
     1-1.0745,-.9978,-1.5909,-2.457,-1.0452,-1.4233,-2.5170,-1.2082,
     2-1.1742,-2.2648,-1.7785,-.4761,-2.101,-.7692,-.1792,-.165,
     3-.1087,-.766,.332,-2.1763,-.003711,-.6796,-1.8706,.007071/
      DATA CSR3/
     1.5258,1.9055,.5729,1.9745,4.1328,1.4707,1.2515,1.4248,2.553,.8969,
     21.536,1.329,1.6028,.5108,.3398,1.0971,1.6262,.701,.5076,.3316,
     30.8914,.7397,.5148,.07979/
C
      END
C
C
      SUBROUTINE UNCERT
C
C  UNCERTAINTY ANALYSIS FOR STANTON PROGRAM.  FUNCTIONAL RELATIONSHIPS
C  ARE DIFFERENT FOR THE VARIOUS OPERATING MODES.
C
C
C THE FOLLOWING PROCEDURE CALCULATES UNCERTAINTY INTERVALS BY THE
C PROCEDURE OF KLINE AND MCLINTOCK.   THE UNCERTAINTY INTERVALS FOR
C THE MEASURED (INDEPENDENT) VARIABLES ARE:
C     DCMP      : % OF ROTOMETER READING
C     DDELP     : MANOMETER (INCHES-H20)
C     DPAMB     : AMBIENT PRESSURE (PSF)
C     DP5LO     :TRANSDUCER CALIBRATION-PM5 FOR P<1.0 "H20 (%)
C     DP5HI     :TRANSDUCER CALIBRATION-PM5 FOR P>1.0 "H20 (%)
C     DP97LO    :TRANSDUCER CALIBRATION-PM97 FOR P<0.05 "H20 (%)
C     DP97HI    :TRANSDUCER CALIBRATION-PM97 FOR P>0.05 "H20 (%)
C           MINIMUM AND MAXIMUM LIMITS ARE ALSO SET ON THE
C           TRANSDUCER UNCERTAINTIES
C     DQRADP    : % OF RADIATION ENERGY TRANSFER
C     DTEMPA    : TEMPERATURE (F) - ACTIVE RUNS
C     DTEMPP    : TEMPERATURE (F) - PASSIVE RUNS
```

```
C      DWIND     : INDICATED WATTMETER READING (WATTS)
C      DXX       : STATIC TAP LOCATIONS (INCHES)
C      DENZRP    : ENTHALPY THICKNESS AT START OF PLATES(X=0)  (%)
C      DMUP      : ABSOLUTE VISCOSITY EQUATION  (%)
C
C      DXX AND DMUP ARE SET TO ZERO FOR NORMAL CALCULATIONS DESIGNED TO
C      HIGHLIGHT EXPERIMENTAL PROBLEMS.  TO RELATE TO THE 'REST OF THE
C      WORLD', THESE INTERVALS ARE GIVEN FINITE VALUES.
C
       REAL KCOND(24),KCONV(24),KFLOW(24),KFUDGE(24),KPROP,KS(24),
      1     KV(48),KW,MA,MDOT(24),MV,NPWR,ISO(24)
       REAL M1,M2,M3,M4,N,NN
C
       INTEGER CMFLAG,DATE,ENBLFG,RUN,TITLE(18)
C
       COMMON /A/ AR,BETA,B1T1,B3T3,CMFLAG,COEF1,COEF23,CP,DATE,DEN,
      1  ENBLFG,E1,E2,EMISS,EPS,ER1,ER2,ER3,F12,F13,F22,I,INSTOT,J,KCOND,
      2    KCONV,KFLOW,KFUDGE,KPROP,KS,KV,KW,KLM,MA,MDOT,MV,NPWR,NPLATE,
      3    NSTAT,P,PBAR,PROTA, DELP ,PVAP,Q1,Q2,Q3,QHEAT,
      4    QHEATA,QHTA,QLOSS,RA,RCF,REPS,RHOA,RHOH,RHOL,RHOV,RHOZRO,RUN,
      5    RH1,RH2,RH3,RHUM,RM,T,TAMB,TBASE,TCOV,TGAS,TROT,
      6    TROTA,T1,T2,T3,VAPH,VAPL,VEPS,WCORR,WSCALE,WSTDI,
      7  ISO,REENCP(24),ENTHCP(24),ENTHZR,
      8    AREA(24),BB(24),CFHT(24),CM(24),CONLAT(24),DELH(25),
      9    DELTAT(24),DUDX(48),DUDXS(24),ECONV(24),ED(24),ENDEN(24),
      1    ENNET(24),EO(24),ENTH(24),ET(24),EU(24),F(24),GS(24),H(24),
      2    HTFRAC(24),HTRANS(24),INSTK(48),MASSK(24),PK(48),
      A    PROT(24),PROTAB(24),PSAT(9),PSTAT(48),QCOND(24),
      3    QRAD(24),REENTH(24),REENW(25),RHOG(48),
      4    RHOSAT(9),ST(24),STCP(24),TAVG(24),TEMP(9),TIME60(48),
      5    TO(24),TOEFF(24),TD(24),TITLE,TT(24),TU(24),V(48),
      6    VISCG(48),VISCGS(24),UG(24),VZERO(24),WACT(24),WIND(24),
      7    WNET(24),WSTD(24),X(48),XS(24),XSTCP(24),XMDOT(24)
       COMMON /B/ DCMP,DDELP,DPAMB,DP5HI,DP5LO,DP97HI,DP97LO,DQRADP,
      1          DTEMPA,DTEMPP,DTBASE,DTT,DTROT,DTGAS,DWIND,DXX,F2,F3,F4,
      2            F6,F7,F8,DEL,DDUDXS(24),DISO(24),DENZRP,
      3            DB(24),DBND(24),DCM(24),DDL2(24),DDL2ND(24),DF(24),
      4            DFND(24),DHTF(24),DMDOT(24),DMDOTN(24),DPSTAT(48),
      5            DQRAD(24),DRE(24),DREND(24),DRHOG(24),DST(24),
      6            DSTND(24),DUG(24),DUGND(24),DV(48),DDUDX(48),
      7            CLR1(24),CLR2(24),CLR3(24),CLR4(24),CSR1(24),
      8            CSR2(24),CSR3(24),DVISCG(24),DEL2,DMUP,MNPLAT,
      9             D97MIN,D97MAX,D5MIN,D5MAX,PTOTAL,NPORT,MNPORT
C
C CALCULATED UNCERTAINTY INTERVALS
C
       DCM(I)=DCMP*CM(I)/100.
       DQRAD(I)=DQRADP*QRAD(I)/100.
       DPBAR=DPAMB*29.96/2116.
C
C      VELOCITY HEAD (DELP) UNCERTAINTY INTERVAL
C
       DPRES=DDELP
       IF(INSTOT.NE.1) GO TO 5062
       IF( DELP .LT.0.05) DPRES= DELP *DP97LO
       IF( DELP .GE.0.05) DPRES= DELP *DP97HI
 5062  IF(INSTOT.NE.2) GO TO 5061
       IF(DPRES.LT.D97MIN) DPRES=D97MIN
       IF(DPRES.GT.D97MAX) DPRES=D97MAX
       IF( DELP .LT.1.0) DPRES= DELP *DP5LO
       IF( DELP .GE.1.0) DPRES= DELP *DP5HI
```

```
      IF(DPRES.LT.D5MIN) DPRES=D5MIN
      IF(DPRES.GT.D5MAX) DPRES=D5MAX
C
 5061 DO 305 J=1,NPORT
C
C     STATIC PRESSURE UNCERTAINTY INTERVALS
C
      DPSTAT(J)=DDELP
      IF(INSTK(J).NE.1) GO TO 5060
      IF(PSTAT(J).LT.0.05) DPSTAT(J)=PSTAT(J)*DP97LO
      IF(PSTAT(J).GE.0.05) DPSTAT(J)=PSTAT(J)*DP97HI
      IF(DPSTAT(J).LT.D97MIN) DPSTAT(J)=D97MIN
      IF(DPSTAT(J).GT.D97MAX) DPSTAT(J)=D97MAX
 5060 IF(INSTK(J).NE.2) GO TO 305
      IF(PSTAT(J).LT.1.0) DPSTAT(J)=PSTAT(J)*DP5LO
      IF(PSTAT(J).GE.1.0) DPSTAT(J)=PSTAT(J)*DP5HI
      IF(DPSTAT(J).LT.D5MIN) DPSTAT(J)=D5MIN
      IF(DPSTAT(J).GT.D5MAX) DPSTAT(J)=D5MAX
  305 CONTINUE
C
C  TOTAL PRESSURE UNCERTAINTY INTERVAL
C
      DPTOT=SQRT(DPRES**2 + DPSTAT(2)**2)
C
C TEMPERATURE UNCERTAINTIES - ACTIVE OR PASSIVE RUN
C
      DTEMP=DTEMPA
      DTBASE=DTEMPA
      DTT=DTEMPA
      DTROT=DTEMPA
      DTGAS=DTEMPA
      IF(WIND(I).NE.0.0) GO TO 720
      DTEMP=DTEMPP
      DTBASE=DTEMPP
      DTT=DTEMPP
      DTROT=DTEMPP
      DTGAS=DTEMPP
  720 CONTINUE
C
C   GENERALLY USED CONSTANTS
C
      XMDOT(I)=ABS(MDOT(I))
      A1=KCOND(I)/30.
      IF(XMDOT(I).LE.0.0044)  A1=A1 + CONLAT(I)*(1.-XMDOT(I)/0.0044)
      IF(XMDOT(I).LE.0.0002) A1=A1 + 0.015*12./3600.
      A2=0.0
      IF(XMDOT(I).LE.0.0044) A2=-CONLAT(I)/0.0044
      C1=1.+30.*XMDOT(I)*KCONV(I)
      C2=1/(64.4*778.)
      C3=2116/29.96
      C5=BETA*KW/(1055.*.5*1.023)
      DEL2=DEL/2.
C
C   XMDOT(I) UNCERTAINTY
C
      IF(CM(I).EQ.0.0) GO TO 150
      IF(PROT(I).LE.-0.1) M1=KFLOW(I)*2.01258
      IF(PROT(I).GT.-0.1) M1=(KFLOW(I)+KFUDGE(I))*2.01258
      M2=SQRT((PBAR+PROT(I)/25.4)*2116./29.96/(RM*TROTA*0.075))
      M3=WSTD(I)
      IF(CMFLAG.EQ.1) M4=.075/60.*(F6+F7*F8*COS(F8*(CM(I)-2.)))
```

```
      IF(CMFLAG.EQ.2) M4=.075/60.*(F2+F3*F4*COS(F4*CM(I)))
      IF(CMFLAG.EQ.3.AND.MASSK(I).EQ.1) M4=.075/60.*(F6+F7*F8*
     1    COS(F8*(CM(I)-2.)))
      IF(CMFLAG.EQ.3.AND.MASSK(I).EQ.2) M4=.075/60.*(F2+F3*F4*
     1  COS(F4*CM(I)))
      X1=DCM(I)*M1*M2*M4
      C6=M1*M3*C3/(2*M2*0.075*RM*TROTA)
      X2=DPBAR*C6
      X3=-DTROT*C6*(PBAR+PROT(I)/25.4)/TROTA
C
      DMDOT(I)=SQRT(X1**2+X2**2+X3**2)
      DMDOTN(I)=DMDOT(I)/XMDOT(I)*100.
C
  150 IF (CM(I).EQ.0.0) DMDOT(I)=0.0
      IF (CM(I).EQ.0.0) DMDOTN(I)=0.0
C
      II=2*I-1
C
C
C DTAVG UNCERTAINTY
C
      DTAVG=SQRT(11.*DTEMP**2)/5.
C
      IF(ENBLFG.EQ.1) GO TO 105
      IF(I.NE.1) GO TO 215
C
C DUG AND DUDX UNCERTAINTY
C
      DO 210 M=1,NPORT
C
      C4=SQRT(64.4*5.2*RM)
      N=C4*SQRT((PTOTAL-PSTAT(M))*(TGAS+460.))
      D=SQRT(C3*PBAR+5.2*PSTAT(M))
      U1=DPTOT*1/D*C4/2.*C4/N*(TGAS+460.)
      U2=DTGAS*1/D*C4/2.*C4/N*(PTOTAL-PSTAT(M))
      U3=-DPBAR*N/D**3*C3/2.
      U4=-DPSTAT(M)*(1/D*C4/2.*C4/N*(TGAS+460.)+N/D**3*5.2/2.)
C
      DV(M)=SQRT(U1**2+U2**2+U3**2+U4**2)
  210 CONTINUE
C
      DO 211 M=2,MNPORT
      N=12.*(V(M+1)-V(M-1))
      D=X(M+1)-X(M-1)
      DX1=DV(M+1)*12./D
      DX2=-DV(M-1)*12./D
      DX3=DXX*12.*N/D**2
C
      DDUDX(M)=SQRT(DX1**2+DX2**2+2.*DX3**2)
C
  211 CONTINUE
C
      N=12.*(V(2)-V(1))
      D=X(2)-X(1)
      DX11=DV(2)*12./D
      DX12=-DV(1)*12./D
      DX13=DXX*12.*N/D**2
C
      DDUDXS(1)=SQRT(DX11**2+DX12**2+2.*DX13**2)
C
      DUG(1)=DV(1)
```

```
      DUGND(1)=DUG(1)/UG(1)*100.
C
      DO 212 M=2,NPLATE
      MM=2*M-1
      DDUDXS(M)=DDUDX(MM)
      DUG(M)=DV(MM)
      DUGND(M)=DUG(M)/UG(M)*100.
  212 CONTINUE
  215 CONTINUE
C
C
C STANTON OR HTFRAC UNCERTAINTY - FOLLOWING MODES ARE CALCULATED AT GIVE
C STATEMENT NUMBER: BLOW-100, SUCK-200, IMPERMEABLE-300, SUCK ENBAL-400,
C BLOW ENBAL-500
C
  105 IF(CM(I).EQ.0.0) GO TO 300
      IF(PROT(I).LE.-0.1) GO TO 200
C
  100 IF(ENBLFG.EQ.1) GO TO 500
C
C  STANTON NUMBER - BLOWING
C
      N=ENDEN(I)-QRAD(I)-A1*(TAVG(I)-TBASE)-XMDOT(I)*(TAVG(I)-TT(I))*
     1  CP*C1
      D=(CP*(TT(I)+(TAVG(I)-TT(I))*C1-TGAS)-C2*UG(I)**2)*
     1    UG(I)*RHOG(II)
      B1=DWIND*C5/D
      B2=-DQRAD(I)/D
      B3=DTAVG*(-1/D*(A1+XMDOT(I)*CP*C1)+N/D**2*(UG(I)*RHOG(II)*CP*C1))
      B4=DTBASE*A1/D
      B5=DTT*(1/D*XMDOT(I)*CP*C1+N/D**2*CP*UG(I)*RHOG(II)*30.*XMDOT(I)*
     1    KCONV(I))
      B6=DTGAS*(N/D**2*(CP*UG(I)*RHOG(II) + D/(TGAS+460.)))
      B7=DMDOT(I)*(1/D*((TBASE-TAVG(I))*A2-(TAVG(I)-TT(I))*CP*(1.+
     1  60.*XMDOT(I)*KCONV(I)))-N/D**2*CP*UG(I)*RHOG(II)*30.*KCONV(I)*
     2  (TAVG(I)-TT(I)))
      B8=DUG(I)*(N/D**2*(2.*C2*UG(I)**2*RHOG(II)-D/UG(I)))
      B9=DPBAR*(-N/D**2*C3*D/(RHOG(II)*RM*(TGAS+460.)))
C
      DST(I)=SQRT(B1**2+B2**2+B3**2+B4**2+B5**2+B6**2+B7**2+B8**2+
     1   B9**2)
      DSTND(I)=DST(I)/ST(I)*100.
C
C UNCERTAINTY IN ISO
C
      XI1=DTT*CP*(1.-C1)
      XI2=DTAVG*CP*C1
      XI3=-DTGAS*CP
      XI4=-DUG(I)*2.*C2*UG(I)
      XI5=DMDOT(I)*CP*(TAVG(I)-TT(I))*30.*KCONV(I)

      DISO(I)=SQRT(XI1**2+XI2**2+XI3**2+XI4**2+XI5**2)
C
      GO TO 600
C
C  STANTON NUMBER - IMPERMEABLE
C
  300 N=ENDEN(I)-QRAD(I)-A1*(TAVG(I)-TBASE)
      D=(CP*(TAVG(I)-TGAS)-C2*UG(I)*UG(I))*UG(I)*RHOG(II)
      B1=DWIND*C5/D
      B2=-DQRAD(I)/D
```

```
      B3=-DTAVG*(A1/D+N/D**2*CP*UG(I)*RHOG(II))
      B4=DTBASE*A1/D
      B6=DTGAS*(N/D**2*(CP*UG(I)*RHOG(II) + D/(TGAS+460.)))
      B8=DUG(I)*(N/D**2*(2.*C2*UG(I)**2*RHOG(II)-D/UG(I)))
      B9=DPBAR*(-N/D**2*C3*D/(RHOG(II)*RM*(TGAS+460.)))
C
      DST(I)=SQRT(B1**2+B2**2+B3**2+B4**2+B6**2+B8**2+B9**2)
      DSTND(I)=DST(I)/ST(I)*100.
C
C UNCERTAINTY IN ISO
C
      XI1=DTAVG*CP
      XI2=-DTGAS*CP
      XI3=-DUG(I)*2.*C2*UG(I)

      DISO(I)=SQRT(XI1**2+XI2**2+XI3**2)
C
      GO TO 600
C
C  STANTON NUMBER - SUCKING
C
  200 IF(ENBLFG.EQ.1) GO TO 400
      N=ENDEN(I)-QRAD(I)-A1*(TAVG(I)-TBASE)-0.0264*XMDOT(I)*WIND(I)*CP
      D=UG(I)*RHOG(II)*(CP*(TAVG(I)-0.0044*WIND(I)-TGAS)-C2*UG(I)*UG(I))
      B1=DWIND*(1/D*(C5-.0264*XMDOT(I)*CP)+N/D**2*CP*UG(I)*RHOG(II)
     1  *0.0044)
      B2=-DQRAD(I)/D
      B3=-DTAVG*(1/D*A1+N/D**2*CP*UG(I)*RHOG(II))
      B4=DTBASE*A1/D
      B6=DTGAS*(N/D**2*(CP*UG(I)*RHOG(II) + D/(TGAS+460.)))
      B7=DMDOT(I)*(1/D*((TBASE-TAVG(I))*A2-.0264*WIND(I)*CP))
      B8=DUG(I)*(N/D**2*(2.*C2*UG(I)**2*RHOG(II)-D/UG(I)))
      B9=DPBAR*(-N/D**2*C3*D/(RHOG(II)*RM*(TGAS+460.)))
      DST(I)=SQRT(B1**2+B2**2+B3**2+B4**2+B6**2+B7**2+B8**2+B9**2)
      DSTND(I)=DST(I)/ST(I)*100.
C
C UNCERTAINTY IN ISO
C
      XI1=DTAVG*CP
      XI2=-DTGAS*CP
      XI3=-DUG(I)*2.*C2*UG(I)
      XI4=-DWIND*CP*.0044

      DISO(I)=SQRT(XI1**2+XI2**2+XI3**2+XI4**2)
C
      GO TO 600
C
C  HTFRAC - SUCKING ENERGY BALANCE
C
  400 N=XMDOT(I)*CP*(TAVG(I)+.022*WIND(I)-TGAS)*100.
      D=ENDEN(I)-QRAD(I)-A1*(TAVG(I)-TBASE)
      B1=DWIND*((-N/D**2)*C5+.022*XMDOT(I)*CP*100./D)
      B2=DQRAD(I)*N/D**2
      B3=DTAVG*(A1*N/D**2+XMDOT(I)*CP*100./D)
      B4=DTBASE*(-A1*N/D**2)
      B7=DMDOT(I)*(N/(D*XMDOT(I))+N/D**2*(TAVG(I)-TBASE)*A2)
      B6 =-DTGAS*1./D*XMDOT(I)*CP*100.
C
      DHTF(I)=SQRT(B1**2+B2**2+B3**2+B4**2+B6**2+B7**2)
      GO TO 800
C
```

```
C  HTFRAC - BLOWING ENERGY BALANCE
C
  500 NN=XMDOT(I)*CP*C1*100.
      N=NN*(TT(I)-TAVG(I))
      D=ENDEN(I)-QRAD(I)-A1*(TAVG(I)-TBASE)
      B1=DWIND*(-N/D**2)*C5
      B2=DQRAD(I)*N/D**2
      B3=DTAVG*(1/D*(-NN)+N/D**2*A1)
      B4=DTBASE*(-A1*N/D**2)
      B7=DMDOT(I)*(1/D*(N/XMDOT(I)+XMDOT(I)*(TT(I)-TAVG(I))*CP*30.*
     1  KCONV(I))+N/D**2*(TAVG(I)-TBASE)*A2)
      B10=DTT*(1/D*NN)
C
      DHTF(I)=SQRT(B1**2+B2**2+B3**2+B4**2+B7**2+B10**2)
      GO TO 800
  600 CONTINUE
C
C     RHOG(II) UNCERTAINTY
C
      N=C3*PBAR+5.2*PSTAT(II)
      D=RM*(TGAS+460.)
      R1=DPBAR*C3*1/D
      R2=DPSTAT(II)*5.2*1/D
      R3=-DTGAS*N/D**2*RM
C
      DRHOG(I)=SQRT(R1**2+R2**2+R3**2)
C
C     B UNCERTAINTY
C
      IF(CM(I).EQ.0.0) GO TO 151
      BB1=DMDOT(I)*1/(UG(I)*RHOG(II)*ST(I))
      BB2=-DUG(I)*BB(I)/UG(I)
      BB3=-DRHOG(I)*BB(I)/RHOG(II)
      BB4=-DST(I)*BB(I)/ST(I)
C
      DB(I)=SQRT(BB1**2+BB2**2+BB3**2+BB4**2)
      DBND(I)=DB(I)/BB(I)*100.
C
C
C     F UNCERTAINTY
C
      FF1=DMDOT(I)*1/(UG(I)*RHOG(II))
      FF2=-DUG(I)*F(I)/UG(I)
      FF3=-DRHOG(I)*F(I)/RHOG(II)
C
      DF(I)=SQRT(FF1**2+FF2**2+FF3**2)
      DFND(I)=DF(I)/ABS(F(I))*100.
C
  151 IF(CM(I).NE.0.0) GO TO 152
      DB(I)=0.0
      DBND(I)=0.0
      DF(I)=0.0
      DFND(I)=0.0
  152 CONTINUE
C
C
C  VISCGS  UNCERTAINTY
C
      DMU=DMUP*VISCG(II)*RHOG(II)/100.
      N=11.*RM*TGAS + .0175*RM*TGAS**2
      D=1.E06*(C3*PBAR + 5.2*PSTAT(II))
```

```
      V1=-DPBAR*N/D**2*C3*1.E06
      V2=-DPSTAT(I)*N/D**2*5.2*1.E06
      V3=DTGAS*1/D*(11.*RM+ .35*RM*TGAS)
      V4=DMU*1/RHOG(II)
C
      DVISCG(I)=SQRT(V1**2 + V2**2 + V3**2 + V4**2)
C
  120 CONTINUE
  800 RETURN
      END
C
C
C
C
      SUBROUTINE UNCER
C
C
      REAL KCOND(24),KCONV(24),KFLOW(24),KFUDGE(24),KPROP,KS(24),
     1     KV(48),KW,MA,MDOT(24),MV,NPWR,ISO(24)
      REAL M1,M2,M3,M4,N,NN,SUM(24),DSUM(24)
C
      INTEGER CMFLAG,DATE,ENBLFG,RUN,TITLE(18)
C
      COMMON /A/ AR,BETA,B1T1,B3T3,CMFLAG,COEF1,COEF23,CP,DATE,DEN,
     1  ENBLFG,E1,E2,EMISS,EPS,ER1,ER2,ER3,F12,F13,F22,I,INSTOT,J,KCOND,
     2    KCONV,KFLOW,KFUDGE,KPROP,KS,KV,KW,KLM,MA,MDOT,MV,NPWR,NPLATE,
     3    NSTAT,P,PBAR,PROTA, DELP ,PVAP,Q1,Q2,Q3,QHEAT,
     4    QHEATA,QHTA,QLOSS,RA,RCF,REPS,RHOA,RHOH,RHOL,RHOV,RHOZRO,RUN,
     5    RH1,RH2,RH3,RHUM,RM,T,TAMB,TBASE,TCOV,TGAS,TROT,
     6    TROTA,T1,T2,T3,VAPH,VAPL,VEPS,WCORR,WSCALE,WSTDI,
     7  ISO,REENCP(24),ENTHCP(24),ENTHZR,
     8    AREA(24),BB(24),CFHT(24),CM(24),CONLAT(24),DELH(25),
     9    DELTAT(24),DUDX(48),DUDXS(24),ECONV(24),ED(24),ENDEN(24),
     1    ENNET(24),EO(24),ENTH(24),ET(24),EU(24),F(24),GS(24),H(24),
     2    HTFRAC(24),HTRANS(24),INSTK(48),MASSK(24),PK(48),
     A    PROT(24),PROTAB(24),PSAT(9),PSTAT(48),QCOND(24),
     3    QRAD(24),REENTH(24),REENW(25),RHOG(48),
     4    RHOSAT(9),ST(24),STCP(24),TAVG(24),TEMP(9),TIME60(48),
     5    TO(24),TOEFF(24),TD(24),TITLE,TT(24),TU(24),V(48),
     6    VISCG(48),VISCGS(24),UG(24),VZERO(24),WACT(24),WIND(24),
     7    WNET(24),WSTD(24),X(48),XS(24),XSTCP(24),XMDOT(24)
      COMMON /B/ DCMP,DDELP,DPAMB,DP5HI,DP5LO,DP97HI,DP97LO,DQRADP,
     1          DTEMPA,DTEMPP,DTBASE,DTT,DTROT,DTGAS,DWIND,DXX,F2,F3,F4,
     2            F6,F7,F8,DEL,DDUDXS(24),DISO(24),DENZRP,
     3            DB(24),DBND(24),DCM(24),DDL2(24),DDL2ND(24),DF(24),
     4            DFND(24),DHTF(24),DMDOT(24),DMDOTN(24),DPSTAT(48),
     5            DQRAD(24),DRE(24),DREND(24),DRHOG(24),DST(24),
     6            DSTND(24),DUG(24),DUGND(24),DV(48),DDUDX(48),
     7            CLR1(24),CLR2(24),CLR3(24),CLR4(24),CSR1(24),
     8            CSR2(24),CSR3(24),DVISCG(24),DEL2,DMUP,MNPLAT,
     9             D97MIN,D97MAX,D5MIN,D5MAX,PTOTAL,NPORT,MNPORT
C
      DENZR=DENZRP*ENTHZR/100.
C
C UNCERTAINTY CALCULATION FOR ENTH AND REENTH
C
C
C SUM(1) IS UNDEFINED, BY SET TO ZERO HERE FOR COMPUTATIONAL EASE.
C
      SUM(1)=0.0
      DSUM(1)=0.0
```

```
      START=ENTHZR*UG(1)*ISO(1)
      DSTART=SQRT((DENZR*UG(1)*ISO(1))**2 + (DUG(1)*ENTHZR*ISO(1))**2
     1  + (DISO(1)*ENTHZR*UG(1))**2)
C
      DO 100 I=2,NPLATE
      SUM(I)=SUM(I-1) + 1./3.*UG(I-1)*ISO(I-1)*(ST(I-1)+F(I-1))
      DSUM(I)=SQRT(DSUM(I-1)*DSUM(I-1) + 1./9.*((DUG(I-1)*ISO(I-1)*
     1  (ST(I-1)+F(I-1)))**2 + (DISO(I-1)*UG(I-1)*(ST(I-1)+F(I-1)))**2
     2  + (ISO(I-1)*UG(I-1))**2*(DST(I-1)*DST(I-1)+DF(I-1)*DF(I-1))))
  100 CONTINUE
C
      D1=DENZR
      D5=DST(1)/6.
      D6=DF(1)/6.
C
      DDL2(1)=SQRT(D1*D1+D5*D5+D6*D6)
      DDL2ND(1)=DDL2(1)/ENTH(1)*100.
C
      R1=DENZR*UG(1)/VISCGS(1)
      R3=-DVISCG(1)/(VISCGS(1)*VISCGS(1))*( ENTHZR*UG(1) +
     1  1./6.*UG(1)*(ST(1)+F(1)))
      R4=DUG(1)*(1./6.*(ST(1)+F(1))/VISCGS(1)+ ENTHZR/VISCGS(1))
      R6=DST(1)*UG(1)/(6.*VISCGS(1))
      R7=DF(1)*UG(1)/(6.*VISCGS(1))
C
      DRE(1)=SQRT(R1*R1+R3*R3+R4*R4+R6*R6+R7*R7)
      DREND(1)=DRE(1)/REENTH(1)*100.
C
      DO 110 I=2,NPLATE
        D1=DSTART/(UG(I)*ISO(I))
        D2=DSUM(I)/(UG(I)*ISO(I))
        D3=-DUG(I)*(SUM(I)+START)/(UG(I)*UG(I)*ISO(I))
        D4=-DISO(I)*(SUM(I)+START)/(UG(I)*ISO(I)*ISO(I))
        D5=DST(I)/6.
        D6=DF(I)/6.
C
        DDL2(I)=SQRT(D1*D1+D2*D2+D3*D3+D4*D4+D5*D5+D6*D6)
        DDL2ND(I)=DDL2(I)/ENTH(I)*100.
C
      R1=DSTART/(VISCGS(I)*ISO(I))
      R2=DSUM(I)/(VISCGS(I)*ISO(I))
      R3=-DVISCG(I)/(VISCGS(I)*VISCGS(I))*((START+SUM(I))/ISO(I) +
     1  1./6.*UG(I)*(ST(I)+F(I)))
      R4=DUG(I)*1./6.*(ST(I)+F(I))/VISCGS(I)
      R5=-DISO(I)/(VISCGS(I)*ISO(I)*ISO(I))*(START+SUM(I))
      R6=DST(I)*UG(I)/(6.*VISCGS(I))
      R7=DF(I)*UG(I)/(6.*VISCGS(I))
C
      DRE(I)=SQRT(R1*R1+R2*R2+R3*R3+R4*R4+R5*R5+R6*R6+R7*R7)
      DREND(I)=DRE(I)/REENTH(I)*100.
C
  110 CONTINUE
  800 RETURN
      END
C
C
```

PROFILE PROGRAM

```
C
C
C     TEMPERATURE PROFILE PROGRAM :  THE RAW TEMPERATURE PROFILE DATA ARE
C     UTILIZED TO CALCULATE TEMPERATURE VERSUS DISTANCE IN VARIOUS DIMENS
C     AND NON-DIMENSIONAL COORDINATES.  THESE PROFILES ARE INTEGRATED, ALO
C     WITH THE VELOCITY RESULTS CALCULATED BY ANOTHER PROGRAM, TO
C     OBTAIN ENTHALPY THICKNESS AND THUS ENTHALPY THICKNESS REYNOLDS NO.
C
C     THE LATEST COMPILATION OF THIS PROGRAM WAS 120169.
C
C
      COMMON  AREA(60),AREAD(60),AREAM(60),CF2(10),DP(60),DDELT1(10),
     1   DDELT2(10),DELM(10),DELMCM(10),DELTA2(10),DFV(10),DKV(10),
     2  DHV(10),DIMT(60),DIMYH(60),DIMYM(60),DISPL(60),DREMOM(10),
     3   DUV(10,60),DUUG(10,60),H(10),IS,KEYREF(10),NTPTS(10),NVPTS(10),
     4  PBAR(10),PR(10),PSTAT(10),REDEL(24),REENTH(10),REMOM(10),RC(10),
     5   RHUM(10),ST(10),STN(24),T(60),TAMB(10),TR(60),DREENT(10),
     6   TBAR(60),TD(10),TEMP(60),TGAST(10),TIME60(10,60),
     7   TITLE(18),TMV(10,60),TO(10),TPLATE(10),TPLUS(60),
     8   TU(10),TX(10),U(60),UINFT(10),UINFV(10),UPLUS(60),UUG(10,60),
     9   UUGNEW(60),UV(10,60),U2(60),VDELT1(10),VDELT2(10),VF(10),
     1   VH(10),VK(10),VMDOT(10),VREMCM(10),VREX(10),VVZERO(10),VX(10),
     2 VYDEL(10,60),X(10),YPLUS(60),YRAWT(10,60),YTMP(60),YVEL(10,60)
     3  ,UTAU(60),DELH(10),IBAR,PER1(24),RE1(24),CP(60),ENTH(24)
      COMMON /A/ DUUGNW(60),DUVNW(60),RHOG(60),VISCO(60),DCF2(10),
     1        DDIMT(60),DYPLUS(60),DUPLUS(60),DTPLUS(60),
     2        IDELH,DDELH(10),Z(60),DZ(60),C1,RM,N,PSAT,RHOSAT,TEMPS
     3        ,DST(10),DAREA(60),DDIMYH(60),DYPLND(60),DUPLND(60),
     4        DTPLND(60),DYND(60),DUUGND(60),DTND(60),DDELTA(10),
     5        DELY,DTEMPA,DPAMB,DMUF,NNTPTS,DDELND(10),DREND(10),
     6          DTEMP(60),DVISCO(60),DIMYHP(10,60),DIMTP(10,60),
     7          YPLUSP(10,60),TPLUSP(10,60),ENTHNW(24),DPRTMP
C
C
      INTEGER VDATE(10),VRUN(10),TDATE(10),TRUN(10),VTRAV(10),PLATE(10),
     1 PTITLE(4,60),XLABEL(4,40),YLABEL(4,40),R,XTYPE(4),YTYPE(4),
     2 XTEN(4),YTEN(4),L2(13),LL2(4,13),N1(60),N5(40),N6(40),N18(13)
C
      REAL IS(60),PSAT(9),RHOSAT(9),TEMPS(9),IBAR(60),XLENGT(4),
     1  YLENGT(4),XZERO(4),XEND(4),X1(4),YZERO(4),YEND(4),Y1(4),
     2 XX(13,50),YY(13,50)
C
C
C
C
    1 FORMAT(2F10.0,F3.0)
    2 FORMAT(I1,9X,I6,4X,I1,9X,F10.0,I2,8X,3F10.0)
    3 FORMAT(18A4,2X,I1)
    6 FORMAT(F10.0,I1,1X,I1,1X,I2)
   16 FORMAT(8F10.0)
  530 FORMAT(I6,I1,I1,F6.3,E10.4,F8.5,F7.3,F7.4,F8.5,E9.3,15X,I2)
  531 FORMAT(3F8.6,F8.2,F8.6)
  533 FORMAT(/4E9.3,E8.2,E9.3)
  534 FORMAT(2XF6.4,F8.4,F8.5,F8.6,32X,2F8.5)
  889 FORMAT(1H1)
  905 FORMAT(5X'PROBE THERMOCOUPLE REFERENCED TO FREE STREAM'/)
  906 FORMAT(5X'PROBE THERMOCOUPLE REFERENCED TO ICE'/)
  900 FORMAT(30X'INPUT SECTION'40X                '(THIS PROGRAM WAS COMPIL
     1ED ON 120169)'///,10X,18A4// 5X'THERMOCOUPLE PROBE HEIGHT='F5.3,
     210X,'NUMBER OF TRAVERSES='I2///)
```

```
  901 FORMAT(//5X'TRAVERSE   ','RUN   ',4X,
     1'POSITION   ','NO. OF POINTS   ','UINF'4X'STANTON NO.'3X
     2 'ST.NO.UNCERTAINTY'/7X12,
     3  5X,I6,'-',I1,4X,F7.2,7X,I2,9XF5.1,6XF7.5,10XF7.5)
  902 FORMAT(/4X,'  TO     TU     TD     TGAS     TAMB    '5X,'PSTAT',
     1  2X'   RHUM    PBAR '/ 5XF5.3,1XF5.3,1XF5.3,2XF5.3,1XF7.3,1X,
     2      5XF7.4,2XF5.2,2XF6.2//)
  903 FORMAT( 18X'INTEGRATED'/,
     1        5X'MICROMETER','   VOLTAGE(MV)     COUNTER ')
  904 FORMAT(8XF5.3,7XF6.3,8XF5.0)
  915 FORMAT(7(1X,3(F7.5,F6.0,F6.4,1X)/),1X,3(F7.5,F6.0,F6.4,1X))
  950 FORMAT(1H1///45X'VELOCITY INPUT DATA'/)
  951 FORMAT(5X'TRAVERSE   RUN   POSITION  NO. OF POINTS  '3X'CF/2'6X,
     1   'UINF      K     ',
     2'      F  '4X'MDOT     VZERO     REX'/7X,I2,4X,I6,'-',I1,2XF5.2,8X,I2,
     3  11XF7.5,3X,  F5.1,1XE10.3,2XF6.3,2XF6.3,2XF5.2,2XE9.3//)
  952 FORMAT(2X, 87H  0.99  DISPLACEMENT MOMENTUM    H   MOMENTUM
     1                      UNCERTAINTIES      /
     2      2X,  116H  POINT  THICKNESS   THICKNESS          RE
     3  K           F        DISP.THK.    MOM.THK.       H        MOM.RE.   ,
     4 3X'CF/2'/
     5 4XF5.3,3XF5.3,7XF5.3,4XF5.2,F8.2,4X,3(2XE9.3),1X3(2XE9.3),3XF7.5,
     6  //)
  953 FORMAT(50X'UNCERTAINTIES'/5X'Y'10X'U'6X'Y/DELTA'4X'U/UINF'8X
     1  'L/UINF'8X'U')
  954 FORMAT(2XF6.4,3XF8.4,3XF8.5,3XF8.6,3X,2(3XF8.5))
  956 FORMAT(///30X'TEMPERATURE INPUT DATA'/)
  958 FORMAT(///5X'CF/2 QUOTED ABOVE IS CALCULATED FROM STANTON NUMBER V
     1IA REYNOLDS ANALOGY')
  959 FORMAT(///5X'CF/2 QUOTED ABOVE IS BEST ESTIMATE FROM HYDRODYNAMIC
     1DATA')
C
C    INPUTS HERE
C
C
C READ UNCERTAINTY INTERVALS
C
      READ(5,3620) DTEMPA,DPRTMP,DPAMB,DMUP,DELY
 3620 FORMAT(6F10.0)
C
      WRITE(6,889)
C
C NRUNS - # OF COMPLETE TEST RUNS
C NTRAV - # OF TRAVERSES PER TEST RUN
C IPUNCH: 0 - NO PUNCH     1 - PUNCH
C
      READ(5,6) TPRBHT,NRUNS,IPUNCH,NPL
      IF(NPL.EQ.0) NPL=24
C
C
      DO 550 LOOP=1,NRUNS
C
C
      READ(5,3) TITLE,NTRAV
      WRITE(6,900) TITLE,TPRBHT,NTRAV
C
C
C
C ALL TEMPERATURE DATA IS READ IN THE 4000 LOOP
C
  156 DO 4000 N=1,NTRAV
```

```
C
C    USE KEYREF =1 IF TMV IS REFERENCED TO TICE(32 F)
C    USE KEYREF =0 IF TMV IS REFERENCED TO TGAS
C
      READ(5,2) KEYREF(N),TDATE(N),TRUN(N),TX(N),NTPTS(N),UINFT(N),
     1  ST(N),DST(N)
      IF(N.EQ.1) WRITE(6,956)
      IF(N.GT.1) WRITE(6,889)
      WRITE(6,901) N,TDATE(N),TRUN(N),TX(N),NTPTS(N),UINFT(N),
     1 ST(N),DST(N)
      READ(5,16) TO(N),TU(N),TD(N),TGAST(N),TAMB(N),PSTAT(N),RHUM(N),
     1     PBAR(N)
      WRITE(6,902)TO(N),TU(N),TD(N),TGAST(N),TAMB(N),PSTAT(N),RHUM(N),
     1     PBAR(N)
      NNTPTS=NTPTS(N)+1
      IF(KEYREF(N).EQ.0) WRITE (6,905)
      IF(KEYREF(N).EQ.1) WRITE (6,906)
      WRITE (6,903)
      DO 350 I=2,NNTPTS
      READ(5,1) YRAWT(N,I),TMV(N,I),TIME60(N,I)
      WRITE(6,904) YRAWT(N,I),TMV(N,I),TIME60(N,I)
  350 CONTINUE
 4000 CONTINUE
C
C ALL VELOCITY DATA IS READ IN 4001 LOOP
C
      WRITE(6,950)
      DO 4001 N=1,NTRAV
C
C  READ IN BLANK CARD HERE UNTIL FINAL CF/2 IS AVAILABLE
C  FROM HYDRODYNAMIC RESULTS
C
      READ(5,16) CF2(N),DCF2(N)
      DUMMY=CF2(N)
      IF(CF2(N).EQ.0.0) CF2(N)=ST(N)/1.16
      IF(DCF2(N).EQ.0.0) DCF2(N)=0.1*CF2(N)
C
      READ(5,530) VDATE(N),VRUN(N),VTRAV(N),VX(N),VK(N),VF(N),UINFV(N),
     1 VMDOT(N),VVZERO(N),VREX(N),NVPTS(N)
      IF(N.GT.1) WRITE (6,889)
      WRITE(6,951) VTRAV(N),VDATE(N),VRUN(N),VX(N),NVPTS(N),CF2(N),
     1     UINFV(N),VK(N),VF(N),VMDOT(N),VVZERO(N),VREX(N)
      READ(5,531) VDELT1(N),VDELT2(N),VH(N),VREMOM(N),DELM(N)
C
C  UNCERTAINTY DATA CALCULATED BY VELOCITY PROGRAM
C
      READ(5,533) DKV(N),DFV(N),DDELT1(N),DDELT2(N),DHV(N),
     1  DREMOM(N)
      WRITE(6,952) DELM(N),VDELT1(N),VDELT2(N),VH(N),VREMOM(N),DKV(N),
     1             DFV(N),DDELT1(N),DDELT2(N),DHV(N),DREMOM(N),DCF2(N)
C
      NNVPTS=NVPTS(N)+1
      WRITE(6,953)
      DO 800 J=2,NNVPTS
          READ(5,534) YVEL(N,J),UV(N,J),VYDEL(N,J),UUG(N,J),
     1    DUUG(N,J),DUV(N,J)
      WRITE(6,954) YVEL(N,J),UV(N,J),VYDEL(N,J),UUG(N,J),DUUG(N,J),
     1DUV(N,J)
  800 CONTINUE
      IF(DUMMY.EQ.0.0) WRITE(6,958)
      IF(DUMMY.GT.0.0) WRITE(6,959)
```

```
C
 4CC1 CONTINUE
C
C EACH TRAVERSE IS COMPUTED IN 75 LOOP
C
      DO 75 N = 1,NTRAV
C
C
      NNTPTS=NTPTS(N)+1
      NNVPTS=NVPTS(N)+1
      PR(N)=0.705
      RC(N) = PR(N)**.333
 1004 P = PBAR(N)*2116./29.96+PSTAT(N)*5.2
C
C   MILLIVOLT CONVERSION
C
      IF(TAMB(N).LT.10.) TAMB(N)=TCALIB(TAMB(N))
      IF(TU(N).EQ.0.0) TU(N)=TO(N)
      IF(TD(N).EQ.0.0) TD(N)=TU(N)
      TMVWAL=(3.*TO(N)+TU(N)+TD(N))/5.
      TPLATE(N)=TCALIB(TMVWAL)
   46 TMVGAS=TGAST(N)
      TGAST(N)=TCALIB(TGAST(N))
C
C     TEMPERATURE DEPENDENT PROPERTY CORRECTIONS
C
 1005 DO 44 NN=1,9
  44  IF(TEMPS(NN).GT.TAMB(N)) GO TO 45
  45  M = NN-1
      RHOV = RHOSAT(M) + (TAMB(N)-TEMPS(M))*(RHOSAT(NN)-RHOSAT(M))/10.0
      PVAP=RHUM(N)*(PSAT(M)+(TAMB(N)-TEMPS(M))*(PSAT(NN)-PSAT(M))/10.0)
      RHOA = (P-PVAP)/(53.3*(TAMB(N)+460.0)) + (RHUM(N)*RHOV)
      ZMV = RHUM(N)*RHOV/RHOA
      ZMA = 1.0 - ZMV
      RM = 1545.0*(ZMA/28.9 + ZMV/18.0)
C
C
C  SETTING INITIAL CONDITIONS
C
      YTMP(1)=0.0
      T(1)=TPLATE(N)
      TIME60(N,1)=0.0
      YVEL(N,1) = 0.0
      UUG(N,1) = 0.0
      DUUG(N,1)=0.0
      DUV(N,1)=0.0
C
C  TIME60=600 IS EQUIVALENT TO 10 SECONDS OF MV INTEGRATION
C
C    THE 1633 LOOP DETERMINES THERMOCOUPLE READING AND Y POSITION
C    AT EACH DATA POINT
C
 1009 DO 1633 I=2,NNTPTS
      IF(TIME60(N,I).LE.0.0) GO TO 1011
      CONST=60.
      TMV(N,I)=CONST/TIME60(N,I)*TMV(N,I)
 1011 KEY=KEYREF(N)+1
C
C GO TO (TGAS, ICE) REFERENCE
C
      GO TO (1001,1003),KEY
```

```
C
C   TMVGAS IS ADDED ONTO TEMP DIFFERENCE READING TO CONVERT TO DEGREES
C   IN THE PROPER RANGE OF THE MV-F TABLES.
C
 1001 TMV(N,I)=TMV(N,I)+TMVGAS
C
C   T(I) IS THE TEMPERATURE IN DEGREES RECORDED BY THE THERMOCOUPLE
C
 1003 T(I)=TCALIB(TMV(N,I))
C
C THE Y POSITION IS CORRECTED FOR PROBE HEIGHT AND MICROMETER SETTING
C
      IF(I.NE.1) YTMP(I) = YRAWT(N,I) - YRAWT(N,2) + 0.5*TPRBHT
 1633 CONTINUE
C
C     USING COLD WALL VELOCITY DATA
C
C
      IF(UINFT(N).EQ.0.0) UINFT(N)=UINFV(N)
      IF(TX(N).EQ.0.0) TX(N)=VX(N)
C
C
C THE FOLLOWING CODE ENSURES THAT THE LAST VELOCITY Y IS
C GREATER THAN THE LAST THERMAL Y
C
      IF(YTMP(NNTPTS).LT.YVEL(N,NNVPTS)) GO TO 1006
      NNVPTS=NNVPTS+1
      YVEL(N,NNVPTS)=1.1*YTMP(NNTPTS)
      UUG(N,NNVPTS)=UUG(N,NNVPTS-1)
      DUUG(N,NNVPTS)=DUUG(N,NNVPTS-1)
      DUV(N,NNVPTS)=DUV(N,NNVPTS-1)
C
C VELOCITY INTERPOLATION TO FIT Y STATIONS WHERE TEMPERATURE DATA WAS
C TAKEN
C
 1006 DO 40 I=1,NNTPTS
          DO 37 J=1,NNVPTS
          IF(YVEL(N,J)-YTMP(I)) 37,38,39
   39     UUGNEW(I)=UUG(N,J-1)+(YTMP(I)-YVEL(N,J-1))/(YVEL(N,J)-
     1    YVEL(N,J-1))*(UUG(N,J)-UUG(N,J-1))
          DUUGNW(I)=DUUG(N,J-1)+(YTMP(I)-YVEL(N,J-1))/(YVEL(N,J)-
     1    YVEL(N,J-1))*(DUUG(N,J)-DUUG(N,J-1))
          DUVNW(I)=DUV(N,J-1)+(YTMP(I)-YVEL(N,J-1))/(YVEL(N,J)-
     1    YVEL(N,J-1))*(DUV(N,J)-DUV(N,J-1))
          GO TO 36
   38     UUGNEW(I)=UUG(N,J)
          DUUGNW(I)=DUUG(N,J)
          DUVNW(I)=DUV(N,J)
          GO TO 36
   37     CONTINUE
   36 U2(I)=UUGNEW(I)*UUGNEW(I)*UINFT(N)*UINFT(N)
C
C THE ASSUMPTION IN USING COLD WALL VELOCITY PROFILES WITH HOT
C WALL TEMPERATURE PROFILES IS THAT U/UINF VERSUS Y/DELTA IS PRESERVED.
C SEE W.H.THIELBAHR THESIS FOR DISCUSSION OF THIS POINT.  WHEN COMPARING
C INTERPOLATED VELOCITIES TO VELOCITY INPUT, RECALL THAT UINF(TEMP) IS
C NOT NECESSARILY EXACTLY EQUAL TO UINF(VEL).
C
      CP(I)=.24
      C1=1./(2.*32.17*778.16)
      TEMP(I)=T(I)-RC(N)*C1/CP(I)*U2(I)
```

```
      RHOG(I)=P/(RM*(TEMP(I)+460.))
      VISCO(I)=(11.0 + 0.0175*TEMP(I))/(1000000.*RHOG(I))
   40 CONTINUE
C
C
C  THE 450 LOOP FINDS STAGNATION ENTHALPY REFERENCED TO FREE STREAM AFTER
C  FIRST DETERMINING STATIC TEMPERATURE FROM THE THERMOCOUPLE READING
C  VIA A RECOVERY FACTOR RELATIONSHIP.  THE NEED EXISTS TO EXAMINE THE
C  RECOVERY FACTOR USED HERE.
C
C   IT IS VERY DIFFICULT TO MAINTAIN A CONSTANT FREE STREAM TEMPERATURE
C  CONDITION DURING A TEST RUN.  WHEN THE PROBE TEMPERATURE IS REFERENCED
C  TO ICE, AND TGAS HAS CHANGED SLIGHTLY, AN ERROR IS INTRODUCED INTO
C  THE STAGNATION ENTHALPY COMPUTATION BECAUSE A CONSTANT TGAS IS FED
C  INTO THIS PROGRAM.  AN ALTERNATIVE TESTING TECHNIQUE IS TO REFERENCE
C  TO TGAS AND WORK WITH THE MEASURED TEMPERATURE DIFFERENCE. IN THE
C  PROFILE CALCULATIONS, THE LAST POINT IS TAKEN AS THE GAS TEMPERATURE.
C
C  T(I)-THERMOCOUPLE TEMPERATURE
C  TEMP(I)-STATIC TEMPERATURE
C  IS(I)- STAGNATION ENTHALPY REFERENCED TO FREE STREAM
C  TBAR-    (T-TGAS)/(TWALL-TGAS)
C  DIMT-    (TWALL-T)/(TWALL-TGAS) = 1 - TBAR
C
      DO 450 I=1,NNTPTS
      IS(I)=(CP(I)*TEMP(I)  +  U2(I)*C1) -  (CP(NNTPTS)*TEMP(NNTPTS
     1    )  +  U2(NNTPTS)*C1)
  450 CONTINUE
C
C
C     INTEGRAL PARAMETER CALCULATIONS
C
C
C  AREA-ENTHALPY THICKNESS
C  AREAM-MOMENTUM THICKNESS
C  AREAD-DISPLACEMENT THICKNESS
C
      AREA(1) = 0.0
      AREAM(1) = 0.0
      AREAD(1) = 0.0
      DO 70 I=1,NNTPTS
      IBAR(I)=IS(I)/IS(1)
      TBAR(I)=(TEMP(I)-TEMP(NNTPTS))/(TPLATE(N)-TEMP(NNTPTS))
      DIMT(I)=1.-TBAR(I)
      DIMTP(N,I) = DIMT(I)
      TR(I)=(TEMP(NNTPTS)+460.)/(TEMP(I)+460.)
      IF(I.EQ.1) GO TO 70
      AREA(I)=0.5*(YTMP(I)-YTMP(I-1))*(UUGNEW(I-1)*IBAR(I-1)
     1*TR(I-1)+UUGNEW(I)*IBAR(I)*TR(I))    + AREA(I-1)
      AREAM(I) = 0.5*(YTMP(I)-YTMP(I-1))*(UUGNEW(I-1)*(1.0-UUGNEW(
     1I-1))*TR(I-1)+UUGNEW(I)*(1.0-UUGNEW(I))*TR(I))  + AREAM(I-1)
      AREAD(I)=0.5*(YTMP(I) - YTMP(I-1))*((1.-UUGNEW(I-1)*TR(I-1))
     1+ (1. - UUGNEW(I)*TR(I))) + AREAD(I-1)
   70 CONTINUE
      DELTA2(N)= AREA(NNTPTS)
      DELMOM(N) = AREAM(NNTPTS)
      DISPL(N) = AREAD(NNTPTS)
      REMOM(N) = UINFT(N)*DELMOM(N)/(VISCO(NNTPTS)*12.0)
      REENTH(N) = UINFT(N)*DELTA2(N)/(VISCO(NNTPTS)*12.0)
      H(N) = DISPL(N)/DELMOM(N)
```

```
C  THERMAL BOUNDARY LAYER THICKNESS
C
      DO 72 I=10,NNTPTS
      IF(DIMT(I).GE.0.99) GO TO 173
   72 CONTINUE
  173 DELH(N)=YTMP(I-1) +(0.99-DIMT(I-1))/(DIMT(I)-DIMT(I-1))*
     1    (YTMP(I)-YTMP(I-1))
      IDELH=I
C
C  THERMAL AND HYDRODYNAMIC Y/B.L. THICKNESS
C
C
      DO 210 I=1,NNTPTS
      DIMYM(I)=YTMP(I)/DELM(N)
      DIMYH(I) = YTMP(I)/DELH(N)
  210 DIMYHP(N,I) = DIMYH(I)
C
C     CALCULATION OF + PARAMETERS
C
C UTAU IS BASED ON LOCAL RHO IN THIS PROGRAM
C
      DO 651 I=1,NNTPTS
      UTAU(I)=SQRT(CF2(N)*TR(I))*UINFT(N)
      TPLUS(I) =DIMT(I)*UTAU(I)/(ST(N)*UINFT(N))
      TPLUSP(N,I) = TPLUS(I)
      YPLUS(I) = YTMP(I)*UTAU(I)/(VISCO(NNTPTS)*12.)
      YPLUSP(N,I)=YPLUS(I)
C
  669 U(I)=UUGNEW(I)*UINFT(N)
      UPLUS(I) = U(I)/UTAU(I)
  651 CONTINUE
C
      CALL UNCERT
C
C
C
C         OUTPUT SECTION
C
   12 FORMAT(///3X,18A4//,
     1 2X'TEMP. RUN  VEL. RUN'3X'PLATE'4X'X'8X'ST       CF/2'6X'UINF'
     1,6X'TGAS'6X'TWALL'/2X,I6,'-',I1,3X,I6,'-',I1,4X,I2,
     2  4XF5.2,3XF7.5,4XF7.5,3XF5.1,5XF5.1,6XF5.1///3X
     3   'THERMAL    HYDRO.     ENTHALPY   MOMENTUM   ENTHALPY   MOMENTU
     4M   NO. DATA'/2X'B.L. THK.  B.L. THK.      THK.       THK.      ',
     5 '  RE.         RE.        POINTS',
     6 /4XF5.3,6XF5.3,6XF6.4,5XF6.4,4XF6.0,5XF6.0,8XI2///)
  812 FORMAT(1X18A4/1X,I6,1X,I1,1X,I6,1X,I1,1X,I2,1XF5.2,2(1XF7.5),
     1  3(1XF5.1)/2(1XF5.3),2(1XF6.4),2(1XF6.0),1X,I2)
  817 FORMAT(1XF6.1,2(1XF6.1),4(1XF5.3),1XF6.4,2(1XF5.1))
  819 FORMAT(1X,I1,1X,I2,1XF5.2,3(1XF5.1),2(1XF7.5),1XF5.3,1XF6.4,1XF5.0
     1 )
  821 FORMAT(1X,I1,1X,I2,4(1XF6.4),2(1XF6.0),2(1XF5.3))
  861 FORMAT(2(1X,I2,1XF7.5,2(1XF6.0),1XF5.1,1XF5.3))
  916 FORMAT(30X'PROFILE OUTPUT'//'    YPLUS    UPLUS    TPLUS   Y/DELH
     1  U/UINF   TBAR   Y/DELM    Y        U        T'/)
  917 FORMAT(2XF6.1,2(3XF6.1),4XF5.3,4XF5.3,4XF5.3,2XF5.3,3XF6.4,
     1 3XF5.1,3XF5.1)
  918 FORMAT(///,40X' SUMMARY '///,2X'N'3X'PLATE'5X'X    TPLATE  ',
     1  'TGAS   UINF     ST          CF/2       F      ENTH. THK.',
     2 5X'ENTH. THK. RE.'/)
  919 FORMAT(2XI1,4X,I2,3X,2XF5.2,2XF5.1,2XF5.1,2XF5.1,3XF7.5,4XF7.5,
```

```
     1   4XF5.3,5XF6.4,12XF5.0)
  920 FORMAT(/96X'UNCERTAINTIES'/
     12X'N'3X'PLATE'5X'DISPL. THK.      MOMENTUM THK.     MOMENTUM RE.
     2     H'18X'ENTH. THK.'11X'ENTH. THK. RE.',
     3/16X'VEL    PROF      VEL    PROF      VEL    PROF      VEL    PROF'
     410X'ABSOLUTE'6X'%'8X'ABSOLUTE'6X'%'/)
  921 FORMAT(2X11,4X12,7XF6.4,1XF6.4,3XF6.4,1XF6.4,3XF6.0,1XF6.0,4XF5.3,
     12XF5.3,10XF6.4,4XF5.1,8XF5.0,5XF5.1)
  960 FORMAT(//////30X'STANTON NUMBER,ADJUSTED ENTH. THK. REYNOLDS NO.,
     1AND 2-D CHECK'/
     2//2(5X'PLATE'5X'ST'5X'REDEL'5X'REDEL'5X' % '5X'DELTA2'5X)/
     3  2(22X'(ST)'6X'(PROF)'3X'ERROR'15X)/)
  961 FORMAT(2(6X,I2,4XF7.5,2XF6.0,5XF5.0,3XF5.1,5XF5.3,6X))
 1555 FORMAT(1H1,30X'   OUPUT SECTION ')
 1556 FORMAT(/3X,18A4//)
 1557 FORMAT(3X,18A4)
 3070 FORMAT(1H1,////,45X'UNCERTAINTY INTERVALS'///18X'ABSOLUTE VALUES',
     1 46X'PERCENTAGE VALUES'3X,///'    YPLUS    UPLUS    TPLUS   Y/DELH
     1  U/UINF    TBAR'                                  11X'YPLUS   UPLUS
     2TPLUS    Y/DELH   U/UINF    TBAR'/)
 3071 FORMAT(2XF6.1,2(3XF6.1),4XF5.3,4XF5.3,4XF5.3,9XF5.1,3XF5.1,
     1 3XF5.1,5XF5.1,4XF5.1,2XF5.1)
C
C
C  PLATE NUMBER IS DETERMINED FROM THE X POSITION
C
      DO 133 KK=1,24
      XL=4*KK
      IF(XL.GT.TX(N)) GO TO 134
  133 CONTINUE
  134 PLATE(N)=KK
C
      IF(N.EQ.1) WRITE(6,1555)
      IF(N.GT.1) WRITE(6,889)
  655 WRITE(6,12) TITLE,TDATE(N),TRUN(N),VDATE(N),VRUN(N),PLATE(N),
     1  TX(N),ST(N),CF2(N),UINFT(N),
     2TEMP(NNTPTS),TPLATE(N),DELH(N),DELM(N),DELTA2(N),DELMOM(N),
     3 REENTH(N),REMOM(N),NNTPTS
      IF(IPUNCH.EQ.1) WRITE(7,812) TITLE,TDATE(N),TRUN(N),VDATE(N),
     1  VRUN(N),PLATE(N),TX(N),ST(N),CF2(N),
     2UINFT(N),TEMP(NNTPTS),TPLATE(N),DELH(N),DELM(N),DELTA2(N),
     3 DELMOM(N),REENTH(N),REMOM(N),NNTPTS
      WRITE(6,916)
      DO 517 I=1,NNTPTS
      WRITE(6,917) YPLUS(I),UPLUS(I),TPLUS(I),DIMYH(I),UUGNEW(I),
     1DIMT(I),DIMYM(I),YTMP(I),U(I),TEMP(I)
      IF(IPUNCH.EQ.1) WRITE(7,817) YPLUS(I),UPLUS(I),TPLUS(I),
     1  DIMYH(I),UUGNEW(I),DIMT(I),DIMYM(I),YTMP(I),U(I),TEMP(I)
  517 CONTINUE
C
      WRITE(6,3070)
      DO 3075 I=1,NNTPTS
      WRITE(6,3071) DYPLUS(I),DUPLUS(I),DTPLUS(I),DDIMYH(I),DUUGNW(I),
     1 DDIMT(I),DYPLND(I),DUPLND(I),DTPLND(I),DYND(I),DUUGND(I),DTND(I)
 3075 CONTINUE
C
   75 CONTINUE
C
C
C     WRITE SUMMARY
C
```

```
 1108 WRITE(6,689 )
      WRITE(6,1556) TITLE
       WRITE(6,918)
       WRITE(6,919) (N,PLATE(N),TX(N),TPLATE(N),TEMP(NTPTS(N)+1),
     1   UINFT(N),ST(N),CF2(N),VF(N),DELTA2(N),REENTH(N),N=1,NTRAV)
       WRITE(6,920)
       WRITE(6,921) (N,PLATE(N),VDELT1(N),DISPL(N),VDELT2(N),DELMOM(N),
     1   VREMOM(N),REMOM(N),VH(N),H(N),DDELTA(N),
     2   DDELND(N),DREENT(N),DREND(N),N=1,NTRAV)
C
      IF(IPLACH.EQ.0) GO TO 1830
      WRITE(7,1557) TITLE
      DO 1819 N=1,NTRAV
       WRITE(7,819) N,PLATE(N),TX(N),TPLATE(N),TEMP(NTPTS(N)+1),
     1   UINFT(N),ST(N),CF2(N),VF(N),DELTA2(N),REENTH(N)
 1819 CONTINUE
      DO 1821 N=1,NTRAV
        WRITE(7,821) N,PLATE(N),VDELT1(N),DISPL(N),VDELT2(N),
     1   DELMOM(N),VREMOM(N),REMOM(N),VH(N),H(N)
 1821 CONTINUE
C
 1830 CONTINUE
C
C
C THE FOLLOWING SECTION PRINTS OUT INFORMATION ON THE
C UNCERTAINTY INTERVALS USED IN THE UNCERTAINTY CALCULATIONS.
C
C
C     HEADING AND EXPLANATION
      WRITE(6,1900)
 1900 FORMAT(///////,20X,'PRIME UNCERTAINTY INTERVALS USED'
     1,3X,'(ESTIMATED AT 20:1 ODDS)'//)
      WRITE(6,1901)
 1901 FORMAT(2X,'VARIABLE',5X,'VALUE ASSIGNED',10X,'VARIABLE MEANING'
     1,44X,'UNITS'/)
      WRITE(6,909) DTEMPA
  909 FORMAT(2X,'DTEMPA',7X,F5.3,19X,'TEMPERATURE',49X,'DEG. F.')
      WRITE(6,908) DPRTMP
  908 FORMAT(2X'DPRTMP'7XF5.3,19X'PROBE TEMPERATURE NEAR WALL(FIRST 15 P
     1OINTS)'16X'DEG. F.')
      WRITE(6,910) DPAMB
  910 FORMAT(2X,'DPAMB',8X,F5.2,19X,'AMBIENT PRESSURE',44X,'LBF/FT2')
      WRITE(6,911) DMUP
  911 FORMAT(2X'DMUP',7X,F5.1,21X,'ABSOLUTE VISCOSITY',42X,'%')
      WRITE(6,907) DELY
  907 FORMAT(2X'DELY'9X,F6.4,18X,'PROBE POSITION REL. TO WALL',33X,
     1 'INCHES')
      WRITE(6,689)
C
 1550 CONTINUE
  550 CONTINUE
      STOP
      END
C
C
C
C
      FUNCTION TCALIB(T)
C      THIS FUNCTION SUPPLIES THE THERMOCOUPLE CALIBRATION
      A=-2220.703
      B=781.25
```

```
      E=7.950782
      D=0.256
      TCALIB=A+B*SQRT(E+D*T)+ 5C.
      RETURN
      END
C
C
C
C
C
C
C
C
      BLOCK DATA
C
C
      COMMON  AREA(60),AREAD(60),AREAM(60),CF2(10),DP(60),DDELT1(10),
     1   DDELT2(10),DELM(10),DELMOM(10),DELTA2(10),DFV(10),DKV(10),
     2  DHV(10),DIMT(60),DIMYH(60),DIMYM(60),DISPL(60),DREMOM(10),
     3   DUV(10,60),DUUG(10,60),H(10),IS,KEYREF(10),NTPTS(10),NVPTS(10),
     4  PBAR(10),PR(10),PSTAT(10),REDEL(24),REENTH(10),REMOM(10),RC(10),
     5   RHOM(10),ST(10),STN(24),T(60),TAMB(10),TR(60),DREENT(10),
     6   TBAR(60),TD(10),TEMP(60),TGAST(10),TIME60(10,60),
     7   TITLE(18),TMV(10,60),TC(10),TPLATE(10),TPLUS(60),
     8   TU(10),TX(10),U(60),UINFT(10),UINFV(10),UPLUS(60),UUG(10,60),
     9   UUGNEW(60),UV(10,60),U2(60),VDELT1(10),VDELT2(10),VF(10),
     1   VH(10),VK(10),VMDOT(10),VREMOM(10),VREX(10),VVZERO(10),VX(10),
     2 VYDEL(10,60),X(10),YPLUS(60),YRAWT(10,60),YTMP(60),YVEL(10,60)
     3  ,UTAU(60),DELH(10),IBAR,PER1(24),RE1(24),CP(60),ENTH(24)
      COMMON /A/ DUUGNW(60),DUVNW(60),RHOG(60),VISCO(60),DCF2(10),
     1        DDIMT(60),DYPLUS(60),DUPLUS(60),DTPLUS(60),
     2        IDELH,DDELH(10),Z(60),CZ(60),C1,RM,N,PSAT,RHOSAT,TEMPS
     3        ,DST(10),DAREA(60),DDIMYH(60),DYPLND(60),DUPLND(60),
     4        DTPLND(60),DYND(60),DUUGND(60),DTND(60),DDELTA(10),
     5        DELY,DTEMPA,DPAMB,CMUF,NNTPTS,DDELND(10),DREND(10),
     6          DTEMP(60),DVISCO(60),DIMYHP(10,60),DIMTP(10,60),
     7          YPLUSP(10,60),TPLUSP(10,60),ENTHNW(24),DPRTMP
C
      INTEGER VDATE(10),VRUN(10),TDATE(10),TRUN(10),VTRAV(10),PLATE(10),
     1 PTITLE(4,60),XLABEL(4,40),YLABEL(4,40),R,XTYPE(4),YTYPE(4),
     2 XTEN(4),YTEN(4),L2(13),LL2(4,13),N1(60),N5(40),N6(40),N18(13)
C
      REAL IS(60),PSAT(9),RHOSAT(9),TEMPS(9),IBAR(60),XLENGT(4),
     1  YLENGT(4),XZERO(4),XEND(4),X1(4),YZERO(4),YEND(4),Y1(4),
     2 XX(13,50),YY(13,50)
C
      DATA TEMPS/
     1140.0,50.0,60.0,70.0,80.0,90.0,100.0,110.0,120.0/
      DATA PSAT/
     1117.53,25.65,36.90,52.20,73.00,100.40,136.50,183.60
     2,243.70/
C
      DATA RHOSAT/
     110.0C0409,0.000587,0.000830,0.001153,
     2C.001580,0.002139,0.002853,0.003770,0.004920/
C
C
      END
C
C
C
```

```
C
C
C
      SUBROUTINE UNCERT
C
C UNCERTAINTY ANALYSIS FOR PROFILE PROGRAM
C
C  THIS PROCEDURE CALCULATES UNCERTAINTY INTERVALS BY THE PROCEDURE OF
C  KLINE AND MCLINTOCK.  THE UNCERTAINTY INTERVALS FOR THE MEASURED
C  VARIABLES AND/OR THE UNCERTAINTIES CALCULATED BY THE VELOCITY PROGRAM
C  ARE DEFINED AS:
C       DTEMPA    : TEMPERATURE (F)
C       DPRTMP    : TEMPERATURE OBTAINED WITH PROBE (F)
C       DPAMB     : AMBIENT PRESSURE (PSF)
C       DMUP      : ABSOLUTE VISCOSITY (%)
C       DELY      : PROBE POSITION RELATIVE TO WALL (IN)
C
C  CERTAIN UNCETAINTY INTERVALS, PREVIOUSLY CALCULATED, WHICH ARE USED
C  IN THIS PROCEDURE ARE:
C       DUUG      : U/UINF  (1)
C       DUV       : VELOCITY (FPS)
C       DCF2      : SKIN FRICTION COEFFICIENT (1)
C       DST       : STANTON NUMBER (1)
C
      COMMON  AREA(60),AREAD(60),AREAM(60),CF2(10),DP(60),DDELT1(10),
     1   DDELT2(10),DELM(10),DELMLM(10),DELTA2(10),DFV(10),DKV(10),
     2  DHV(10),DIMT(60),DIMYH(60),DIMYM(60),DISPL(60),DREMOM(10),
     3   DUV(10,60),DUUG(10,60),H(10),IS,KEYREF(10),NTPTS(10),NVPTS(10),
     4  PBAR(10),PR(10),PSTAT(10),REDEL(24),REENTH(10),REMOM(10),RC(10),
     5   RHUM(10),ST(10),STN(24),T(60),TAMB(10),TR(60),DREENT(10),
     6   TBAR(60),TD(10),TEMP(60),TGAST(10),TIME60(10,60),
     7   TITLE(18),TMV(10,60),TO(10),TPLATE(10),TPLUS(60),
     8   TU(10),TX(10),U(60),UINFT(10),UINFV(10),UPLUS(60),UUG(10,60),
     9   UUGNEW(60),UV(10,60),U2(60),VDELT1(10),VDELT2(10),VF(10),
     1   VH(10),VK(10),VMDOT(10),VREMOM(10),VREX(10),VVZERO(10),VX(10),
     2 VYDEL(10,60),X(10),YPLUS(60),YRAWT(10,60),YTMP(60),YVEL(10,60)
     3  ,UTAU(60),DELH(10),IBAR,PER1(24),RE1(24),CP(60),ENTH(24)
      COMMON /A/ DUUGNW(60),DUVNW(60),RHOG(60),VISCO(60),DCF2(10),
     1        DDIMT(60),DYPLUS(60),DUPLUS(60),DTPLUS(60),
     2        IDELH,DDELH(10),Z(60),DZ(60),C1,RM,N,PSAT,RHOSAT,TEMPS
     3        ,DST(10),DAREA(60),DDIMYH(60),DYPLND(60),DUPLND(60),
     4        DTPLND(60),DYND(60),DUUGND(60),DTND(60),DDELTA(10),
     5        DELY,DTEMPA,DPAMB,DMUP,NNTPTS,DDELND(10),DRENO(10),
     6          DTEMP(60),DVISCO(60),DIMYHP(10,60),DIMTP(10,60),
     7          YPLUSP(10,60),TPLUSP(10,60),ENTHNW(24),DPRTMP
C
      INTEGER VDATE(10),VRUN(10),TDATE(10),TRUN(10),VTRAV(10),PLATE(10),
     1 PTITLE(4,60),XLABEL(4,40),YLABEL(4,40),R,XTYPE(4),YTYPE(4),
     2 XTEN(4),YTEN(4),L2(13),LL2(4,13),N1(60),N5(40),N6(40),N18(13)
C
      REAL IS(60),PSAT(9),RHOSAT(9),TEMPS(9),IBAR(60),XLENGT(4),
     1  YLENGT(4),XZERO(4),XEND(4),X1(4),YZERO(4),YEND(4),Y1(4),
     2 XX(13,50),YY(13,50)
C
C
      REAL NN,N1V,N2V,N1Y,N2Y,NC,NT,NDH,N1D,N2D,N3D,NN1,NN2,NN3,DMU(60),
     1  NN4,NN5
C
C  CALCULATED UNCERTAINTY INTERVALS
C
      DYTMP=DELY
```

```
      DTPLAT=SQRT(11.*DTEMPA**2)/5.
      DPBAR=DPAMB*29.96/2116.
      DTMP=DTPLAT
      DAREA(1)=0.0
 1000 FORMAT(/2X11(1X,E10.3))
 1001 FORMAT(///)
C     PRINT 1000, DYTMP,DTPLAT,DPBAR,DTMP
C     PRINT 1001
C
      DO 90 I=1,NNTPTS
C
C  TEMP(I)
C
C BECAUSE OF POSSIBLE THERMOCOUPLE ERRORS DUE TO RADIATION AND
C CONDUCTION AND ALSO ERRORS DUE TO INHOMOGENEOUS WIRES IN A TEMP-
C ERATURE GRADIENT, A HIGHER UNCERTAINTY IS APPLIED HERE TO THE FIRST
C 15 POINTS ABOVE THE WALL(PRESUMING THAT MOST PROFILES HAVE 25 TO
C 30 POINTS).  IN THE OUTER REGION, THE SMALL GRADIENTS LEAD TO MORE
C CERTAIN READINGS.
C
      IF(I.GT.1) DTMP=DPRTMP
      IF(I.GT.16) DTMP=DTEMPA
      T1=DTMP
      T2=-DUVNW(I)*2.*RC(N)*C1/CP(I)*U2(I)
      DTEMP(I)=SQRT(T1**2 + T2**2)
C     PRINT 1000, T1,T2,DTEMP(I)
   90 CONTINUE
C     PRINT 1001
C
          DO 100 I=1,NNTPTS
C
      CMU(I)=DMUP*VISCO(I)*RHOG(I)/100.
      IF(I.GT.1) DUUGND(I)=DUUGNW(I)/UUGNEW(I)*100.
      IF(I.GT.1) DTMP=DTEMPA
      IF(I.GT.1) GO TO 88
      DLLGND(1)=0.0
      DTND(1)=0.0
      DYPLND(1)=0.0
      DUPLND(1)=0.0
      DYND(1)=0.0
      DTPLND(1)=0.0
   88 CONTINUE
C
C  DIMT(I)
C
      NN=TEMP(I) - TEMP(NNTPTS)
      DD=TPLATE(N) - TEMP(NNTPTS)
      D1=-DTEMP(I)/DD
      D2=DTEMP(NNTPTS)*(1./DD - NN/DD**2)
      D3=DTPLAT*NN/DD**2
      DDIMT(I)=SQRT(D1**2 + D2**2 + D3**2)
      IF(I.GT.1) DTND(I)=DDIMT(I)/DIMT(I)*100.
C     PRINT 1000, DMU(I),DTEMP(I),NN,DD,D1,D2,D3,DDIMT(I),DTND(I)
C
C
C  VISCOSITY
C
      N1V=11. + 0.0175*TEMP(I)
      N2V=RM*(TEMP(I) + 460.)
      DV=1.0E06*(PBAR(N)*2116./29.96 + PSTAT(N)*5.2)
      V1=DTEMP(I)*(0.0175*N2V/DV + RM*N1V/DV)
```

```
      V2=-DPBAR*N1V*N2V/DV**2*1.0E06*2116./29.96
      V3=DMU(I)*N2V/DV
      DVISCO(I)=SQRT(V1**2 + V2**2 + V3**2)
C     PRINT 1000, N1V,N2V,DV,V1,V2,V3,DVISCO(I)
C
C  YPLUS(I)
C
      N1Y=YTMP(I)*UINFT(N)
      N2Y=CF2(N)*(TEMP(NNTPTS) + 460.)
      D1Y=VISCO(I)*12.
      D2Y=TEMP(I) + 460.
      Y8=DELY*UINFT(N)*SQRT(N2Y)/(D1Y*SQRT(D2Y))
      Y2=-DTEMP(I)*N1Y*SQRT(N2Y)/(SQRT(D2Y)*D2Y*D1Y*2.)
      Y3=DTEMP(NNTPTS)*N1Y*CF2(N)/(D1Y*SQRT(D2Y*N2Y)*2.)
      Y4=DUVNW(NNTPTS)*YTMP(I)*SQRT(N2Y)/(D1Y*SQRT(D2Y))
      Y5=-DVISCO(I)*N1Y*12.*SQRT(N2Y)/(SQRT(D2Y)*D1Y**2)
      Y6=DCF2(N)*N1Y/(D1Y*(SQRT(D2Y*N2Y)*2.))*(TEMP(NNTPTS)+460.)
      DYPLUS(I)=SQRT(Y8*Y8 + Y2**2 + Y3**2 + Y4**2 + Y5**2 + Y6*Y6)
      IF(I.GT.1) DYPLND(I)=DYPLUS(I)/YPLUS(I)*100.
C     PRINT 1000, N1Y,N2Y,D1Y,D2Y,Y6,Y2,Y3,Y4,Y5,DYPLUS(I),DYPLND(I)
C
C  UPLUS(I)
C
      NU=U(I)*SQRT(TEMP(I)+460.)
      DU=SQRT(CF2(N)*(TEMP(NNTPTS)+460.))*UINFT(N)
      U1=DUVNW(I)*SQRT(TEMP(I)+460.)/DU
      U6=DTEMP(I)*U(I)/(2.*DU*SQRT(TEMP(I)+460.))
      U3=-DUVNW(NNTPTS)*NU/(DU*UINFT(N))
      U4=-DTEMP(NNTPTS)*NU/(2.*DU*(TEMP(NNTPTS)+460.))
      U5=-DCF2(N)*NU/(2.*DU*CF2(N))
      DUPLUS(I)=SQRT(U1**2 + U6**2 + U3**2 + U4**2 + U5**2)
      IF(I.GT.1) DUPLND(I)=DUPLUS(I)/UPLUS(I)*100.
C     PRINT 1000, NU,DU,U1,U6,U3,U4,U5,DUPLUS(I),DUPLND(I)
C
C  TPLUS(I)
C
      NT=DIMT(I)*SQRT(CF2(N)*(TEMP(NNTPTS)+460.))
      DT=ST(N)*SQRT((TEMP(I)+460.))
      TP1=DDIMT(I)*SQRT(CF2(N)*(TEMP(NNTPTS)+460.))/DT
      TP2=DTEMP(NNTPTS)*NT/(2.*DT*(TEMP(NNTPTS)+460.))
      TP3=-DST(N)*NT*SQRT(TEMP(I)+460.)/DT**2
      TP4=-DTEMP(I)*NT*ST(N)/(2.*DT**2*SQRT(TEMP(I)+460.))
      TP5=DCF2(N)*DIMT(I)*SQRT(TEMP(NNTPTS)+460.)/(2.*DT*SQRT(CF2(N)))
      DTPLUS(I)=SQRT(TP1**2 + TP2**2 + TP3**2 + TP4**2 + TP5**2)
      IF(I.GT.1) DTPLND(I)=DTPLUS(I)/TPLUS(I)*100.
C     PRINT 1000, NT,DT,TP1,TP2,TP3,TP4,TP5,DTPLUS(I),DTPLND(I)
C
C DELTA2(N) - IBAR(1)*TR(I)
C
      AA=RC(N)*C1/CP(I)
      N1D=T(NNTPTS)-AA*U2(NNTPTS)+460.
      D1D=T(I)-AA*U2(I)+460.
      N2D=CP(I)*T(I)+C1*U2(I)*(1.-RC(N))-CP(NNTPTS)*T(NNTPTS)-C1*U2(NNTP
     1TS)*(1.-RC(N))
      D2D=CP(1)*T(1)-CP(NNTPTS)*T(NNTPTS)-C1*U2(NNTPTS)*(1.-RC(N))
      N3D=N1D*N2D
      D3D=D1D*D2D
      Z(I)=N3D/D3D
      X6=-DTPLAT*N3D*D1D/D3D**2*CP(1)
      X2=DTMP*(N1D*CP(I)/D3D - N3D/D3D**2*D2D)
      X3=DTEMPA*((N2D-N1D*CP(NNTPTS))/D3D+N3D/D3D**2*CP(NNTPTS)*D1D)
```

```
      X4=DUVNW(I)*(N1D*2.*C1*(1.-RC(N))*U(I)/D3D+N3D/D3D**2*D2D*2.*AA*
     1 U(I))
      X5=DUVNW(NNTPTS)*((-N2D*2.*AA*U(NNTPTS)-N1D*2.*C1*(1.-RC(N))*U(NNT
     1PTS))/D3D - N3D/D3D**2*D1D*(-2.*C1*(1.-RC(N))*U(NNTPTS)))
      DZ(I)=SQRT(X6**2 + X2**2 + X3**2 + X4**2 + X5**2)
C     PRINT 1000,AA,N1D,D1D,N2D,D2D,N3D,D3D,Z(I)
C     PRINT 1000,X6,X2,X3,X4,X5,DZ(I)
C     PRINT 1001
C
C TO BE CONTINUED
C
C
  100 CONTINUE
C
C  THERMAL BL THICKNESS
C
C IDELH IS THE VALUE OF THE INDEX I FOR THE FIRST DIMT(I) > 0.99
C
      NDH=0.99 - DIMT(IDELH-1)
      DDH=DIMT(IDELH) - DIMT(IDELH-1)
      DH1=DELY*(1.-NDH/DDH)
      DH2=DELY*NDH/DDH
      DH3=-DDIMT(IDELH)*NDH/DDH**2*(YTMP(IDELH)-YTMP(IDELH-1))
      DH4=DDIMT(IDELH-1)*(YTMP(IDELH)-YTMP(IDELH-1))*(NDH/DDH**2-1./DDH)
      DDELH(N)=SQRT(DH1**2 + DH2**2 + DH3**2 + DH4**2)
C
C
      DO 115 I=1,NNTPTS
C
C  YTMP/DELH
C
      DDIMYH(I)=SQRT((DELY/DELH(N))**2 + (DDELH(N)*YTMP(I)/DELH(N)**2)
     1**2)
      IF(I.GT.1) DYND(I)=DDIMYH(I)/DIMYH(I)*100.
C     PRINT 1000, NDH,DDH,DH1,DH2,DH3,DH4,DDELH(N),DDIMYH(I),DYND(I)
C
  115 CONTINUE
C     PRINT 1001
C
C DELTA2(N) CONTINUED
C
      A1=DELY*.5*(DUGNEW(NNTPTS)*Z(NNTPTS)+DUGNEW(NNTPTS-1)*Z(NNTPTS-1))
      A2=-DELY*.5*(DUGNEW(1)*Z(1)+DUGNEW(2)*Z(2))
C     NN5=.5*(YTMP(2) - YTMP(1))
C     A3=DUUGNW(NNTPTS)*NN4*Z(NNTPTS)  =0 SINCE Z(NNTPTS)=0
C     A4=DUUGNW(1)*NN5*Z(1)     =0 SINCE DUUGNW(1)=0
C     A6=DZ(1)*NN5*UUGNEW(1)    =0 SINCE UUGNEW(1)=0
      NN4=.5*(YTMP(NNTPTS)-YTMP(NNTPTS-1))
      A5=DZ(NNTPTS)*NN4*UUGNEW(NNTPTS)
C
      SUM1=0.0
      SUM2=0.0
      SUM3=0.0
      NNN=NNTPTS-1
      DO 110 I=2,NNN
         NN1=.5*(UUGNEW(I-1)*Z(I-1) - UUGNEW(I+1)*Z(I+1))
         NN2=.5*(YTMP(I+1) - YTMP(I-1))*Z(I)
         NN3=.5*(YTMP(I+1) - YTMP(I-1))*UUGNEW(I)
         SUM1=DELY*DELY*NN1*NN1  + SUM1
         SUM2=DUUGNW(I)*DUUGNW(I)*NN2*NN2  + SUM2
         SUM3=DZ(I)*DZ(I)*NN3*NN3 + SUM3
```

```
C      PRINT 1000,UUGNEW(I),Z(I),YTMP(I),DELY,DUUGNW(I),DZ(I)
C      PRINT 1000, NN1,NN2,NN3,SUM1,SUM2,SUM3
  110 CONTINUE
C
C      PRINT 1000, A1,A2,A5,SUM1,SUM2,SUM3,DZ(NNTPTS),NN4,UUGNEW(NNTPTS)
       DDELTA(N)=SQRT(A1*A1+A2*A2+A5*A5+SUM1+SUM2+SUM3)
       DDELND(N)=DDELTA(N)/DELTA2(N)*100.
C
C ENTHALPY THICKNESS REYNOLDS NO.
C
       R1=DDELTA(N)*UINFT(N)/(12.*VISCO(NNTPTS))
       R2=DUVNW(NNTPTS)*DELTA2(N)/(12.*VISCO(NNTPTS))
       R3=-DVISCO(NNTPTS)*DELTA2(N)*UINFT(N)/(12.*VISCO(N)**2)
       DREENT(N)=SQRT(R1**2 + R2**2 + R3**2)
       DREND(N)=DREENT(N)/REENTh(N)*100.
C      PRINT 1000, DDELTA(N),DDELND(N),R1,R2,R3,DREENT(N),DREND(N)
C      PRINT 1001
C
       RETURN
       END
C
C
```

ENERGY PROGRAM

```
C
C
C  THIS PROGRAM IS DESIGNED TO:
C       1. ADJUST THE ENTHALPY THICKNESSES, INTEGRATED FROM THE
C          STANTON DATA, ON THE BASIS OF A STARTING VALUE COMPUTED
C          FROM THE PROFILE DATA.
C       2. COMPARE THE PROFILE ENTHALPY THICKNESS TO THAT FROM THE
C          INTEGRATION OF THE ENERGY EQUATION,IE, CHECK THE ENERGY
C          BALANCE.
C       3. PLOT STANTON NO. VS REDEL2 AND PUNCH ALL THE RESULTS.
C  ALL THE STANTON RUNS ASSOCIATED WITH EACH PROFILE RUN CAN BE
C  ADJUSTED AT ONE TIME(ENTIRE SET IS HERE DEFINED TO BE A DATA RUN).
C  AS MANY DATA RUNS AS DESIRED CAN BE PLOTTED ON ONE PLOT.
C         IF A PLOT OF DEL2 VS X FOR THE PROFILE DATA AND FOR THE
C  VALUES FROM THE INTEGRATION IS DESIRED, IT CAN BE OBTAINED BY USING
C  THE PUNCHED OUTPUT WITH A PLOT PROGRAM.
C
C
C   COMPILED 11/2/69
C
      INTEGER PLATE(10),PTITLE(4,60),XLABEL(4,40),YLABEL(4,40),R,
     1  XTYPE(2),YTYPE(2),XTEN(2),YTEN(2),OPTION,DATE,RUN
      DIMENSION XLENGT(2),YLENGT(2),LL2(2,13)
     1             ,XZERO(2),XEND(2),X1(2),YZERO(2),YEND(2),Y1(2),
     2DELTA2(10),STN(15,24),REDEL(24),ENTH(24),REDELN(15,24),ENTHNW(24),
     3 L2(15),XX(13,100),YY(13,100),N5(40),N6(40),N1(60),Q(24),FR(24)
     4 ,N18(13),TITLE(18),TOEFF(24),F(24),UG(24),XINT(25),X(25),
     5 XST(24),TERM(25),XPROF(10),ENTHCK(10),VISCGS(24)
      REAL ISO(24)
C
C
C
C    INPUTS HERE
C
C
C PLOT INFORMATION
C
C
C  THE PLOT SPECIFICATIONS WERE READ IN THIS SECTION.  THE ACTUAL
C  CARDS HAVE BEEN REMOVED, BUT ANY PLOTTING ROUTINE CAN BE UTILIZED.
C
C
C DEFINITIONS:   SEVERAL STANTON RUNS WILL BE ADJUSTED BY THE RESULTS
C   OF A SINGLE PROFILE RUN.  STANTON RUN=1 TO 24 PLATES OF STANTON
C   DATA.  DATA RUN=ALL STANTON RUNS ASSOCIATED WITH ONE PROFILE RUN.
C
C
C  IPUNCH - 0-NO PUNCH  1-PUNCH
C  IPLOT  - 0-NO PLOT  1-PLOT
C  NPLOTS - NUMBER OF PLOTS TO BE PREPARED
C  NDATA - NUMBER OF DATA RUNS DESIRED ON EACH PLOT
C  NCURV - NUMBER OF STANTON RUNS PER DATA RUN
C  NTRAV - NUMBER OF TRAVERSES IN THE PROFILE RUN USED FOR 2-D CHECK
C  MTRAV - PLATE CORRESPONDING TO DELTA2 USED FOR ADJUSTMENT
C  OPTION - OPTION TO SELECT BASIS FOR STARTING VALUE IN ENERGY
C           EQUATION.  1  FOR AVERAGE BASED ON PROFILES,  2 FOR A
C           PARTICULAR PROFILE,  3 FOR A PRESELECTED STARTING VALUE
C           WHICH IS ENTERED AT "READ(5,9)" STATEMENT.
C  XDEL -    X  CORRESPONDING TO XDELTA USED FOR ADJUSTMENT WHEN OPTION=3
C  NCST - SET TO 1 FOR CONSTANT PROPERTY CORRECTION TO STANTON DATA
```

```
C NF - FIRST PLATE TO BE PLOTTED
C NL - LAST PLATE TO BE PLOTTED
C
C
      READ(5,6) NPLOTS,IPUNCH,IPLOT
    6 FORMAT(I2,1X,I1,1X,I1)
   61 FORMAT(I1,1X,I1,1X,I2,1X,I2)
C
C
      DO 1550 LOOP=1,NPLOTS
C
 1605 NN=0
      KD=1
      READ(5,61) NDATA,NCST,NF,NL
C
 1610 READ(5,9) NCURV,NTRAV,MTRAV,OPTION,XDEL,XDELTA
      XDEL=XDEL/12.
      XDELTA=XDELTA/12.
      WRITE(6,889)
      WRITE(6,3235)
 3235 FORMAT(5X'TEMPERATURE PROFILE DATA'//4X'PLATE'5X'I'5X'DELTA2'/)
 3236 FORMAT(5X,I2,5XF5.2,2XF7.4)
C
C INSERT TITLE CARD THAT GOES WITH TEMP OUTPUT SUMMARY. IT WILL BE
C SKIPPED.
C
      DO 110 N=1,NTRAV
      READ(5,10) PLATE(N),XPROF(N),DELTA2(N)
      IF(OPTION.NE.2) GO TO 3365
      IF(PLATE(N).EQ.MTRAV) XDEL=XPROF(N)/12.
      IF(PLATE(N).EQ.MTRAV) XDELTA=DELTA2(N)/12.
 3365 WRITE(6,3236) PLATE(N),XPROF(N),DELTA2(N)
  110 CONTINUE
C
    9 FORMAT(I2,1X,I2,1X,I2,1X,I1,3X,2F10.0/)
   10 FORMAT(3X,I2,1XF5.2,41XF6.4)
C
      DO 200 NC=1,NCURV
C
      NNN=NC + NN
      IF(NC.NE.1) WRITE(6,889)
C
C INITIALIZE STANTON DATA
C
      DO 588 I=1,24
         STN(NNN,I)=0.0
         REDEL(I)=0.0
  588    ENTH(I)=0.0
C
C
      READ(5,905) TITLE,DATE,RUN
C
      READ(5,132) TAMB,TGAS
       DO 135 I=1,24
      READ(5,131) TOEFF(I),STN(NNN,I),REDEL(I),ENTH(I),F(I),UG(I)
      IF(NCST.EQ.1) STN(NNN,I)=STN(NNN,I)*(((TOEFF(I)+460.)/
     1  (TGAS+460.))**0.4)
  135 CONTINUE
  131 FORMAT(3X,F6.2,6X,F7.5,F6.0,F6.4,F8.4,F6.2)
  132 FORMAT(/1XF6.2,15XF6.2)
      WRITE(6,906) TITLE,DATE,RUN
```

```
      WRITE(6,140)
      WRITE(6,141) TAMB,TGAS
      WRITE(6,1916)
      DO 150 I=1,24
      WRITE(6,131) TOEFF(I),STN(NNN,I),REDEL(I),ENTH(I),F(I),UG(I)
  150 CONTINUE
C
  140 FORMAT(///10X'STANTON PROGRAM REDUCED DATA'/)
  141 FORMAT(5X'TAMB=' F5.1,10X'TGAS=' F5.1/)
C
  861 FORMAT(1X,I2,1XF7.5,1XF6.0,1XF6.4,1X,F3.0)
  889 FORMAT(1H1)
  905 FORMAT(1X,18A4/5X,I8,12X,I4)
  906 FORMAT(//10X,18A4/25X,I6,'-',I1)
  907 FORMAT(2X18A4)
  960 FORMAT(//2(5X'PLATE'5X'ST'5X'REDEL'5X'ENTH')/)
  961 FORMAT(2(6X,I2,4XF7.5,2XF6.0,4XF6.4))
 1916 FORMAT(4X'TOEFF'8X'ST'4X'REDEL'1X'ENTH'5X'F'5X'UG'/)
 1917 FORMAT(5XI2,3XF7.5,1XF6.0,4XF6.4,9XI2,3XF7.5,1XF6.0,4XF6.4)
C
      CP=.24
      DEL=1./3.
      XST(1)=1./6.
      DO 3200 I=1,24
      IF(I.GT.1) XST(I)=XST(I-1) + 1./3.
      ISO(I)=CP*(TOEFF(I)-TGAS) - UG(I)*UG(I)/(64.4*778.)
      VISCGS(I)=ENTH(I)*UG(I)/(12.*REDEL(I))
      Q(I)=STN(NNN,I)*UG(I)*ISO(I)
      FR(I)=F(I)*UG(I)*ISO(I)
 3200 CONTINUE
C
C
C INTEGRAL IN ENERGY EQUATION IS EVALUATED HERE
C
       XINT(1)=0.0
       DO 3205 J=2,25
 3205  XINT(J)=XINT(J-1) + 1./3.*(Q(J-1)+FR(J-1))
C
C  STARTING CONSTANT IN ENERGY EQUATION IS EVALUATED HERE.  METHOD
C  USED DEPENDS ON OPTION SPECIFIED IN INPUT.
C
C
C X(I) - X AT EDGE OF EACH PLATE
C START - UG*ISO*DELTA2 AT X=0
C
      X(1)=0.0
      DO 3214 JJ=2,24
 3214 X(JJ)=X(JJ-1) + 1./3.
C
      SUM1=0.0
      SUM2=0.0
      SUM3=0.0
C
      WRITE(6,2136)
 2136 FORMAT(///)
C
      MMM=1
      IF(OPTION.EQ.1) MMM=NTRAV
      DO 3215 MM=1,MMM
      IF(OPTION.NE.1) GO TO 3318
         XDEL=XPROF(MM)/12.
```

```
         XDELTA=DELTA2(MM)/12.
 3318 CONTINUE
      DO 3210 J=2,24
      IF(X(J).GE.XDEL) GO TO 3220
 3210 CONTINUE
 3220 XXINT=XINT(J-1)+(XDEL-X(J-1))*(XINT(J)-XINT(J-1))/(X(J)-X(J-1))
      DO 3211 J=2,24
 3211 IF(XST(J).GE.XDEL) GO TO 3212
 3212 XISO=ISO(J-1)
      IF(XDEL.GT.(XST(J-1)+1./6.)) XISO=ISO(J)
      XUG=UG(J-1)+(XDEL-XST(J-1))*(UG(J)-UG(J-1))/(XST(J)-XST(J-1))
      START=XUG*XISO*XDELTA-XXINT
C
      XSTART=12.*START/(UG(1)*ISO(1))
      XREDEL=XSTART*UG(1)/(VISCGS(1)*12.)
      WRITE(6,2135) XSTART,XREDEL
 2135 FORMAT(3X'STARTING VALUE: ENTHALPY THICKNESS='F7.4,
     1 10X'ENTHALPY REYNOLDS NUMBER='F6.0)
      SUM1=SUM1+START
      SUM2=SUM2+XSTART
      SUM3=SUM3+XREDEL
 3215 CONTINUE
      START=SUM1/MMM
      SUM2=SUM2/MMM
      SUM3=SUM3/MMM
      WRITE(6,3216)
      WRITE(6,2135) SUM2,SUM3
 3216 FORMAT(/7X'AVERAGE')
C
C
C NOW THE ENERGY EQUATION CAN BE EVALUATED ALONG THE ENTIRE TEST
C SECTION. "TERM" IS UG*ISO*ENTH  AT THE EDGE OF EACH PLATE.  "ENTHNW"
C AND "XST" ARE THE VALUES OF ENTHALPY THICKNESS AND X AT THE CENTER
C OF EACH PLATE.
C
       TERM(1)=START
       DO 3230 I=2,25
       TERM(I)=START + XINT(I)
       ENTHNW(I-1) =(.5*(TERM(I-1)+TERM(I))/(UG(I-1)*ISO(I-1)))*12.
      REDELN(NNN,I-1)=UG(I-1)*ENTHNW(I-1)/(VISCGS(I-1)*12.)
 3230 CONTINUE
C
C TWO-DIMENSIONALITY CHECK: ENTHALPY THICKNESS CALCULATED FROM THE
C  PROFILES IS COMPARED TO THAT PREDICTED BY THE ENERGY EQUATION
C
C
C
      WRITE(6,889)
      WRITE(6,906) TITLE,DATE,RUN
       WRITE(6,3325)
       DO 3300 M=1,NTRAV
       DO 3305 J=1,24
 3305  IF(XST(J).GE.(XPROF(M)/12.)) GO TO 3310
 3310  ENTHCK(M)=ENTHNW(J-1)+(XPROF(M)/12.-XST(J-1))*(ENTHNW(J)-
     1 ENTHNW(J-1))/(XST(J)-XST(J-1))
      VEL=UG(J-1)+(XPROF(M)/12.-XST(J-1))/(XST(J)-XST(J-1))*
     1 (UG(J)-UG(J-1))
      XNU=VISCGS(J-1)
      IF((XPROF(M)/12.).GT.(XST(J-1)+1./6.)) XNU=VISCGS(J)
      REYN=VEL*ENTHCK(M)/(XNU*12.)
       ER=(DELTA2(M)-ENTHCK(M))/DELTA2(M)*100.
```

```
      WRITE(6,3320) PLATE(M),XPROF(M),DELTA2(M),ENTHCK(M),ER,REYN
      IF(IPUNCH.EQ.1) WRITE(7,3321) PLATE(M),XPROF(M),DELTA2(M),
     1 ENTHCK(M),ER,REYN
 3300 CONTINUE
 3325  FORMAT(///25X'TWO-DIMENSIONALITY CHECK'//10X'PLATE'10X'X'10X,
     1 'DELTA2'10X'DELTA2'10X'PERCENT'10X'PROFILE'/36X'(PROF)'10X,
     2 ' (ST) '8X,'   ERROR'13X'RE.'/)
 3320 FORMAT(12X,I2,8XF5.2,9XF6.4,10XF6.4,10XF5.1,12XF6.0)
 3321 FORMAT(I2,1X,F5.2,1X,F6.4,1X,F6.4,1X,F5.1,1X,F6.0)
C
C THIS SECTION WRITES OUT THE CORRECTED ST-REDEL RESULTS
C
      WRITE(6,3350)
 3350 FORMAT(////2X,'ADJUSTED RESULTS OF STANTON NUMBER VS ENTHALPY THIC
     1KNESS REYNOLDS NUMBER')
      IF(NCST.EQ.1) WRITE(6,3351)
 3351  FORMAT(20X'CORRECTED TO CONSTANT PROPERTIES')
      WRITE(6,960)
      DO 3140 JJ=1,12
      JK=JJ+12
      WRITE(6,961) JJ,STN(NNN,JJ),REDELN(NNN,JJ),ENTHNW(JJ),
     1 JK,STN(NNN,JK),REDELN(NNN,JK),ENTHNW(JK)
 3140 CONTINUE
C
      IF(IPUNCH.EQ.0) GO TO 3144
      DO 3143 II=1,24
      XJ=4*II-2
      WRITE(7,861) II,STN(NNN,II).REDELN(NNN,II),ENTHNW(II),XJ
 3143 CONTINUE
 3144 CONTINUE
C
  200 CONTINUE
      IF(KD.EQ.NDATA) GO TO 1620
C
C NOW A NEW DATA RUN WILL BE COMPUTED AND SET UP FOR PLOTTING.
C
      NN=NN + NCURV
      KD=KD+1
      GO TO 1610
C
C PLOTTING PREPARATION SECTION
C
 1620 IF(IPLOT.EQ.0) GO TO 1540
C
C  IN THIS SECTION THE PLOT ARRAYS WERE FILLED, AND THE PLOTTING
C  SUBROUTINE WAS CALLED.
C
 1540 CONTINUE
 1550 CONTINUE
      STOP
      END
C
C
```